

JAERI-Research

96-003

NEA/NSC/DOC(96)01



Publication

OECD/NEA
BURNUP CREDIT CRITICALITY BENCHMARK
— RESULT OF PHASE II A —

February 1996

Makoto TAKANO and Hiroshi OKUNO

日本原子力研究所
Japan Atomic Energy Research Institute

OECD/NEA
Burnup Credit Criticality Benchmark
— Result of Phase IIA —

Makoto TAKANO and Hiroshi OKUNO

Department of Fuel Cycle Safety Research
Tokai Research Establishment
Japan Atomic Energy Research Institute
Tokai-mura, Naka-gun, Ibaraki-ken

(Received January 5, 1996)

The report describes the final result of the Phase IIA of the Burnup Credit Criticality Benchmark conducted by OECD/NEA. In the Phase IIA benchmark problems, the effect of an axial burnup profile of PWR spent fuels on criticality (end effect) has been studied. The axial profiles at 10, 30 and 50 GWd/t burnup have been considered. In total, 22 results from 18 institutes of 10 countries have been submitted.

The calculated multiplication factors from the participants have lain within the band of $\pm 1\% \Delta k$. For the irradiation up to 30 GWd/t, the end effect has been found to be less than 1.0% Δk . But, for the 50 GWd/t case, the effect is more than 4.0% Δk when both actinides and FPs are taken into account, whereas it remains less than 1.0% Δk when only actinides are considered. The fission density data have indicated the importance end regions have in the criticality safety analysis of spent fuel systems.

Keywords: Burnup Credit, Benchmark, Criticality, OECD, NEA, Burnup Profile, Actinide, Fission Product, Calculation, Comparison, PWR Fuel

OECD/NEA
燃焼度クレジット臨界計算ベンチマーク
- フェーズ IIA の結果 -

日本原子力研究所東海研究所燃料サイクル安全工学部
高野 誠・奥野 浩

(1996年1月5日受理)

この報告書は、経済開発機構原子力機関で実施された燃焼度クレジットの臨界ベンチマーク問題フェーズ IIA の最終結果を示したものである。フェーズ IIA のベンチマーク問題では、加圧水型原子炉使用済燃料の軸方向燃焼分布が臨界性に与える効果（端部効果）を検討した。燃焼度 10, 30 及び 50 GWd/t における軸方向分布を考慮した。10ヶ国, 18 機関から合計 22 の結果が提出された。

参加者の中性子増倍率は、 $\pm 1\% \Delta k$ の幅に収まった。30 GWd/t までの照射では、端部効果は $1.0\% \Delta k$ 未満であった。しかし 50 GWd/t の場合では、この効果はアクチノイドと FP を両方考慮したときには $4.0\% \Delta k$ を超え、またアクチノイドのみでは $1.0\% \Delta k$ 未満にとどまった。核分裂密度のデータは、燃焼燃料系の臨界安全解析における端部領域が持つ重要性を示した。

Contents

1. Introduction	1
2. Benchmark Specification	1
3. Participants and Analysis Methods	2
4. Results and Discussions	18
5. Concluding Remarks	26
Acknowledgments	27
References	27
Appendix 1 Specification of Benchmark Problems	59
Appendix 2 Additional Analyses by Participants	93
2.1 Report from ORNL	93
2.2 Additional Figures from Toshiba	103
Appendix 3 Documents on Phase IIA Presented at 1994 Meeting in Paris	109
3.1 Preliminary Results (Figures and Tables) Revised, JAERI	109
3.2 PSI Calculation for NEA Burnup Credit Criticality Benchmark, Phase IIA, PSI	137
3.3 The Effect of Axial Burnup Profile, CEA/DRN	144
3.4 Comparison of SCALE-4 CSAS Modules for Criticality Calculations, PNC	159
Appendix 4 List of Participants	165

目 次

1. 緒 言	1
2. ベンチマーク問題の設定	1
3. 参加者と解析方法	2
4. 結果及び検討	18
5. 結 言	26
謝 辞	27
参考文献	27
付録1 ベンチマーク問題	59
付録2 参加者からの追加の解析	93
2.1 ORNLからのレポート	93
2.2 東芝からの追加の図	103
付録3 パリで1994年に開催された会議でのフェーズIIAに関する配布資料	109
3.1 予備的結果(図表)改訂版[原研]	109
3.2 原子力機関燃焼度クレジット臨界ベンチマーク問題フェーズIIAに対する PSIの計算結果[PSI]	137
3.3 軸方向燃焼度分布の効果[CEA/DRN]	144
3.4 臨界計算におけるSCALE-4のCSASモジュールの比較[動燃]	159
付録4 参加者名簿	165

1. Introduction

The report describes the final result of the Phase IIA of the Burnup Credit Criticality Benchmark conducted by OECD/NEA. In the Phase IIA benchmark problems, a simplified model with spent PWR fuel rods was used to compare criticality safety parameters for flat (average) burnup profiles with those of more realistic axial profiles. In total, 22 results from 18 institutes of 10 countries have been submitted.

For the criticality calculation of a spent fuel system, burnup profile of the spent fuel needs to be considered. The effect of the axial burnup profile on criticality is studied in Phase II of the Burnup Credit Criticality Benchmark. The Phase II is divided into two benchmarks, namely, Phase IIA and Phase IIB. In Phase IIA, the criticality of an infinite array of PWR spent fuel rods is analyzed to grasp the effect of axial burnup profile (end effect). In Phase IIB, the criticality of a spent fuel cask will be evaluated.

The end effect was studied as a function of the initial fuel enrichment, the burnup and the cooling time. Parameters selected for the analysis are: burnups of 10, 30 GWd/t for a 3.6 wt% initial fuel enrichment, burnups of 30, 50 GWd/t for a 4.5 wt% initial fuel enrichment, and 1 and 5 years of cooling time. Further, the effect of fission products on the end effect have also been studied. The multiplication factors of spent fuel systems for these combinations of parameters have been obtained by all participants using their code and data. Here, the end effect is measured by the difference of multiplication factors between the cases with and without burnup profile. The case without the burnup profile has an axially flat burnup distribution, i.e., the same burnup value from top to bottom of the fuel rod, where the burnup value is obtained by averaging axially the burnup by volume.

2. Benchmark Specification

The Phase IIA benchmark consists of 26 cases as listed in Table 2.1. Each case results in an eigenvalue calculation of an infinite cell of a PWR fuel rod as shown in Fig. 2.1, with a

specified burnup profile. The geometry and the atomic number densities of all materials are given in the specification. The region-wise fission density data are also requested for the cases 2, 6 and 19. The benchmark specification was finalized in October 1993 and was published as NEA/NSC/DOC(93)15 (see Appendix 1).

3. Participants and Analysis Methods

The following is a brief description of nuclear data and analysis codes employed by each participant. Additional comments provided by participants are also included here. Table 3.1 summarizes the data and codes used by the participants.

(1) Belgonucleaire, Belgium

a) File Header

- Date: 12 Jan. 1994
- Institute: Belgonucleaire SA, 4 Av. Ariane,
B-1200 Bruxelles, Belgium.
- Participant: Thierry Maldague, Y. Vanderborck
- Computer Codes: LWR-WIMS (1986) + ANISN

b) Analysis Environment

The reference code used for the calculation of the cross sections is LWRWIMS from AEA Technology, Winfrith (U.K.). The cross section library is the 69 group 'WIMS 86' set. The collision probability (PERSEUS) module of the code is used for the generation of 16-group macroscopic cross sections for each region of the problem. These 16-group cross sections are introduced in an S8 ANISN one-dimensional calculation.

(2) CEA/DRN, France

a) File Header

- Date: 17 Feb. 1994 (Eigenvalues),
8 Apr. 1994 (Fission densities)
- Institute: CEA/DRN, 13108 St. Paul les Durance, CEDEX, France
- Participants: A. Santamarina, B. Roque

b) Analysis Environment

- Computer Codes: APOLLO + BISTRO

(3) CEA/IPSN, France

a) File Header

- Date: 21 Jan. 1994
- Institute: CEA/IPSN
- Participants: Louis Maubert, Ali Nouri, Gilles Poullot, Jacques Roussignol

b) Analysis Environment

- Neutron Data Library: APOLLO-1 CEA86 Library (JEF1 + ENDFB) + Hansen and Roach library (for stainless steel only)
- Neutron Data Processing: APOLLO 1 cell code 16 groups Hansen and Roach Lethargy
- Code system: APOLLO 1 cell code + MORET Monte Carlo code 3-D geometry modeling, no nuclide omitted, 1 standard deviation, $\sigma = 0.00100$

(4) BfS/IKE, Germany

a) File Header

- Date: 18 Mar. 1994
- Institute: Bundesamt für Strahlenschutz (BfS), Salzgitter, Germany,
Institut für Kernenergetik und Energiesysteme (IKE), der Universität Stuttgart, Germany.
- Participants: Hans-Heinrich Schweer (BfS)
Wolfgang Bernnat (IKE)

b) Analysis Environment

- Data Library: JEF-1, Multigroup Library generated by NJOY
- Codes: CGM(IKE Development) and MORSE-K Monte Carlo codes
- Number of Groups: 242 (CGM-Calculation, one dimensional, condensation to 60 groups for three dimensional Monte Carlo calculation, [Ref. App.4, NEACRP-Report Result of Phase IA]. The number of energy groups (lower breakpoints) are as used at IKE: 4, 9, 14, 19, 24, 29, 35, 40, 44, 49, 52, 55, 58, 62, 65, 68, 71, 74, 77, 80, 83, 86, 89, 91, 111, 115, 119, 123, 128, 132, 136, 138, 139, 140, 141, 143, 147, 156, 164, 174, 179, 184, 187, 189, 190, 192, 194, 197, 202, 206, 210, 214, 220, 223, 227, 231, 234, 237, 239, 242.

For the cladding material, only Zr-90 was taken, and Cr and Fe were omitted. The statistical error, one standard deviation σ , lies between 0.0013 and 0.0025 depending on the number of

batches and neutrons per batch. For Case numbers 2, 6 and 19 however, the standard deviation is less than 0.0009. The code MORSE-K, as described in IKE-Report Nr.4-11, Dez. 1972, is based on the MORSE code and contains modifications to work with multigroup cross sections in the format of RSYST (RSYST is a program system developed at the IKE Stuttgart). The MORSE-K code uses the combinatorial geometry package to describe the geometry.

(5) GRS, Germany

a) File Header

- Date: 2 Feb. 1994
- Institute: Gesellschaft für Anlagen- und Reaktorsicherheit
- Participants: B. Gmal, W. Weber, W. Heinicke, E.F. Moser

b) Analysis Environment

- Neutron Data Library: 27-group-depletion library, SCALE-4
(27BURNUPLIB)
- Number of Neutron Energy Groups : 27
- Code System: SCALE-4, CSAS25, KENO-Va, 53 batches each one
with 600 neutrons were started.
- Geometry Modeling: 3-D
- Statistical Error: 0.00212 to 0.00380 for one sigma

(6) ENEA, Italy (Analysis Environment was not supplied. This is copied from the Phase IA report.)

a) File Header

- Date: 17 May 1994 (Eigenvalues)
27 May 1994 (Fission Density)
22 Nov. 1994 (Corrections to eigenvalues of
cases 21, 25 and 26.)
- Institute : ENEA, Viale Regina Margherita 125, 00198 Roma,
Italy

- Participant: Francesco Siciliano

b) Analysis Environment (Copied from the Phase IA report)

- Computer Code : MCNP-V3
- Data Library : The following nuclides were processed by the
NJOY code employing the JEF-1 library :

H-1,	O-16,	Cr-24,	Fe-26,	Gd-155,
U-234,	U-235,	U-236,	U-238,	Pu-238,
Pu-239,	Pu-240,	Pu-241,	Pu-242.	

The following nuclides were processed by the THEMIS code employing the JEF-1 library:

Tc-99, Rh-103, Cs-133, Nd-143, Nd-145,
Sm-149, Sm-150, Sm-151, Sm-152, Eu-153.

The original ENDL-85 MCNP library is employed for the following nuclides:

Zr-40, Ag-109, Sn-50, Np-237, Am-241, Am-243.

No. of Groups : (Continuous)

(7) JAERI(1), Japan

a) File Header

- Date: 15 Jan. 1994
- Institute: Japan Atomic Energy Research Institute, Tokai, Ibaraki, Japan.
- Participants: Makoto Takano, Yoshitaka Naito

b) Analysis Environment

- Nuclear Data File : JENDL-3
- Nuclear Data Processing: MGCL-ACE code
- Neutron Energy Groups : 137-group (MGCL library)
- Macroscopic Cross section : The MAIL code of JACS code system was used to produce 137 group macroscopic cross section sets. In the macroscopic cross section sets, all resonance absorbers are self-shielded by employing f-tables.
- Fuel Pin Calculation : The KENO-IV of the JACS code system was used to model the geometry in 3-dimensions for the eigenvalue calculation.

(8) JAERI(2), Japan

a) File Header

- Date: 15 Jan. 1994
- Institute: Japan Atomic Energy Research Institute, Tokai, Ibaraki, Japan.
- Participants: Makoto Takano, Yoshitaka Naito

b) Analysis Environment

- Nuclear Data File : JENDL-3
- Nuclear Data Processing: NJOY (modified)
- Neutron Energy Groups : (Continuous)
- Fuel Pin Calculation : The MCNP-4.2 code was used to model the geometry in 3-dimensions for the eigenvalue calculation.

(9) JINS(1), Japan

a) File Header

- Date: 31 Jan. 1994
- Institute : Japan Institute of Nuclear Safety, Tokyo, Japan.
- Participants: Susumu Mitake (Japan Institute of Nuclear Safety),
Osamu Sato (Mitsubishi Research Institute Inc.)

b) Analysis Environment

- Computer code: SCALE-4 (CSASI)+KENO-Va with SCALE 27-group
cross section library
- Nuclear Data File : ENDF-B/4, B/5
- Neutron cross section library: 27 groups burnup library of
SCALE-4
- Cross section processing: CSASI sequence (with NITAWL-II)

The CSASI sequence (BONAMI, NITAWL, ICE) in SCALE-4 system was used. The 27 groups neutron cross section library of AMPX master interface was changed to AMPX working interface by BONAMI-S code. These AMPX working libraries were processed via NITAWL-II with Nordheim Integral method, then microscopic effective cross section files for each nuclide were created. The microscopic library is converted to macroscopic library by using the ICE-S code. The heterogeneity effect was taken into account using the Dancoff correction factor of square pitch lattice of infinite length cylindrical fuel pins by using NITAWL-II code. Each of the macroscopic effective cross sections for all axial zones were calculated individually by the above processes. Each of the macroscopic cross section files was gathered by the WAX code in SCALE-4 system.

- Method for criticality calculation: 3-dimensional multi-group
Monte Carlo
- No. of histories: 203 generations x 300 histories
- Skipped generations: 3 generations
- Criticality calculation code: KENO-Va
- Omitted cases: None

(10) JINS(2), Japan

a) File Header

- Date: 31 Jan. 1994
- Institute : Japan Institute of Nuclear Safety, Tokyo, Japan.

- Participants: Susumu Mitake (Japan Institute of Nuclear Safety),
Osamu Sato (Mitsubishi Research Institute Inc.)

b) Analysis Environment

- Computer code: KENO-Va with MGCL-JINS 137-group cross section library
- Nuclear Data File : ENDF-B/4
- Neutron cross section library : 137 groups MGCL-JINS library
- Cross section processing: MAIL-PIJ code

The MAIL-PIJ code is used for the cross section processing with MGCL-JINS library. MAIL-PIJ has two methods available to correct heterogeneity effect for resonance self-shielding correction. One method consists in using Dancoff correction factors for square or hexagonal pitch lattices of cylindrical fuel pins, and another is the method based on Tone's formula using the first collision probabilities of fuel and moderators. The Dancoff corrections were used for these calculations. Epithermal total cross sections for moderator regions are assumed to be 1.487/cm. Cladding materials are assumed to be Zircaloy-2, because the cross section of natural Zr is not included in MGCL-JINS.

- Method for criticality calculation: 3-dimensional multi-group Monte Carlo
- No. of histories: 203 generations x 300 histories
- Skipped generations: 3 generations
- Criticality calculation code: KENO-Va
- Omitted cases: Case 2, 3, 6, 7, 10, 11, 15, 16, 19, 20, 23, 24.

For the analysis with MGCL-JINS, because some fission product (FP) nuclide (except Tc-99, Ag-109, Cs-133, Sm-149 and Gd-155) are not included in MGCL-JINS library, only cases not considering FPs were calculated.

(11) PNC, Japan

a) File Header

- Date: 14 Jan. 1994
- Institute : PNC, Tokai, Japan
- Participants: Ichiro Nojiri

b) Analysis Environment

- Computer code: SCALE-4 (CSAS25)

- Nuclear Data File: ENDF-B/4, B/5
- Neutron cross section library: 27 groups burn up library of SCALE-4
- Cross section processing: BONAMI-S, NITAWL-II
- Statistical error for eigenvalues: 0.00154

(12) Tohoku University, Japan

a) File Header

- Date: 06 Feb. 1994
07 Jun. 1994 (Revised)
- Institute: Tohoku University, Sendai, Japan
- Participants :Kenya Suyama, Tomohiko Iwasaki, Naohiro Hirakawa

b) Analysis Environment

- Nuclear Data File: JENDL-3 (U-234 and Pu-238 from ENDF-85 and BMCCS at OK respectively)
- Nuclear Data Processing: NJOY (modified)
- Neutron Energy Groups : (Continuous)
- Fuel Pin Calculation: The MCNP-4.2 code was used to model the geometry in 3-dimension for the eigenvalue calculation.

(13) Toshiba, Japan (See also Appendix 2.2)

a) File Header

- Date: 16 Dec. 1993
- Institute : Toshiba/NEL(Nuclear Engineering Laboratory), Kawasaki, Japan.
- Participants: Yoshihira Ando, Munenari Yamamoto

b) Analysis Environment

(1) Neutron data library

- Data source:

U-235,U-238,Pu-239,Pu-240	: ENDF/B-5
Pu-241,Pu-242	: ENDF/B-4
All other actinides	: JENDL-3
FPS	: mostly ENDF/B-4

- FP chain : 45 explicit FPS + 1 lumped pseudo FP model,
[S.Iijima et al., J.Nucl.Sci.Technol., 19,96 (1982)]

* Mo-95 is not treated as an explicit FP in this FP model, while it has been taken into account as one of the major contributors to the pseudo FP poisoning as described in the above reference.

- * Zr is treated as Zircaloy-2 (including Cr, Fe)
- FP yield data : based on Rider&Meek compilation
[B.F.Rider et al., NEDO-12154-2 (GE) (1977)]

(2) Neutron data processing

CRECT-J

(3) Neutron energy groups

Fast and Epi-thermal (0.6825eV - 10MeV):

68 groups (GAM-type)

Thermal (0 - 0.6825eV):

30 groups (THERMOS-type)

(4) Code system

TGBLA/ALEX

(5) Geometry modeling

Radial : 1D Transport (Cylinder)

Axial : 2D Diffusion (XY)

- Note concerning calculations:

Cell averaged 3 group constants (fast, epi-thermal, thermal) for fuel, end plug and water region through TGBLA with reflective boundary conditions and multiplication factors by 2D diffusion code ALEX using 3 group constants estimated by TGBLA were calculated.

(6) Omitted nuclides etc

Omitted nuclide : Mo-95

Lumped nuclides : Cr, Fe, Zr

(7) Employed convergence limit

1.0E-05 : Outer Iteration

1.0E-05 : Inner Iteration

(8) Other related information

(A) K-Infinity Values by TGBLA Unit Cell Calculation

Geometry Data :

Fuel Radius = 0.412 cm

Cladding Thickness = 0.063 cm

Cell Pitch = 1.33 cm

*K-infinity values shown in figures of Appendix 2.2

(B) Conditions in 2D diffusion calculation

(i) Boundary Condition

X-axis : Vacuum (Albedo = 0.0)

Y-axis : Reflective (Albedo = 1.0)

(ii) No. of Meshes

X-axis : 189

Y-axis : 3

(iii) Mesh Sizes along X-axis

Water (Top): 5.0cm x 4, 1.0cm x 10

(bottom) : 1.0cm x 10, 5.0cm x 4

End Plug : 0.35cm x 5

Fuel (Region 1,2,8,9) : 0.5cm x 10

(Region 3,7) : 1.0cm x 10

(Region 4,6) : 2.0cm x 10

(Region 5) : 4.0cm x 35, 5.7cm x 1, 4.0cm x 35

(iv) Mesh Sizes along Y-axis

All Regions: 1.33cm x 3

(14) CSN, Spain

a) File Header

- Date : 31 Jan. 1994

- Institute : CONSEJO DE SEGURIDAD NUCLEAR (CSN),
MADRID SPAIN

- Participant: Jose M. Conde, M. Recio

b) Analysis Environment

- Nuclear Data File : mainly from ENDF-B/4, some from ENDF-B/5
and JEF-2

- Nuclear Data Processing: NJOY

- Neutron Energy Groups : 70 groups, E4LTJB7

- Analysis Procedure:

The Studsvik-CMS (Core Management System) has been used for this work. 70 Energy Groups were used for the 2-D calculation in CASMO-3, 2 Groups were used for the 3-D calculation in SIMULATE-3. CASMO-3 is a two dimensional transport theory code used to generate the cross sections needed to run SIMULATE-3. Cross sections for the different state-points are functionalized by means of the TABLES code. SIMULATE-3 is a two-group 3-D nodal simulator. The nuclides Mo-95, Tc-99 and Ru-101 are not included in the CASMO library, and hence have not been considered. A 3-D calculation has been performed using an array of single pins infinite in the radial direction. The model contains 85 axial nodes 5 cm high, 6 nodes each to model the top and bottom reflector and 73 to model the active fuel length. The active fuel length is thus reduced to 365 cm in this

model, from the original value of 365.7 cm. It has been verified that the impact of this change on reactivity is negligible (<7 pcm for the worst case), while the code convergence is eased greatly. The axial reflector length is 30 cm on top and bottom. Convergence limit used has been 1E-5 on the eigenvalue.

(15) E. M. Systems, Sweden

a) File Header

- Date : 31 Jan. 1994
23 Mar. 1994 (Corrections)
- Institute : E Mennerdahl Systems
- Participant : Dennis Mennerdahl

b) Analysis Environment

- Computer Code: SCALE-4.0 with 27-group burnup library
- Analysis Procedure:

NITAWL Resonance Treatment. No homogenization of pin cells. Complete criticality modules from SCALE 4.0. Implementation made from full tape version for the Intel 80486-type personal computers. FORTRAN compiler from Silicon Valley Software (SVS). Symmetry was used for the geometry model.

Number of neutrons for the flat (average) burnup was 103 000 from which 3000 neutrons were skipped. Cases treated: 1, 3, 5, 7, 9, 11, 13, 14, 16, 18, 20, 22, 24 and 26.

Number of neutrons for the profiled burnup was 703 000 from which 103 000 neutrons were skipped. Cases treated: 2, 4, 6, 8, 10, 12, 15, 17, 19, 21, 23 and 25.

Atomic densities for Zircaloy and Water were calculated by SCALE and were not taken from the input specifications. (Very small insignificant differences).

(16) PSI, Switzerland

a) File Header

- Date: 28 Jan. 1994
- Institute: Paul Scherrer Institute
- Participants: Peter Grimm, Jean-Marie Paratte

b) Analysis Environment

The results given here were obtained using the ETOBOX and BOXER codes of the ELCOS light water neutronics code package (Refs. 1 and 2) developed at PSI. ETOBOX processes cross section

data in ENDF/B format and produces a cross section library for BOXER. BOXER performs cell and two-dimensional transport and depletion calculations.

Data Library and Processing Methods

The BOXLIB cross section library for BOXER used in the present calculations contains cross sections for 34 actinide nuclides (from Th-232 through Cm-248), 55 fission products considered explicitly, and two pseudo fission products. For some fission products which contribute little to the absorption the resonance cross sections are given for infinite dilution only. The source of cross section data for all nuclides is JEF-1, except for Gd-155, whose cross sections are taken from JENDL-2.

The BOXLIB cross section library contains microscopic neutron cross sections collapsed to 70 groups. The group structure is the 69 group WIMS structure with an extra group between 10 and 15 MeV. However, the upper boundary of the thermal energy range is 1.3 eV instead of 4 eV. P0 and P1 scattering matrices (P2 transport corrected) are given for most isotopes. The weighting spectrum used for the collapsing in ETOBOX is a spectrum calculated in many microgroups for a typical LWR cell in the fast range, a 1/E spectrum at intermediate energies, and a modified Maxwellian spectrum in the thermal range. In the fast range ($E > 907$ eV) the resonance cross sections (both resolved and unresolved resonances) are Doppler broadened and collapsed to groups for three temperatures and 4 values of the dilution cross section. In the resonance range between 1.3 eV and 907 eV (important low energy resonances of plutonium isotopes are included) pointwise lists of Doppler broadened cross sections are produced for three to seven temperatures (depending on the nuclide). For the unresolved resonances these lists are produced for four dilutions. The spacing of the points depends on the variation of the cross sections with lethargy, so that the cross section values between the points can be accurately reconstructed by interpolation. The minimum spacing of the points is $1.0E-5$ lethargy units. Typical numbers of energy points for actinides are 7000 to 8000 between 1.3 and 907 eV.

The thermal scattering matrices for most nuclides are calculated using the free gas model. For the moderator nuclides and especially for hydrogen in water the $S(\alpha, \beta)$ matrices given in the basic cross section files are used.

Cell and Transport Code

In the cell module of BOXER the resonance cross sections are self-shielded by a two region collision probability calculation in 7000 to 8000 lethargy points between 1.3 and 907 eV and by an interpolation versus temperature and equivalent dilution cross section above this value. The fluxes in fine groups and in each zone are calculated by means of an integral transport method in cylindrical geometry. The fission source is assumed to be flat over all zones containing fissile nuclides. The scattering source in each zone can be flat or represented by a polynomial of the radius. In the epithermal range (above 1.3 eV) P1 corrected isotropic scattering is used. In the thermal range P1 anisotropy can be taken into account. The cells are calculated with white boundary conditions or with the outgoing partial current from a previously calculated cell as a fixed source at the periphery. The fundamental mode spectrum (i.e. for $k\text{-eff} = 1$) is determined by a B1 leakage calculation for the homogenized cell in 70 groups with an iterative search for the critical buckling.

The fine group fluxes in the homogeneous (i.e. non-cell) materials are computed by a one-dimensional transport calculation in slab geometry, preserving the mean chord length of each material in the two-dimensional grid. Then the cross sections are collapsed to between 6 and 15 groups. The two-dimensional transport calculations are performed by a transmission probability method which couples the meshes by surface currents. The outgoing current moments are obtained by the solution of the integral transport equation using the following approximations:

- The hemisphere of the flight angles is divided into four quadrants. The surface current in each quadrant is represented by a linear function in space and a first order spherical harmonics expansion in the flight directions.

- The scattering and fission source within the mesh is approximated by a linear function of the spatial variables.
- The scattering anisotropy is taken into account by the P1 matrix.

Calculational Models and Options Used

A cell calculation with white boundary conditions was performed for each of the axial fuel regions. The end plugs were also homogenized with the surrounding water by a cell calculation using the outgoing partial current of the largest axial fuel zone as a fixed source at the boundary. The water reflector was treated as a homogeneous material. One half of the whole configuration (taking into account the symmetry with respect to the axial middle of the fuel rod) was modelled in a one-dimensional transport calculation with homogenized cell cross sections using the transmission probability method described above.

Eight energy groups with upper boundaries of 15 MeV, 821 keV, 907, 16, 4, 1.3, 0.625, and 0.14 eV were used for the calculation of the axial configuration. The mesh widths for this calculation varied between 1 cm near the interfaces of different materials (including different axial fuel zones) and 5 cm in the middle of zone 5, the total number of meshes is 77. A convergence criterion of $1.0E-5$ was employed for the fluxes. Such a tight criterion was found necessary to obtain reasonably converged fluxes, specially for the quite irregular distributions in the cases with axial burnup profile. The adequacy of these approximations was checked by calculations for cases 2 and 19 in which the number of groups and meshes, respectively, were doubled and with a flux convergence criterion of $1.0E-6$. The effects of the mesh width and of the flux convergence were found to be negligible, whereas doubling the energy group number resulted in k-eff changes of 30 to 70 pcm and in region fission density changes of less than 0.4%.

References

1. J.M. Paratte, K. Foskolos, P. Grimm, C. Maeder, "Das PSI-Codesystem ELCOS zur stationaeren Berechnung von Leichtwasserreaktoren", Proceedings of Jahrestagung Kerntechnik, Travemuende p. 59 (1988)
2. P. Grimm, J.M. Paratte, "Validation of the EIR LWR Calculation Methods for Criticality Assessment of Storage Pools", EIR Report 603 (1986)

(17) AEA Technology, U.K.

a) File Header

- Date: 4 Feb. 1994
- Institute: AEA Technology Center Winfrith
- Participant : Jim Gulliford, David Hanlon

b) Analysis Environment

MONKBTHERM version of MONK6B was used in the calculations with the JEF2 DICE Nuclear Data Library provided by Christine Eaton (Generated 06 Aug 1993). NJOY was used to produce 8220 group cross-sections. The technique used is described in AEA Reactor Services Report No. AEA-RS-1246. The geometry was modelled in 3-D. No nuclides were omitted. Two calculations per case were run. Each to a one standard deviation level of approximately 0.15%. The results of the two calculations were averaged to produce a mean k-effective and a standard error of approximately 0.1%. Calculations carried out on SUN Sparc Station IPX workstation "DIMPLE". It was not possible to calculate the fission densities using MONK6BTHERM.

(18) BNFL, UK

a) File Header

- Date: 21 Feb. 1994
2 Sep. 1994 (Revision of eigenvalues and fission density data of cases 2, 6 and 19.)
- Institute: British Nuclear Fuels plc,
Risley, Warrington, England.

- Participant : P. R. Thorne, P. E. Broome

b) Analysis Environment

- Code: MONK6B (operated under SCO UNIX Version 2)
- Data Library: MONK6 8220 point energy with added fission products from JEF-2

- Energy Groups: Continuous Energy
- Geometry Modeling: 3D, reflection plane used
- Nuclides: All nuclides modeled -fission products not part of MONK6 standard library- processed from JEF2
- Convergence: Standard deviation of k-eff not greater than 0.0025

(19&20) Department of Transport, UK

a) File Header

- Date: 11 Feb. 1994
- Institute: United Kingdom Department of Transport
- Participant: Jim Stewart

b) Analysis Environment

- Computer Code: MONK6B (SCO UNIX PC version -SCO7)
- Data Library: MONK7 8220 point energy library (MONK6 library with added fission products)
- Geometry: 3D model
- Convergence: Standard deviation of k-eff approximately 0.0015, error on fission scores: 1-10%.
- Nuclides:

DOT(1): UKNDL options chosen where possible, all nuclides included (Case 19)

DOT(2): Data set adjustment was removed (Case 20)

(see Section 4.1 (2) c) for more detail)

(21&22) ORNL, USA (see also Appendix 2.1)

a) File Header

- Date: 5 Jan 1994
- Institute : Oak Ridge National Laboratory
- Participant: Mark D. DeHart, Cecil V. Parks,
Stephen M. Bowman

b) Analysis Environment

* ORNL(1):

- Neutron Library: SCALE ENDF/B-IV and ENDF/B-V based library 27BURNUPLIB.
- Number of Energy Groups: 27 (14 fast, 13 thermal)
- Description of Code System:

The CSAS25 sequence of SCALE 4.2 invokes BONAMI-S to perform resonance shielding calculations, using the Bondarenko method, followed by NITAWL-II calculations (using the Nordheim Integral treatment) to perform resolved resonance range cross-section processing for any nuclides possessing resonance parameter data. The cross-section working library thus produced is used by the Monte Carlo code KENO.Va to calculate k-effective.

Geometry Modeling: 3-D half-length fuel pin, taking advantage of symmetry at the axial midplane.

Omitted Nuclides: None. All nuclides set forth in problem specifications were modelled.

Statistical Errors: Monte Carlo calculations were based on 500 generations with 1000 neutrons per generation, for a total of 500,000 histories. Statistical uncertainty ranged from 0.0007 to 0.0010.

* ORNL(2)

- Neutron Library: SCALE library 44GROUPNDF5. This library is a broad group collapse of the 238GROUPNDF5 library, collapsed using a "typical" LWR fuel pin spectrum. Both libraries include all 300+ isotopes available in ENDF/B-V, plus ENDF/B-VI oxygen.

- Number of Energy Groups: 44 (22 fast, 22 thermal)

- Description of Code System: the same as ORNL(1)

- Geometry Modeling: the same as ORNL(1)

- Omitted Nuclides: the same as ORNL(1)

4. Results and Discussions

4.1 Multiplication factors

The multiplication factors of all participants are listed in Tables 4.1 and 4.3 showing up to four digits after the decimal point. In these tables, the average and 2σ values are calculated for each case, where the value σ is obtained by;

$$\sigma = \sqrt{\frac{\sum_{i=1}^n (x_i - \bar{x})^2}{n}}$$

n : Number of data, \bar{x} : Average, x_i : i -th data

The values of 2σ vary from 0.0096 to 0.0232. In both 3.6 and 4.5 wt% enriched fuel, the largest 2σ value results for fresh fuel cases, i.e., cases 1 and 14. Further, it is generally observed that the cases with fission products show larger 2σ values than the cases without fission products, except for the 10 GWd/t burnup cases where the fission products have a smaller effect on the multiplication factor than in other higher burnup cases. Similar results were obtained in the Phase IA exercise [1].

The statistical errors in the eigenvalue calculation are also tabulated in Tables 4.2 and 4.4. The tables show that the statistical error varies approximately from 0.001 to 0.005. For choosing the number of neutron histories, two criteria seem to have been used by: some have performed the Monte Carlo calculation until the statistical error was below 0.001 and the others below around 0.003.

(1) Comparison of Phase IA and Phase IIA results

Comparing the results of Phases IA and IIA, an axial leakage effect on the multiplication factor can be observed. In the Phase IA, the benchmark model is a fuel rod cell of infinite length, hence, no neutrons leak from the system. In the Phase IIA, however, the benchmark model reflects the actual axial geometry, and the axial neutron leakage exists. The cases with 3.6wt% for the fresh fuel and burnup of 30 GWd/t after 1 and 5 years of cooling, have been analyzed for both Phases IA and IIA (without axial burnup profile), and the averaged values of the

neutron multiplication factor for all the participants are compared in the following table.

Comparison of Phase IA and Phase IIA results
(Initial Fuel Enrichment = 3.6 wt%)

Burnup (GWd/t)	Fresh	30	30	30	30
Cooling Time (year)	N/A	1	1	5	5
Fission Products	N/A	Yes	No	Yes	No
Case No. of Phase IA	1	2	4	6	8
Case No. of Phase IIA	1	7	9	11	13
Multiplication Factor					
Phase IA	1.4378	1.1402	1.2456	1.1123	1.2284
Phase IIA	1.4335	1.1358	1.2419	1.1062	1.2256
Difference ($\Delta k = IA - IIA$)	0.0043	0.0044	0.0037	0.0061	0.0028

Although the Phases IA and IIA have employed slightly different atomic number densities, the leakage effect in an axially homogeneous assembly is considered to be very small and the Phase IIA results shown in the following sections correspond to the situation neutron leakage from the system is zero or almost negligible (about 0.3% in $\Delta k/k$).

(2) Comparison of results from participants

The multiplication factors calculated by the participants are compared for each benchmark case in Figs. 4.1 and 4.2. These bar charts may be of help to participants to compare their results against those of other participants.

Figures 4.3 and 4.4 as well as Tables 4.5 and 4.6 show the difference (ratio) in percent (%) of multiplication factor of individual cases from the average value of each benchmark case. For example in Fig. 4.3, the bar corresponding to the results from Belgonucleaire for Case 3 shows that the deviation is 1.1 % larger than the average multiplication factor of Case 3.

From Figs. 4.3 and 4.4, the following are observed;

a) Results of Belgonucleaire

The results of cases with fission products differ more than +1.0 % from the average multiplication factor and the difference becomes larger with the burnup value. Here, the case numbers with fission products are 2, 3, 6, 7, 10, 11, 15, 16, 19, 20, 23, and 24.

The multiplication factors are obtained by the ANISN code using cross section data generated by LWR-WIMS code. The library for LWR-WIMS is WIMS1986. In the previous Phase IA benchmark, the LWR-WIMS code with WIMS1986 library was also used by three participants, i.e., Belgonucleaire, AEA(Culcheth) and AEA(Winfrith), and their results showed the same tendency as observed here. In the calculation, no nuclide is omitted. Therefore, it is concluded that the library is the main cause of the difference. The following describes how the WIMS1986 library has been produced.

In the WIMS1986 library [2], the fission products are not self-shielded but integral adjustments have been made by AEA based on the experimental results and operation experience from many LWRs. The integral adjustments have been performed so that the reactivity can be estimated correctly as a function of burnup. As a result of the integral adjustments, the capture cross section of all fission products is reduced to 85 % of the former WIMS1981 library.

b) Results of GRS, JINS(1), PNC, E.M.Systems and ORNL(1)

All the above institutes have employed the SCALE-4 (Version 4.0 or 4.2) code together with 27BURNUPLIB and all results show a deviation about -1.0 % (see Figs. 4.3 and 4.4). The differences do not seem to depend on the presence of fission products.

The 27BURNUPLIB library is generated from ENDF-B/4 but the ORNL has performed another analysis, shown as ORNL(2), by using ENDF-B/5 based library called 44GROUPEP5. These figures show that the ORNL(2) result has come very close to the average values by using the 44GROUPEP5 library. Since there are 5 SCALE-4 users in the Phase IIA benchmark, the replacement of the SCALE-4 library from 27BURNUPLIB to 44GROUPEP5 will reduce the discrepancies of the multiplication factors among participants (see also Appendix 2.1).

c) Results of AEA, BNFL and DOT(1)

The results from these institutes have been obtained by using the MONK-6 code. Although, slightly different libraries named MONK6B and MONK6BTHRM were used, all these results differ by about +1.0 % from the average values.

In order to explain this difference, Mr. Stewart of Department of Transport, UK, has performed a complementary calculation which is shown as DOT(2). The explanation of the difference between DOT(1) and DOT(2) [3] is as follows:

DOT(1) represents the standard method of running MONK, and would be the results obtained by a person carrying out the normal calculation route. The data sets used with DOT(1) have been adjusted to compensate for a small underprediction of reactivity for uranium systems, and a small overprediction for plutonium systems. The intention is that, with this standard data sets, MONK should not underpredict k_{eff} (nor should it overpredict significantly). The data set can be used without adjustment by running the MONK code in a non-standard manner. It would not normally be acceptable to run the code using unadjusted data, but an unpublished keyword allows this to be done, this is how the DOT(2) results were produced. Although the manner of running is not standard for MONK, it may be closer to the methodology employed with other codes. It would not be surprising if the DOT(2) results showed better comparison with other methods than the DOT(1) results, but the DOT(1) results will remain the normal MONK results.

d) Result of CSN

The CSN results show differences of about +1.0 % for the cases with the fission products. The calculation has been performed by the CASMO-3 and SIMULATE-3 codes with E4LTJB7 library, however, the code does not include the fission products of Mo-95, Tc-99 and Ru-101. These omitted nuclides are considered to be the main reason of the difference [4].

In fact, careful investigation has been performed to compare the CSN results both with the average results and with those of participants using codes and methods known to CSN. As a result, it is found that the agreement is quite good in general, but

that CSN solutions are slightly higher for the cases with fission products included. This is due to the fact that three absorbent nuclides are not included in the CASMO library. To demonstrate this, additional calculations have been performed including the absorption of these nuclides by means of another nuclide of similar absorption cross section. The reactivity obtained in these cases has a deviation from other participants' results of a similar size as that for the non-fission product cases.

e) Results of JAERI(1) and JINS(2)

By considering the sources of the differences described under points a) through d), Figure 4.3 has been re-drawn as shown in Fig. 4.5 for the purpose of a more coherent comparison. In this figure, in fact, some results are removed, such as the results by SCALE-4 with 27BURNUPLIB to be represented by ORNL(2), all MONK-6 results but DOT(2) and the results of the cases with the fission products of Belgonucleaire and CSN. All the results but JAERI(1) and JINS(2) show better agreement in this figure.

The JAERI(1) and JINS(2) have the library generated from different neutron data files, namely, JENDL-3 and ENDF-B/4 respectively; both libraries, however, are produced by using the same processing code included in the JACS code system, named MGCL-ACE code. Considering the facts that the libraries of JAERI(1) and (2) methods are both based on JENDL-3 data file, and the ENDF-B/4 results by SCALE have shown the negative deviations, it is considered that the neutron data or cross section processing codes in JACS may produce a positive bias.

After identifying the causes of the discrepancies in this way, the deviation is expected to converge to less than $\pm 0.5 \% \Delta k$.

f) French results (CEA/DRN and CEA/IPSN)

Calculations based on the APOLLO code are in agreement, whether using the SN or Monte Carlo code for the RZ assembly calculation. The CEA results are always consistent with the average k_{eff} within 0.5 %.

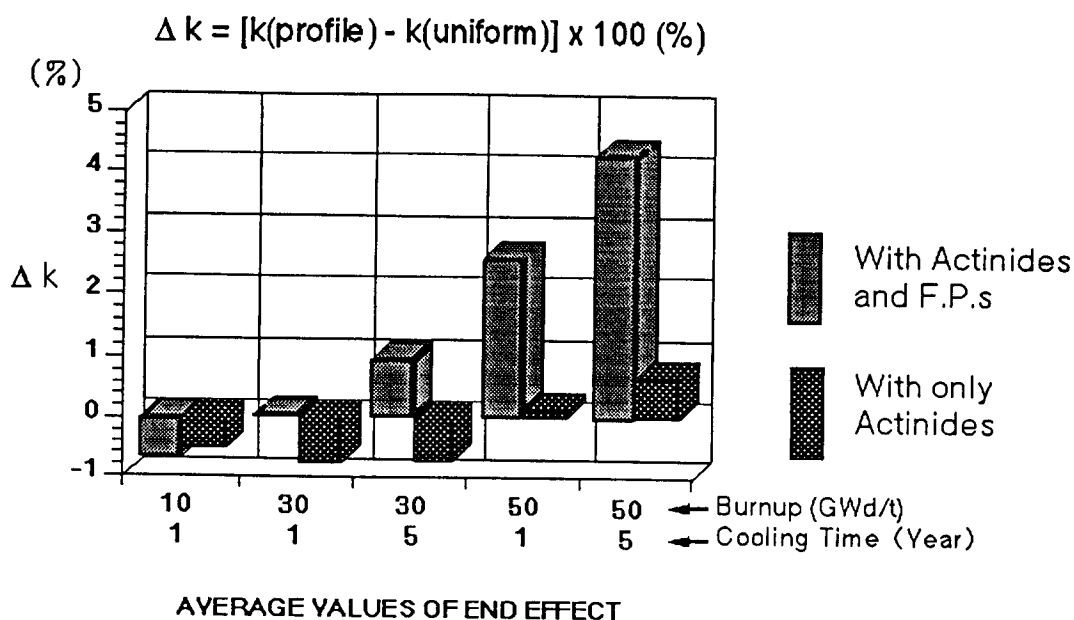
4.2 End Effect

In the report, the end effect is measured by Δk (%), defined as:

$$\Delta k(\%) = [k_1 - k_2] \times 100$$

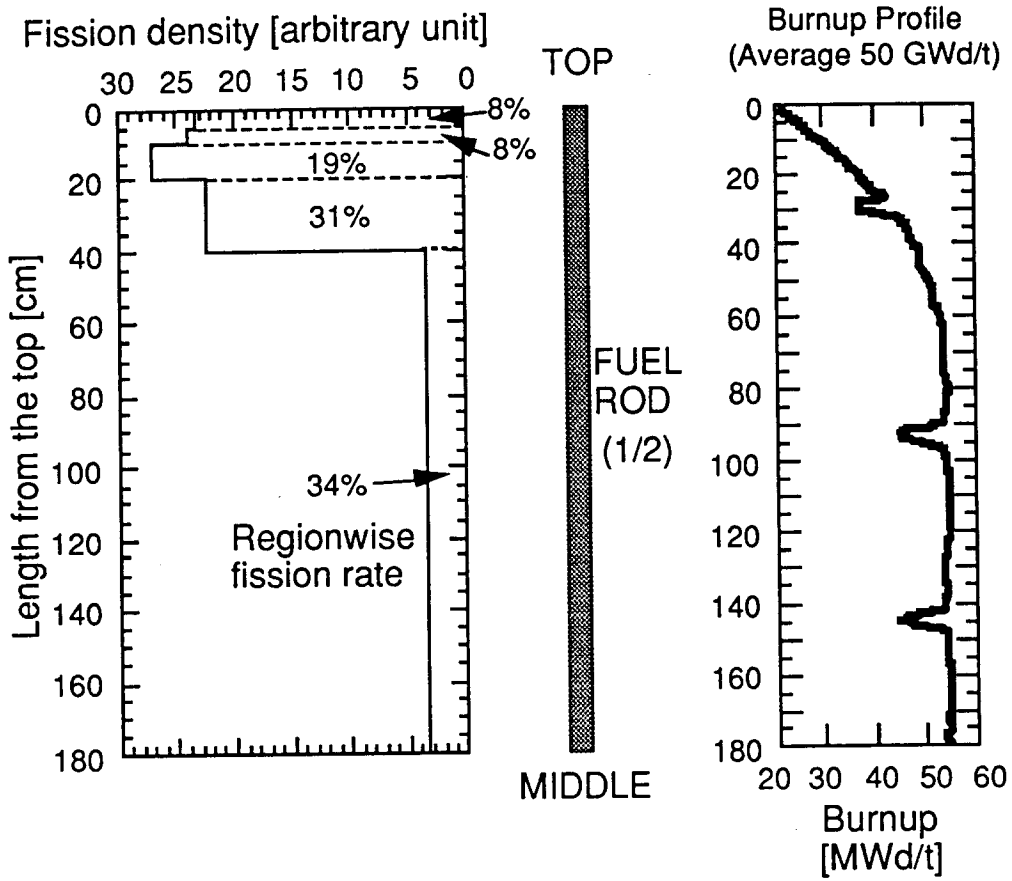
where k_1 and k_2 are the multiplication factors of the cases with and without burnup profile, respectively. When the value of Δk is positive, it means that the use of burnup profile makes the multiplication factor higher than when it is assumed to be axially flat.

The end effect (Δk) is shown in Table 4.7 and Fig. 4.6. In the table, both the average and the 2σ values are also given. The 2σ values are relatively large since the Δk values are the difference of two close values. However, the general tendencies are clearly seen in Fig. 4.6: the end effect becomes larger with burnup and cooling time. The fission products have a positive Δk effect for higher burnup cases since the accumulation of fission products is smaller at both fuel ends than in the central region making the end region relatively more reactive. All of the average Δk values excluding the 4.5 wt% enrichment at burnup 30 GWd/t case, are plotted below. The figure below shows that up to 30 GWd/t, the end effect has been found to be less than 1.0 % Δk but for the 50 GWd/t case, the end effect is more than 4.0 % Δk when both actinides and FPs are taken into account, whereas it remains less than 1.0 % Δk when only actinides are considered. Although these tendencies are believed to be representative in general, the effects of both neutron leakage from the system and axial asymmetry of material composition may make a considerable difference in aspect of the problem. This point will be studied by using a fuel cask model in Phase IIB.



4.3 Fission Density

The fission density data provided by the participants are displayed in Table 4.8. Some of the original data submitted were not fission densities (fissions/cm³·s) but fission rates (fissions/s), therefore these data have been converted into fission densities by dividing by the volumes of the respective region. The adjusted data for the cases 2, 6 and 19 are shown in Table 4.9 and Figs. 4.7 to 4.9. Further, the fission rate of each axial region is shown in Figs. 4.10 to 4.12 in which the sum of fission rates over all regions has been normalized to one. From these figures, it is found that the regions 1 through 4 contribute about 50 % and 70 % of the total fissions for the 30 GWd/t case (case 6) and 50 GWd/t case (case 19), respectively. The figure below shows the relation among the region-wise fission rate, the burnup distribution and the fuel length for the 50 GWd/t case. The figure also shows the importance of the top (end) regions: in the top 40 cm region of the rod almost 70 % of total fission rate occurs. Therefore, adequate modeling and flux convergence at both fuel ends are essential to obtain reliable eigenvalues of highly irradiated spent fuel systems.



Fission density distribution, fuel length and fuel burnup distribution for the case 19 (burnup: 50 GWd/t, initial ^{235}U enrichment: 5 wt%, cooling time: 1 year, both fission products and burnup profile are included)

5. Concluding Remarks

In the Phase IIA benchmark, infinite arrays of spent fuel rods have been analyzed in order to study the effect of the burnup profile on reactivity (end effect). Comparing the 22 submitted results, the following three points need to be remarked:

(1) Comparison of multiplication factors

The 22 results have been compared for each of the 26 cases. The multiplication factors deviate from the average about $\pm 1.0\%$ Δk . It has been found that the deviation is mainly caused by difference in the cross section treatment. After identifying the causes of the discrepancies, the deviation is expected to converge to less than $\pm 0.5\%$ Δk . It should be noted, however, that the convergence of the results does not guarantee the absolute accuracy of the results.

In some criticality codes, the cross section is adjusted intentionally so that the code should never underestimate the multiplication factor. Although this may be justified for this specific application of the code, the user should keep this in mind when comparing results with other codes.

(2) End effect

The end effect becomes prominent as burnup and cooling time increase. The fission products provide a positive component to the end effect since the accumulation of fission products is smaller at both fuel ends than the central region and this makes the end region relatively more reactive.

For irradiation up to 30 GWd/t, the end effect has been found small, i.e. less than 1.0% Δk . However, for the 50 GWd/t case, the end effect is more than 4.0% Δk when both actinides and FPs are taken into account, whereas it remains less than 1.0% Δk when only actinides are considered. Although these tendencies are believed to be representative in general, the effects of both neutron leakage from the system and axial asymmetry of material composition may make a considerable difference in aspect of the problem. This point will be studied in the next benchmark exercise.

(3) Fission density

Although the 40 cm regions at both fuel ends occupy only 22 % of the total fuel volume, it is found that they contribute almost 70 % of total fission rate of the fuel for the 50 GWd/t case. This shows the importance of the end regions for the criticality analysis of highly irradiated spent fuel systems.

All data from the participants and data used to produce tables and figures in the report are available upon request in computer readable form (stored in WINGZ format on Macintosh) for your further analysis.

Acknowledgments

The authors would like to thank the participants in the international benchmark study for their contributions to the work and for their helpful comments in the preparation of this report. They also wish to thank Dr. E. Whitesides of ORNL, the chairman of the group, for conducting the meeting to make it fruitful, Drs. Y. Naito and Dr. Y. Nomura of JAERI for their valuable comments and discussions during the work, and Mr. T. Suzaki of JAERI for his careful reading the manuscript and useful comments. Finally, they would particularly thank Dr. E. Sartori and his staff at the NEA for their contribution in organizing the exercise and arranging the meetings.

References

- [1] M. Takano, "OECD/NEA Burnup Credit Criticality Benchmark - Result of Phase-1A-", NEA/NSC/DOC(93)22, JAERI-M 94-003 (1994).
- [2] Th. Maldague, Private communication.
- [3] J.T.Stewart, Private communication.
- [4] J.M.Conde, Private communication.

Table 2.1 Case Numbers 1 to 26 and Various Parameters

Case Number	1	2	3	4	5	6	7	8	9	10	11	12	13
Initial Fuel Enrichment (w/o)	3.6	3.6	3.6	3.6	3.6	3.6	3.6	3.6	3.6	3.6	3.6	3.6	3.6
Burnup (GWd/t)	Fresh	10	10	10	10	30	30	30	30	30	30	30	30
Cooling Time (years)	N/A	1	1	1	1	1	1	1	1	5	5	5	5
Fission Products	N/A	Yes	Yes	No	No	Yes	Yes	No	No	Yes	Yes	No	No
Burnup Profile	N/A	Yes	No	Yes	No	Yes	No	Yes	No	Yes	No	Yes	No

Case Number	14	15	16	17	18	19	20	21	22	23	24	25	26
Initial Fuel Enrichment (w/o)	4.5	4.5	4.5	4.5	4.5	4.5	4.5	4.5	4.5	4.5	4.5	4.5	4.5
Burnup (GWd/t)	Fresh	30	30	30	30	50	50	50	50	50	50	50	50
Cooling Time (years)	N/A	1	1	1	1	1	1	1	1	5	5	5	5
Fission Products	N/A	Yes	Yes	No	No	Yes	Yes	No	No	Yes	Yes	No	No
Burnup Profile	N/A	Yes	No	Yes	No	Yes	No	Yes	No	Yes	No	Yes	No

Table 3.1 Summary of Participants, Data and Codes for Phase II A Analysis

No.	COUNTRY	INSTITUTE	PARTICIPANT	NUCLEAR		DATA		CALCULATION			REMARKS
				Origin	Library	No of Groups	CODE	MODEL	1σ(%)		
1	Belgium	Belgonucleaire	Maldague		WIMS-1986	69	LWR-WIMS+ANISN	1-D		Collision Probability > 16-group S8 ANISN	
2	France	CEA/DRN	Santamarina	JEF-1	CEA-86	99	APOLLO1+BISTRO	2-D			
3	France	CEA/PSN	Maubert	JEF-1+ENDFB	CFA-86+H.R.	99	APOLLO1+MORET	3-D	-0.1	APOLLO1(Cell) > MORET(Monte Carlo)	
4	Germany	BIS/KE	Schweer	JEF-1	(NJOY)	242	CGM+MORSE-K	3-D	-0.25	Only Zr-90 for Cladding	
5	Germany	GRS	Gmal	ENDF-B/4,B/5	27BURNUPLIB	27	SCALE-4	3-D	-0.3	CSAS25	
6	Italy	ENEA	Siciliano	JEF-1+ENDL-85	(NJOY)	(Continuous)	MCNP-3	3-D	-0.20		
7	Japan	JAERI(1)	Takano	JENDL-3	MGCL	137	JACS(KENO)	3-D	-0.1	MAIL3+KENOIV	
8	Japan	JAERI(2)	Takano	JENDL-3	(NJOY)	(Continuous)	MCNP-4.2	3-D	-0.1		
9	Japan	JINS(1)	Mitake	ENDF-B/4,B/5	27BURNUPLIB	27	SCALE-4	3-D	-0.3	CSASI (NITAWL-II)>KENO-Va	
10	Japan	JINS(2)	Mitake	ENDF-B/4	MGCL+JINS	137	MAIL-Plus-KENO-V.a	3-D	-0.3	Excl. FP cases	
11	Japan	PNC	Nojiri	ENDF-B/4,B/5	27BURNUPLIB	27	SCALE-4	3-D	-0.15	CSAS25	
12	Japan	Tohoku Univ.	Suyama	JENDL-3	(NJOY)	(Continuous)	MCNP-4.2	3-D	-0.1	U-234 < ENDL-85, Pu-238 < BMCCS at Ok	
13	Japan	Toshiba	Ando	JENDL-3,ENDF-B/4,B/5	B-4.5,J-3	95	TGBLA/ALEX	2-D	(1E-5)	Excl. Mo-95, Lumped Cr,Fe,Zr	
14	Spain	CSN	Conde	ENDF-B/4,B/5,JEF-2	E4LTJ87	70	CASMO-3+SIMULATE-3	3-D	(1E-5)	Excl. Mo,Tc,Ru	
15	Sweden	E.M. Systems	Mennerdahl	ENDF-B/4,B/5	27BURNUPLIB	27	SCALE-4.0	3-D	-0.15		
16	Switzerland	PSI	Grimm	JEF-1	BOXLIB	70	BOXER	1-D	(1E-5)	Gd-155 from JENDL-2	
17	U.K.	AEA Technology	Gulliford	JEF-2 DICE	MONKBTHRM	(Continuous)	MONK6B	3-D	-0.1		
18	U.K.	BNFL	Thorne	UKNDL+JEF2	MONK6B	(Continuous)	MONK6B	3-D	-0.25		
19	U.K.	DOT(1)	Stewart	UKNDL+JEF2	MONK6B	(Continuous)	MONK6B	3-D	-0.15	Am,Np,Ag,Eu < UKENDL	
20	U.K.	DOT(2)	Stewart	UKNDL+JEF2	MONK6B	(Continuous)	MONK6B	3-D	-0.15	No Dataset Adjustment	
21	U.S.A.	ORNL(1)	DeHart	ENDF-B/4,B/5	27BURNUPLIB	27	SCALE-4.2	3-D	-0.1	CSAS25	
22	U.S.A.	ORNL(2)	DeHart	ENDF-B/5	44GROUPNDF5	44	SCALE-4.2	3-D	-0.1	CSAS25	

8-Nov-94

Table 4.1 Multiplication Factors from Participants (3.6 w/o Initial Fuel Enrichment)

No.	COUNTRY	INSTITUTE	CODE	1	2	3	4	5	6	7	8	9	10	11	12	13
				Case												
				Burnup (GWd/t)												
				Cooling time (years)												
				Fission Products												
				Burnup Profile												
1	Belgium	Belgonucleaire	LWR-WIMS>ANISN	1.4400	1.3203	1.3271	1.3644	1.3707	1.1534	1.1542	1.2341	1.2434	1.1319	1.1249	1.2173	1.2260
2	France	CEA/DRN	APOLLO-1>BISTRO	1.4373	1.3062	1.3140	1.3629	1.3688	1.1362	1.1320	1.2330	1.2418	1.1152	1.1035	1.2183	1.2250
3	France	CEA/PSN	APOLLO-1>MORET	1.4371	1.3046	1.3139	1.3599	1.3612	1.1334	1.1304	1.2331	1.2391	1.1184	1.0997	1.2175	1.2247
4	Germany	BfS/KE	CGM+MORSE-K	1.4363	1.3068	1.3113	1.3628	1.3694	1.1360	1.1371	1.2322	1.2451	1.1134	1.1056	1.2169	1.2215
5	Germany	GRS	SCALE-4	1.4126	1.2987	1.3009	1.3435	1.3549	1.1239	1.1229	1.2280	1.2312	1.1073	1.0963	1.2092	1.2170
6	Italy	ENEA	MCNP-3	1.4323	1.3053	1.3138	1.3646	1.3692	1.1302	1.1397	1.2306	1.2442	1.1087	1.1087	1.2134	1.2279
7	Japan	JAERI(1)	JACS(KENO)	1.4421	1.3129	1.3203	1.3670	1.3759	1.1482	1.1406	1.2407	1.2453	1.1274	1.1129	1.2254	1.2303
8	Japan	JAERI(2)	MCNP-4.2	1.4303	1.3005	1.3087	1.3580	1.3652	1.1325	1.1328	1.2304	1.2412	1.1128	1.1046	1.2168	1.2247
9	Japan	JINS(1)	SCALE-4	1.4196	1.2904	1.3027	1.3504	1.3509	1.1231	1.1308	1.2249	1.2331	1.1114	1.0952	1.2082	1.2163
10	Japan	JINS(2)	MAIL-PIJ>KENO5.a	1.4472			1.3748	1.3779			1.2487	1.2486			1.2314	1.2366
11	Japan	PNC	SCALE-4	1.4201	1.2945	1.3027	1.3469	1.3529	1.1267	1.1290	1.2260	1.2313	1.1019	1.1009	1.2109	1.2177
12	Japan	Tohoku Univ.	MCNP-4.2	1.4293	1.3041	1.3084	1.3585	1.3612	1.1380	1.1331	1.2363	1.2399	1.1162	1.1030	1.2200	1.2227
13	Japan	Toshiba	TGBLA	1.4337	1.3055	1.3140	1.3608	1.3673	1.1371	1.1357	1.2312	1.2405	1.1167	1.1076	1.2161	1.2237
14	Spain	CSN	CASMO-3>SIMULATE-3	1.4290	1.3080	1.3160	1.3590	1.3651	1.1481	1.1460	1.2350	1.2437	1.1280	1.1174	1.2195	1.2264
15	Sweden	E. M. Systems	SCALE-4	1.4240	1.2979	1.3043	1.3524	1.3592	1.1318	1.1300	1.2258	1.2375	1.1130	1.1017	1.2118	1.2217
16	Swiss.	PSI	BOXER	1.4321	1.3026	1.3110	1.3592	1.3655	1.1356	1.1342	1.2326	1.2419	1.1149	1.1056	1.2170	1.2249
17	U.K.	AEA	MONK6B	1.4496	1.3174	1.3263	1.3765	1.3839	1.1406	1.1451	1.2459	1.2548	1.1239	1.1135	1.2278	1.2356
18	U.K.	BNFL	MONK6B	1.4526	1.3177	1.3224	1.3748	1.3783	1.1401	1.1390	1.2415	1.2492	1.1179	1.1092	1.2197	1.2339
19	U.K.	DOT(1)	MONK6B	1.4541	1.3176	1.3267	1.3728	1.3801	1.1455	1.1419	1.2442	1.2526	1.1220	1.1081	1.2275	1.2351
20	U.K.	DOT(2)	MONK6B	1.4242	1.3008	1.3070	1.3566	1.3630	1.1333	1.1325	1.2328	1.2407	1.1154	1.1024	1.2179	1.2258
21	U.S.A.	ORNL(1)	SCALE-4.2(27G)	1.4206	1.2941	1.3032	1.3500	1.3568	1.1293	1.1298	1.2267	1.2372	1.1080	1.1014	1.2117	1.2200
22	U.S.A.	ORNL(2)	SCALE-4.2(44G)	1.4322	1.3048	1.3109	1.3599	1.3654	1.1322	1.1348	1.2314	1.2405	1.1120	1.1081	1.2137	1.2252
				Case 1	Case 2	Case 3	Case 4	Case 5	Case 6	Case 7	Case 8	Case 9	Case 10	Case 11	Case 12	Case 13
				1.4335	1.3053	1.3126	1.3607	1.3665	1.1360	1.1358	1.2339	1.2419	1.1160	1.1062	1.2176	1.2256
				0.0217	0.0161	0.0159	0.0175	0.0174	0.0155	0.0138	0.0129	0.0119	0.0144	0.0136	0.0119	0.0113

Table 4.2 Statistical Error of Eigenvalue Calculation (One Standard Deviation)

No.	COUNTRY	INSTITUTE	CODE	1	2	3	4	5	6	7	8	9	10	11	12	13
1	Belgium	Belgonucleaire	LWR-WIMS>ANISN	Fresh	10	10	10	10	30	30	30	30	30	30	30	30
2	France	CEA/DRN	(Deterministic Method)	N/A	1	1	1	1	1	1	1	1	1	5	5	5
3	France	CEA/IPSN	APOLLO-1>BISTRO	N/A	Yes	Yes	No	No	Yes	Yes	No	No	Yes	Yes	No	No
4	Germany	BIS/KE	APOLLO-1>MORET	N/A	Yes	No	Yes	No	Yes	No	Yes	No	Yes	No	Yes	No
5	Germany	GRS	CGM+MORSE-K	Standard deviation 0.00100												
6	Italy	ENEA	SCALE-4	Standard deviation from 0.0013 to 0.0025 (less than 0.0009 for Cases 2, 6 and 19)												
7	Japan	JAERI(1)	MCNP-3	0.0027	0.0027	0.0029	0.0028	0.0035	0.0030	0.0022	0.0033	0.0031	0.0028	0.0021	0.0032	0.0033
8	Japan	JAERI(1)	JACS(KENO)	0.0017	0.0017	0.0013	0.0013	0.0013	0.0019	0.0013	0.0020	0.0016	0.0018	0.0016	0.0016	0.0016
9	Japan	JAERI(2)	MCNP-4.2	0.0008	0.0008	0.0008	0.0009	0.0008	0.0009	0.0008	0.0009	0.0008	0.0009	0.0008	0.0009	0.0009
10	Japan	JINS(1)	SCALE-4	0.0008	0.0010	0.0009	0.0009	0.0009	0.0009	0.0011	0.0012	0.0011	0.0012	0.0012	0.0011	0.0011
11	Japan	JINS(2)	MAIL-PIJ>KENO5.a	0.0029	0.0028	0.0027	0.0025	0.0032	0.0029	0.0032	0.0033	0.0030	0.0026	0.0027	0.0025	0.0028
12	Japan	PNC	SCALE-4	0.0033			0.0033	0.0032			0.0026	0.0035			0.0036	0.0030
13	Japan	Tohoku Univ.	SCALE-4	Standard deviation 0.00154 (Typical)												
14	Spain	Toshiba	MCNP-4.2	0.0010	0.0007	0.0008	0.0008	0.0010	0.0008	0.0009	0.0008	0.0010	0.0008	0.0010	0.0008	0.0009
15	Sweden	CSN	TGBLA	(Deterministic Method, Convergence criterion for the outer iteration 1.0e-5, for inner iteration 1.0e-5)												
16	Swiss.	E. M. Systems	CASMO-3>SIMULATE-3	(Deterministic Method, Convergence criterion for the eigenvalue 1.0e-5)												
17	U.K.	PSI	SCALE-4	0.0016	0.0006	0.0014	0.0007	0.0015	0.0007	0.0016	0.0007	0.0016	0.0007	0.0014	0.0007	0.0014
18	U.K.	AEA	BOXER	(Deterministic Method, Convergence criterion for flux 1.0e-5)												
19	U.K.	BNFL	MONK6B	0.0009	0.0010	0.0009	0.0009	0.0009	0.0010	0.0010	0.0009	0.0009	0.0010	0.0010	0.0010	0.0010
20	U.K.	DOT(1)	MONK6B	Standard deviation less than 0.0025												
21	U.S.A.	ORNL(1)	SCALE-4.2(27G)	Standard deviation on keff approximately 0.0025 (0.0008 for selected cases)												
22	U.S.A.	ORNL(2)	SCALE-4.2(44G)	Standard deviation on keff approximately 0.0025 (0.0008 for selected cases)												

7-Nov-94 16:22:22

Table 4.6 Relative Difference from Average k Value (4.5 w/o Initial Fuel Enrichment)
[Calculation/Average - 1.0]*100

No.	COUNTRY	INSTITUTE	CODE	14	15	16	17	18	19	20	21	22	23	24	25	26
				Case												
				Burnup (GWd/t)												
				Cooling time (years)												
				Fission Products												
				Burnup Profile												
1	Belgium	Belgonucleaire	LWR-WIMS>ANISN	0.45	1.24	1.66	0.11	0.09	1.72	1.95	-0.11	-0.03	1.72	1.94	-0.04	-0.09
2	France	CEA/DRN	APOLLO-1>BISTRO	0.33	-0.08	-0.20	0.01	-0.04	-0.13	-0.46	0.01	-0.05	0.04	-0.47	0.13	0.00
3	France	CEA/PSN	APOLLO-1>MORET	-0.38	-0.03	-0.38	0.01	-0.08	-0.27	-0.52	-0.03	-0.48	-0.18	-0.66	-0.18	-0.23
4	Germany	BfS/IKF	CGM+MORSE-K	0.25	-0.04	0.08	-0.09	-0.17	0.18	-0.25	0.17	0.26	-0.03	-0.07	0.55	-0.17
5	Germany	GRS	SCALE-4	-1.38	-1.02	-0.74	-1.24	-0.86	-1.70	-0.85	-0.75	-1.06	-1.66	-0.88	-0.97	-0.47
6	Italy	ENEA	MCNP-3	0.24	-0.38	0.04	-0.28	0.09	0.13	-0.08	0.07	0.02	-0.71	0.03	-0.03	-0.08
7	Japan	JAERI(1)	JACS(KENO)	0.57	0.94	0.64	0.44	0.46	1.01	0.53	0.67	0.51	-0.01	-0.82	0.02	-0.20
8	Japan	JAERI(2)	MCNP-4.2	-0.33	-0.43	-0.25	-0.22	-0.18	-0.24	-0.27	-0.25	-0.03	-0.13	0.04	-0.25	0.12
9	Japan	JINS(1)	SCALE-4	-1.06	-1.34	-1.08	-0.43	-0.46	-1.20	-0.61	-0.42	-0.81	-0.79	-0.31	-0.39	-0.39
10	Japan	JINS(2)	MAIL-PIJ>KENO5.a	0.92			1.36	1.07			1.36	0.75			0.62	0.92
11	Japan	PNC	SCALE-4	-0.87	0.14	-1.11	-0.17	-0.94	-1.28	-0.55	-0.75	-0.37	-0.79	-0.65	-0.45	-0.58
12	Japan	Tohoku Univ.	MCNP-4.2	-0.44	0.12	-0.34	-0.03	-0.31	0.03	-0.35	0.16	-0.28	0.10	-0.24	0.10	-0.24
13	Japan	Toshiba	TGBLA	0.06	0.09	0.10	-0.20	-0.09	0.02	0.06	-0.25	-0.16	0.10	0.15	-0.16	-0.15
14	Spain	CSN	CASMO-3>SIMULATE-3	-0.38	0.83	0.80	-0.08	-0.03	1.44	1.22	0.16	0.11	1.63	1.27	0.26	0.09
15	Sweden	E. M. Systems	SCALE-4	-0.76	-0.29	-0.49	-0.50	-0.54	-0.28	-0.27	-0.26	-0.20	-0.16	-0.41	-0.28	-0.35
16	Swiss.	PSI	BOXER	-0.11	-0.13	-0.12	-0.17	-0.08	-0.08	-0.05	-0.08	0.05	-0.08	-0.04	-0.01	0.07
17	U.K.	AEA	MONK6B	1.59	0.90	0.82	0.94	0.94	0.81	0.71	0.57	1.01	0.69	0.76	0.51	0.92
18	U.K.	BNFL	MONK6B	1.29	0.37	0.63	0.86	0.91	0.18	0.25	0.25	0.43	-0.15	0.62	0.28	0.45
19	U.K.	DOT(1)	MONK6B	1.36	0.44	0.79	0.68	0.78	0.52	0.20	0.77	0.77	0.79	0.25	1.00	0.73
20	U.K.	DOT(2)	MONK6B	-0.64	-0.56	-0.29	-0.18	0.06	-0.12	-0.27	-0.12	0.07	-0.09	-0.27	0.30	0.10
21	U.S.A.	ORNL(1)	SCALE-4.2(27G)	-0.72	-0.66	-0.48	-0.70	-0.50	-0.64	-0.39	-0.70	-0.31	-0.37	-0.20	-0.68	-0.40
22	U.S.A.	ORNL(2)	SCALE-4.2(44G)	0.01	-0.14	-0.09	-0.10	-0.10	-0.10	0.00	-0.48	-0.21	0.08	-0.05	-0.34	-0.07

Table 4.8 Fission Density Data from Participants

No	COUNTRY	INSTITUTE	CASE 2					CASE 6					CASE 19				
			3.6w/o, Burnup(10GWd/t), C.time(1y), F.P.(Yes)					3.6w/o, Burnup(30GWd/t), C.time(1y), F.P.(Yes)					4.5w/o, Burnup(50GWd/t), C.time(1y), F.P.(Yes)				
			Reg.-1	Reg.-2	Reg.-3	Reg.-4	Reg.-5	Reg.-1	Reg.-2	Reg.-3	Reg.-4	Reg.-5	Reg.-1	Reg.-2	Reg.-3	Reg.-4	Reg.-5
1	Belgium	Belgonucleaire	0.0200	0.0220	0.0600	0.1580	1.2520	0.1050	0.1130	0.2740	0.5550	1.1750	0.2430	0.2500	0.5670	0.9720	1.0870
2	France	CEA/DRN	0.0142	0.0161	0.0434	0.1117	0.8146	0.0549	0.0588	0.1412	0.2736	0.4715	0.0857	0.0883	0.1974	0.3247	0.3039
3	France	CEA/PSN	0.0163	0.0179	0.0506	0.1264	0.7886	0.0561	0.0603	0.1393	0.2739	0.4703	0.0794	0.0862	0.1946	0.3278	0.3119
4	Germany	BfS/IKF	0.0143	0.0165	0.0428	0.1105	0.8159	0.0515	0.0535	0.1284	0.2480	0.5186	0.0857	0.0850	0.1919	0.3216	0.3158
5	Germany	GRS	0.1296	0.1540	0.2168	0.2192	0.2804	0.1533	0.1685	0.2280	0.2630	0.1872	0.2378	0.2357	0.2633	0.2049	0.0583
6	Italy	ENEA	0.0701	0.1011	0.1860	0.2638	0.3789	0.1420	0.1658	0.2645	0.3188	0.1089	0.1949	0.2306	0.3029	0.2493	0.0223
7	Japan	JAERI(1)															
8	Japan	JAERI(2)	0.1247	0.1382	0.1856	0.2463	0.3052	0.2046	0.2134	0.2564	0.2560	0.0696	0.2415	0.2371	0.2665	0.2247	0.0302
9	Japan	JINS(1)	0.1372	0.1584	0.1945	0.2451	0.2647	0.1872	0.2044	0.2381	0.2406	0.1298	0.2253	0.2414	0.2590	0.2293	0.0449
10	Japan	JINS(2)															
11	Japan	PNC	0.1283	0.1383	0.1941	0.2414	0.2978	0.2033	0.2166	0.2574	0.2479	0.0749	0.2290	0.2380	0.2684	0.2225	0.0421
12	Japan	Tohoku Univ.															
13	Japan	Toshiba	0.1158	0.1354	0.1867	0.2504	0.3118	0.1974	0.2167	0.2634	0.2594	0.0633	0.2285	0.2409	0.2726	0.2280	0.0300
14	Spain	CSN	0.1236	0.1404	0.1856	0.2429	0.3076	0.2081	0.2216	0.2581	0.2486	0.0636	0.2420	0.2465	0.2663	0.2164	0.0289
15	Sweden	E. M. Systems	0.1321	0.1465	0.1907	0.2486	0.2821	0.2066	0.2162	0.2566	0.2530	0.0676	0.2376	0.2386	0.2679	0.2227	0.0332
16	Swiss.	PSI	0.1212	0.1384	0.1881	0.2486	0.3037	0.2019	0.2172	0.2614	0.2555	0.0640	0.2331	0.2413	0.2706	0.2248	0.0302
17	U.K.	AEA															
18	U.K.	BNFL	0.1292	0.1382	0.1845	0.2465	0.3016	0.2010	0.2123	0.2531	0.2435	0.0902	0.2398	0.2431	0.2645	0.2149	0.0377
19	U.K.	DOT(1)	0.1259	0.1402	0.1904	0.2477	0.2958	0.2093	0.2196	0.2636	0.2529	0.0546	0.2456	0.2415	0.2670	0.2169	0.0289
20	U.K.	DOT(2)	0.1208	0.1368	0.1908	0.2517	0.2999	0.2066	0.2135	0.2616	0.2501	0.0682	0.2375	0.2409	0.2683	0.2239	0.0294
21	U.S.A.	ORNL(1)	0.1267	0.1436	0.1929	0.2511	0.2857	0.2068	0.2127	0.2557	0.2542	0.0707	0.2280	0.2352	0.2669	0.2330	0.0368
22	U.S.A.	ORNL(2)	0.1178	0.1317	0.1786	0.2467	0.3252	0.1944	0.2028	0.2501	0.2529	0.0998	0.2337	0.2356	0.2647	0.2291	0.0369

8-Nov-94 16:27:59

Table 4.9 Adjusted Fission Densities (Data of Belgonucleaire, CEA/DRN, CEA/IPSN and Bfs/IKE are Volume Averaged)

No	COUNTRY	INSTITUTE	CASE 2					CASE 6					CASE 19				
			3.6w/o, Burnup(10GWd/t), C.time(1y), F.P.(Yes)					3.6w/o, Burnup(30GWd/t), C.time(1y), F.P.(Yes)					4.5w/o, Burnup(50GWd/t), C.time(1y), F.P.(Yes)				
			Reg.-1	Reg.-2	Reg.-3	Reg.-4	Reg.-5	Reg.-1	Reg.-2	Reg.-3	Reg.-4	Reg.-5	Reg.-1	Reg.-2	Reg.-3	Reg.-4	Reg.-5
1	Belgium	Belgonucleaire	0.1288	0.1416	0.1931	0.2543	0.2821	0.1963	0.2113	0.2561	0.2594	0.0769	0.2298	0.2364	0.2681	0.2298	0.0360
2	France	CEA/DRN	0.1310	0.1485	0.2001	0.2575	0.2629	0.2039	0.2184	0.2623	0.2541	0.0613	0.2351	0.2422	0.2708	0.2227	0.0292
3	France	CEA/IPSN	0.1373	0.1508	0.2131	0.2662	0.2325	0.2070	0.2225	0.2570	0.2527	0.0607	0.2232	0.2423	0.2735	0.2303	0.0307
4	Germany	Bfs/IKE	0.1319	0.1522	0.1974	0.2549	0.2635	0.2065	0.2146	0.2575	0.2486	0.0728	0.2393	0.2374	0.2679	0.2245	0.0309
5	Germany	GRS	0.1296	0.1540	0.2168	0.2192	0.2804	0.1533	0.1685	0.2280	0.2630	0.1872	0.2378	0.2357	0.2633	0.2049	0.0583
6	Italy	ENEA	0.0701	0.1011	0.1860	0.2638	0.3789	0.1420	0.1658	0.2645	0.3188	0.1089	0.1949	0.2306	0.3029	0.2493	0.0223
7	Japan	JAERI(1)															
8	Japan	JAERI(2)	0.1247	0.1382	0.1856	0.2463	0.3052	0.2046	0.2134	0.2564	0.2560	0.0696	0.2415	0.2371	0.2665	0.2247	0.0302
9	Japan	JINS(1)	0.1372	0.1584	0.1945	0.2451	0.2647	0.1872	0.2044	0.2381	0.2406	0.1298	0.2253	0.2414	0.2590	0.2293	0.0449
10	Japan	JINS(2)															
11	Japan	PNC	0.1283	0.1383	0.1941	0.2414	0.2978	0.2033	0.2166	0.2574	0.2479	0.0749	0.2290	0.2380	0.2684	0.2225	0.0421
12	Japan	Tohoku Univ.															
13	Japan	Toshiba	0.1158	0.1354	0.1867	0.2504	0.3118	0.1974	0.2167	0.2634	0.2594	0.0633	0.2285	0.2409	0.2726	0.2280	0.0300
14	Spain	CSN	0.1236	0.1404	0.1856	0.2429	0.3076	0.2081	0.2216	0.2581	0.2486	0.0636	0.2420	0.2465	0.2663	0.2164	0.0289
15	Sweden	E. M. Systems	0.1321	0.1465	0.1907	0.2486	0.2821	0.2066	0.2162	0.2566	0.2530	0.0676	0.2376	0.2386	0.2679	0.2227	0.0332
16	Swiss.	PSI	0.1212	0.1384	0.1881	0.2486	0.3037	0.2019	0.2172	0.2614	0.2555	0.0640	0.2331	0.2413	0.2706	0.2248	0.0302
17	U.K.	AEA															
18	U.K.	BNFL	0.1292	0.1382	0.1845	0.2465	0.3016	0.2010	0.2123	0.2531	0.2435	0.0902	0.2398	0.2431	0.2645	0.2149	0.0377
19	U.K.	DOT(1)	0.1259	0.1402	0.1904	0.2477	0.2958	0.2093	0.2196	0.2636	0.2529	0.0546	0.2456	0.2415	0.2670	0.2169	0.0289
20	U.K.	DOT(2)	0.1208	0.1368	0.1908	0.2517	0.2999	0.2066	0.2135	0.2616	0.2501	0.0682	0.2375	0.2409	0.2683	0.2239	0.0294
21	U.S.A.	ORNL(1)	0.1267	0.1436	0.1929	0.2511	0.2857	0.2068	0.2127	0.2557	0.2542	0.0707	0.2280	0.2352	0.2669	0.2330	0.0368
22	U.S.A.	ORNL(2)	0.1178	0.1317	0.1786	0.2467	0.3252	0.1944	0.2028	0.2501	0.2529	0.0998	0.2337	0.2356	0.2647	0.2291	0.0369
		Average	0.1240	0.1408	0.1927	0.2490	0.2934	0.1964	0.2093	0.2556	0.2562	0.0824	0.2323	0.2391	0.2694	0.2249	0.0343
		2* sigma	0.0286	0.0238	0.0186	0.0193	0.0598	0.0364	0.0314	0.0179	0.0322	0.0631	0.0218	0.0073	0.0175	0.0177	0.0157

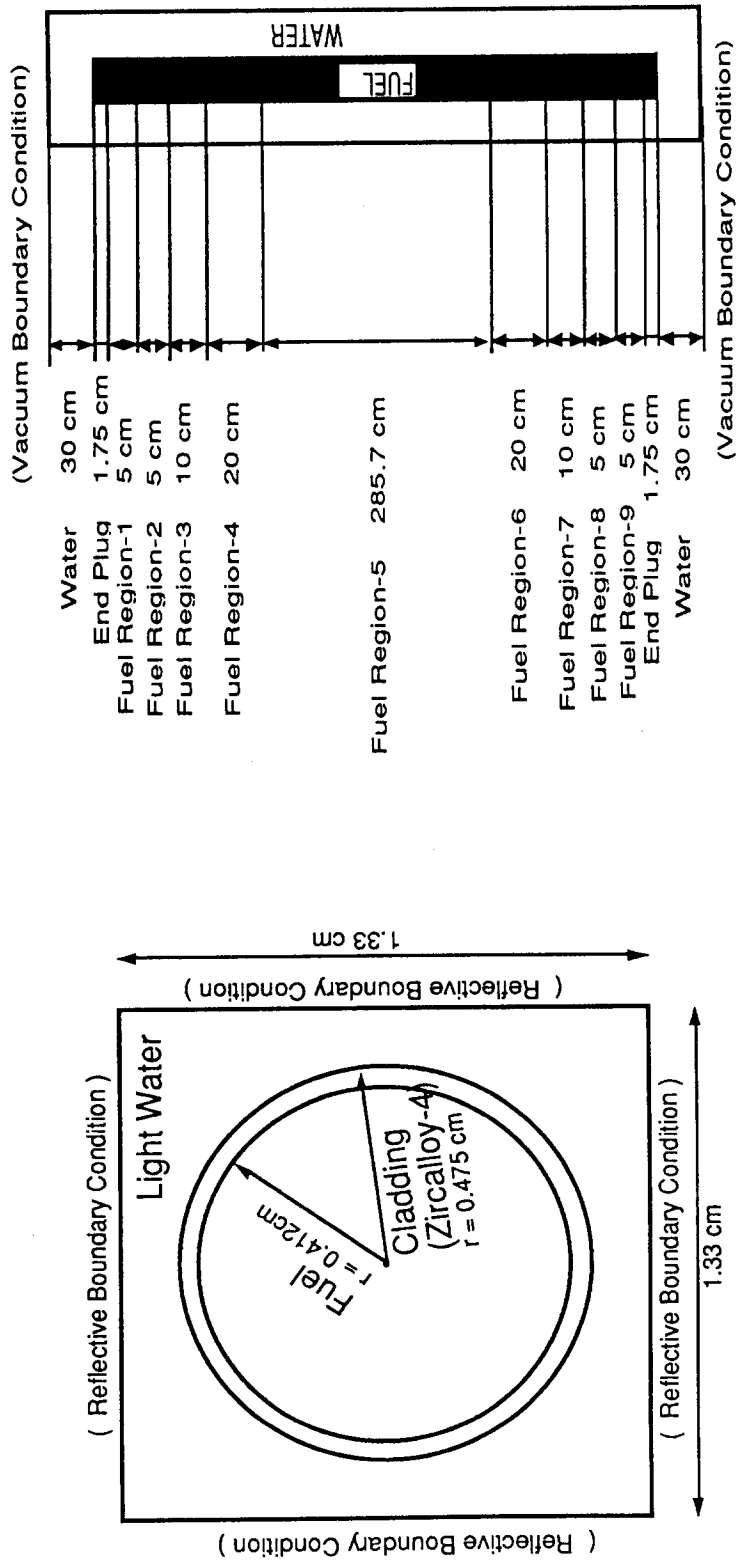


Fig. 2.1 Geometrical Model of Benchmark Problem

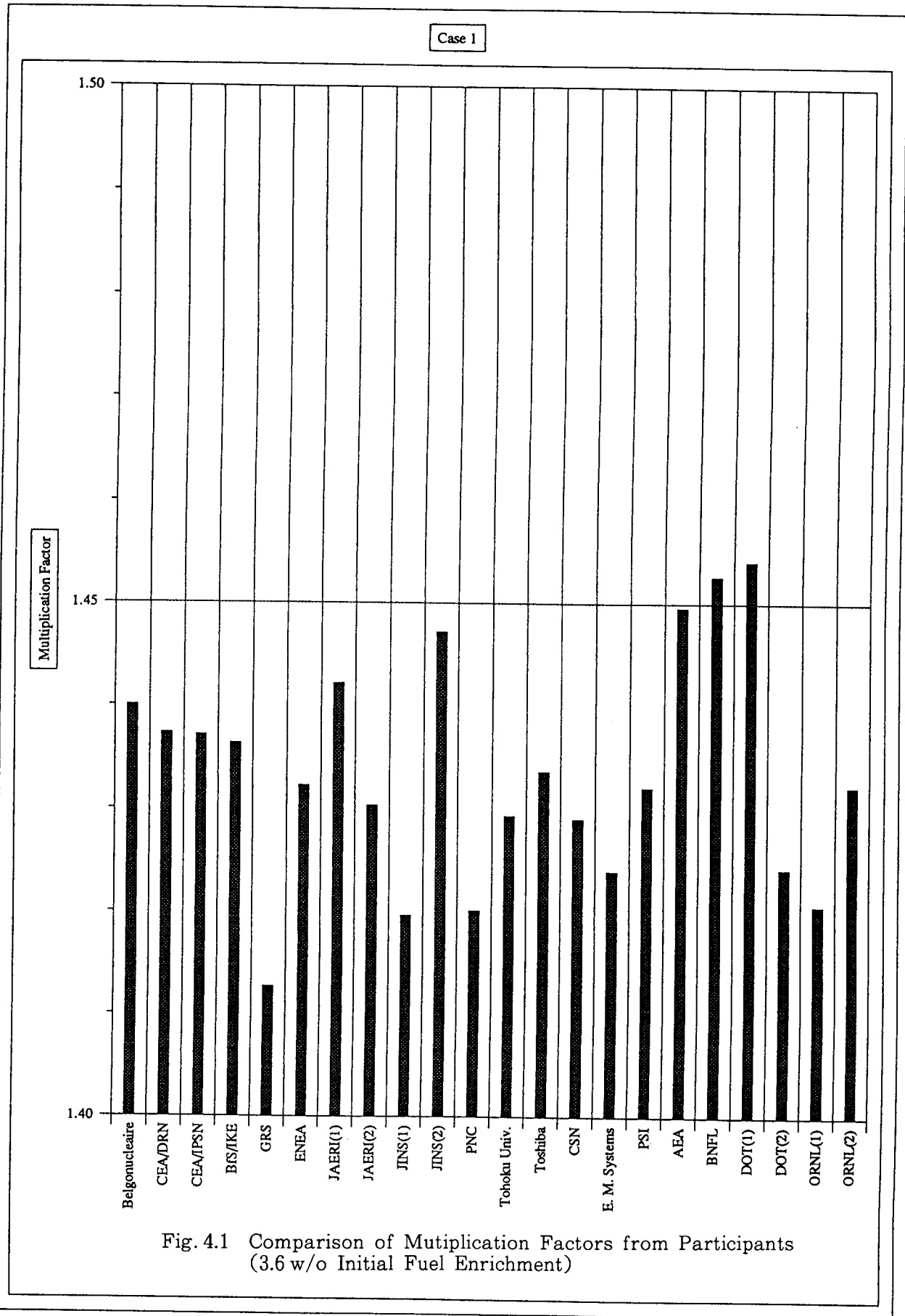


Fig. 4.1 Comparison of Multiplication Factors from Participants (3.6 w/o Initial Fuel Enrichment)

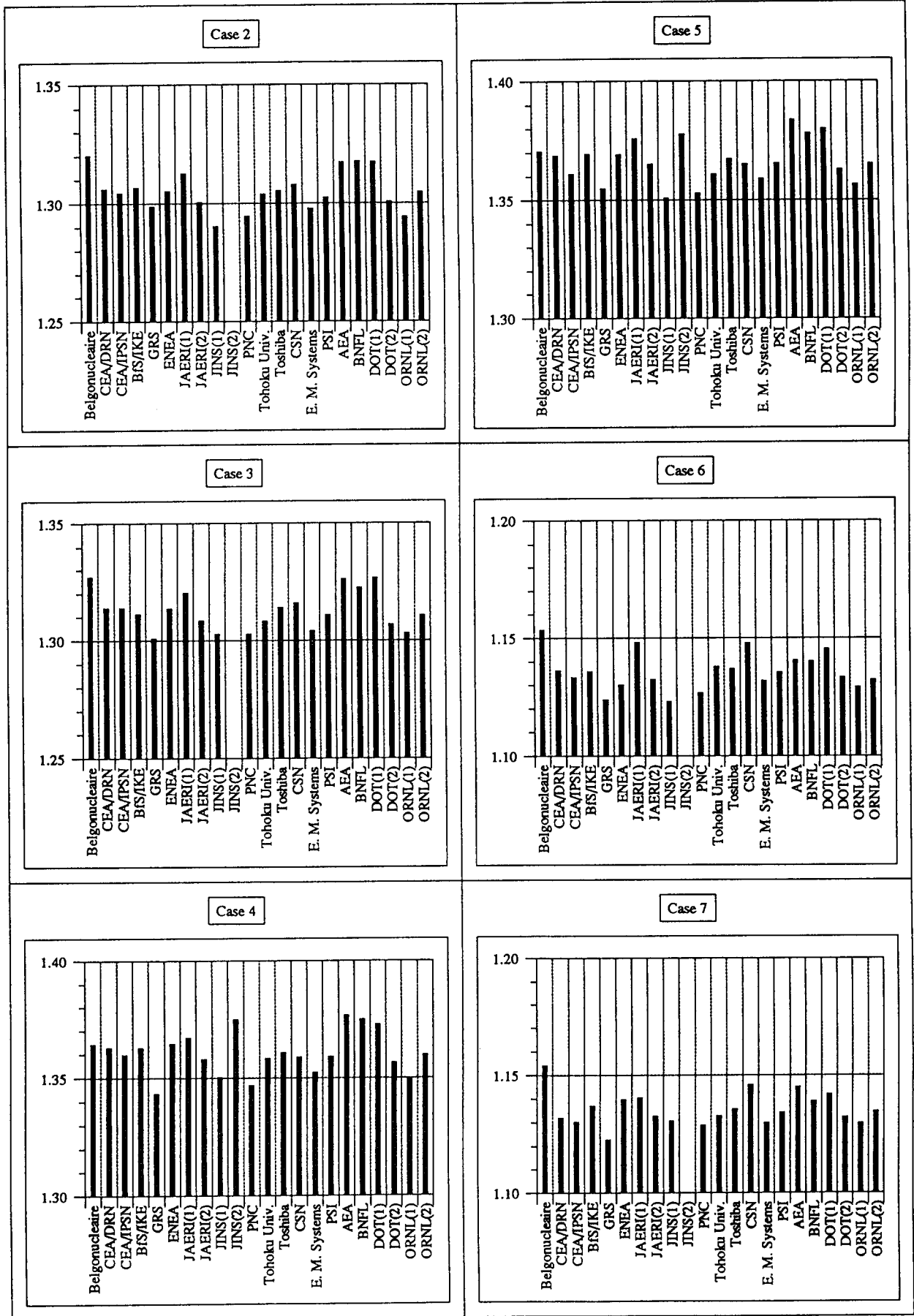


Fig. 4.1 (Continued)

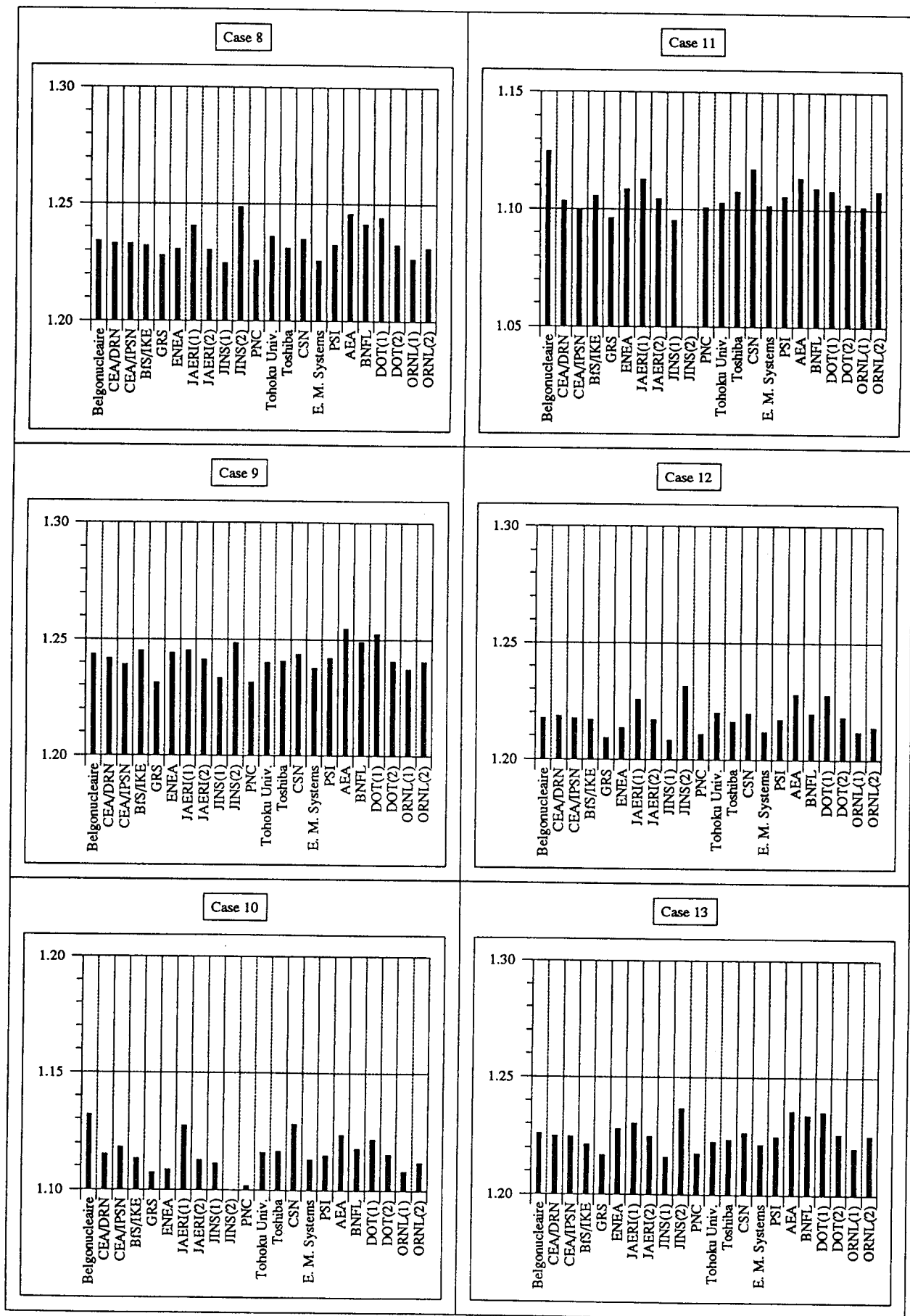
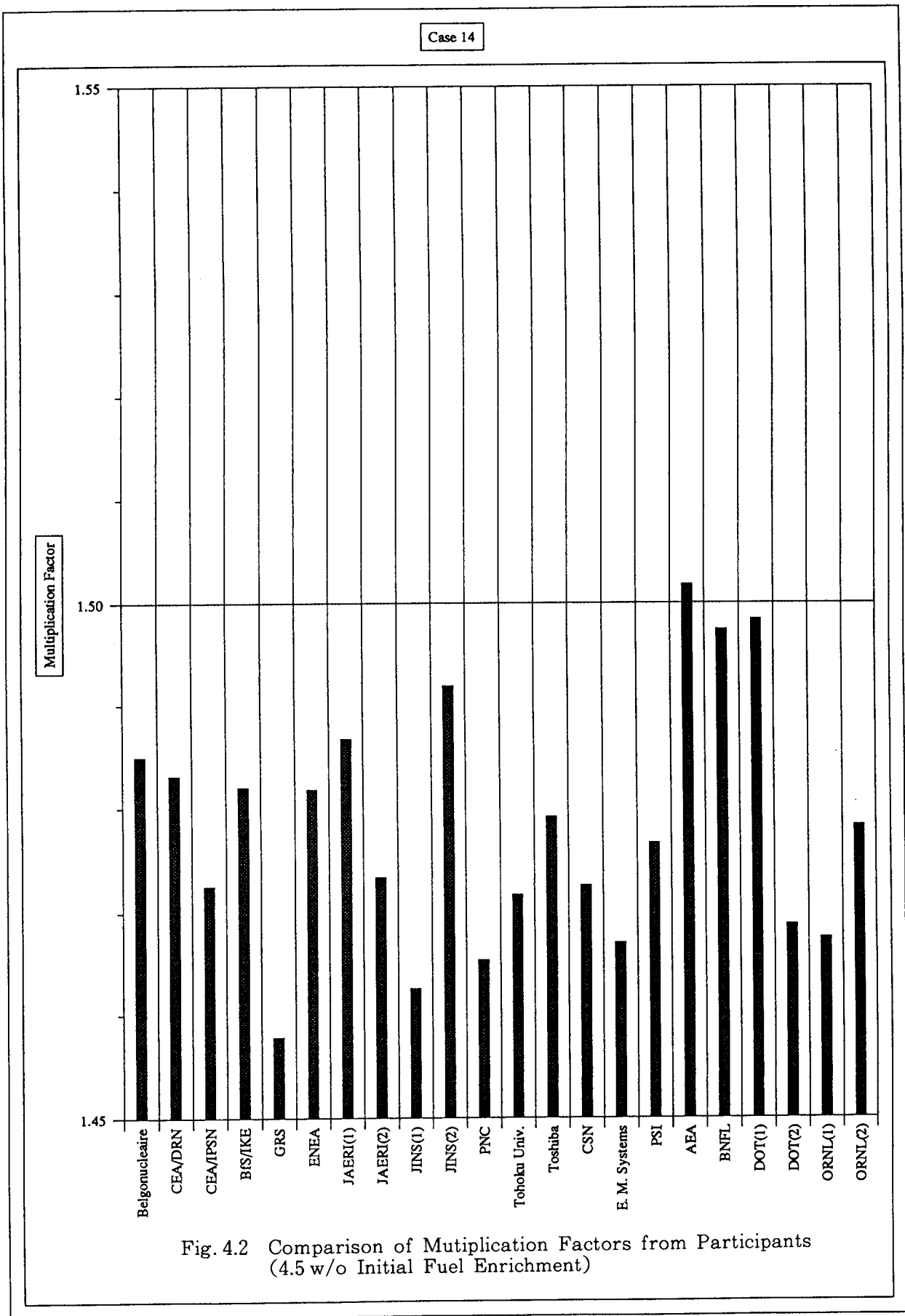


Fig. 4.1 (Continued)



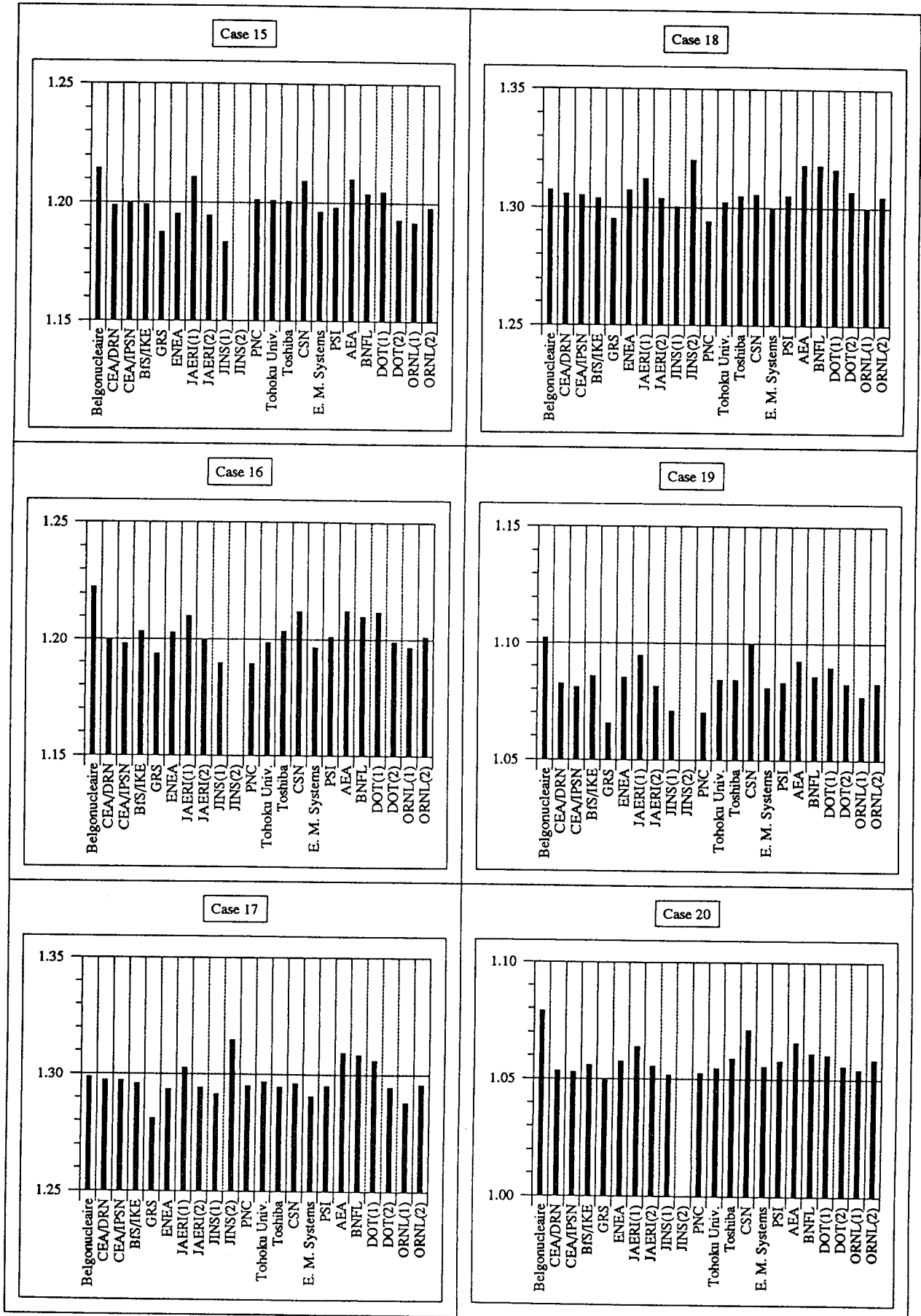


Fig. 4.2 (Continued)

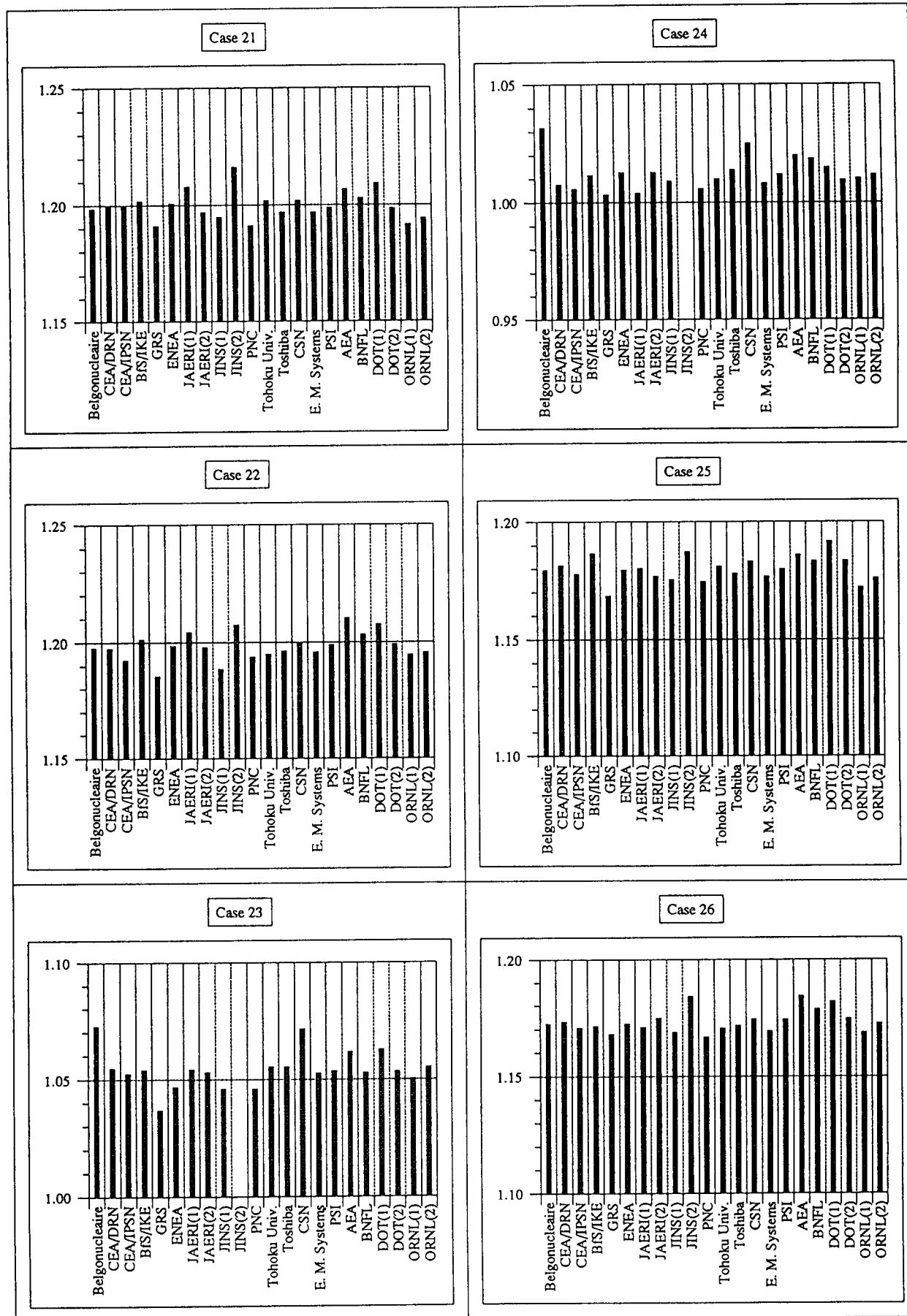
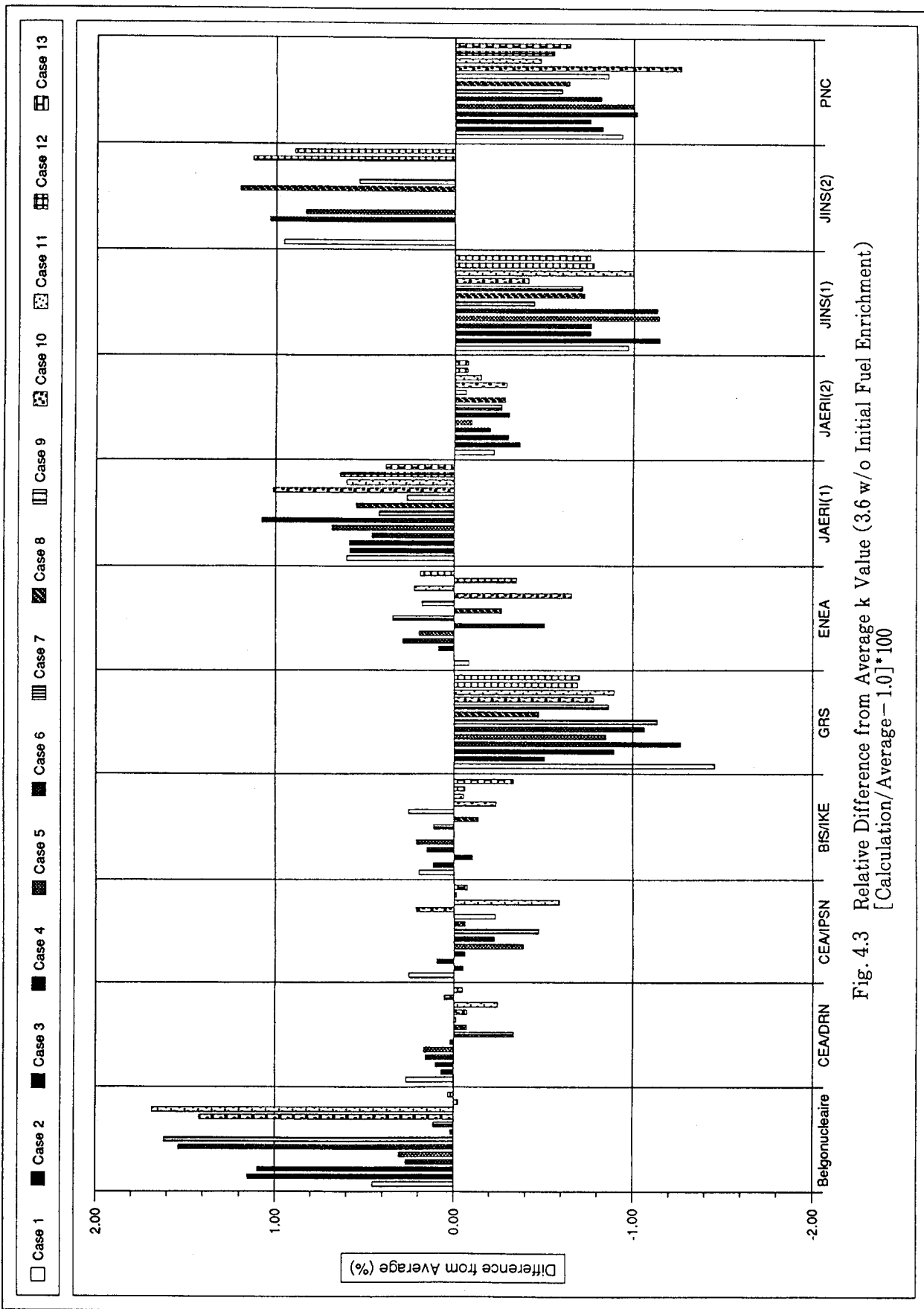


Fig. 4.2 (Continued)



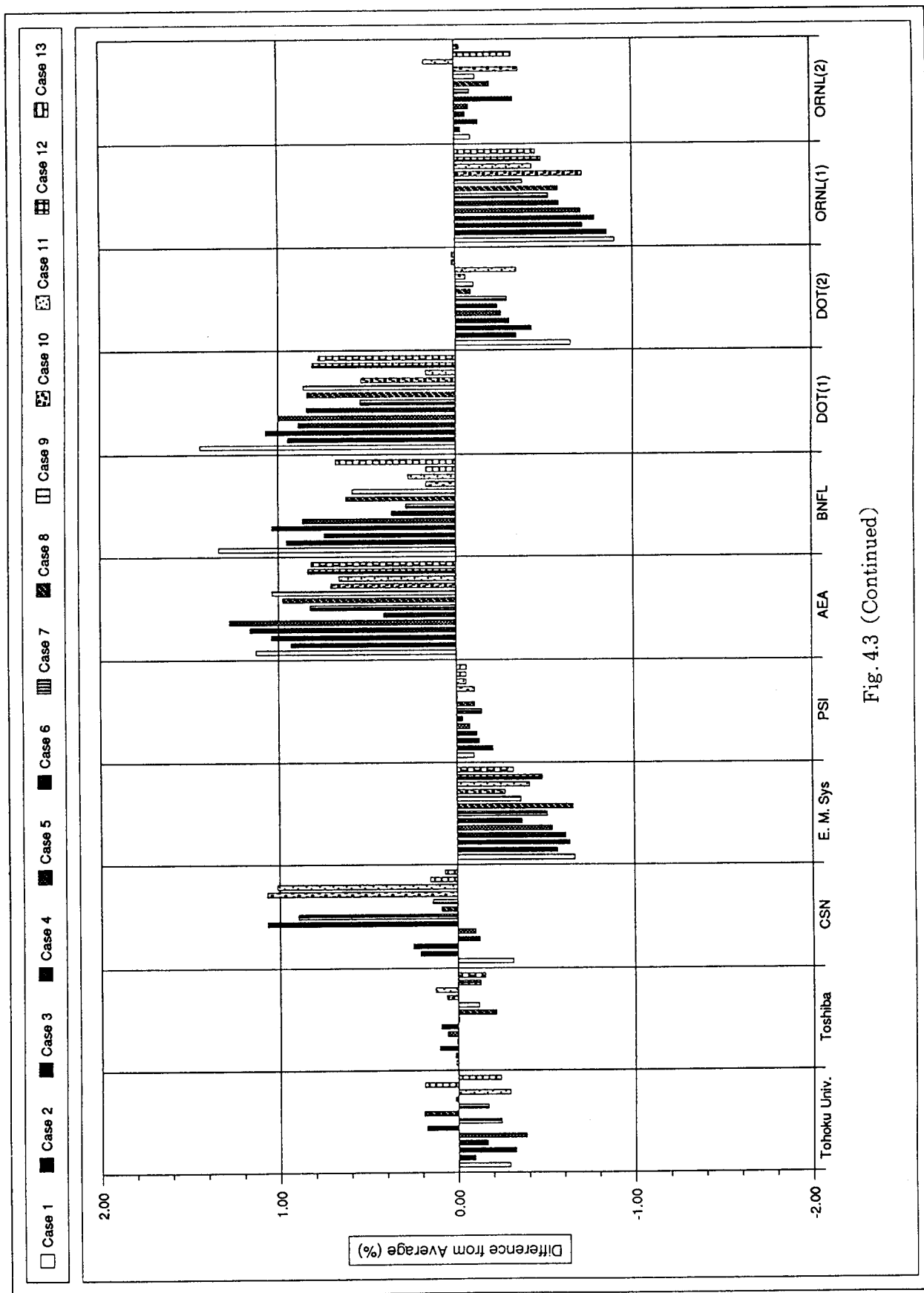


Fig. 4.3 (Continued)

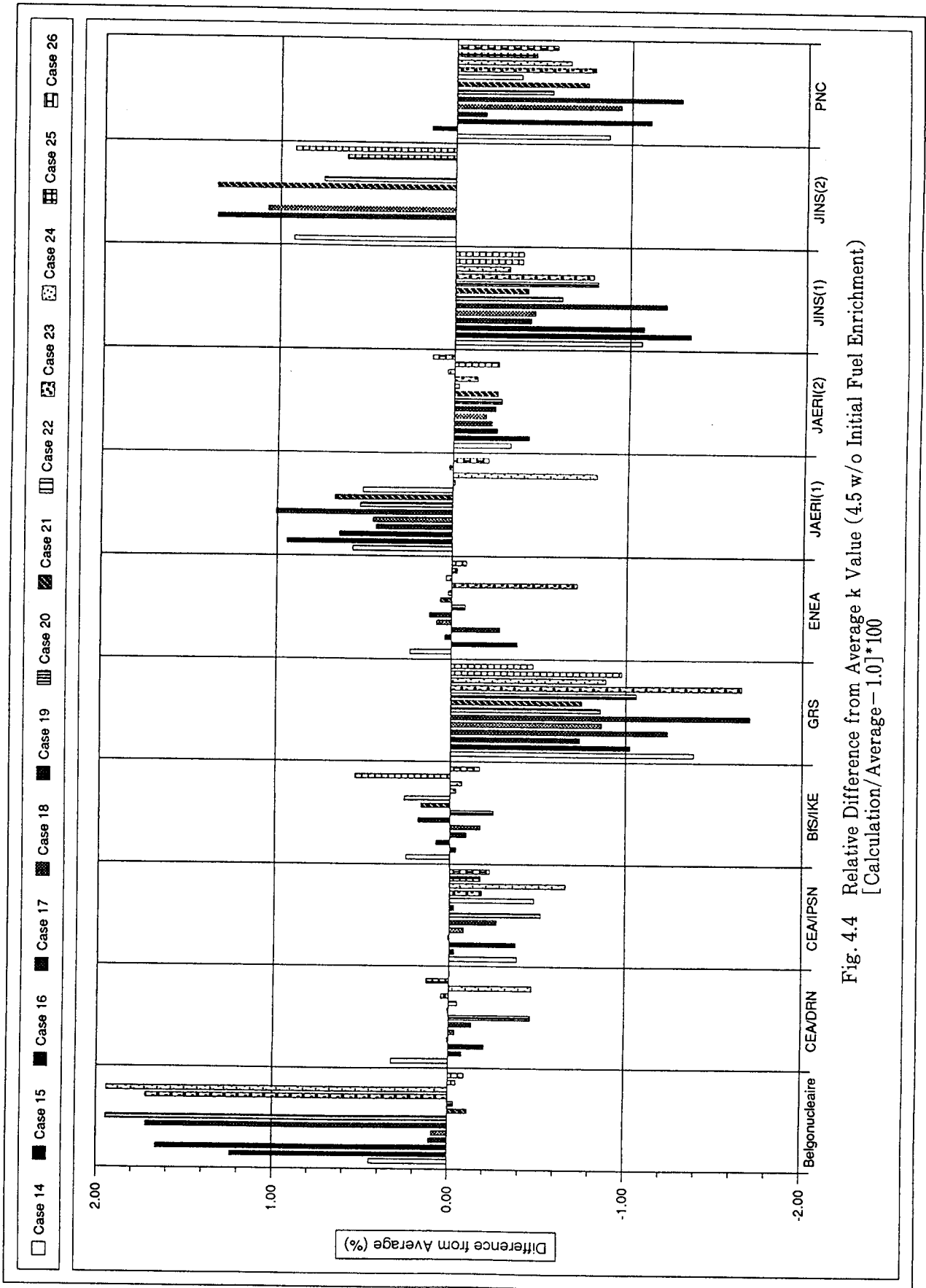


Fig. 4.4 Relative Difference from Average k Value (4.5 w/o Initial Fuel Enrichment)
 [Calculation/Average - 1.0] * 100

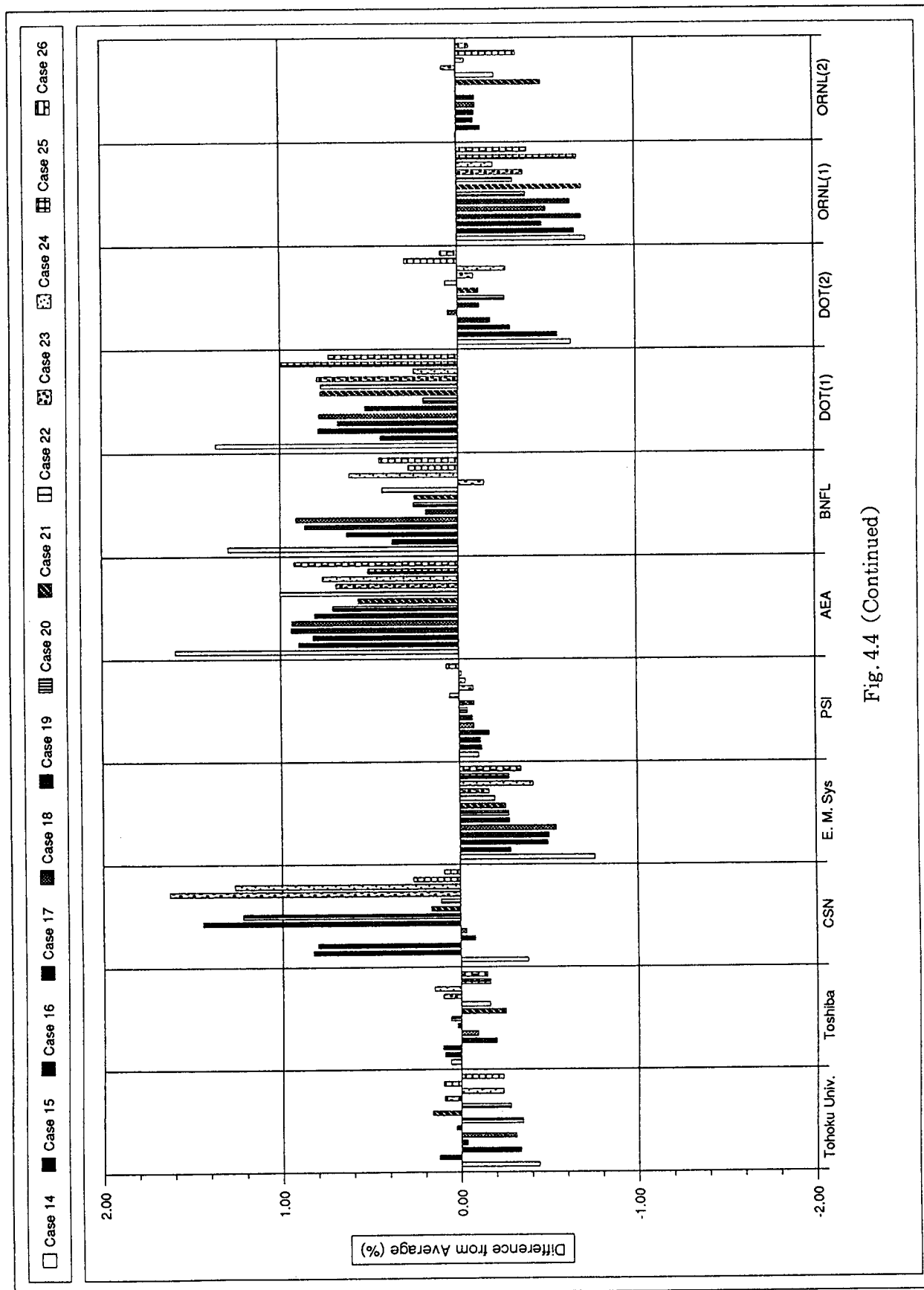


Fig. 4.4 (Continued)

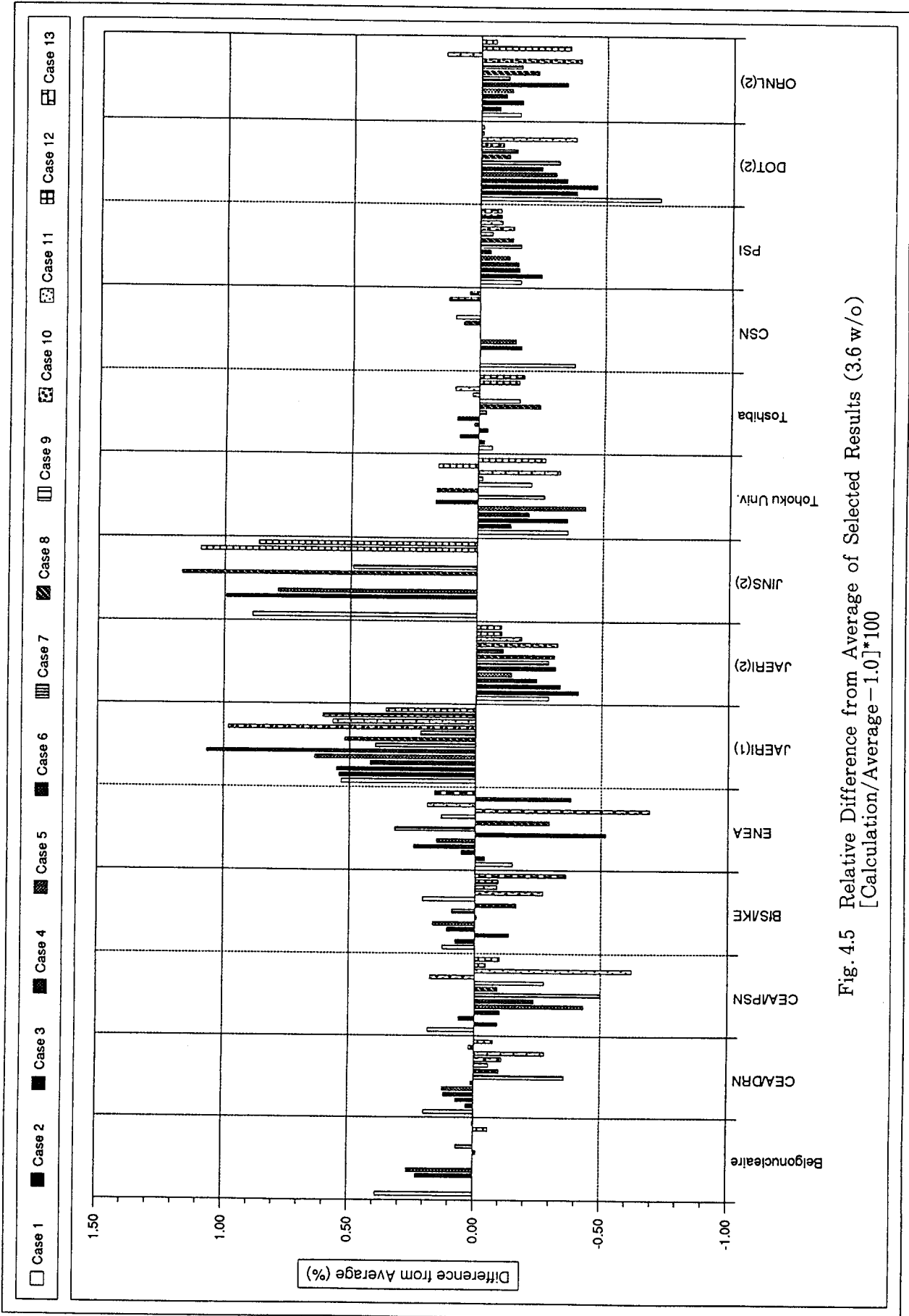


Fig. 4.5 Relative Difference from Average of Selected Results (3.6 w/o)
 [Calculation/Average - 1.0]*100

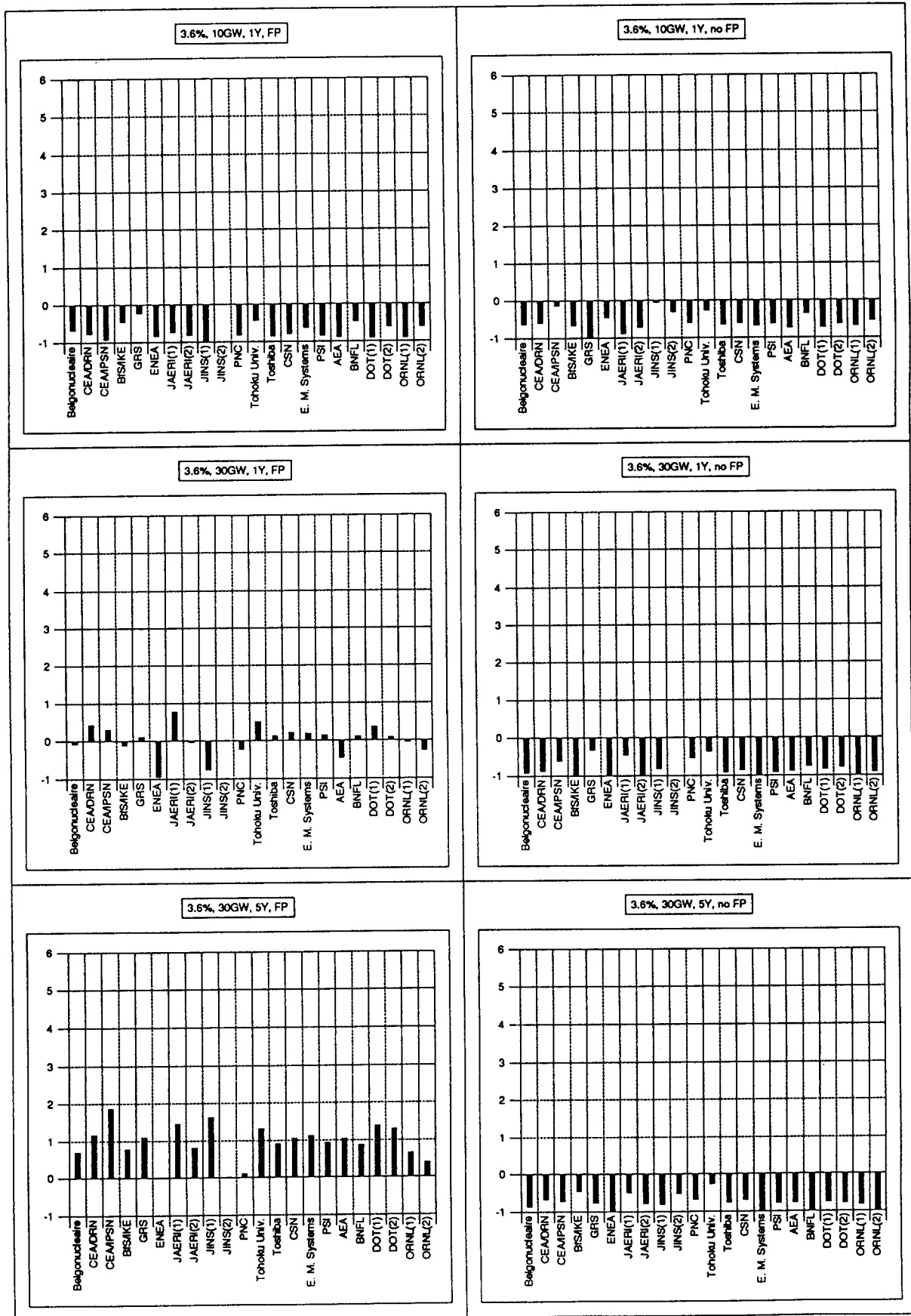


Fig. 4.6 Effect of Burnup Profile in Delta k (%)

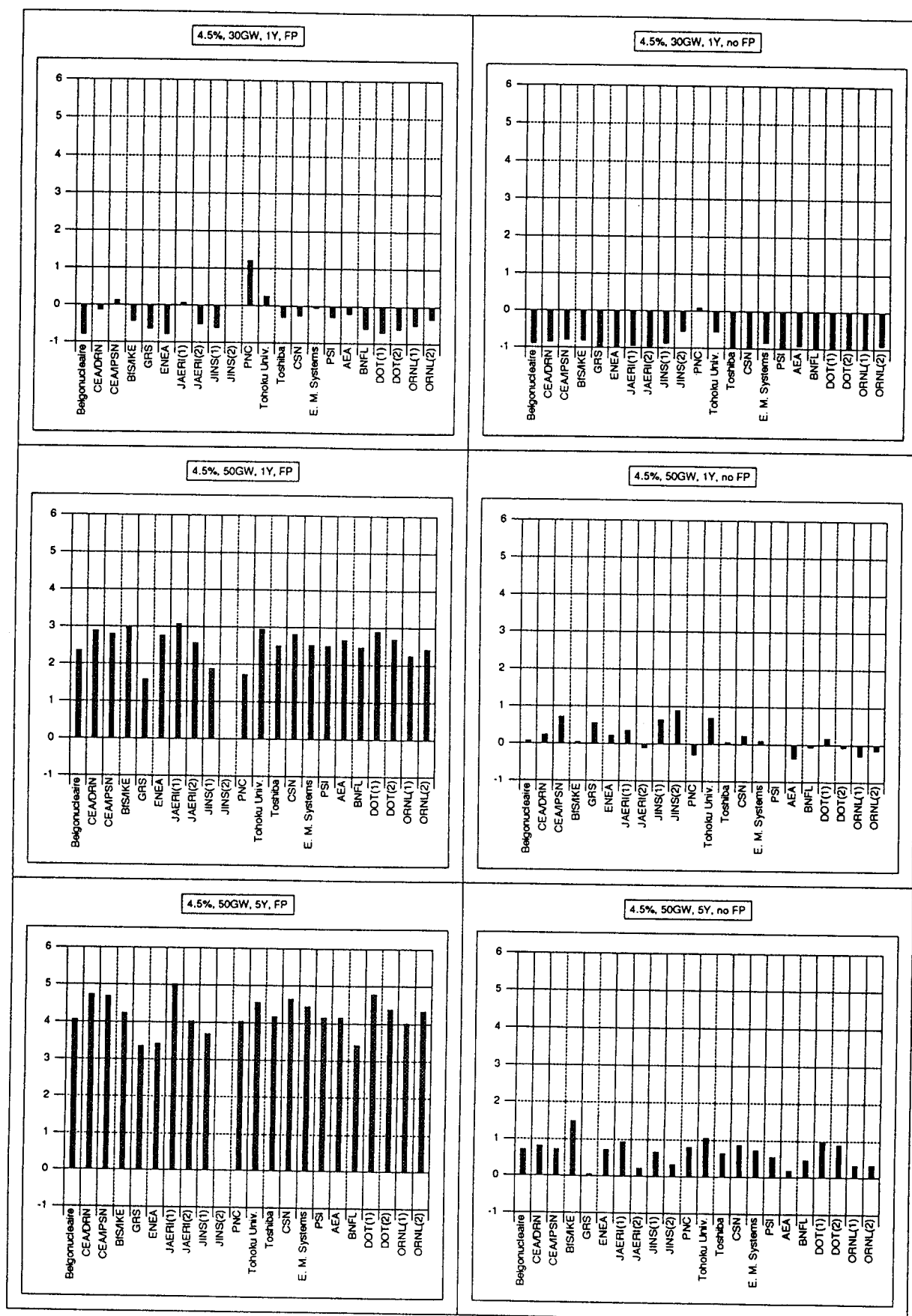


Fig. 4.6 (Continued)

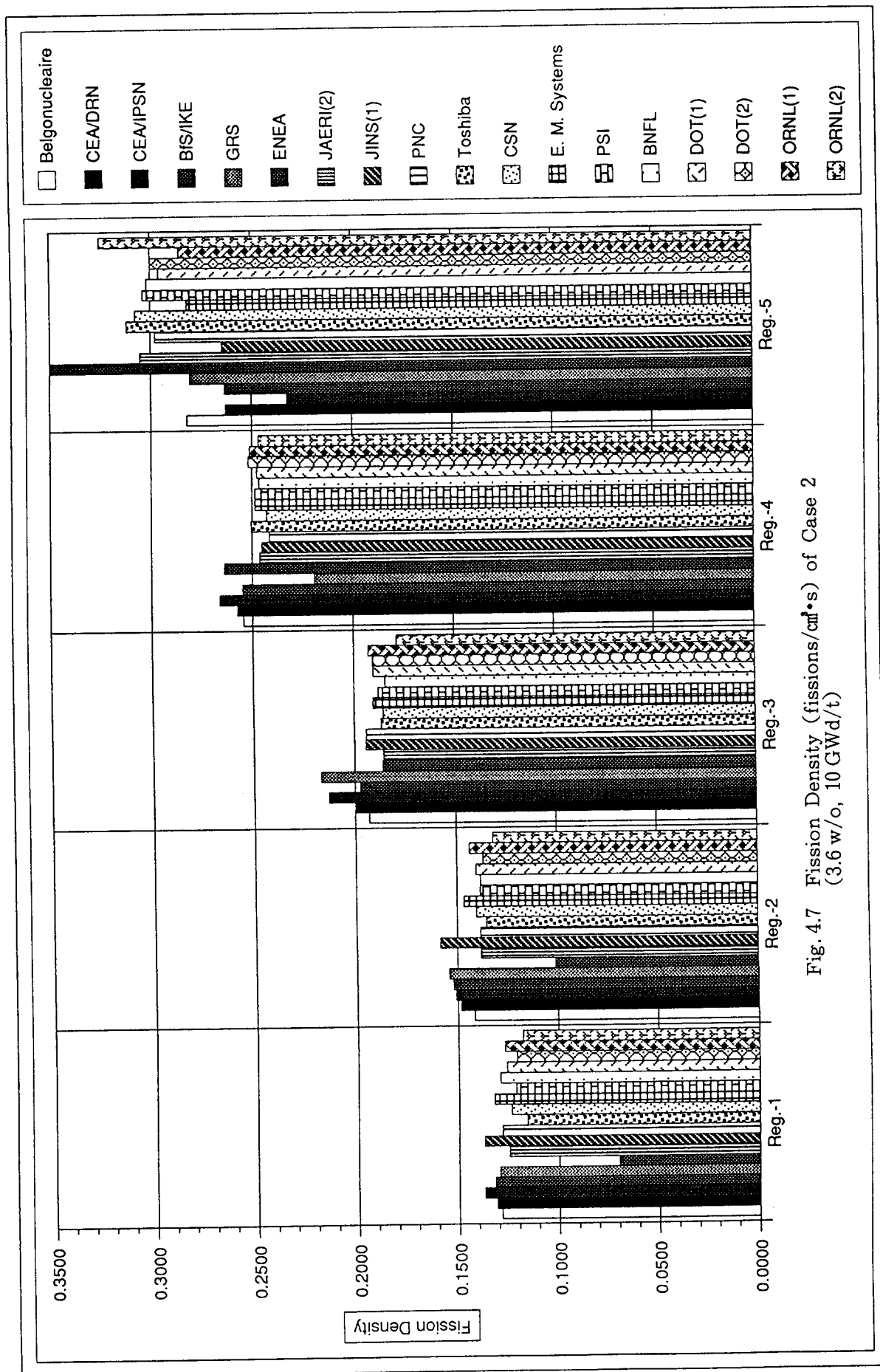


Fig. 4.7 Fission Density (fissions/cm²·s) of Case 2 (3.6 w/o, 10 GWd/t)

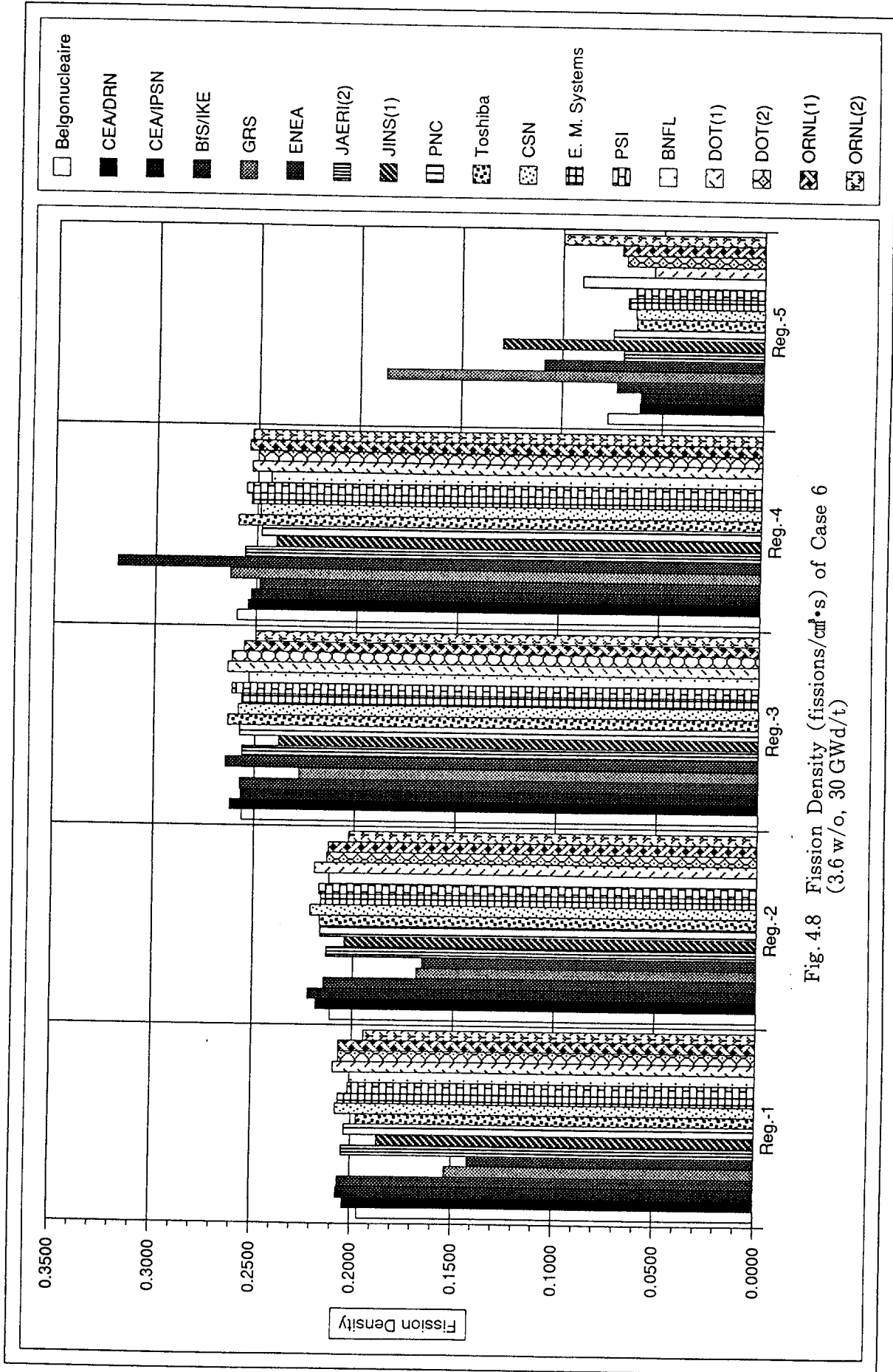


Fig. 4.8 Fission Density (fissions/cm²·s) of Case 6 (3.6 w/o, 30 GWd/t)

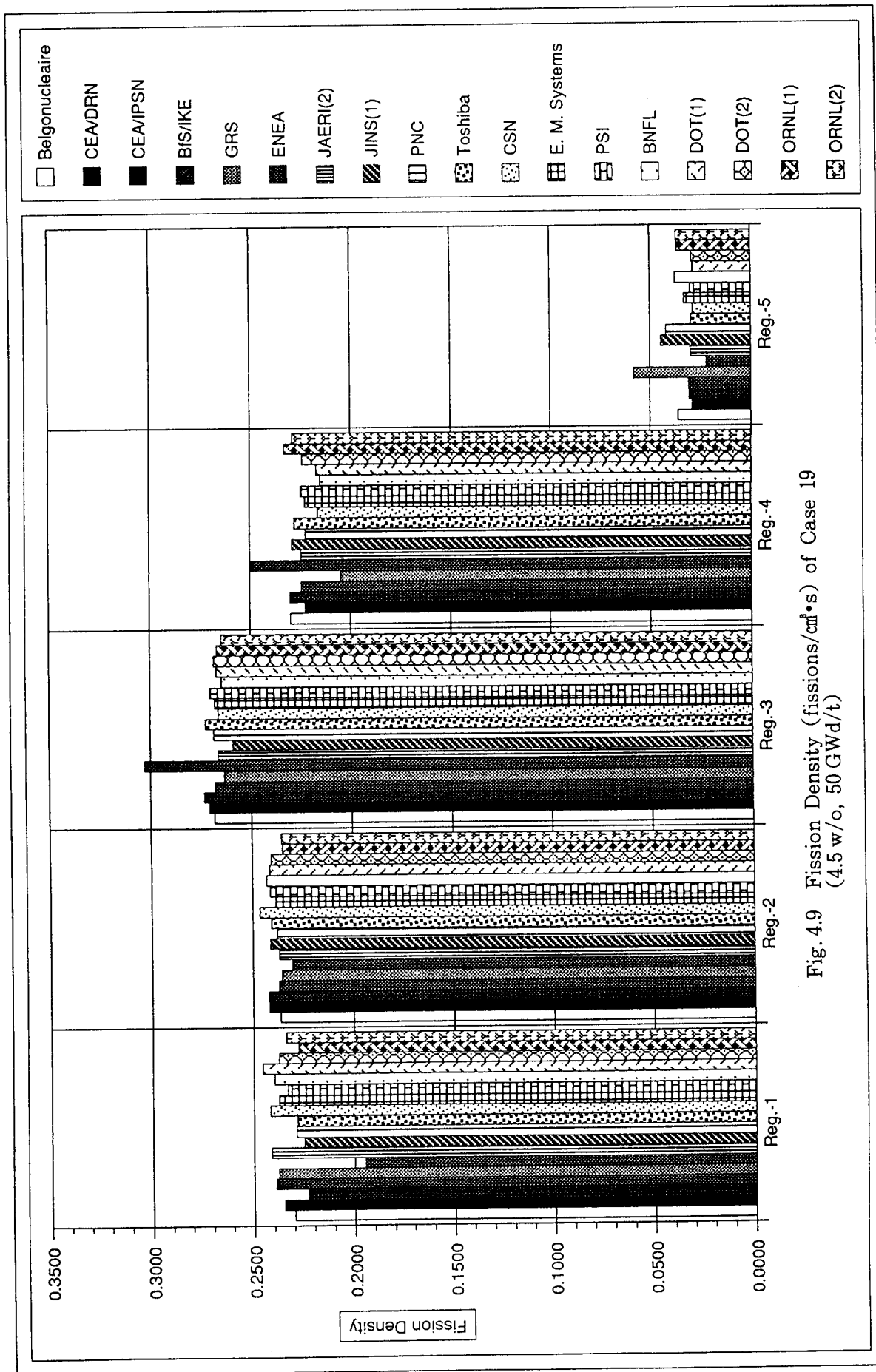


Fig. 4.9 Fission Density (fissions/cm²·s) of Case 19 (4.5 w/o, 50 GWd/t)

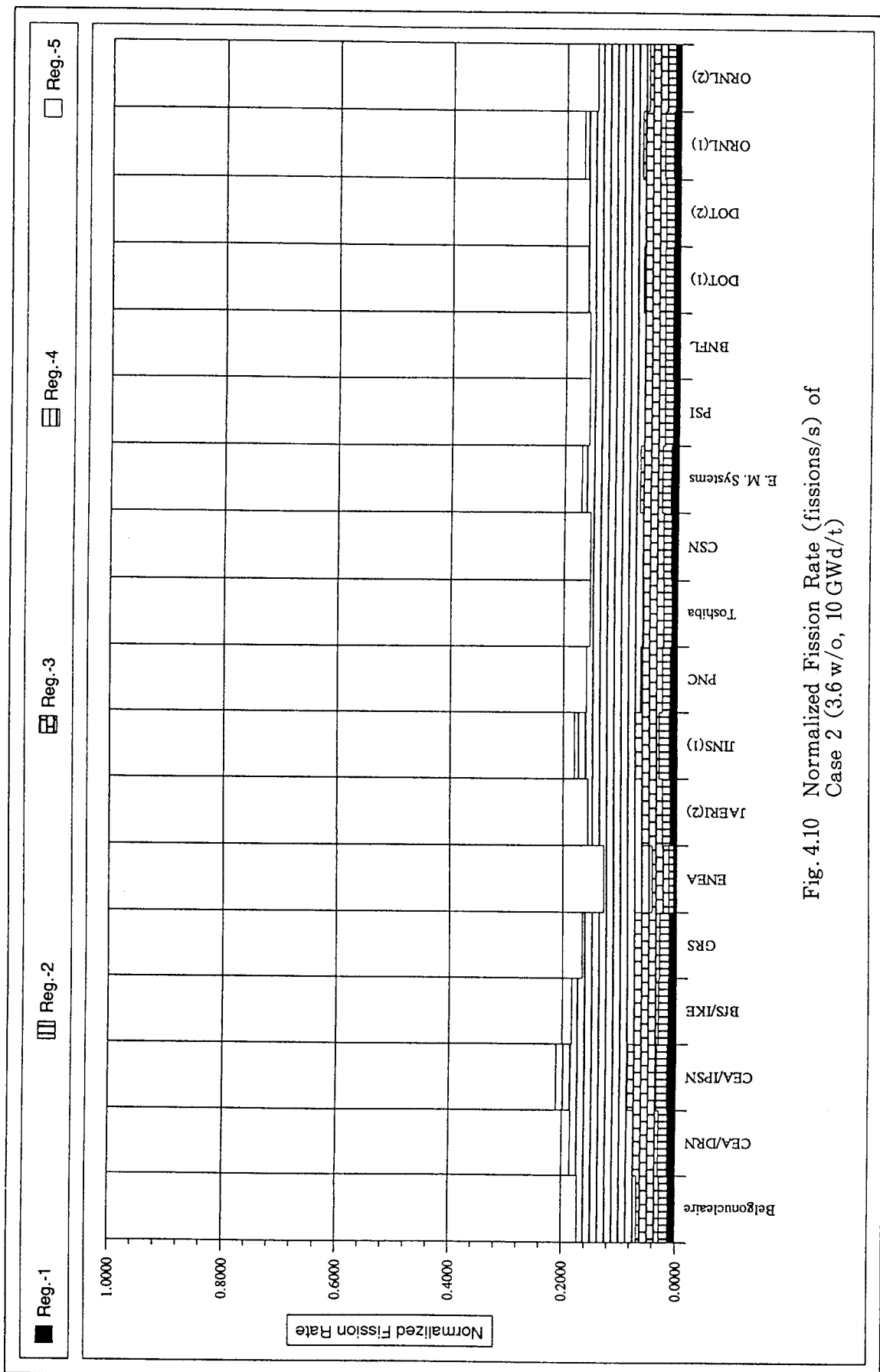


Fig. 4.10 Normalized Fission Rate (fissions/s) of Case 2 (3.6 w/o, 10 GWd/t)

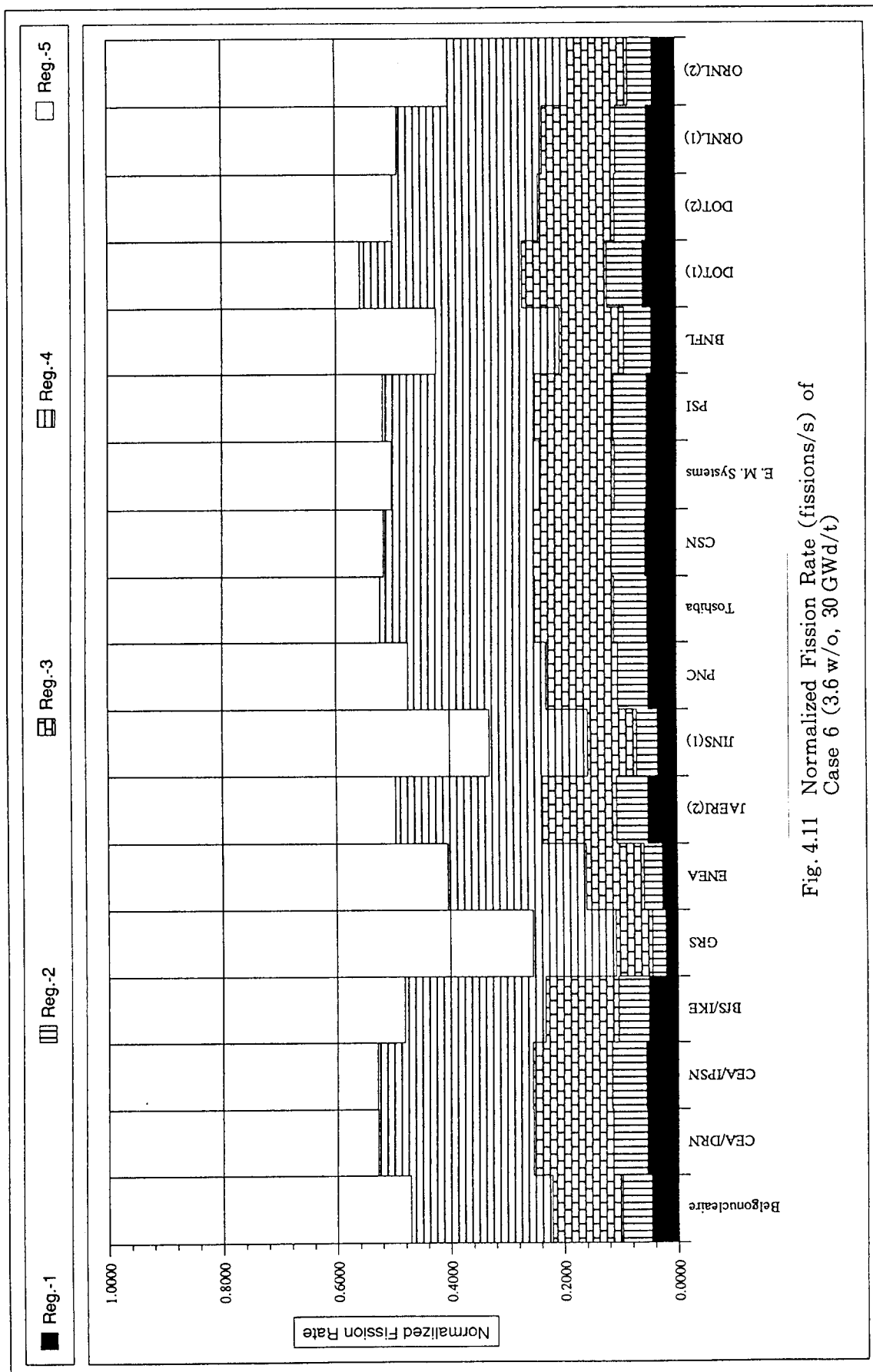


Fig. 4.11 Normalized Fission Rate (fissions/s) of Case 6 (3.6 w/o, 30 GWd/t)

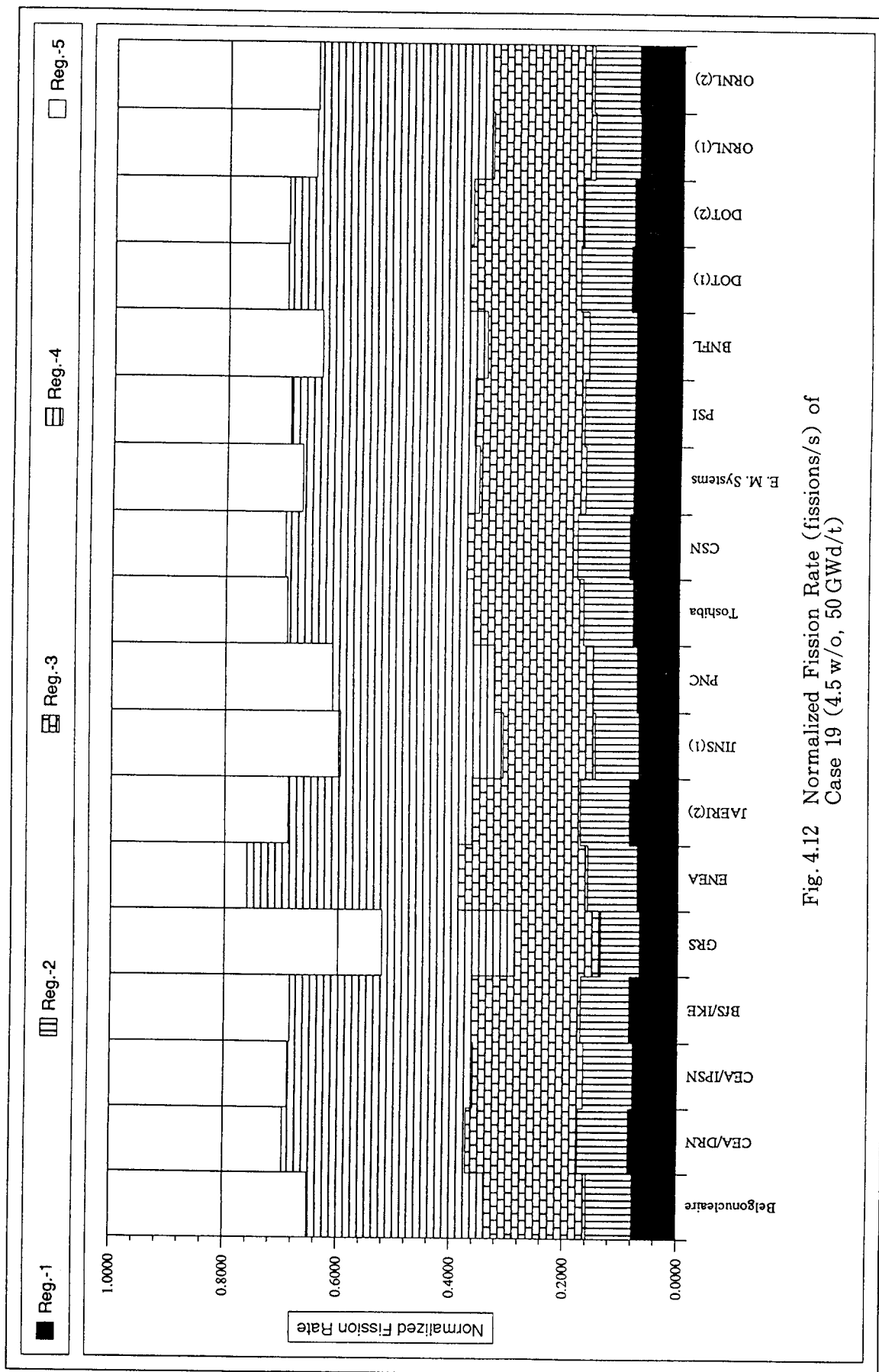


Fig. 4.12 Normalized Fission Rate (fissions/s) of Case 19 (4.5 w/o, 50 GWd/t)

Appendix 1 Specification of Benchmark Problems

Burnup Credit Criticality Benchmark
Phase IIA Effect of Axial Burnup Profile
(Infinite fuel pin array in water)

Burnup Credit Criticality Benchmark
Phase II-A Effect of Axial Burnup Profile
(Infinite fuel pin array in water)

Makoto TAKANO*, Michaele BRADY and Alan SANTAMARINA
JAERI Sandia National Lab. CEA Cadarache

OCTOBER 1993

*E-mail address; Internet	takano@s4a.tokai.jaeri.go.jp
Bitnet	J3520@JPNJAERI
Telefax	(81)-292-82-6479

1. Introduction

For the criticality calculation of a spent fuel system, burnup profile of the spent fuel needs to be considered. The effect of the axial burnup profile on criticality will be studied in Phase II of the Burnup Credit Criticality Benchmark. The Phase II will be divided by two programs, namely, Phase II-A and Phase II-B. In Phase II-A, the criticality calculation of an infinite array of PWR spent fuel rods is performed to grasp the effect of axial burnup profile (end effect) on criticality. In Phase II-B, the criticality of a spent fuel cask will be evaluated.

It is considered that the end effect is a function of the initial fuel enrichment, the burnup and the cooling time. The selection of these parameter values were discussed at meetings in Paris and at ORNL. The selected parameters are 10, 30 GWd/t burnups for 3.6 w/o initial fuel enrichment, 30, 50 GWd/t burnups for 4.5 w/o initial fuel enrichment, 1 and 5 years of cooling times. Further, the the effect of fission products on the end effect is also investigated. The multiplication factors of spent fuel systems with these combinations of parameters will be obtained by all participants using their code and data. Here, the end effect is measured by the difference of multiplication factors between the cases with and without burnup distribution.

It is expected that the results will be helpful to know the degree of importance of the end effect in the burnup credit. The results can be utilized, for example, to obtain a unique Dk value of the end effect, by which the criticality of the spent fuel system can be evaluated by disregarding the burnup profile but employing the average burnup over the rod then simply adding the Dk value.

The burnup profiles of spent fuels at 10, 30, 40 and 50 GWd/t have been measured and supplied for the benchmark by Dr. A. Santamarina and Dr. P. Albarede. The profiles are digitized to obtain region-wise burnup values for the benchmark problem. In total, 60 sets of atomic number densities have been prepared by Dr. M. Brady (see Appendix A).

2. Geometry Data

The geometry of the fuel pin cell is defined by the following data. The cell is used to obtain the multiplication factor of the infinite fuel pin array.

A. Radial dimensions (see Fig. 1)

Fuel Cell Pitch	1.33 cm
Fuel Radius	0.412 cm
Cladding Inner Radius	0.412 cm
Outer Radius	0.475 cm
Radial Boundary Condition	Reflective

B. Axial dimensions (see Fig. 2)

Fuel length	365.7 cm
End plug(Each side)	1.75 cm
Water thickness(Each side)	30.0 cm
Axial Boundary Condition	Vacuum

C. Axial Fuel Modeling

There are 9 regions from top to bottom of the fuel.

Region 1	(Fuel top)	5 cm
Region 2		5 cm
Region 3		10 cm
Region 4		20 cm
Region 5 (Central region)		285.7 cm
Region 6		20 cm
Region 7		10 cm
Region 8		5 cm
Region 9	(Fuel bottom)	5 cm

3. Material Data (at 300 K)

A. Fuel

Fresh Fuel (3.6 w/o) (for Case 1 in Table 1)	Number density (atoms/barn*cm)	
	U-234	7.5174E-06
	U-235	8.4209E-04
	U-236	3.7268E-06
	U-238	2.2254E-02
	O	4.6215E-02
Fresh Fuel (4.5 w/o) (for Case 2 in Table 1)	Number density (atoms/barn*cm)	
	U-234	8.4100E-06
	U-235	1.0526E-03
	U-236	6.4752E-06
	U-238	2.2042E-02
	O	4.6219E-02

The number densities of spent fuels are given in Appendix A.

B. Cladding and End plug

Zircalloy-4	Number density (atoms/barn*cm)	
	Cr	7.5891E-05
	Fe	1.4838E-04
	Zr	4.2982E-02

C Moderator

Water	Number density (atoms/barn*cm)	
	H	6.6621E-02
	O	3.3310E-02

4. Parameters and Case Numbers

In total 26 cases of multiplication factors are requested to be evaluated. Parameters and case numbers for reference are tabulated in Table 1. For the cases of No FP, the following fission products should be omitted from the nuclides listed in Appendix A.

Mo-95, Tc-99, Ru-101, Rh-103, Ag-109, Cs-133, Sm-147, Sm-149, Sm-150, Sm-151, Sm-152, Nd-143, Nd-145, Eu-153, Gd-155

For Cases 2, 6 and 19, the fission densities of Region 1 to 5 are also requested. The fission density is defined as;

$$\text{Fission Density} = \int \sum_f \phi \, dE \quad (\text{per unit fuel volume}),$$

and the sum of fission densities of 5 regions should be normalized to unity, i.e.,

$$\sum_{i=1 \sim 5}^{\text{Region}} \text{Fission Density of Region } i = 1.0 .$$

5. Requested Information and Results

Please forward the results by an electronic mail to Dr. Takano at JAERI. The e-mail is the most convenient way for us to receive your data. Please avoid sending the results by a diskette. In Phase-IA, we had many problems in handling diskettes recorded by various PCs since we have no full IBM PC compatible in our laboratory. However, the results recorded as a text file on a 3.5 inch HD diskette of Macintosh or MSDOS may be also accepted.

Line No.	Contents
1	Date
2	Institute
3	Contact Person
4	E-mail address or Telefax Number of the contact person
5	Computer Code
6 to 31	Multiplication Factors of Cases 1 to 26
32 to 36	Fission densities from Region 1 to 5 of Case 2
37 to 41	Fission densities from Region 1 to 5 of Case 6
42 to 46	Fission densities from Region 1 to 5 of Case 19
47~	Please describe your analysis environment here. It will be included in Phase IIA report. The description should include; Institute and Country, Participants, Neutron data library, Neutron data processing code or method,

Neutron energy groups,
Description of your code system,
Geometry modeling (3-D , 2-D etc.),
Omitted nuclides if any.
Employed convergence limit or statistical errors for
eigenvalues
Other related information.

6. Schedule

Mid October	Distribution of the specification
Mid January	Results should be sent to JAERI
Mid March	Distribution of draft report Phase-IIA
End March	Comments to draft report Phase IIA
End April	Final draft of Phase IIA for NSC

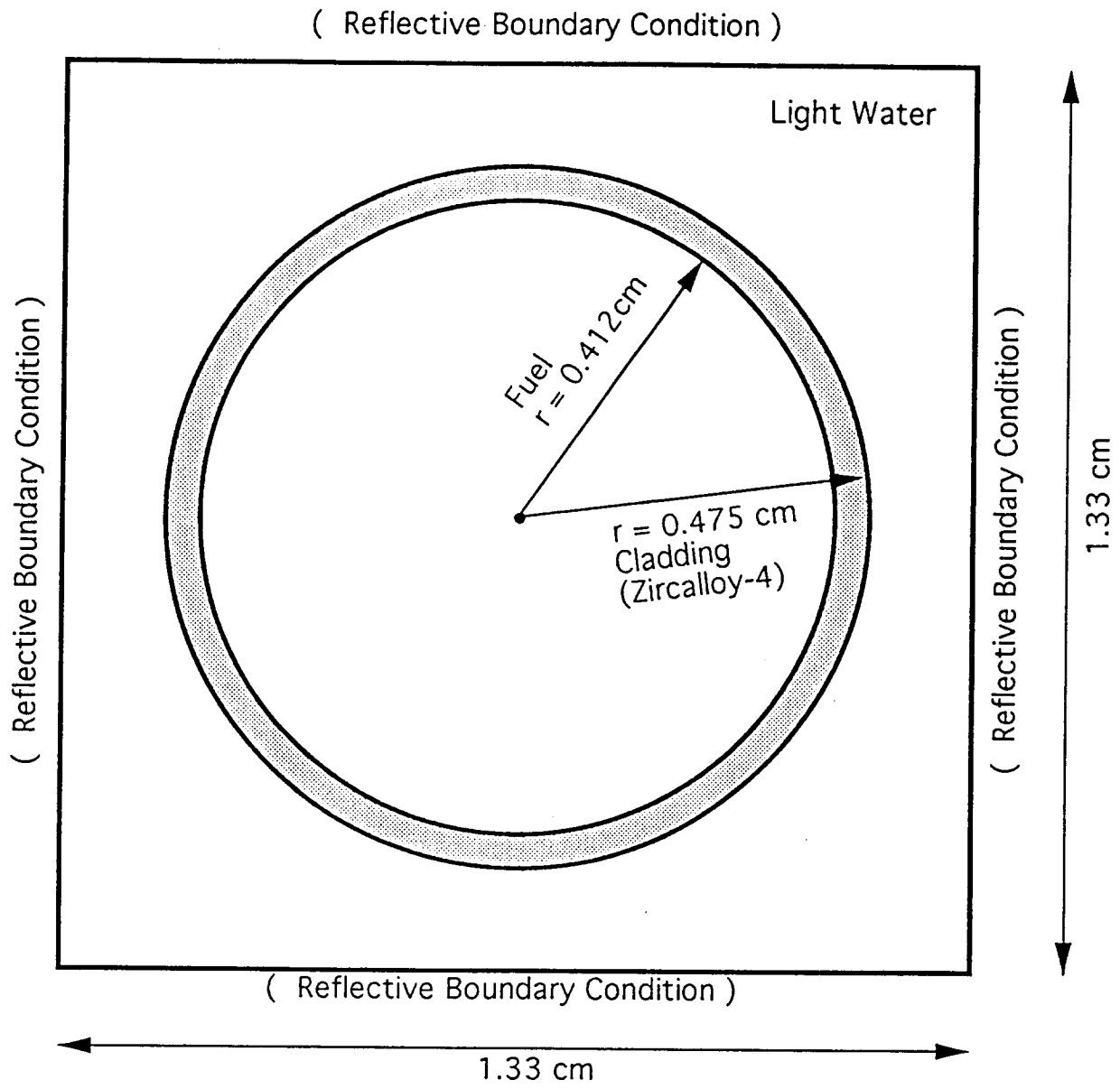


Fig. 1 Radial Dimensions

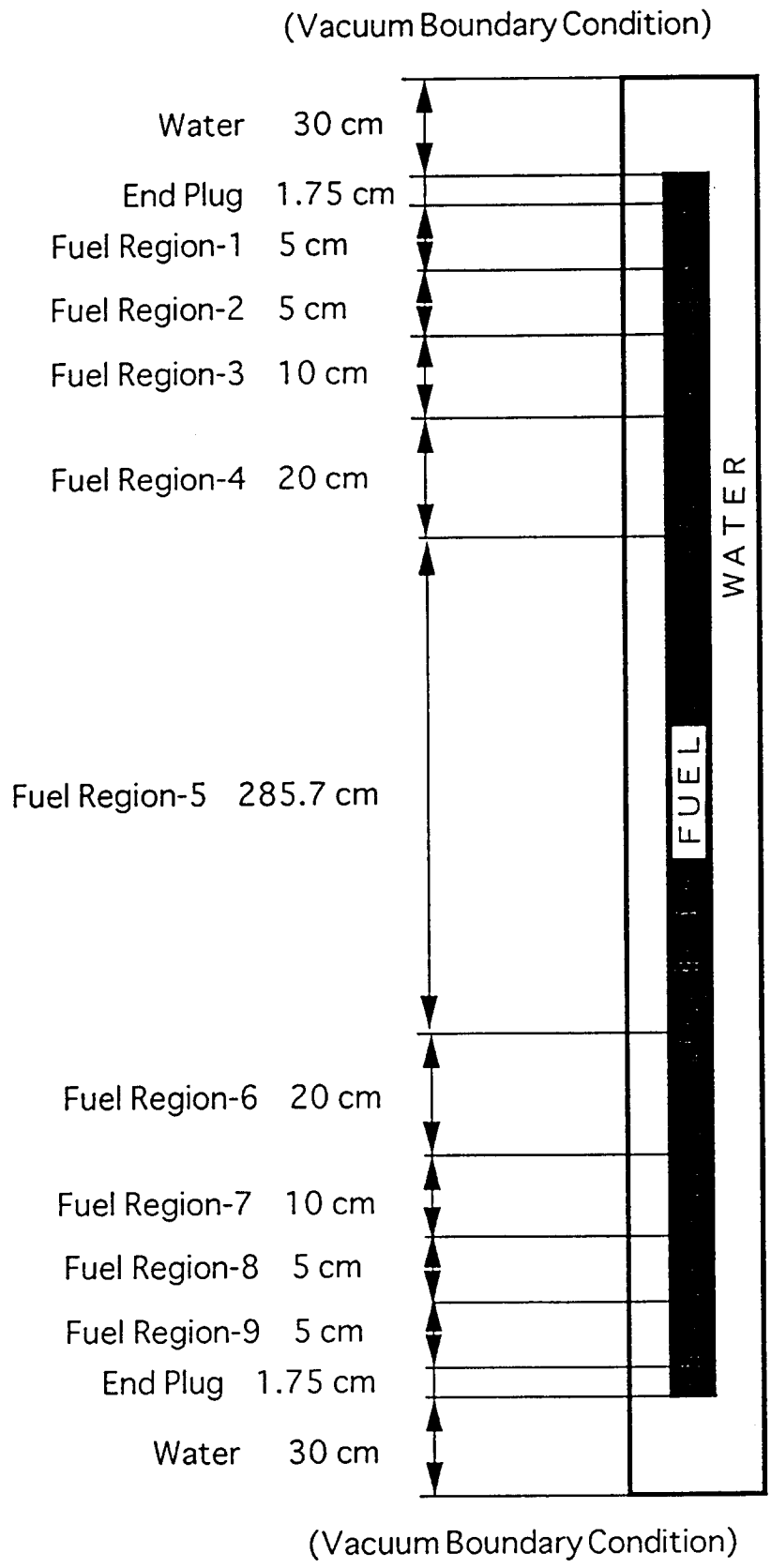


Fig.2 Axial Dimensions

Table 1 Parameters and Case Numbers

		Initial Fuel Enrichment																															
		3.6 w/o					4.5 w/o																										
		Burnup					Burnup																										
Cooling Time	F.P.s	Burnup Profile	Fresh	10 GWd/t	30 GWd/t	40 GWd/t	Fresh	30 GWd/t	50 GWd/t	50 GWd/t																							
			CASE NUMBERS	1	2	3	4	5	N/A	6	7	8	9	10	11	12	13	14	15	16	17	18	N/A	N/A	N/A	N/A	19	20	21	22	23	24	25
1 year	Yes	Yes	No	Yes	No	Yes	No	Yes	No	Yes	No	Yes	No	Yes	No	Yes	No	Yes	No	Yes	No	Yes	No	Yes	No	Yes	No	Yes	No	Yes	No	Yes	No
5 years	Yes	Yes	No	Yes	No	Yes	No	Yes	No	Yes	No	Yes	No	Yes	No	Yes	No	Yes	No	Yes	No	Yes	No	Yes	No	Yes	No	Yes	No	Yes	No	Yes	No

The multiplication factors of 26 cases and related information should be sent to JAERI by 15 January 1994.

Fission Densities of Regions 1 to 5 for Cases 2, 6 and 19 are also requested.

Table 2 Parameters and Data Set Numbers of Appendix A for Analysis

		Initial Fuel Enrichment						
		3.6 w/o			4.5 w/o			
		Burnup						
		Fresh	10 GWd/t	30 GWd/t	40 GWd/t	Fresh	30 GWd/t	50 GWd/t
Cooling Time	F.P.s	Data Set Numbers for Atomic Number Densities						
	Burnup Profile							
1 year	Yes	See	11,13,15,17,19	21,23,25,27,29	N/A	See	41,43,45,47,49	51,53,55,57,59
	No	Chap.3	1	3	N/A	Chap.3	7	9
	Yes		11,13,15,17,19	21,23,25,27,29	N/A		41,43,45,47,49	51,53,55,57,59
	No		1	3	N/A		7	9
5 years	Yes		N/A	22,24,26,28,30	N/A		N/A	52,54,56,58,60
	No		N/A	4	N/A		N/A	10
	Yes		N/A	22,24,26,28,30	N/A		N/A	52,54,56,58,60
	No		N/A	4	N/A		N/A	10

Please DO NOT MIXUP Case Numbers and Data Set Numbers.
(Case Numbers are NOT equal to Data Set Numbers.)

For cases of No F.P.s, omit F.P. nuclides as described in Chap.4.

Appendix A

Atomic Number Densities of Spent Fuels

Prepared by Dr. M. Brady

INFORMATION REGARDING THE CALCULATION
OF ORIGEN-S/SAS2H ISOTOPICS TO GENERATE
THE SPENT FUEL ATOMIC NUMBER DENSITIES FOR PHASE II A
PWR assembly design description for tabulated cases

Parameter	Data
 Assembly general data	
Designer	Westinghouse
Lattice	17 x 17
Water temperature,	570 K
Water density, av, g-cm ⁻³	0.7295
Soluble boron cycle av, ppm (wt)	550
Number of fuel rods	264
Number of guide tubes	24
Number of instrument tubes	1
 Fuel rod data	
Type fuel pellet UO ₂	
Fellet stack density, % TD	94.5
Rod pitch, cm	1.25984
Rod OD, cm	0.94966
Rod ID, cm	0.83566
Pellet diameter, cm	0.81915
Active fuel length, cm	365.8
Effective fuel temperature, K	811
Clad temperature, K	620
Clad material	Zircalloy
 Guide tube data	
Inner radius, cm	0.5715
Outer radius, cm	0.61214
Tube material	Zircalloy

Operating History Data and Fuel Isotopic Content of PWR Cases

Specific Power: 40 kW/kgU

Case Descriptions:

Case 1 - 4 cycle depletion of 3.6 wt% U-235 fuel assembly to 14 Gwd/MTU

	Cycle 1	Cycle 2	Cycle 3	Cycle 4
Burnup (Gwd/MTU)	3	3	4	4
Uptime (Days)	75	75	100	100
Downtime (Days)	0	0	0	62.5

Case 2 - 5 cycle depletion of 3.6 wt% U-235 fuel assembly to 50 Gwd/MTU

Uniform cycles with the following cycle data:

Burnup (Gwd/MTU)	10
Uptime (Days)	250
Downtime (Days)	62.5

Case 3 - 6 cycle depletion of 4.5 wt% U-235 fuel assembly to 60 Gwd/MTU

Uniform cycles with the following cycle data:

Burnup (Gwd/MTU)	10
Uptime (Days)	250
Downtime (Days)	62.5

Uranium Content (wt%)

3.6 wt% U-235		4.5 wt% U-235	
U-234	0.032	U-234	0.0358
U-235	3.600	U-235	4.5000
U-236	0.016	U-236	0.0278
U-238	96.352	U-238	95.4364

Notes on how the nuclide concentrations were obtained:

The nuclide concentrations for the 3.6 wt% 10 GWd/MTU assembly were obtained from Case 1. The concentrations for the 3.6 wt% 30 and 40 GWd/MTU assemblies were obtained from Case 2. The concentrations for the 4.5 wt% 30 and 50 GWd/MTU assemblies were obtained from Case 3. The SAS2 multi-cycle depletions saved nuclide concentrations at the end of each cycle prior to downtime in a single dataset (e.g., the 4.5 wt% depletion saved concentrations at 10, 20, 30, 40, 50 and 60 GWd/MTU). A utility program then interpolated on the values saved at these burnups to obtain the nuclide concentrations at the specified burnups for each axial region and for the assembly average burnup. (Since the assembly average burnups are consistent with the burnups where concentrations were saved, these interpolations are trivial but convenient.) The interpolated concentrations were then input to ORIGEN-S, where they were decayed for 1 year and 5 year cooling times. The concentrations for each axial region of a fuel assembly are taken from a single SAS2 multi-cycle depletion by interpolating between different cycles in the depletion. The result of this method is that the nuclide concentrations for the lower burnup regions at the end of the assemblies are generated at the same specific power as the higher burnup region in the center of the assembly. In our judgment, the effects of this approximation on k-eff are minor. The assembly average nuclide concentrations are based on the assembly average burnup, not on a volume-weighted average of the axial region concentrations. The assembly average burnup is already volume-weighted, and this method is consistent with the way that concentrations would be generated for an axially uniform assembly average analysis.

Isotopics for Phase IIA

	Data set No. 1 3.6wt%u235, 10gwd/mtu cooling time (yr)=1.0	Data set No. 2 3.6wt%u235, 10gwd/mtu cooling time (yr)=5.0	Data set No. 3 3.6wt%u235, 30gwd/mtu cooling time (yr)=1.0
*****	u-234 6.5794E-06	u-234 6.5852E-06	u-234 4.8804E-06
**	u-235 5.9967E-04	u-235 5.9968E-04	u-235 2.8377E-04
	u-236 4.7807E-05	u-236 4.7812E-05	u-236 9.9398E-05
	u-238 2.2103E-02	u-238 2.2103E-02	u-238 2.1759E-02
	pu-238 1.8519E-07	pu-238 1.8036E-07	pu-238 2.8704E-06
	pu-239 8.4685E-05	pu-239 8.4675E-05	pu-239 1.3551E-04
	pu-240 1.1749E-05	pu-240 1.1744E-05	pu-240 4.2931E-05
	pu-241 4.7672E-06	pu-241 3.9295E-06	pu-241 2.8085E-05
	pu-242 3.3278E-07	pu-242 3.3278E-07	pu-242 7.4143E-06
	am-241 2.7770E-07	am-241 1.1109E-06	am-241 2.1081E-06
	am-243 1.7490E-08	am-243 1.7484E-08	am-243 1.3695E-06
	np-237 2.2679E-06	np-237 2.2724E-06	np-237 1.0284E-05
	mo-95 1.4902E-05	mo-95 1.5117E-05	mo-95 4.1124E-05
	tc-99 1.4751E-05	tc-99 1.4751E-05	tc-99 4.0326E-05
	ru-101 1.2768E-05	ru-101 1.2768E-05	ru-101 3.8144E-05
	rh-103 8.4763E-06	rh-103 8.4798E-06	rh-103 2.3427E-05
	ag-109 6.7934E-07	ag-109 6.7934E-07	ag-109 3.6406E-06
	cs-133 1.6145E-05	cs-133 1.6145E-05	cs-133 4.3935E-05
	sm-147 1.3283E-06	sm-147 3.4563E-06	sm-147 3.9475E-06
	sm-149 1.4063E-07	sm-149 1.4063E-07	sm-149 1.7755E-07
	sm-150 3.0773E-06	sm-150 3.0773E-06	sm-150 1.0241E-05
	sm-151 3.8042E-07	sm-151 3.6888E-07	sm-151 5.9020E-07
	sm-152 1.4113E-06	sm-152 1.4113E-06	sm-152 4.2236E-06
	nd-143 1.3086E-05	nd-143 1.3086E-05	nd-143 3.0965E-05
	nd-145 9.0337E-06	nd-145 9.0337E-06	nd-145 2.4165E-05
	eu-153 7.1408E-07	eu-153 7.1408E-07	eu-153 3.3822E-06
	gd-155 1.1869E-08	gd-155 4.3474E-08	gd-155 6.3853E-08
	o 4.6215E-02	o 4.6215E-02	o 4.6215E-02

ISOTOPICS FOR AVERAGE

BURNUP CASES

**

Data set No. 4	Data set No. 5	Data set No. 6	Data set No. 7
3.6wt%u235, 30gwd/mtu cooling time (yr)=5.0	3.6wt%u235, 40gwd/mtu cooling time (yr)=1.0	3.6wt%u235, 40gwd/mtu cooling time (yr)=5.0	4.5wt%u235, 30gwd/mtu cooling time (yr)=1.0
u-234 4.9710E-06	u-234 4.1448E-06	u-234 4.3224E-06	u-234 5.7455E-06
u-235 2.8379E-04	u-235 1.8507E-04	u-235 1.8509E-04	u-235 4.3273E-04
u-236 9.9416E-05	u-236 1.1190E-04	u-236 1.1192E-04	u-236 1.1635E-04
u-238 2.1759E-02	u-238 2.1565E-02	u-238 2.1565E-02	u-238 2.1595E-02
pu-238 2.8294E-06	pu-238 5.6243E-06	pu-238 5.5437E-06	pu-238 2.6453E-06
pu-239 1.3550E-04	pu-239 1.4152E-04	pu-239 1.4151E-04	pu-239 1.4176E-04
pu-240 4.2953E-05	pu-240 5.5277E-05	pu-240 5.5398E-05	pu-240 3.8360E-05
pu-241 2.3150E-05	pu-241 3.6150E-05	pu-241 2.9797E-05	pu-241 2.5933E-05
pu-242 7.4143E-06	pu-242 1.3914E-05	pu-242 1.3914E-05	pu-242 5.3890E-06
am-241 7.0135E-06	am-241 2.8937E-06	am-241 9.2066E-06	am-241 1.9697E-06
am-243 1.3690E-06	am-243 3.4343E-06	am-243 3.4330E-06	am-243 9.1029E-07
np-237 1.0314E-05	np-237 1.4570E-05	np-237 1.4610E-05	np-237 1.0650E-05
mo-95 4.1322E-05	mo-95 5.2430E-05	mo-95 5.2617E-05	mo-95 4.2217E-05
tc-99 4.0326E-05	tc-99 5.1400E-05	tc-99 5.1399E-05	tc-99 4.0848E-05
ru-101 3.8144E-05	ru-101 5.0489E-05	ru-101 5.0489E-05	ru-101 3.8040E-05
rh-103 2.3431E-05	rh-103 2.9115E-05	rh-103 2.9120E-05	rh-103 2.3005E-05
ag-109 3.6406E-06	ag-109 5.3636E-06	ag-109 5.3636E-06	ag-109 3.0914E-06
cs-133 4.3935E-05	cs-133 5.5752E-05	cs-133 5.5752E-05	cs-133 4.4521E-05
sm-147 7.4917E-06	sm-147 4.8850E-06	sm-147 8.5053E-06	sm-147 4.1903E-06
sm-149 1.7755E-07	sm-149 1.7826E-07	sm-149 1.7826E-07	sm-149 1.9919E-07
sm-150 1.0241E-05	sm-150 1.3787E-05	sm-150 1.3787E-05	sm-150 1.0286E-05
sm-151 5.7230E-07	sm-151 6.6650E-07	sm-151 6.4628E-07	sm-151 6.7718E-07
sm-152 4.2238E-06	sm-152 5.3740E-06	sm-152 5.3742E-06	sm-152 4.1136E-06
nd-143 3.0965E-05	nd-143 3.6479E-05	nd-143 3.6479E-05	nd-143 3.3064E-05
nd-145 2.4165E-05	nd-145 3.0439E-05	nd-145 3.0439E-05	nd-145 2.4862E-05
eu-153 3.3822E-06	eu-153 4.8428E-06	eu-153 4.8429E-06	eu-153 3.1728E-06
gd-155 2.3399E-07	gd-155 1.0618E-07	gd-155 3.8944E-07	gd-155 5.8933E-08
o 4.6215E-02	o 4.6215E-02	o 4.6215E-02	o 4.6219E-02

Data set No. 8	Data set No. 9	Data set No. 10
4.5wt&u235, 30gwd/mtu cooling time (yr)=5.0	4.5wt&u235, 50gwd/mtu cooling time (yr)=1.0	4.5wt&u235, 50gwd/mtu cooling time (yr)=5.0
u-234 5.8288E-06	u-234 4.2810E-06	u-234 4.5595E-06
u-235 4.3275E-04	u-235 2.0683E-04	u-235 2.0685E-04
u-236 1.1637E-04	u-236 1.4592E-04	u-236 1.4594E-04
u-238 2.1595E-02	u-238 2.1232E-02	u-238 2.1232E-02
pu-238 2.6014E-06	pu-238 8.8422E-06	pu-238 8.6947E-06
pu-239 1.4175E-04	pu-239 1.5300E-04	pu-239 1.5299E-04
pu-240 3.8367E-05	pu-240 6.1274E-05	pu-240 6.1487E-05
pu-241 2.1376E-05	pu-241 4.1552E-05	pu-241 3.4251E-05
pu-242 5.3890E-06	pu-242 1.7100E-05	pu-242 1.7100E-05
am-241 6.4992E-06	am-241 3.5503E-06	am-241 1.0805E-05
am-243 9.0995E-07	am-243 4.8107E-06	am-243 4.8089E-06
np-237 1.0678E-05	np-237 1.9862E-05	np-237 1.9909E-05
mo-95 4.2421E-05	mo-95 6.5040E-05	mo-95 6.5226E-05
tc-99 4.0847E-05	tc-99 6.2619E-05	tc-99 6.2619E-05
ru-101 3.8040E-05	ru-101 6.2443E-05	ru-101 6.2443E-05
rh-103 2.3009E-05	rh-103 3.3579E-05	rh-103 3.3584E-05
ag-109 3.0914E-06	ag-109 6.2520E-06	ag-109 6.2520E-06
cs-133 4.4521E-05	cs-133 6.7704E-05	cs-133 6.7704E-05
sm-147 7.9467E-06	sm-147 6.0644E-06	sm-147 6.7704E-05
sm-149 1.9919E-07	sm-149 1.9567E-07	sm-149 9.9022E-06
sm-150 1.0286E-05	sm-150 1.7185E-05	sm-150 1.9567E-07
sm-151 6.5663E-07	sm-151 8.1981E-07	sm-151 1.7185E-05
sm-152 4.1139E-06	sm-152 6.3275E-06	sm-152 7.9494E-07
nd-143 3.3064E-05	nd-143 4.4452E-05	sm-152 6.3277E-06
nd-145 2.4862E-05	nd-145 3.7428E-05	nd-143 4.4452E-05
eu-153 3.1728E-06	eu-153 5.9933E-06	nd-145 3.7428E-05
gd-155 2.1404E-07	gd-155 1.4556E-07	eu-153 5.9934E-06
o 4.6219E-02	o 4.6219E-02	gd-155 5.3051E-07
		o 4.6219E-02

	Data set No. 11	Data set No. 12	Data set No. 13
	3.6wt%u235, 10gwd/mtu	3.6wt%u235, 10gwd/mtu	3.6wt%u235, 10gwd/mtu
	cooling time (yr)=1.0	cooling time (yr)=5.0	cooling time (yr)=1.0
	axial locations 1 & 9	axial locations 1 & 9	axial locations 2 & 8
	(3.618 Gwd/MTU)	(3.618 Gwd/MTU)	(4.311 Gwd/MTU)
	u-234	u-234	u-234
	u-235	u-235	u-235
	u-236	u-236	u-236
	u-238	u-238	u-238
	pu-238	pu-238	pu-238
	pu-239	pu-239	pu-239
	pu-240	pu-240	pu-240
	pu-241	pu-241	pu-241
	pu-242	pu-242	pu-242
	am-241	am-241	am-241
	am-243	am-243	am-243
	np-237	np-237	np-237
	mo-95	mo-95	mo-95
	tc-99	tc-99	tc-99
	ru-101	ru-101	ru-101
	rh-103	rh-103	rh-103
	ag-109	ag-109	ag-109
	cs-133	cs-133	cs-133
	sm-147	sm-147	sm-147
	sm-149	sm-149	sm-149
	sm-150	sm-150	sm-150
	sm-151	sm-151	sm-151
	sm-152	sm-152	sm-152
	nd-143	nd-143	nd-143
	nd-145	nd-145	nd-145
	eu-153	eu-153	eu-153
	gd-155	gd-155	gd-155
	o	o	o
	7.1727E-06	7.1731E-06	7.1073E-06
	7.4542E-04	7.4543E-04	7.2820E-04
	2.1526E-05	2.1527E-05	2.4671E-05
	2.2201E-02	2.2201E-02	2.2191E-02
	1.4782E-08	1.4322E-08	2.2662E-08
	3.9529E-05	3.9524E-05	4.5703E-05
	2.3787E-06	2.3777E-06	3.2047E-06
	4.2604E-07	3.5118E-07	6.7465E-07
	5.5378E-09	5.5377E-09	1.2935E-08
	2.1921E-08	9.6399E-08	3.5244E-08
	1.2915E-12	1.2910E-12	3.2474E-12
	5.7921E-07	5.7959E-07	7.2613E-07
	5.4768E-06	5.6240E-06	6.5196E-06
	5.4625E-06	5.4624E-06	6.4947E-06
	4.5948E-06	4.5948E-06	5.4795E-06
	2.9969E-06	2.9994E-06	3.5905E-06
	1.3026E-07	1.3026E-07	1.7303E-07
	5.9784E-06	5.9784E-06	7.1063E-06
	4.7018E-07	1.3987E-06	5.6264E-07
	1.2328E-07	1.2328E-07	1.2673E-07
	8.8301E-07	8.8301E-07	1.0822E-06
	2.3324E-07	2.2616E-07	2.5674E-07
	4.2030E-07	4.2031E-07	5.2286E-07
	5.0905E-06	5.0905E-06	6.0185E-06
	3.3973E-06	3.3973E-06	4.0303E-06
	1.8745E-07	1.8745E-07	2.3222E-07
	4.2592E-09	1.5670E-08	5.0199E-09
	4.6215E-02	4.6215E-02	4.6215E-02

 Axially Dependent Isotopics

The axial regions are of
 the following widths:

- 1 & 9 - 5 cm
- 2 & 8 - 5 cm
- 3 & 7 - 10 cm
- 4 & 6 - 20 cm
- 5 - 285.7 cm

The shapes of the burnup profiles were taken from data provided by A. Santamarina and P. Albarede of C.E.N. - Cadarache. The case of an average burnup of 10 Gwd/MTU used the French EOC1 profile, the cases of 30 and 40 Gwd/MTU used the EOC3 profile and the 50 Gwd/MTU case used the EOC4 profile.

Data set No. 14	Data set No. 15	Data set No. 16	Data set No. 17
3.6wt&u235, 10gwd/mtu cooling time (yr)=5.0 axial locations 2 & 8 (4.311 Gwd/MTU)	3.6wt&u235, 10gwd/mtu cooling time (yr)=1.0 axial locations 3 & 7 (5.647 Gwd/MTU)	3.6wt&u235, 10gwd/mtu cooling time (yr)=5.0 axial locations 3 & 7 (5.647 Gwd/MTU)	3.6wt&u235, 10gwd/mtu cooling time (yr)=1.0 axial locations 4 & 6 (7.558 Gwd/MTU)
u-234 7.1079E-06	u-234 6.9819E-06	u-234 6.9833E-06	u-234 6.8042E-06
u-235 7.2821E-04	u-235 6.9597E-04	u-235 6.9598E-04	u-235 6.5206E-04
u-236 2.4673E-05	u-236 3.0535E-05	u-236 3.0537E-05	u-236 3.8459E-05
u-238 2.2191E-02	u-238 2.2170E-02	u-238 2.2170E-02	u-238 2.2141E-02
pu-238 2.1957E-08	pu-238 4.5152E-08	pu-238 4.3819E-08	pu-238 9.4031E-08
pu-239 4.5698E-05	pu-239 5.6731E-05	pu-239 5.6724E-05	pu-239 7.0502E-05
pu-240 3.2034E-06	pu-240 4.9284E-06	pu-240 4.9264E-06	pu-240 7.6945E-06
pu-241 5.5609E-07	pu-241 1.3069E-06	pu-241 1.0773E-06	pu-241 2.5613E-06
pu-242 1.2935E-08	pu-242 4.6519E-08	pu-242 4.6519E-08	pu-242 1.3880E-07
am-241 1.5318E-07	am-241 7.0854E-08	am-241 2.9930E-07	am-241 1.4450E-07
am-243 3.2462E-12	am-243 1.1026E-09	am-243 1.1022E-09	am-243 6.0436E-09
np-237 7.2675E-07	np-237 1.0344E-06	np-237 1.0356E-06	np-237 1.5325E-06
mo-95 6.6812E-06	mo-95 8.5164E-06	mo-95 8.7008E-06	mo-95 1.1341E-05
tc-99 6.4946E-06	tc-99 8.4682E-06	tc-99 8.4681E-06	tc-99 1.1253E-05
ru-101 5.4795E-06	ru-101 7.1866E-06	ru-101 7.1866E-06	ru-101 9.6322E-06
rh-103 3.5931E-06	rh-103 4.7355E-06	rh-103 4.7385E-06	rh-103 6.3753E-06
ag-109 1.7303E-07	ag-109 2.6703E-07	ag-109 2.6703E-07	ag-109 4.2798E-07
cs-133 7.1063E-06	cs-133 9.2639E-06	cs-133 9.2639E-06	cs-133 1.2312E-05
sm-147 1.6463E-06	sm-147 7.4136E-07	sm-147 2.1071E-06	sm-147 9.9805E-07
sm-149 1.2673E-07	sm-149 1.3232E-07	sm-149 1.3232E-07	sm-149 1.3783E-07
sm-150 1.0822E-06	sm-150 1.4931E-06	sm-150 1.4931E-06	sm-150 2.1420E-06
sm-151 2.4895E-07	sm-151 2.9689E-07	sm-151 2.8788E-07	sm-151 3.4245E-07
sm-152 5.2287E-07	sm-152 7.2402E-07	sm-152 7.2403E-07	sm-152 1.0196E-06
nd-143 6.0185E-06	nd-143 7.7663E-06	nd-143 7.7663E-06	nd-143 1.0171E-05
nd-145 4.0303E-06	nd-145 5.2361E-06	nd-145 5.2361E-06	nd-145 6.9273E-06
eu-153 2.3222E-07	eu-153 3.2705E-07	eu-153 3.2705E-07	eu-153 4.8217E-07
gd-155 1.8445E-08	gd-155 6.5311E-09	gd-155 2.3961E-08	gd-155 8.7956E-09
o 4.6215E-02	o 4.6215E-02	o 4.6215E-02	o 4.6215E-02

Data set No. 18	Data set No. 19	Data set No. 20	Data set No. 21
3.6wt&u235, 10gwd/mtu	3.6wt&u235, 10GWD/MTU	3.6wt&u235, 10GWD/MTU	3.6wt&u235, 30GWD/MTU
cooling time (yr)=5.0	cooling time (yr)=1.0	cooling time (yr)=5.0	cooling time (yr)=1.0
axial locations 4 & 6	axial location 5	axial location 5	axial location 1 & 9
(7.558 Gwd/MTU)	(11.069 GWD/MTU)	(11.069 GWD/MTU)	(12.330GWD/MTU)
u-234 6.8071E-06	u-234 6.4825E-06	u-234 6.4898E-06	u-234 6.3705E-06
u-235 6.5207E-04	u-235 5.7794E-04	u-235 5.7795E-04	u-235 5.5336E-04
u-236 3.8462E-05	u-236 5.1643E-05	u-236 5.1649E-05	u-236 5.5957E-05
u-238 2.2141E-02	u-238 2.2086E-02	u-238 2.2086E-02	u-238 2.2066E-02
pu-238 9.1440E-08	pu-238 2.3783E-07	pu-238 2.3183E-07	pu-238 3.1141E-07
pu-239 7.0494E-05	pu-239 9.0069E-05	pu-239 9.0059E-05	pu-239 9.4448E-05
pu-240 7.6913E-06	pu-240 1.3567E-05	pu-240 1.3561E-05	pu-240 1.5417E-05
pu-241 2.1112E-06	pu-241 5.8526E-06	pu-241 4.8242E-06	pu-241 7.7995E-06
pu-242 1.3880E-07	pu-242 4.5786E-07	pu-242 4.5786E-07	pu-242 6.5918E-07
am-241 5.9217E-07	am-241 3.4621E-07	am-241 1.3690E-06	am-241 4.6500E-07
am-243 6.0413E-09	am-243 2.7360E-08	am-243 2.7350E-08	am-243 4.5209E-08
np-237 1.5349E-06	np-237 2.6147E-06	np-237 2.6203E-06	np-237 3.0436E-06
mo-95 1.1547E-05	mo-95 1.6430E-05	mo-95 1.6647E-05	mo-95 1.8236E-05
tc-99 1.1253E-05	tc-99 1.6254E-05	tc-99 1.6254E-05	tc-99 1.7833E-05
ru-101 9.6322E-06	ru-101 1.4134E-05	ru-101 1.4134E-05	ru-101 1.5775E-05
rh-103 6.3786E-06	rh-103 9.3808E-06	rh-103 9.3844E-06	rh-103 1.0455E-05
ag-109 4.2798E-07	ag-109 7.9998E-07	ag-109 7.9998E-07	ag-109 9.6301E-07
cs-133 1.2312E-05	cs-133 1.7790E-05	cs-133 1.7790E-05	cs-133 1.9552E-05
sm-147 2.7278E-06	sm-147 1.4711E-06	sm-147 3.7534E-06	sm-147 1.6643E-06
sm-149 1.3783E-07	sm-149 1.4238E-07	sm-149 1.4238E-07	sm-149 1.5514E-07
sm-150 2.1420E-06	sm-150 3.4955E-06	sm-150 3.4955E-06	sm-150 3.8040E-06
sm-151 3.3206E-07	sm-151 3.9505E-07	sm-151 3.8307E-07	sm-151 4.1111E-07
sm-152 1.0196E-06	sm-152 1.5804E-06	sm-152 1.5804E-06	sm-152 1.7856E-06
nd-143 1.0171E-05	nd-143 1.4304E-05	nd-143 1.4304E-05	nd-143 1.5611E-05
nd-145 6.9273E-06	nd-145 9.9329E-06	nd-145 9.9329E-06	nd-145 1.0993E-05
eu-153 4.8218E-07	eu-153 8.2472E-07	eu-153 8.2472E-07	eu-153 9.6829E-07
gd-155 3.2233E-08	gd-155 1.3371E-08	gd-155 4.8970E-08	gd-155 1.5168E-08
o 4.6215E-02	o 4.6215E-02	o 4.6215E-02	o 4.6215E-02

Data set No. 22	Data set No. 23	Data set No. 24	Data set No. 25
3.6wt%U235, 30GWD/MTU	3.6wt%U235, 30GWD/MTU	3.6wt%U235, 30GWD/MTU	3.6wt%U235, 30GWD/MTU
cooling time (yr)=5.0	cooling time (yr)=1.0	cooling time (yr)=5.0	cooling time (yr)=1.0
axial location 1 & 9	axial location 2 & 8	axial location 2 & 8	axial location 3 & 7
(12.330GWD/MTU)	(14.041GWD/MTU)	(14.041GWD/MTU)	(18.006GWD/MTU)
u-234 6.3802E-06	u-234 6.2178E-06	u-234 6.2312E-06	u-234 5.8699E-06
u-235 5.5337E-04	u-235 5.2093E-04	u-235 5.2094E-04	u-235 4.5143E-04
u-236 5.5963E-05	u-236 6.1572E-05	u-236 6.1580E-05	u-236 7.3333E-05
u-238 2.2066E-02	u-238 2.2039E-02	u-238 2.2039E-02	u-238 2.1973E-02
pu-238 3.0368E-07	pu-238 4.3069E-07	pu-238 4.2082E-07	pu-238 8.0609E-07
pu-239 9.4437E-05	pu-239 1.0142E-04	pu-239 1.0141E-04	pu-239 1.1449E-04
pu-240 1.5411E-05	pu-240 1.8235E-05	pu-240 1.8228E-05	pu-240 2.4724E-05
pu-241 6.4290E-06	pu-241 9.8114E-06	pu-241 8.0873E-06	pu-241 1.4601E-05
pu-242 6.5918E-07	pu-242 9.7642E-07	pu-242 9.7642E-07	pu-242 2.0114E-06
am-241 1.8281E-06	am-241 6.0188E-07	am-241 2.3164E-06	am-241 9.5617E-07
am-243 4.5192E-08	am-243 7.7068E-08	am-243 7.7039E-08	am-243 2.0891E-07
np-237 3.0511E-06	np-237 3.6522E-06	np-237 3.6618E-06	np-237 5.1708E-06
mo-95 1.8451E-05	mo-95 2.0626E-05	mo-95 2.0840E-05	mo-95 2.6014E-05
tc-99 1.7833E-05	tc-99 2.0170E-05	tc-99 2.0170E-05	tc-99 2.5457E-05
ru-101 1.5775E-05	ru-101 1.7961E-05	ru-101 1.7961E-05	ru-101 2.3014E-05
rh-103 1.0459E-05	rh-103 1.1854E-05	rh-103 1.1857E-05	rh-103 1.4989E-05
ag-109 9.6301E-07	ag-109 1.1788E-06	ag-109 1.1788E-06	ag-109 1.7249E-06
cs-133 1.9552E-05	cs-133 2.2103E-05	cs-133 2.2103E-05	cs-133 2.7859E-05
sm-147 4.1077E-06	sm-147 1.9070E-06	sm-147 4.5466E-06	sm-147 2.4589E-06
sm-149 1.5514E-07	sm-149 1.5939E-07	sm-149 1.5939E-07	sm-149 1.6710E-07
sm-150 3.8040E-06	sm-150 4.4133E-06	sm-150 4.4133E-06	sm-150 5.8464E-06
sm-151 3.9864E-07	sm-151 4.3200E-07	sm-151 4.1889E-07	sm-151 4.7695E-07
sm-152 1.7857E-06	sm-152 2.0469E-06	sm-152 2.0470E-06	sm-152 2.6305E-06
nd-143 1.5611E-05	nd-143 1.7437E-05	nd-143 1.7437E-05	nd-143 2.1378E-05
nd-145 1.0993E-05	nd-145 1.2392E-05	nd-145 1.2392E-05	nd-145 1.5528E-05
eu-153 9.6830E-07	eu-153 1.1667E-06	eu-153 1.1667E-06	eu-153 1.6674E-06
gd-155 5.5547E-08	gd-155 1.8028E-08	gd-155 6.6016E-08	gd-155 2.6254E-08
o 4.6215E-02	o 4.6215E-02	o 4.6215E-02	o 4.6215E-02

Data set No. 26	Data set No. 27	Data set No. 28	Data set No. 29
3.6wt%U235, 30GWD/MTU	3.6wt%U235, 30GWD/MTU	3.6wt%U235, 30GWD/MTU	3.6wt%U235, 30GWD/MTU
cooling time (yr)=5.0	cooling time (yr)=1.0	cooling time (yr)=5.0	cooling time (yr)=1.0
axial location 3 & 7	axial location 4 & 6	axial location 4 & 6	axial location 5
(18.006GWD/MTU)	(24.009GWD/MTU)	(24.009GWD/MTU)	(32.855GWD/MTU)
u-234	u-234	u-234	u-234
5.8952E-06	5.3620E-06	5.4143E-06	4.6622E-06
u-235	u-235	u-235	u-235
4.5145E-04	3.6010E-04	3.6012E-04	2.5228E-04
u-236	u-236	u-236	u-236
7.3343E-05	8.8047E-05	8.8061E-05	1.0372E-04
u-238	u-238	u-238	u-238
2.1973E-02	2.1869E-02	2.1869E-02	2.1705E-02
pu-238	pu-238	pu-238	pu-238
7.9081E-07	1.6598E-06	1.6339E-06	3.5663E-06
pu-239	pu-239	pu-239	pu-239
1.1447E-04	1.2775E-04	1.2773E-04	1.3790E-04
pu-240	pu-240	pu-240	pu-240
2.4717E-05	3.4198E-05	3.4197E-05	4.6744E-05
pu-241	pu-241	pu-241	pu-241
1.2035E-05	2.1718E-05	1.7902E-05	3.0723E-05
pu-242	pu-242	pu-242	pu-242
2.0114E-06	4.3206E-06	4.3206E-06	9.1156E-06
am-241	am-241	am-241	am-241
3.5074E-06	1.5389E-06	5.3328E-06	2.3570E-06
am-243	am-243	am-243	am-243
2.0884E-07	6.2397E-07	6.2374E-07	1.8519E-06
np-237	np-237	np-237	np-237
5.1854E-06	7.6707E-06	7.6933E-06	1.1527E-05
mo-95	mo-95	mo-95	mo-95
2.6225E-05	3.3792E-05	3.3996E-05	4.4455E-05
tc-99	tc-99	tc-99	tc-99
2.5457E-05	3.3109E-05	3.3108E-05	4.3599E-05
ru-101	ru-101	ru-101	ru-101
2.3014E-05	3.0617E-05	3.0617E-05	4.1684E-05
rh-103	rh-103	rh-103	rh-103
1.4993E-05	1.9419E-05	1.9423E-05	2.5173E-05
ag-109	ag-109	ag-109	ag-109
1.7249E-06	2.6462E-06	2.6462E-06	4.1267E-06
cs-133	cs-133	cs-133	cs-133
2.7859E-05	3.6156E-05	3.6156E-05	4.7444E-05
sm-147	sm-147	sm-147	sm-147
5.4627E-06	3.2457E-06	6.6054E-06	4.2452E-06
sm-149	sm-149	sm-149	sm-149
1.6710E-07	1.7425E-07	1.7425E-07	1.7821E-07
sm-150	sm-150	sm-150	sm-150
5.8464E-06	8.0459E-06	8.0459E-06	1.1269E-05
sm-151	sm-151	sm-151	sm-151
4.6248E-07	5.3724E-07	5.2094E-07	6.1328E-07
sm-152	sm-152	sm-152	sm-152
2.6306E-06	3.4583E-06	3.4585E-06	4.5663E-06
nd-143	nd-143	nd-143	nd-143
2.1378E-05	2.6602E-05	2.6602E-05	3.2750E-05
nd-145	nd-145	nd-145	nd-145
1.5528E-05	2.0005E-05	2.0005E-05	2.6033E-05
eu-153	eu-153	eu-153	eu-153
1.6674E-06	2.5019E-06	2.5020E-06	3.8033E-06
gd-155	gd-155	gd-155	gd-155
9.6135E-08	4.2823E-08	1.5685E-07	7.5143E-08
o	o	o	o
4.6215E-02	4.6215E-02	4.6215E-02	4.6215E-02

Data set No. 30	Data set No. 31	Data set No. 32	Data set No. 33
3.6wt%U235, 30GWD/MTU	3.6wt%U235, 40GWD/MTU	3.6wt%U235, 40GWD/MTU	3.6wt%U235, 40GWD/MTU
cooling time (yr)=5.0	cooling time (yr)=1.0	cooling time (yr)=5.0	cooling time (yr)=1.0
axial location 5	axial location 1 & 9	axial location 1 & 9	axial location 2 & 8
(32.855GWD/MTU)	(16.439GWD/MTU)	(16.439GWD/MTU)	(18.722GWD/MTU)
u-234 4.7748E-06	u-234 6.0062E-06	u-234 6.0263E-06	u-234 5.8080E-06
u-235 2.5230E-04	u-235 4.7798E-04	u-235 4.7800E-04	u-235 4.3969E-04
u-236 1.0374E-04	u-236 6.8888E-05	u-236 6.8898E-05	u-236 7.5278E-05
u-238 2.1705E-02	u-238 2.1999E-02	u-238 2.1999E-02	u-238 2.1961E-02
pu-238 3.5160E-06	pu-238 6.4058E-07	pu-238 6.2753E-07	pu-238 8.8941E-07
pu-239 1.3788E-04	pu-239 1.0980E-04	pu-239 1.0978E-04	pu-239 1.1644E-04
pu-240 4.6784E-05	pu-240 2.2172E-05	pu-240 2.2165E-05	pu-240 2.5882E-05
pu-241 2.5324E-05	pu-241 1.2698E-05	pu-241 1.0467E-05	pu-241 1.5470E-05
pu-242 9.1156E-06	pu-242 1.5535E-06	pu-242 1.5535E-06	pu-242 2.2414E-06
am-241 7.7230E-06	am-241 8.1121E-07	am-241 3.0301E-06	am-241 1.0240E-06
am-243 1.8512E-06	am-243 1.4560E-07	am-243 1.4555E-07	am-243 2.4340E-07
np-237 1.1560E-05	np-237 4.5546E-06	np-237 4.5672E-06	np-237 5.4584E-06
mo-95 4.4649E-05	mo-95 2.3909E-05	mo-95 2.4122E-05	mo-95 2.6965E-05
tc-99 4.3598E-05	tc-99 2.3390E-05	tc-99 2.3389E-05	tc-99 2.6392E-05
ru-101 4.1684E-05	ru-101 2.1020E-05	ru-101 2.1020E-05	ru-101 2.3924E-05
rh-103 2.5178E-05	rh-103 1.3768E-05	rh-103 1.3772E-05	rh-103 1.5538E-05
ag-109 4.1267E-06	ag-109 1.5020E-06	ag-109 1.5020E-06	ag-109 1.8295E-06
cs-133 4.7444E-05	cs-133 2.5610E-05	cs-133 2.5610E-05	cs-133 2.8876E-05
sm-147 7.8342E-06	sm-147 2.2431E-06	sm-147 5.1169E-06	sm-147 2.5563E-06
sm-149 1.7821E-07	sm-149 1.6438E-07	sm-149 1.6438E-07	sm-149 1.6822E-07
sm-150 1.1269E-05	sm-150 5.2771E-06	sm-150 5.2771E-06	sm-150 6.1075E-06
sm-151 5.9467E-07	sm-151 4.5972E-07	sm-151 4.4577E-07	sm-151 4.8459E-07
sm-152 4.5665E-06	sm-152 2.4035E-06	sm-152 2.4036E-06	sm-152 2.7326E-06
nd-143 3.2750E-05	nd-143 1.9867E-05	nd-143 1.9867E-05	nd-143 2.2047E-05
nd-145 2.6033E-05	nd-145 1.4306E-05	nd-145 1.4306E-05	nd-145 1.6079E-05
eu-153 3.8033E-06	eu-153 1.4634E-06	eu-153 1.4634E-06	eu-153 1.7629E-06
gd-155 2.7544E-07	gd-155 2.2737E-08	gd-155 8.3258E-08	gd-155 2.7974E-08
o 4.6215E-02	o 4.6215E-02	o 4.6215E-02	o 4.6215E-02

Data set No. 34	Data set No. 35	Data set No. 36	Data set No. 37
3.6wt&U235, 40GWD/MTU	3.6wt&U235, 40GWD/MTU	3.6wt&U235, 40GWD/MTU	3.6wt&U235, 40GWD/MTU
cooling time (yr)=5.0	cooling time (yr)=1.0	cooling time (yr)=5.0	cooling time (yr)=1.0
axial location 2 & 8	axial location 3 & 7	axial location 3 & 7	axial location 4 & 6
(18.722GWD/MTU)	(24.008GWD/MTU)	(24.008GWD/MTU)	(32.012GWD/MTU)
u-234	u-234	u-234	u-234
5.8359E-06	5.3621E-06	5.4144E-06	4.7260E-06
u-235	u-235	u-235	u-235
4.3971E-04	3.6011E-04	3.6013E-04	2.6131E-04
u-236	u-236	u-236	u-236
7.5289E-05	8.8045E-05	8.8059E-05	1.0250E-04
u-238	u-238	u-238	u-238
2.1961E-02	2.1869E-02	2.1869E-02	2.1721E-02
pu-238	pu-238	pu-238	pu-238
8.7306E-07	1.6596E-06	1.6338E-06	3.3524E-06
pu-239	pu-239	pu-239	pu-239
1.1643E-04	1.2775E-04	1.2773E-04	1.3726E-04
pu-240	pu-240	pu-240	pu-240
2.5876E-05	3.4197E-05	3.4196E-05	4.5639E-05
pu-241	pu-241	pu-241	pu-241
1.2752E-05	2.1717E-05	1.7901E-05	2.9970E-05
pu-242	pu-242	pu-242	pu-242
2.2414E-06	4.3201E-06	4.3201E-06	8.5976E-06
am-241	am-241	am-241	am-241
3.7270E-06	1.5388E-06	5.3326E-06	2.2852E-06
am-243	am-243	am-243	am-243
2.4330E-07	6.2387E-07	6.2364E-07	1.7001E-06
np-237	np-237	np-237	np-237
5.4740E-06	7.6703E-06	7.6929E-06	1.1159E-05
mo-95	mo-95	mo-95	mo-95
2.7176E-05	3.3791E-05	3.3995E-05	4.3479E-05
tc-99	tc-99	tc-99	tc-99
2.6392E-05	3.3107E-05	3.3106E-05	4.2640E-05
ru-101	ru-101	ru-101	ru-101
2.3924E-05	3.0616E-05	3.0616E-05	4.0638E-05
rh-103	rh-103	rh-103	rh-103
1.5542E-05	1.9418E-05	1.9422E-05	2.4666E-05
ag-109	ag-109	ag-109	ag-109
1.8295E-06	2.6460E-06	2.6460E-06	3.9821E-06
cs-133	cs-133	cs-133	cs-133
2.8876E-05	3.6155E-05	3.6155E-05	4.6417E-05
sm-147	sm-147	sm-147	sm-147
5.6138E-06	3.2455E-06	6.6053E-06	4.1595E-06
sm-149	sm-149	sm-149	sm-149
1.6822E-07	1.7425E-07	1.7425E-07	1.7807E-07
sm-150	sm-150	sm-150	sm-150
6.1075E-06	8.0456E-06	8.0456E-06	1.0966E-05
sm-151	sm-151	sm-151	sm-151
4.6989E-07	5.3724E-07	5.2094E-07	6.0657E-07
sm-152	sm-152	sm-152	sm-152
2.7327E-06	3.4582E-06	3.4584E-06	4.4661E-06
nd-143	nd-143	nd-143	nd-143
2.2047E-05	2.6601E-05	2.6601E-05	3.2239E-05
nd-145	nd-145	nd-145	nd-145
1.6079E-05	2.0004E-05	2.0004E-05	2.5486E-05
eu-153	eu-153	eu-153	eu-153
1.7629E-06	2.5018E-06	2.5019E-06	3.6786E-06
gd-155	gd-155	gd-155	gd-155
1.0243E-07	4.2820E-08	1.5684E-07	7.1723E-08
o	o	o	o
4.6215E-02	4.6215E-02	4.6215E-02	4.6215E-02

Data set No. 38	Data set No. 39	Data set No. 40	Data set No. 41
3.6wt%U235, 40GWD/MTU cooling time (yr)=5.0 axial location 4 & 6 (32.012GWD/MTU)	3.6wt%U235, 40GWD/MTU cooling time (yr)=1.0 axial location 5 (43.807GWD/MTU)	3.6wt%U235, 40GWD/MTU cooling time (yr)=5.0 axial location 5 (43.807GWD/MTU)	4.5wt%U235, 30GWD/MTU cooling time (yr)=1.0 axial location 1 & 9 (12.330GWD/MTU)
u-234 4.8319E-06	u-234 3.8901E-06	u-234 4.1066E-06	u-234 7.2649E-06
u-235 2.6133E-04	u-235 1.5577E-04	u-235 1.5579E-04	u-235 7.4704E-04
u-236 1.0252E-04	u-236 1.1482E-04	u-236 1.1484E-04	u-236 6.3195E-05
u-238 2.1721E-02	u-238 2.1488E-02	u-238 2.1488E-02	u-238 2.1871E-02
pu-238 3.3050E-06	pu-238 6.8627E-06	pu-238 6.7616E-06	pu-238 2.8641E-07
pu-239 1.3725E-04	pu-239 1.4251E-04	pu-239 1.4249E-04	pu-239 9.3233E-05
pu-240 4.5673E-05	pu-240 5.9179E-05	pu-240 5.9366E-05	pu-240 1.2878E-05
pu-241 2.4703E-05	pu-241 3.8375E-05	pu-241 3.1631E-05	pu-241 6.2410E-06
pu-242 8.5976E-06	pu-242 1.6677E-05	pu-242 1.6677E-05	pu-242 4.2866E-07
am-241 7.5195E-06	am-241 3.1214E-06	am-241 9.8225E-06	am-241 3.7294E-07
am-243 1.6995E-06	am-243 4.4734E-06	am-243 4.4718E-06	am-243 2.9094E-08
np-237 1.1191E-05	np-237 1.6097E-05	np-237 1.6140E-05	np-237 3.1036E-06
mo-95 4.3674E-05	mo-95 5.6436E-05	mo-95 5.6620E-05	mo-95 1.8489E-05
tc-99 4.2639E-05	tc-99 5.5288E-05	tc-99 5.5287E-05	tc-99 1.7929E-05
ru-101 4.0638E-05	ru-101 5.5095E-05	ru-101 5.5095E-05	ru-101 1.5737E-05
rh-103 2.4671E-05	rh-103 3.0949E-05	rh-103 3.0953E-05	rh-103 1.0198E-05
ag-109 3.9821E-06	ag-109 6.0171E-06	ag-109 6.0171E-06	ag-109 7.9138E-07
cs-133 4.6417E-05	cs-133 5.9862E-05	cs-133 5.9862E-05	cs-133 1.9651E-05
sm-147 7.7375E-06	sm-147 5.1613E-06	sm-147 8.7656E-06	sm-147 1.7068E-06
sm-149 1.7807E-07	sm-149 1.7770E-07	sm-149 1.7770E-07	sm-149 1.7444E-07
sm-150 1.0966E-05	sm-150 1.5068E-05	sm-150 1.5068E-05	sm-150 3.7319E-06
sm-151 5.8816E-07	sm-151 6.9223E-07	sm-151 6.7123E-07	sm-151 4.7687E-07
sm-152 4.4663E-06	sm-152 5.7726E-06	sm-152 5.7728E-06	sm-152 1.6948E-06
nd-143 3.2239E-05	nd-143 3.8045E-05	nd-143 3.8045E-05	nd-143 1.6076E-05
nd-145 2.5486E-05	nd-145 3.2614E-05	nd-145 3.2614E-05	nd-145 1.1161E-05
eu-153 3.6787E-06	eu-153 5.3722E-06	eu-153 5.3723E-06	eu-153 9.0062E-07
gd-155 2.6288E-07	gd-155 1.2348E-07	gd-155 4.5301E-07	gd-155 1.4974E-08
o 4.6215E-02	o 4.6215E-02	o 4.6215E-02	o 4.6219E-02

Data set No. 42	Data set No. 43	Data set No. 44	Data set No. 45
4.5wt%U235, 30GWD/MTU	4.5wt%U235, 30GWD/MTU	4.5wt%U235, 30GWD/MTU	4.5wt%U235, 30GWD/MTU
cooling time (yr)=5.0	cooling time (yr)=1.0	cooling time (yr)=5.0	cooling time (yr)=1.0
axial location 1 & 9	axial location 2 & 8	axial location 2 & 8	axial location 3 & 7
(12.330GWD/MTU)	(14.041GWD/MTU)	(14.041GWD/MTU)	(18.006GWD/MTU)
u-234 7.2738E-06	u-234 7.1109E-06	u-234 7.1232E-06	u-234 6.7591E-06
u-235 7.4705E-04	u-235 7.1102E-04	u-235 7.1103E-04	u-235 6.3249E-04
u-236 6.3201E-05	u-236 6.9644E-05	u-236 6.9650E-05	u-236 8.3446E-05
u-238 2.1871E-02	u-238 2.1846E-02	u-238 2.1846E-02	u-238 2.1787E-02
pu-238 2.7907E-07	pu-238 3.9483E-07	pu-238 3.8525E-07	pu-238 7.3356E-07
pu-239 9.3222E-05	pu-239 1.0091E-04	pu-239 1.0090E-04	pu-239 1.1569E-04
pu-240 1.2872E-05	pu-240 1.5353E-05	pu-240 1.5346E-05	pu-240 2.1172E-05
pu-241 5.1443E-06	pu-241 7.9972E-06	pu-241 6.5919E-06	pu-241 1.2395E-05
pu-242 4.2866E-07	pu-242 6.4265E-07	pu-242 6.4265E-07	pu-242 1.3567E-06
am-241 1.4636E-06	am-241 4.9180E-07	am-241 1.8893E-06	am-241 8.1377E-07
am-243 2.9083E-08	am-243 4.8610E-08	am-243 4.8592E-08	am-243 1.2893E-07
np-237 3.1096E-06	np-237 3.7238E-06	np-237 3.7316E-06	np-237 5.2803E-06
mo-95 1.8707E-05	mo-95 2.0938E-05	mo-95 2.1157E-05	mo-95 2.6487E-05
tc-99 1.7929E-05	tc-99 2.0293E-05	tc-99 2.0292E-05	tc-99 2.5652E-05
ru-101 1.5737E-05	ru-101 1.7916E-05	ru-101 1.7916E-05	ru-101 2.2952E-05
rh-103 1.0201E-05	rh-103 1.1560E-05	rh-103 1.1563E-05	rh-103 1.4624E-05
ag-109 7.9138E-07	ag-109 9.7122E-07	ag-109 9.7122E-07	ag-109 1.4313E-06
cs-133 1.9651E-05	cs-133 2.2231E-05	cs-133 2.2231E-05	cs-133 2.8069E-05
sm-147 4.2159E-06	sm-147 1.9623E-06	sm-147 4.6821E-06	sm-147 2.5505E-06
sm-149 1.7444E-07	sm-149 1.8004E-07	sm-149 1.8004E-07	sm-149 1.8905E-07
sm-150 3.7319E-06	sm-150 4.3299E-06	sm-150 4.3299E-06	sm-150 5.7784E-06
sm-151 4.6240E-07	sm-151 5.0124E-07	sm-151 4.8603E-07	sm-151 5.5238E-07
sm-152 1.6949E-06	sm-152 1.9507E-06	sm-152 1.9508E-06	sm-152 2.5243E-06
nd-143 1.6076E-05	nd-143 1.8019E-05	nd-143 1.8019E-05	nd-143 2.2270E-05
nd-145 1.1161E-05	nd-145 1.2599E-05	nd-145 1.2599E-05	nd-145 1.5837E-05
eu-153 9.0062E-07	eu-153 1.0833E-06	eu-153 1.0833E-06	eu-153 1.5474E-06
gd-155 5.4303E-08	gd-155 1.7587E-08	gd-155 6.3779E-08	gd-155 2.4865E-08
o 4.6219E-02	o 4.6219E-02	o 4.6219E-02	o 4.6219E-02

Data set No. 46	Data set No. 47	Data set No. 48	Data set No. 49
4.5wt&U235, 30GWD/MTU cooling time (yr)=5.0 axial location 3 & 7 (18.006GWD/MTU)	4.5wt&U235, 30GWD/MTU cooling time (yr)=1.0 axial location 4 & 6 (24.009GWD/MTU)	4.5wt&U235, 30GWD/MTU cooling time (yr)=5.0 axial location 4 & 6 (24.009GWD/MTU)	4.5wt&U235, 30GWD/MTU cooling time (yr)=1.0 axial location 5 (32.855GWD/MTU)
u-234 6.7821E-06	u-234 6.2417E-06	u-234 6.2892E-06	u-234 5.5185E-06
u-235 6.3251E-04	u-235 5.2583E-04	u-235 5.2585E-04	u-235 3.9296E-04
u-236 8.3455E-05	u-236 1.0149E-04	u-236 1.0151E-04	u-236 1.2236E-04
u-238 2.1787E-02	u-238 2.1693E-02	u-238 2.1693E-02	u-238 2.1547E-02
pu-238 7.1790E-07	pu-238 1.5130E-06	pu-238 1.4854E-06	pu-238 3.3089E-06
pu-239 1.1568E-04	pu-239 1.3159E-04	pu-239 1.3158E-04	pu-239 1.4511E-04
pu-240 2.1165E-05	pu-240 2.9950E-05	pu-240 2.9945E-05	pu-240 4.2146E-05
pu-241 1.0217E-05	pu-241 1.9338E-05	pu-241 1.5940E-05	pu-241 2.8801E-05
pu-242 1.3567E-06	pu-242 3.0288E-06	pu-242 3.0288E-06	pu-242 6.7305E-06
am-241 2.9795E-06	am-241 1.3780E-06	am-241 4.7561E-06	am-241 2.2432E-06
am-243 1.2888E-07	am-243 3.9736E-07	am-243 3.9721E-07	am-243 1.2545E-06
np-237 5.2927E-06	np-237 7.8777E-06	np-237 7.8978E-06	np-237 1.1995E-05
mo-95 2.6703E-05	mo-95 3.4552E-05	mo-95 3.4762E-05	mo-95 4.5717E-05
tc-99 2.5652E-05	tc-99 3.3447E-05	tc-99 3.3447E-05	tc-99 4.4219E-05
ru-101 2.2952E-05	ru-101 3.0530E-05	ru-101 3.0530E-05	ru-101 4.1575E-05
rh-103 1.4628E-05	rh-103 1.8995E-05	rh-103 1.8999E-05	rh-103 2.4774E-05
ag-109 1.4313E-06	ag-109 2.2210E-06	ag-109 2.2210E-06	ag-109 3.5242E-06
cs-133 2.8069E-05	cs-133 3.6529E-05	cs-133 3.6529E-05	cs-133 4.8147E-05
sm-147 5.6683E-06	sm-147 3.4066E-06	sm-147 6.9313E-06	sm-147 4.5297E-06
sm-149 1.8905E-07	sm-149 1.9609E-07	sm-149 1.9609E-07	sm-149 1.9990E-07
sm-150 5.7784E-06	sm-150 8.0419E-06	sm-150 8.0419E-06	sm-150 1.1326E-05
sm-151 5.3562E-07	sm-151 6.1929E-07	sm-151 6.0050E-07	sm-151 7.0207E-07
sm-152 2.5244E-06	sm-152 3.3453E-06	sm-152 3.3455E-06	sm-152 4.4607E-06
nd-143 2.2270E-05	nd-143 2.8054E-05	nd-143 2.8054E-05	nd-143 3.5176E-05
nd-145 1.5837E-05	nd-145 2.0493E-05	nd-145 2.0493E-05	nd-145 2.6836E-05
eu-153 1.5474E-06	eu-153 2.3310E-06	eu-153 2.3310E-06	eu-153 3.5819E-06
gd-155 9.0177E-08	gd-155 3.9606E-08	gd-155 1.4372E-07	gd-155 6.9558E-08
o 4.6219E-02	o 4.6219E-02	o 4.6219E-02	o 4.6219E-02

Data set No. 50	Data set No. 51	Data set No. 52	Data set No. 53
4.5wt%U235, 30GWD/MTU	4.5wt%U235, 50GWD/MTU	4.5wt%U235, 50GWD/MTU	4.5wt%U235, 50GWD/MTU
cooling time (yr)=5.0	cooling time (yr)=1.0	cooling time (yr)=5.0	cooling time (yr)=1.0
axial location 5	axial location 1 & 9	axial location 1 & 9	axial location 2 & 8
(32.855GWD/MTU)	(21.565GWD/MTU)	(21.565GWD/MTU)	(24.023GWD/MTU)
u-234	u-234	u-234	u-234
5.6227E-06	6.4500E-06	6.4862E-06	6.2405E-06
u-235	u-235	u-235	u-235
3.9298E-04	5.6755E-04	5.6757E-04	5.2560E-04
u-236	u-236	u-236	u-236
1.2238E-04	9.4545E-05	9.4556E-05	1.0153E-04
u-238	u-238	u-238	u-238
2.1547E-02	2.1732E-02	2.1732E-02	2.1693E-02
pu-238	pu-238	pu-238	pu-238
3.2553E-06	1.1544E-06	1.1322E-06	1.5152E-06
pu-239	pu-239	pu-239	pu-239
1.4509E-04	1.2592E-04	1.2591E-04	1.3162E-04
pu-240	pu-240	pu-240	pu-240
4.2164E-05	2.6401E-05	2.6395E-05	2.9970E-05
pu-241	pu-241	pu-241	pu-241
2.3740E-05	1.6516E-05	1.3614E-05	1.9354E-05
pu-242	pu-242	pu-242	pu-242
6.7305E-06	2.2623E-06	2.2623E-06	3.0335E-06
am-241	am-241	am-241	am-241
7.2733E-06	1.1411E-06	4.0266E-06	1.3794E-06
am-243	am-243	am-243	am-243
1.2540E-06	2.6232E-07	2.6222E-07	3.9824E-07
np-237	np-237	np-237	np-237
1.2026E-05	6.7920E-06	6.8089E-06	7.8840E-06
mo-95	mo-95	mo-95	mo-95
4.5919E-05	3.1317E-05	3.1530E-05	3.4570E-05
tc-99	tc-99	tc-99	tc-99
4.4219E-05	3.0320E-05	3.0319E-05	3.3465E-05
ru-101	ru-101	ru-101	ru-101
4.1575E-05	2.7452E-05	2.7452E-05	3.0548E-05
rh-103	rh-103	rh-103	rh-103
2.4779E-05	1.7256E-05	1.7260E-05	1.9004E-05
ag-109	ag-109	ag-109	ag-109
3.5242E-06	1.8879E-06	1.8879E-06	2.2230E-06
cs-133	cs-133	cs-133	cs-133
4.8147E-05	3.3140E-05	3.3140E-05	3.6549E-05
sm-147	sm-147	sm-147	sm-147
8.3505E-06	3.0651E-06	6.4488E-06	3.4086E-06
sm-149	sm-149	sm-149	sm-149
1.9990E-07	1.9390E-07	1.9390E-07	1.9611E-07
sm-150	sm-150	sm-150	sm-150
1.1326E-05	7.1174E-06	7.1174E-06	8.0472E-06
sm-151	sm-151	sm-151	sm-151
6.8077E-07	5.9331E-07	5.7531E-07	6.1943E-07
sm-152	sm-152	sm-152	sm-152
4.4610E-06	3.0176E-06	3.0178E-06	3.3471E-06
nd-143	nd-143	nd-143	nd-143
3.5176E-05	2.5793E-05	2.5793E-05	2.8067E-05
nd-145	nd-145	nd-145	nd-145
2.6836E-05	1.8633E-05	1.8633E-05	2.0504E-05
eu-153	eu-153	eu-153	eu-153
3.5819E-06	2.0026E-06	2.0026E-06	2.3329E-06
gd-155	gd-155	gd-155	gd-155
2.5275E-07	3.3040E-08	1.1986E-07	3.9645E-08
o	o	o	o
4.6219E-02	4.6219E-02	4.6219E-02	4.6219E-02

Data set No. 54 4.5wt%U235, 50GWD/MTU cooling time (yr)=5.0 axial location 2 & 8 (24.023GWD/MTU)	Data set No. 55 4.5wt%U235, 50GWD/MTU cooling time (yr)=1.0 axial location 3 & 7 (30.580GWD/MTU)	Data set No. 56 4.5wt%U235, 50GWD/MTU cooling time (yr)=5.0 axial location 3 & 7 (30.580GWD/MTU)	Data set No. 57 4.5wt%U235, 50GWD/MTU cooling time (yr)=1.0 axial location 4 & 6 (40.424GWD/MTU)		
u-234	6.2881E-06	5.6995E-06	5.7868E-06	u-234	4.9433E-06
u-235	5.2562E-04	4.2453E-04	4.2455E-04	u-235	3.0000E-04
u-236	1.0155E-04	1.1761E-04	1.1763E-04	u-236	1.3532E-04
u-238	2.1693E-02	2.1585E-02	2.1585E-02	u-238	2.1413E-02
pu-238	1.4876E-06	2.7719E-06	2.7262E-06	pu-238	5.4525E-06
pu-239	1.3161E-04	1.4250E-04	1.4249E-04	pu-239	1.5066E-04
pu-240	2.9965E-05	3.9132E-05	3.9140E-05	pu-240	5.1412E-05
pu-241	1.5953E-05	2.6524E-05	2.1863E-05	pu-241	3.5395E-05
pu-242	3.0335E-06	5.6472E-06	5.6472E-06	pu-242	1.0893E-05
am-241	4.7603E-06	2.0253E-06	6.6579E-06	am-241	2.9059E-06
am-243	3.9809E-07	9.7389E-07	9.7353E-07	am-243	2.5117E-06
np-237	7.9041E-06	1.0920E-05	1.0948E-05	np-237	1.5563E-05
mo-95	3.4781E-05	4.2926E-05	4.3130E-05	mo-95	5.4612E-05
tc-99	3.3465E-05	4.1532E-05	4.1531E-05	tc-99	5.2747E-05
ru-101	3.0548E-05	3.8751E-05	3.8751E-05	ru-101	5.0881E-05
rh-103	1.9008E-05	2.3367E-05	2.3371E-05	rh-103	2.9052E-05
ag-109	2.2230E-06	3.1774E-06	3.1774E-06	ag-109	4.7134E-06
cs-133	3.6549E-05	4.5257E-05	4.5257E-05	cs-133	5.7263E-05
sm-147	6.9339E-06	4.2601E-06	8.0315E-06	sm-147	5.3175E-06
sm-149	1.9611E-07	1.9936E-07	1.9936E-07	sm-149	1.9993E-07
sm-150	8.0472E-06	1.0496E-05	1.0496E-05	sm-150	1.3997E-05
sm-151	6.0064E-07	6.8230E-07	6.6160E-07	sm-151	7.6073E-07
sm-152	3.3473E-06	4.1841E-06	4.1844E-06	sm-152	5.3313E-06
nd-143	2.8067E-05	3.3502E-05	3.3502E-05	nd-143	3.9984E-05
nd-145	2.0504E-05	2.5263E-05	2.5263E-05	nd-145	3.1783E-05
eu-153	2.3329E-06	3.2545E-06	3.2546E-06	eu-153	4.6704E-06
gd-155	1.4386E-07	6.0994E-08	2.2155E-07	gd-155	1.0133E-07
o	4.6219E-02	4.6219E-02	4.6219E-02	o	4.6219E-02

Data set No. 58	Data set No. 59	Data set No. 60
4.5wt%U235, 50GWD/MTU	4.5wt%U235, 50GWD/MTU	4.5wt%U235, 50GWD/MTU
cooling time (yr)=5.0	cooling time (yr)=1.0	cooling time (yr)=5.0
axial location 4 & 6	axial location 5	axial location 5
(40.424GWD/MTU)	(54.605GWD/MTU)	(54.605GWD/MTU)
u-234	u-234	u-234
5.1152E-06	3.9925E-06	4.3280E-06
u-235	u-235	u-235
3.0002E-04	1.7106E-04	1.7108E-04
u-236	u-236	u-236
1.3534E-04	1.4895E-04	1.4897E-04
u-238	u-238	u-238
2.1413E-02	2.1142E-02	2.1142E-02
pu-238	pu-238	pu-238
5.3656E-06	1.0655E-05	1.0471E-05
pu-239	pu-239	pu-239
1.5064E-04	1.5301E-04	1.5300E-04
pu-240	pu-240	pu-240
5.1484E-05	6.5224E-05	6.5540E-05
pu-241	pu-241	pu-241
2.9175E-05	4.3713E-05	3.6032E-05
pu-242	pu-242	pu-242
1.0893E-05	2.0303E-05	2.0303E-05
am-241	am-241	am-241
9.0866E-06	3.7731E-06	1.1405E-05
am-243	am-243	am-243
2.5108E-06	6.1573E-06	6.1550E-06
np-237	np-237	np-237
1.5602E-05	2.1757E-05	2.1806E-05
mo-95	mo-95	mo-95
5.4806E-05	6.9709E-05	6.9892E-05
tc-99	tc-99	tc-99
5.2746E-05	6.6976E-05	6.6975E-05
ru-101	ru-101	ru-101
5.0881E-05	6.7875E-05	6.7875E-05
rh-103	rh-103	rh-103
2.9057E-05	3.5401E-05	3.5406E-05
ag-109	ag-109	ag-109
4.7134E-06	6.9836E-06	6.9836E-06
cs-133	cs-133	cs-133
5.7263E-05	7.2263E-05	7.2263E-05
sm-147	sm-147	sm-147
9.2075E-06	6.3252E-06	1.0106E-05
sm-149	sm-149	sm-149
1.9993E-07	1.9259E-07	1.9259E-07
sm-150	sm-150	sm-150
1.3997E-05	1.8627E-05	1.8627E-05
sm-151	sm-151	sm-151
7.3765E-07	8.4338E-07	8.1779E-07
sm-152	sm-152	sm-152
5.3316E-06	6.7635E-06	6.7637E-06
nd-143	nd-143	nd-143
3.9984E-05	4.5992E-05	4.5992E-05
nd-145	nd-145	nd-145
3.1783E-05	3.9892E-05	3.9892E-05
eu-153	eu-153	eu-153
4.6705E-06	6.5857E-06	6.5858E-06
gd-155	gd-155	gd-155
3.6871E-07	1.6688E-07	6.0862E-07
o	o	o
4.6219E-02	4.6219E-02	4.6219E-02

Appendix B

Burnup Profiles (10, 30, 40 and 50 GWd/t)

Prepared by Dr. A. Santamarina
and
Dr. P. Albarede

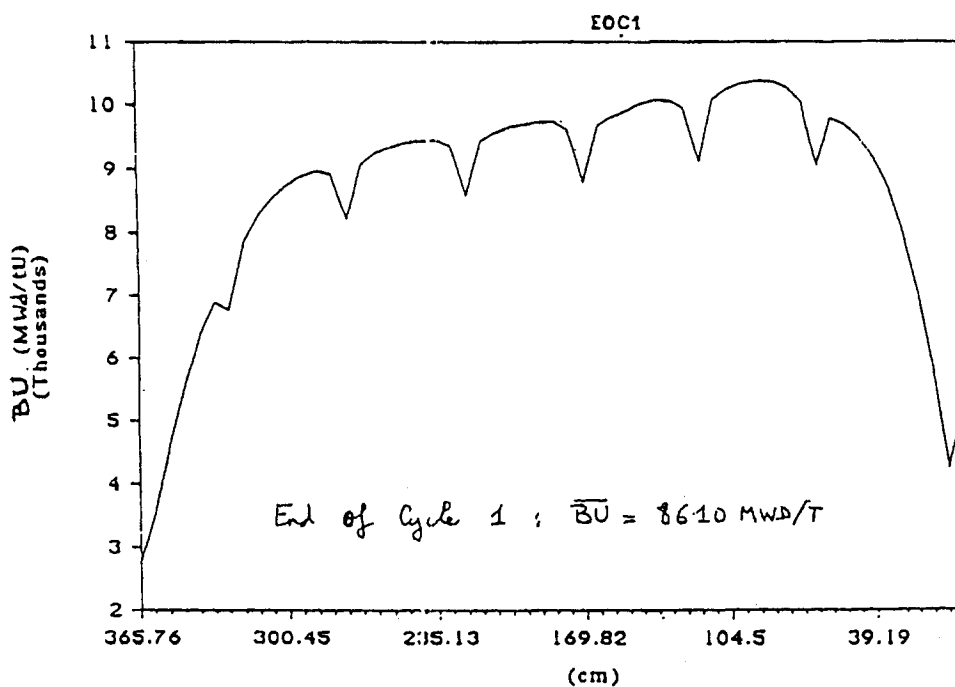


Fig. B.1 Burnup Profile for 10 GWd/t case

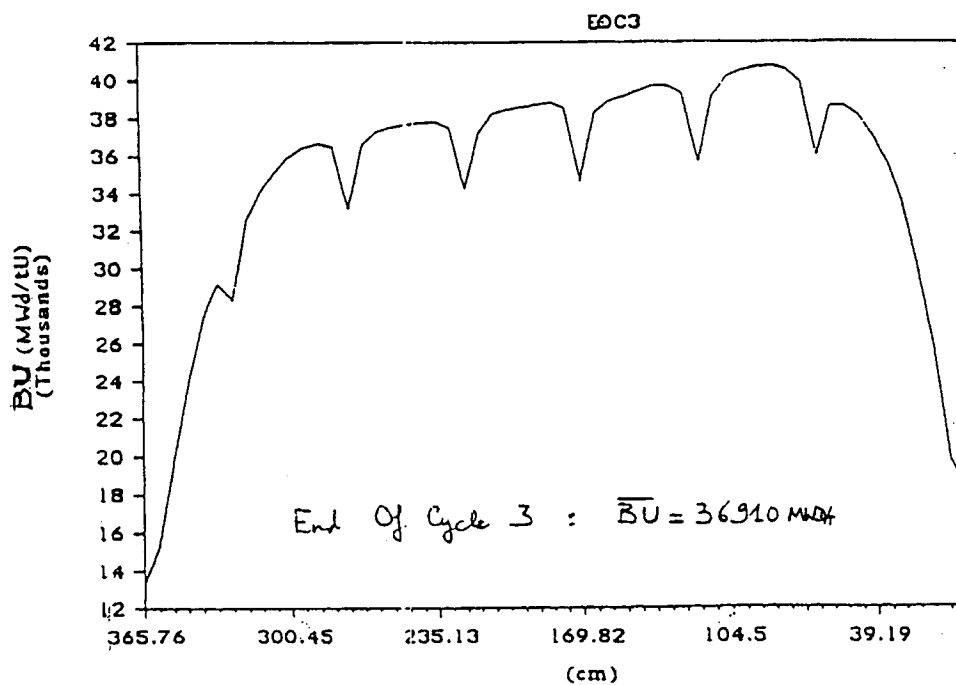


Fig. B.2 Burnup Profile for 30 and 40 GWd/t cases

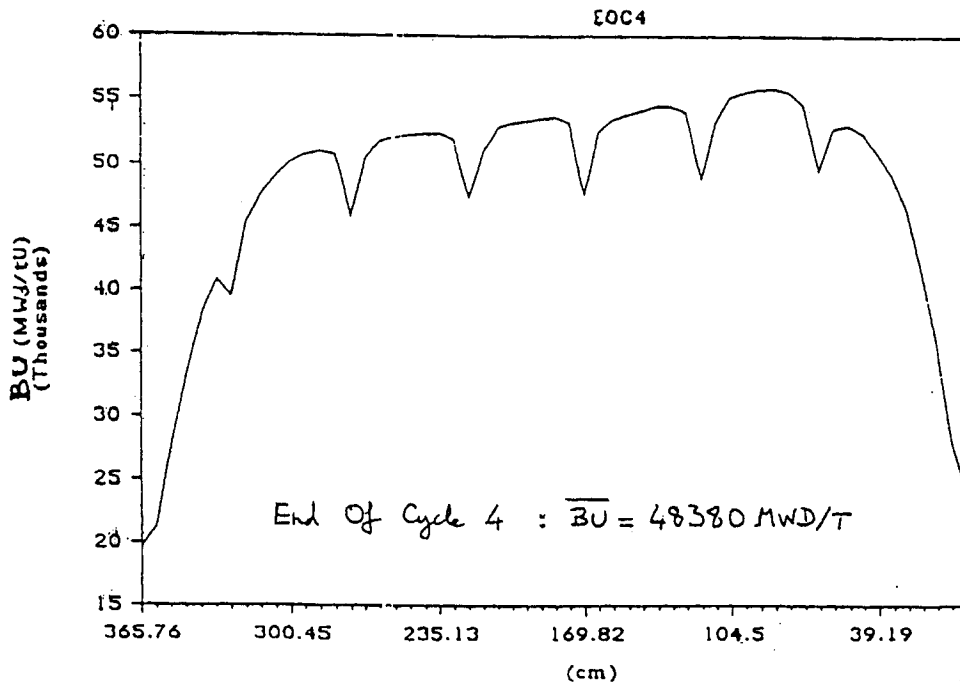


Fig. B.3 Burnup Profile for 50 GWd/t case

Appendix 2 Additional Analyses by Participants

Appendix 2.1 Report from ORNL

Summary of Results for Burnup-Credit Criticality Benchmark

Phase IIA

(Attachments 1 and 2 are omitted)

February 2, 1994

Summary of Results for Burnup-Credit Criticality Benchmark Phase II-A

M. D. DeHart
Oak Ridge National Laboratory*
USA

Introduction

Oak Ridge National Laboratory (ORNL) Phase II-A benchmark calculations [as per NEA/NSC/DOC(93)15, Rev. Oct. 1993] to study the effect of axial burnup profiles have been completed. Results were generated using a configuration-controlled production version of SCALE 4.2 on an IBM RS/6000 with two different SCALE broad-structure cross-section libraries: the 27BURNUPLIB library and the recently developed 44GROUPNDF5 library. 27BURNUPLIB, used by ORNL for most burnup-credit activities to date, is a 27-group library of ENDF/B-IV cross-sections, although most fission product cross-sections were obtained from pre-release ENDF/B-V data. 44GROUPNDF5, a 44-group ENDF/B-V based cross-section library, has been specifically developed for the use in criticality analysis of LWR-type spent fuel assemblies. This summary reports the calculated results, provides a discussion of the trends observed, and briefly proposes preliminary explanations for the trends.

Results and Discussion

Calculations were performed for all of the 42 cases originally proposed in the first draft of the Phase II-A benchmark specifications. Although many of these benchmarks were deleted from the final specification, these additional results are included in this report because they were readily available, and may help in the investigation of trends. The results provided electronically (see Attachments 1-2) to the Phase II-A problem coordinator, Dr. M. Takano of JAERI, are formatted as requested and include only the 26 cases of the final Phase II-A specification.

The Monte Carlo code KENO-V.a, a module of the SCALE 4.2 system, was used to perform the criticality calculations. The KENO geometry was based on a three-dimensional half-length fuel pin, taking advantage of symmetry at the axial midplane. All calculations were based on 500 generations with 1000 neutrons per generation, for a total of 500,000 histories. Because of the

*Managed by Martin Marietta Energy Systems, Inc., under contract DE-AC05-84OR21400 with the U. S. Department of Energy.

stochastic nature of the calculations, all values of k_{eff} have an associated uncertainty, ranging from ± 0.0007 to ± 0.0011 .

Results from both sets of calculations are given in Tables 1 (44-group library) and 2 (27-group library). Note that while k_{∞} values obtained using the 27-group library are lower than those based on 44-group cross-sections (as was expected based on other comparisons of the two libraries), both sets of results illustrate the same trends. Further, the relative differences between corresponding cases with and without the burnup profile are essentially the same for both sets, within the uncertainty of the individual results. Thus calculation of the profile effect for a given set of isotopes is not sensitive to changes between ENDF/B-IV and ENDF/B-V cross-section data. The following trends were observed in both sets of results.

- For low burnups, the effect of the use of the burnup profile gives a smaller value of k_{∞} than the corresponding case with averaged burnup. For high burnups, however, the use of the burnup profile gives a larger value of k_{∞} than that calculated with averaged burnup. In other words, Δk_{axial} ($\equiv k_{\infty, \text{ burnup profile}} - k_{\infty, \text{ averaged profile}}$) is negative for low burnup fuel and positive for high burnup fuel. (Δk_{axial} is a measure of the error in the averaged-burnup model relative to the axial-burnup model.)
- The cross-over point where use of the axial burnup profile is the same as use of the constant (axially averaged) distribution ($\Delta k_{\text{axial}} = 0$) occurs at about 25 GWd/t burnup for 3.6 wt. % enriched fuel and 1 year cooling time, and between 30 and 35 GWd/t burnup for 4.5 wt. % enrichment and 1 year cooling time. Thus, the cross-over point appears to increase with increasing initial enrichment.
- The cross-over point occurs at a lower exposure for a greater cooling time. Increasing the cooling time from 1 year to 5 years caused the cross-over point to decrease to 20 GWd/t for 3.6 wt. % fuel, and between 25 and 30 GWd/t burnup for 4.5 wt. % fuel.
- When fission products are not included, Δk_{axial} is small and close to zero for all exposures and cooling times.
- The trend for Δk_{axial} to increase with burnup appears to be non-linear.

Assuming that both the axial-burnup and averaged-burnup cases would have similar k_{∞} values for very low burnup, then Δk_{axial} would be very close to zero. This suggests that there is an initial decrease in Δk_{axial} as burnup increases, followed by a leveling off and then increase in Δk_{axial} with further exposure. This is illustrated by the Figure 1, which shows the projected behavior of Δk_{axial} as a function of burnup for both 3.6 and 4.5 wt. % enriched fuel and for 1 and 5 years cooling time. The curves are cubic spline

fits to the limited data available, and are not necessarily an accurate representation of the behavior of Δk_{axial} with exposure.

Normalized fission power densities for cases 2, 6, and 19 were also requested in the final benchmark specification. The fission power densities for these cases are shown in Figure 2. For case 2 (3.6 wt. %, 10 GWd/t, 1 y cooling time), the fission density profile strongly resembles a nominal axial flux profile, indicating little burnup effect. However, for cases 6 (3.6 wt. %, 30 GWd/t, 1 y cooling time), and 19 (4.5 wt. %, 50 GWd/t, 1 y cooling time), the effect of burnup is obvious: depleted fuel and burned-in fission products and actinide absorbers significantly reduce the fraction of fissions occurring near the center of the fuel pins, making end regions more significant.

Note that Δk_{axial} increases with increased depression of fission in the center of the fuel for each of the above cases. This behavior suggests that a relationship may exist between the end/center fission density ratio and Δk_{axial} . By approximating the "end region" fission density as the simple average of the fission densities in regions 1-4 of the fuel rod model and assuming the "center region" of the fuel rod is represented by region 5 of the model, one can estimate the ratio of the end-to-center fission densities for each case. Figure 3 shows the end/center ratio plotted as a function of Δk_{axial} for each of the 20 cases which were based on a burnup profile (half of the 40 exposed-fuel cases given in the draft specification). The cases were separated into those containing fission products and those which omitted fission products. Clearly, there is a trend for Δk_{axial} to increase with an increasing end/center fission density ratio. Additionally, it appears that the end/center ratio is significantly decreased when fission products are removed, thus Δk_{axial} is reduced in such cases. Actinide absorbers also affect Δk_{axial} , but to a lesser extent. The error in the use of an averaged-burnup model is due to its inability to properly predict axial variation in fission densities due to the production of parasitic absorbers.

Conclusions

In a no-axial-burnup model, fission products are evenly distributed, and fission densities will remain concentrated near the center region of the rod, giving increased weight to fission product absorption. The results discussed above indicate that the use of an averaged-burnup profile in criticality analysis provides an overprediction of k_{∞} for low-burnup fuel assemblies. This is most likely due to the fact that in the burnup-profile model, fission products are more concentrated near the axial center of the fuel, which is the dominant fission region at low burnup. However, for increasing burnup, the fission density distribution moves outward toward the ends of the fuel rod (as indicated in Figures 2 and 3), where parasitic absorber concentrations are reduced. Hence, a no-axial-burnup profile approximation will underpredict

k_{∞} due to overestimated absorption for burnups high enough to have appreciable parasitic absorption.

Finally, calculations performed using both ENDF/B-IV and ENDF/B-V cross-section libraries demonstrate that the effect of the use of the axial profile is independent of the use of either generation of ENDF/B data.

Table 1. 44 GROUPNDF 5 Cross-section Library
 (Shaded results are those for cases which were not requested in the final benchmark specifications)

		Initial Fuel Enrichment					
		3.6 w/o			4.5 w/o		
Cooling Time	F. P.'s	Burnup = 10 GWd/t	Burnup = 30 GWd/t	Burnup = 40 GWd/t	Burnup = 30 GWd/t	Burnup = 50 GWd/t	
1 year	Yes	1.3048±0.0009	1.1322±0.0010	1.0736±0.0011	1.1980±0.0010	1.0827±0.0009	
	No	1.3109±0.0008	1.1348±0.0008	1.0578±0.0007	1.2014±0.0008	1.0584±0.0007	
	Δ	-0.0061	-0.0026	0.0158	-0.0034	0.0243	
	Yes	1.3599±0.0010	1.2314±0.0011	1.1804±0.0010	1.2959±0.0010	1.1942±0.0009	
	No	1.3654±0.0008	1.2405±0.0009	1.1864±0.0009	1.3050±0.0008	1.1957±0.0008	
	Δ	-0.0055	-0.0091	-0.006	-0.0091	-0.0015	
5 years	Yes	1.2967±0.0009	1.1120±0.0009	1.0460±0.0011	1.1812±0.0010	1.0552±0.0011	
	No	1.3080±0.0008	1.1081±0.0007	1.0173±0.0007	1.1794±0.0008	1.0118±0.0007	
	Δ	-0.0113	0.0039	0.0287	0.0018	0.0434	
	Yes	1.3544±0.0011	1.2137±0.0010	1.1586±0.0010	1.2826±0.0010	1.1760±0.0010	
	No	1.3629±0.0008	1.2252±0.0008	1.1597±0.0008	1.2917±0.0008	1.1725±0.0008	
	Δ	-0.0085	-0.0115	-0.0011	-0.0091	0.0035	
Fresh Fuel, 3.6 w/o		1.4322±0.0008					
Fresh Fuel, 4.5 w/o		1.4784±0.0008					

Table 2. 27 BURNUPLIB Cross-section Library
 (Shaded results are those for cases which were not requested in the final benchmark specifications)

Cooling Time	F. P.'s	Burnup Profile	Initial Fuel Enrichment					
			3.6 w/o			4.5 w/o		
			Burnup = 10 GWd/t	Burnup = 30 GWd/t	Burnup = 40 GWd/t	Burnup = 30 GWd/t	Burnup = 50 GWd/t	Burnup = 50 GWd/t
1 year	Yes	Yes	1.2941±0.0009	1.1293±0.0010	1.0716±0.0010	1.1917±0.0010	1.0769±0.0010	
		No	1.3032±0.0008	1.1298±0.0007	1.0539±0.0007	1.1968±0.0008	1.0543±0.0007	
		Δ	-0.0091	-0.0005	0.0177	-0.0051	0.0226	
	No	Yes	1.3500±0.0010	1.2267±0.0009	1.1737±0.0010	1.2881±0.0010	1.1915±0.0010	
		No	1.3568±0.0008	1.2372±0.0008	1.1818±0.0008	1.2998±0.0008	1.1945±0.0008	
		Δ	-0.0068	-0.0105	-0.0081	-0.0117	-0.0003	
5 years	Yes	Yes	1.2887±0.0010	1.1080±0.0009	1.0448±0.0011	1.1726±0.0009	1.0504±0.0010	
		No	1.2972±0.0008	1.1014±0.0007	1.0160±0.0007	1.1744±0.0008	1.0102±0.0008	
		Δ	-0.0085	0.0066	0.0288	-0.0018	0.0402	
	No	Yes	1.3464±0.0010	1.2117±0.0009	1.1565±0.0010	1.2738±0.0010	1.1720±0.0010	
		No	1.3531±0.0008	1.2200±0.0008	1.1572±0.0008	1.2854±0.0008	1.1687±0.0008	
		Δ	-0.0067	-0.0083	-0.0007	-0.0116	0.0033	

Fresh Fuel, 3.6 w/o 1.4206±0.0008

Fresh Fuel, 4.5 w/o 1.4676±0.0008

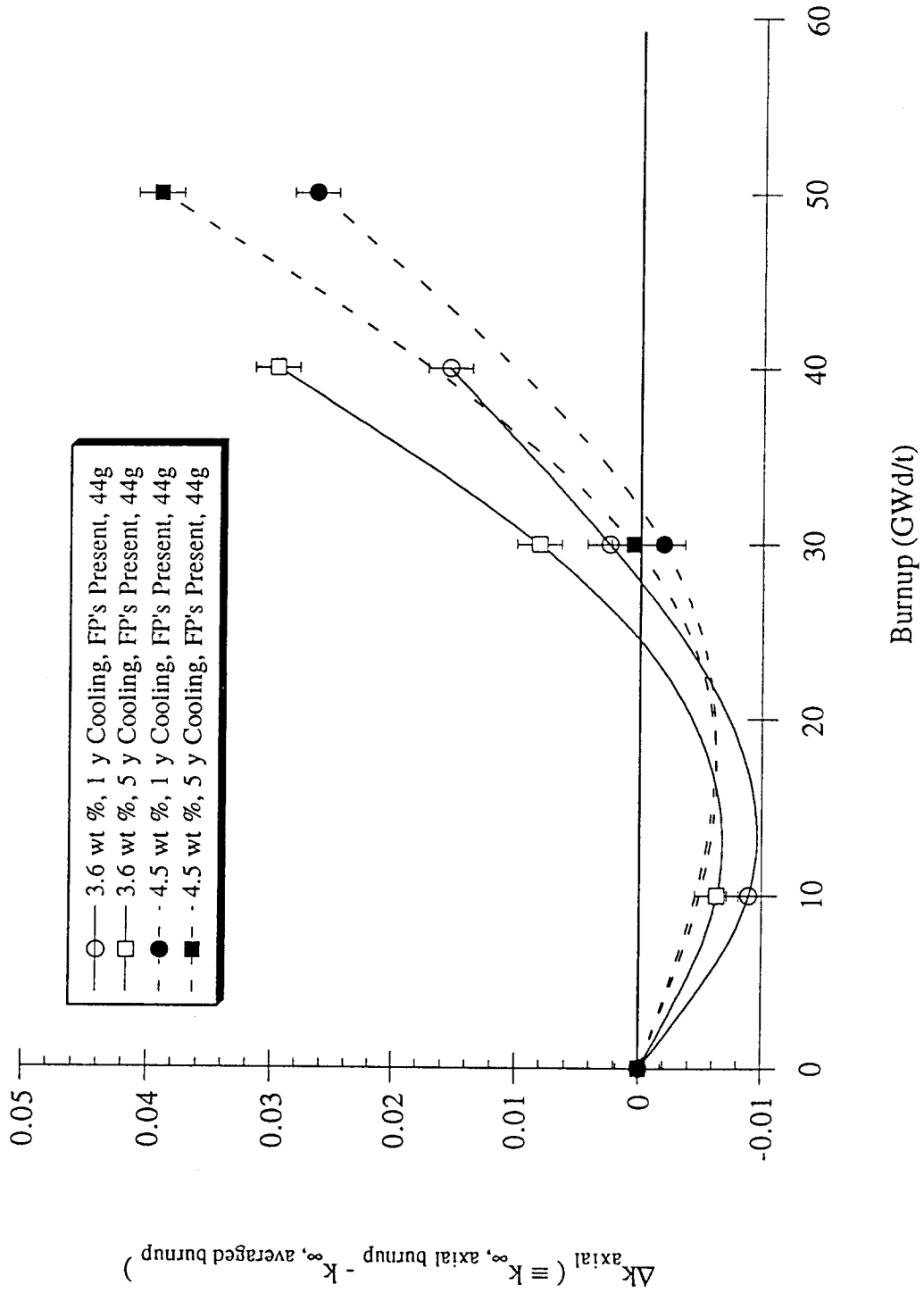


Fig. 1 Variation of Δk_{axial} with Burnup, Cooling Time, and Initial Enrichment

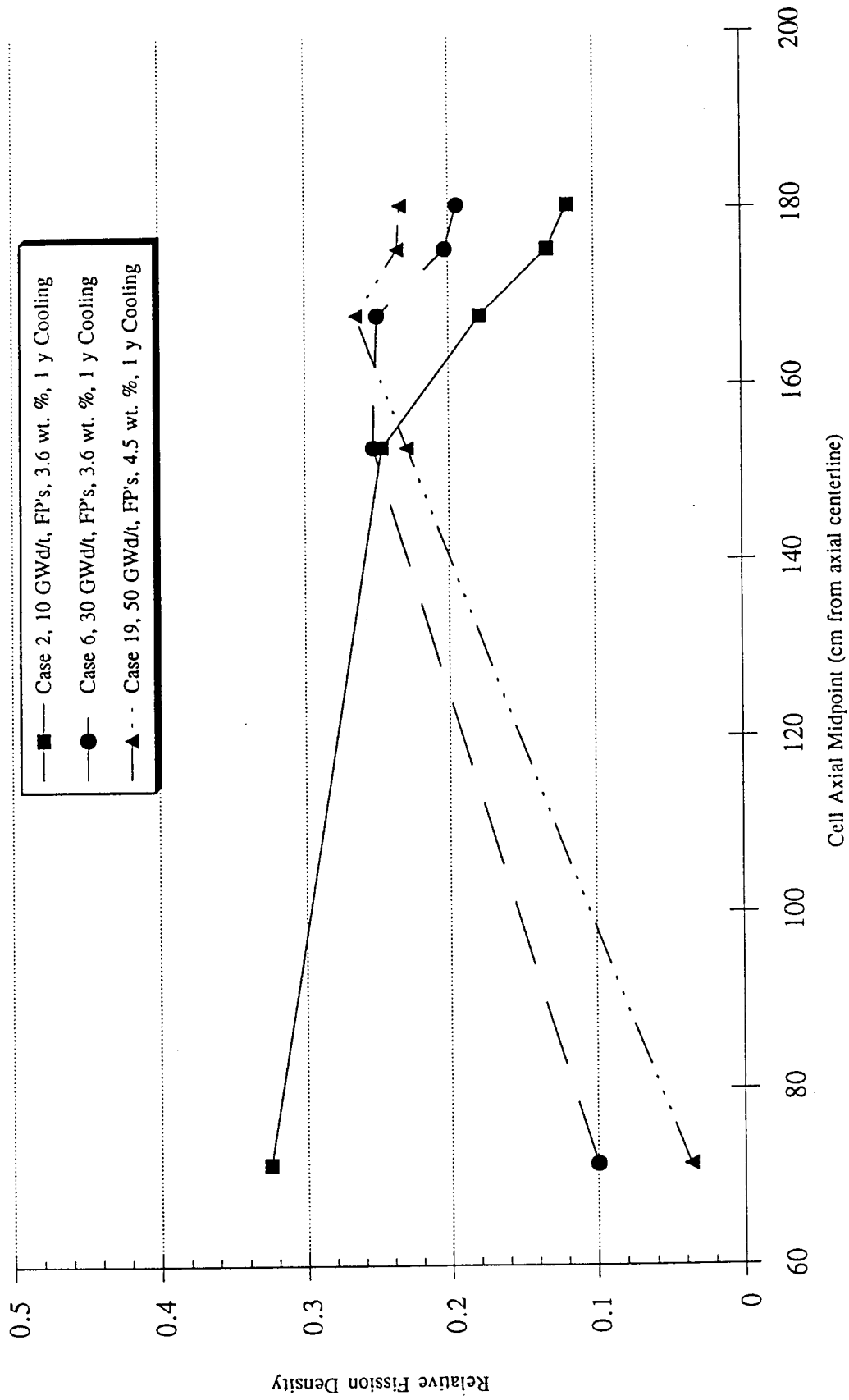


Fig. 2 Fission Power Density Distribution for Various Cases

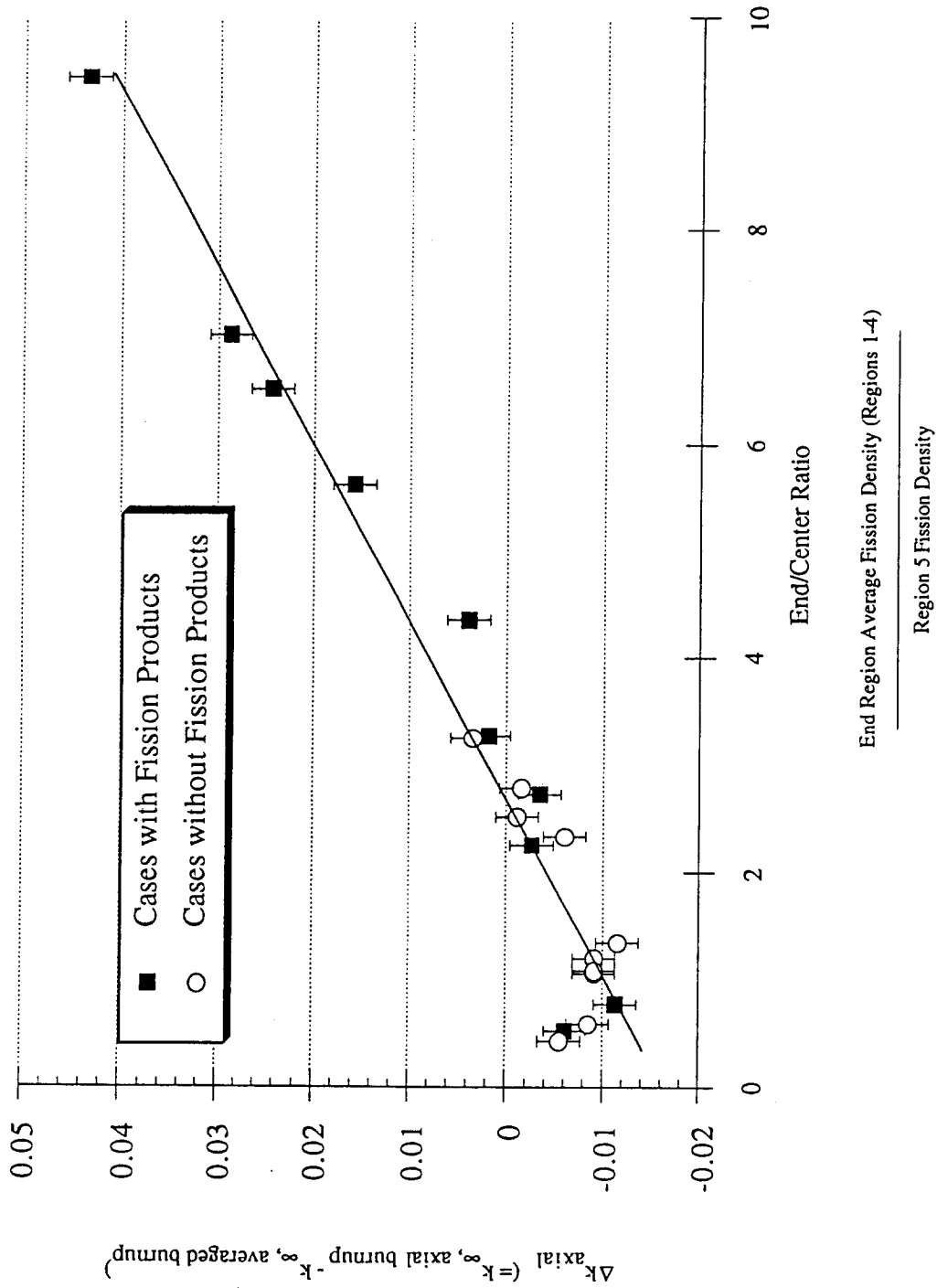


Fig. 3 Δk_{axial} as a Function of End/Center Fission Density Ratio

Appendix 2.2 Additional Figures from Toshiba

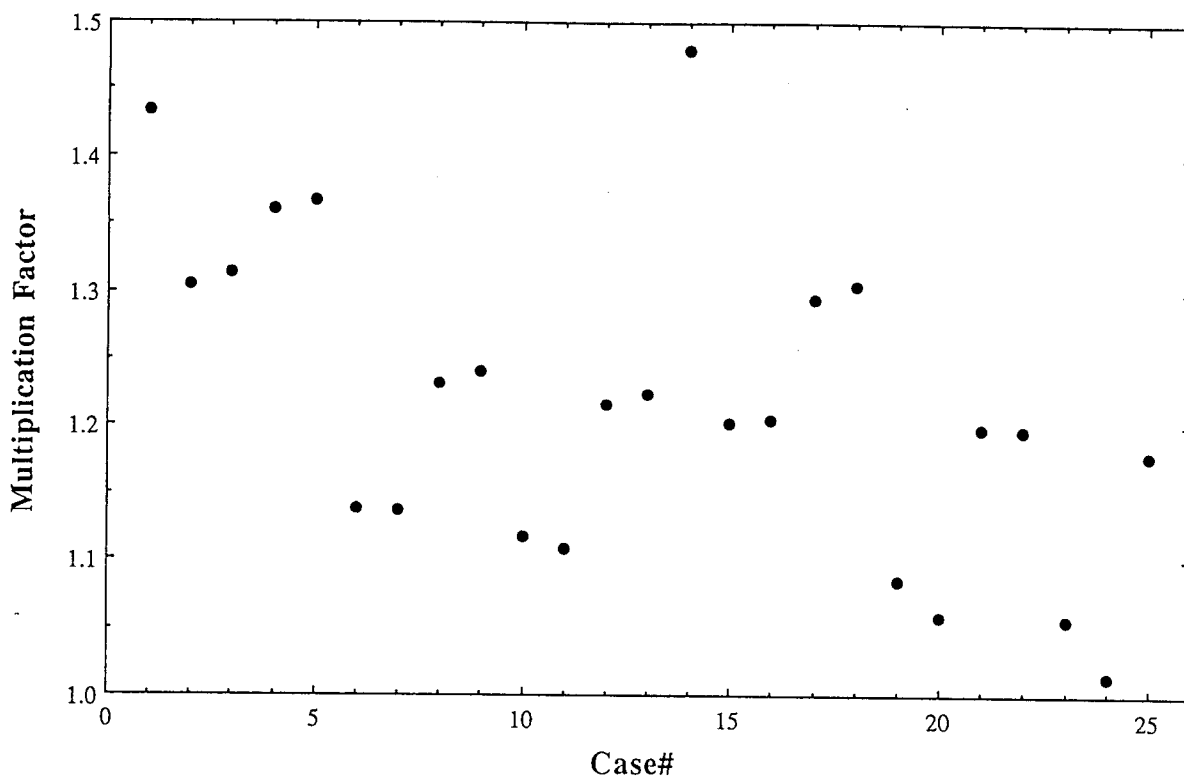


Fig. 1 Comparison of Multiplication Factors by TGBLA/ALEX Calculation

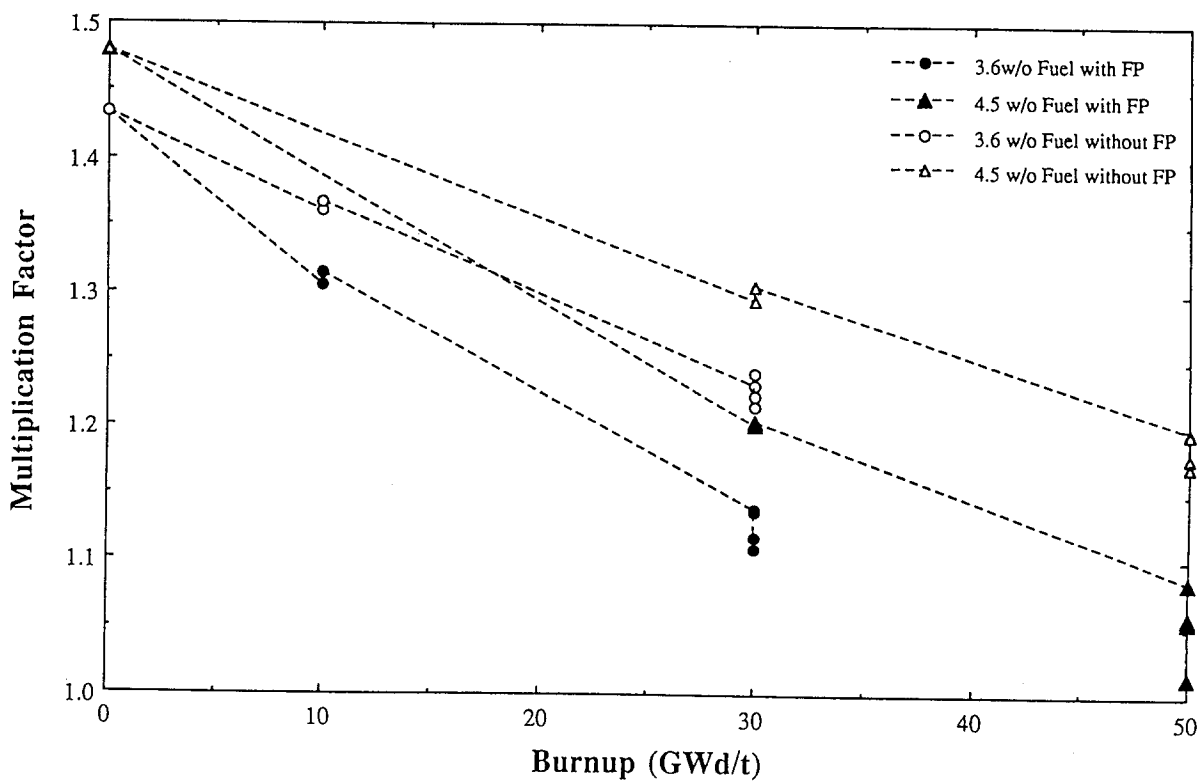


Fig. 2 Comparison of Multiplication Factors by TGBLA/ALEX Calculation

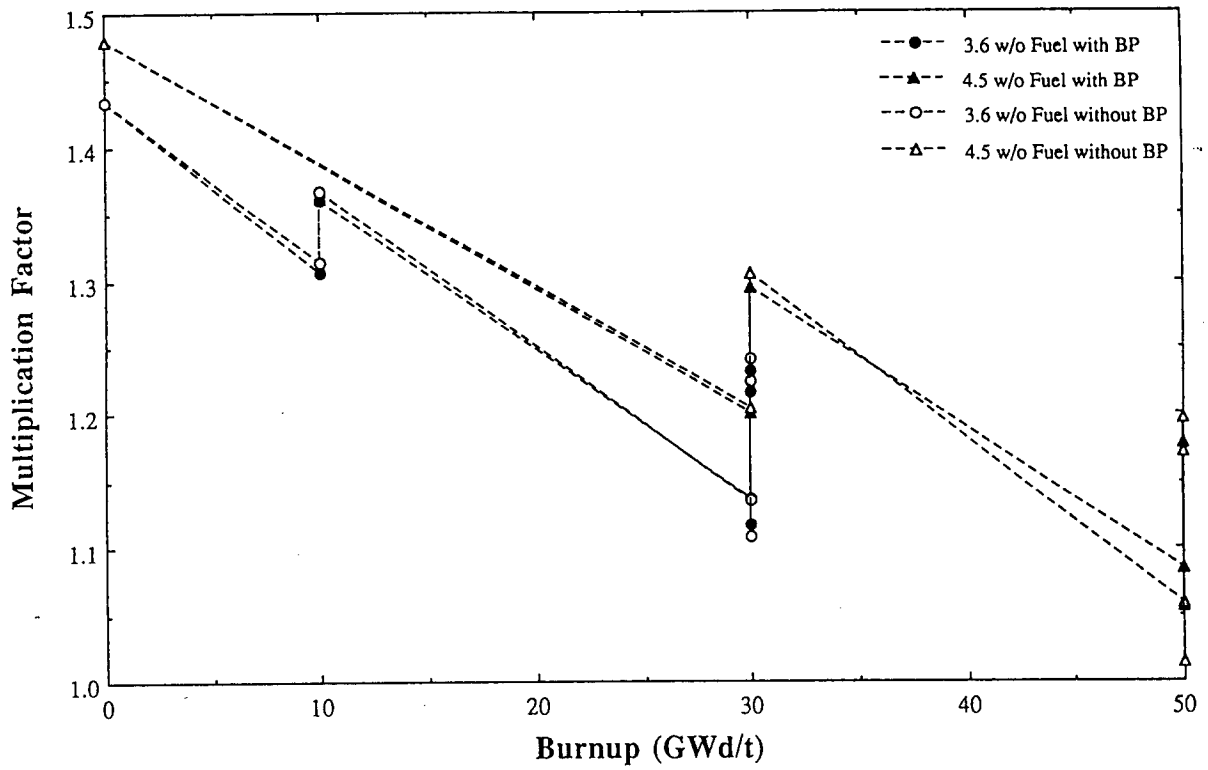


Fig. 3 Comparison of Multiplication Factors by TGBLA/ALEX Calculation

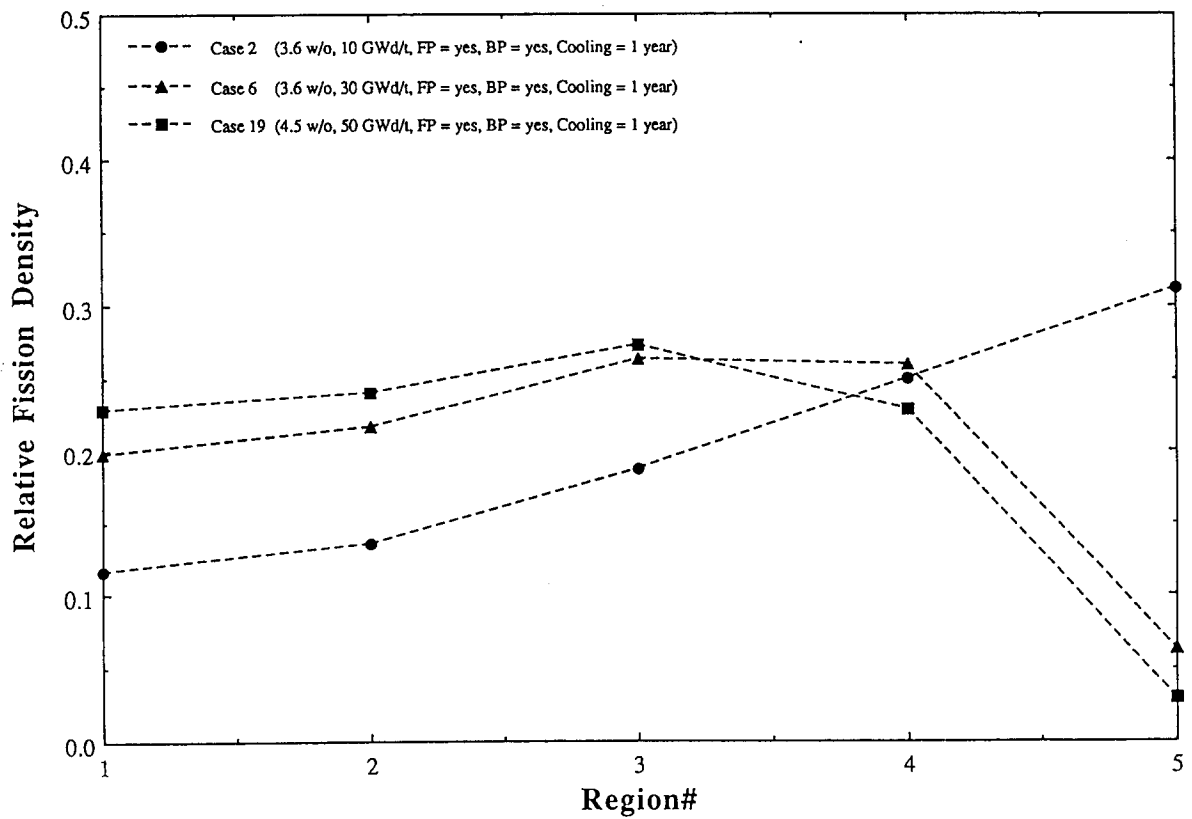


Fig. 4 Comparison of Fission Density Distributions

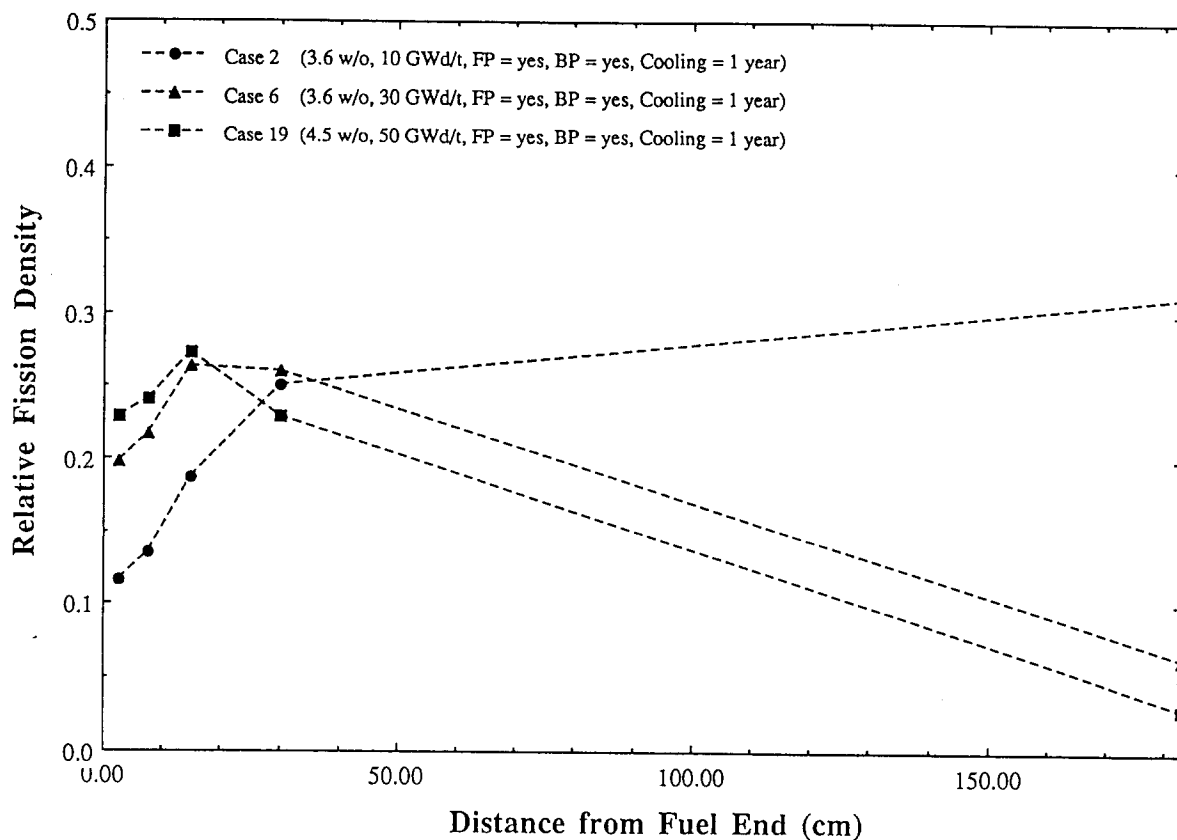


Fig. 5 Comparison of Fission Density Distributions

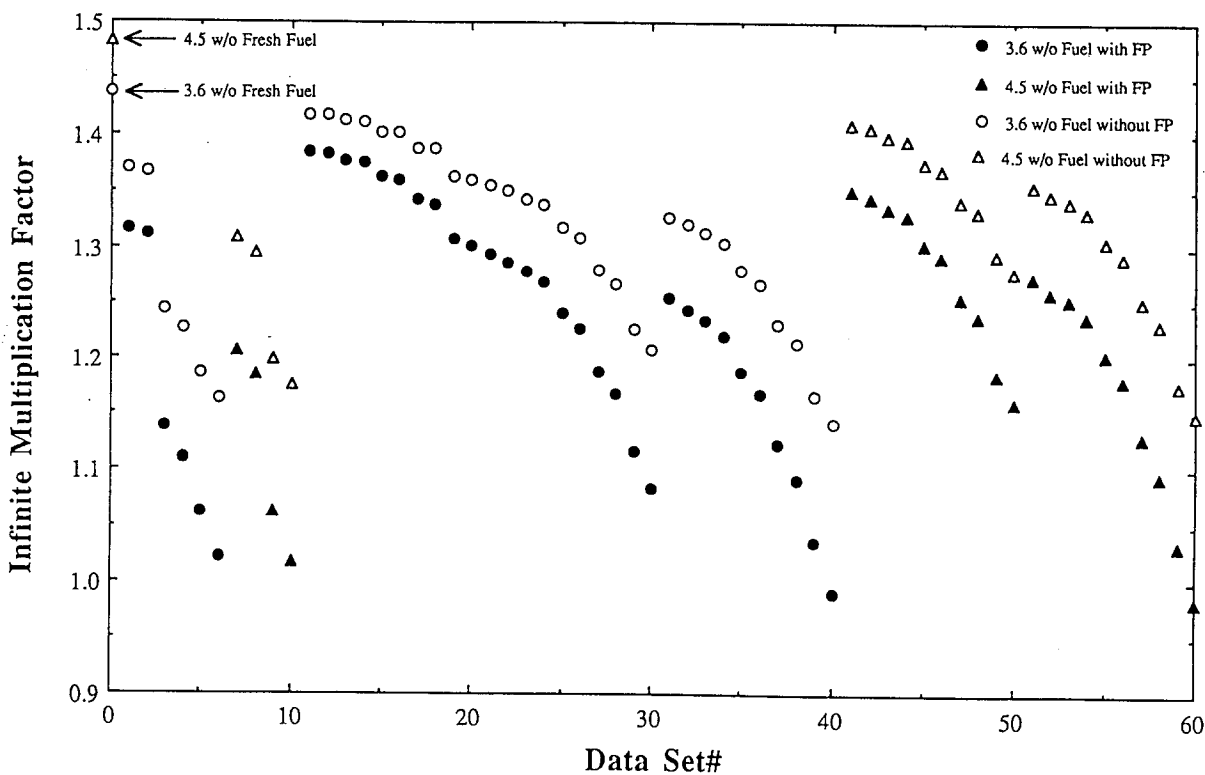


Fig. 6 Comparison of Infinite Multiplication Factors by TGBLA Calculation

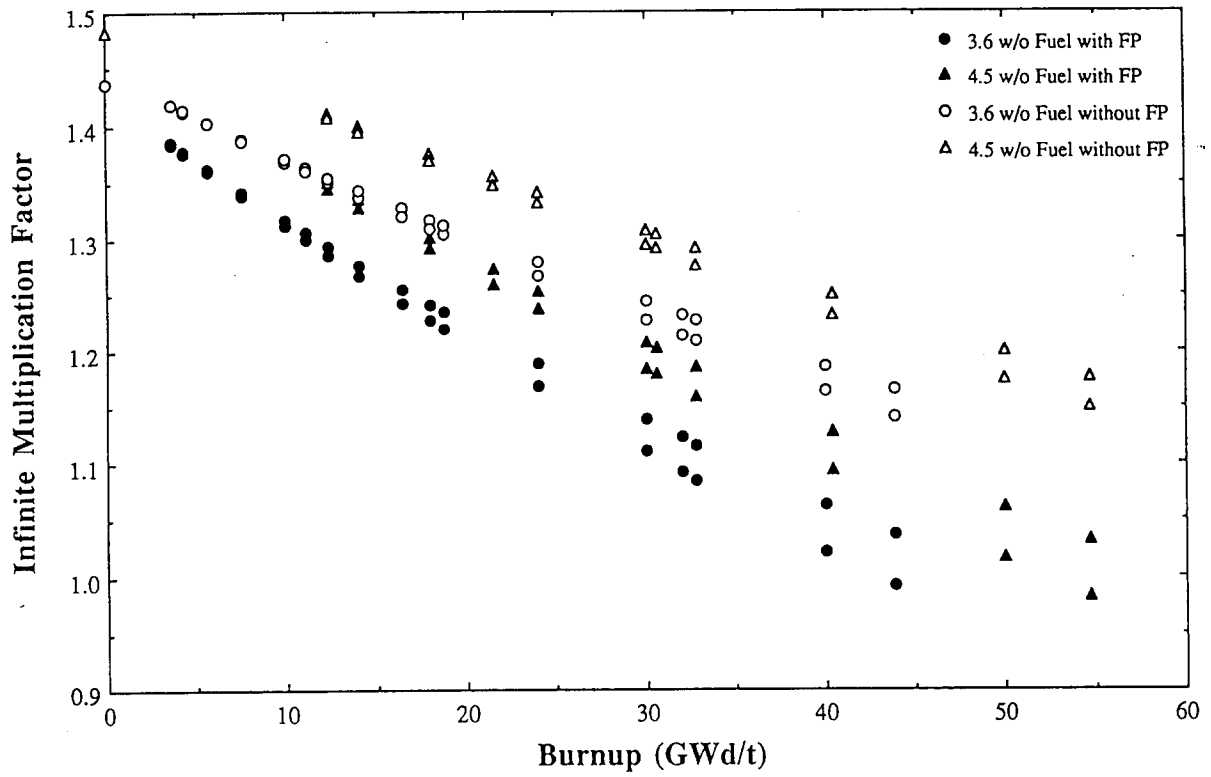


Fig. 7 Comparison of Infinite Multiplication Factors by TGBLA Calculation

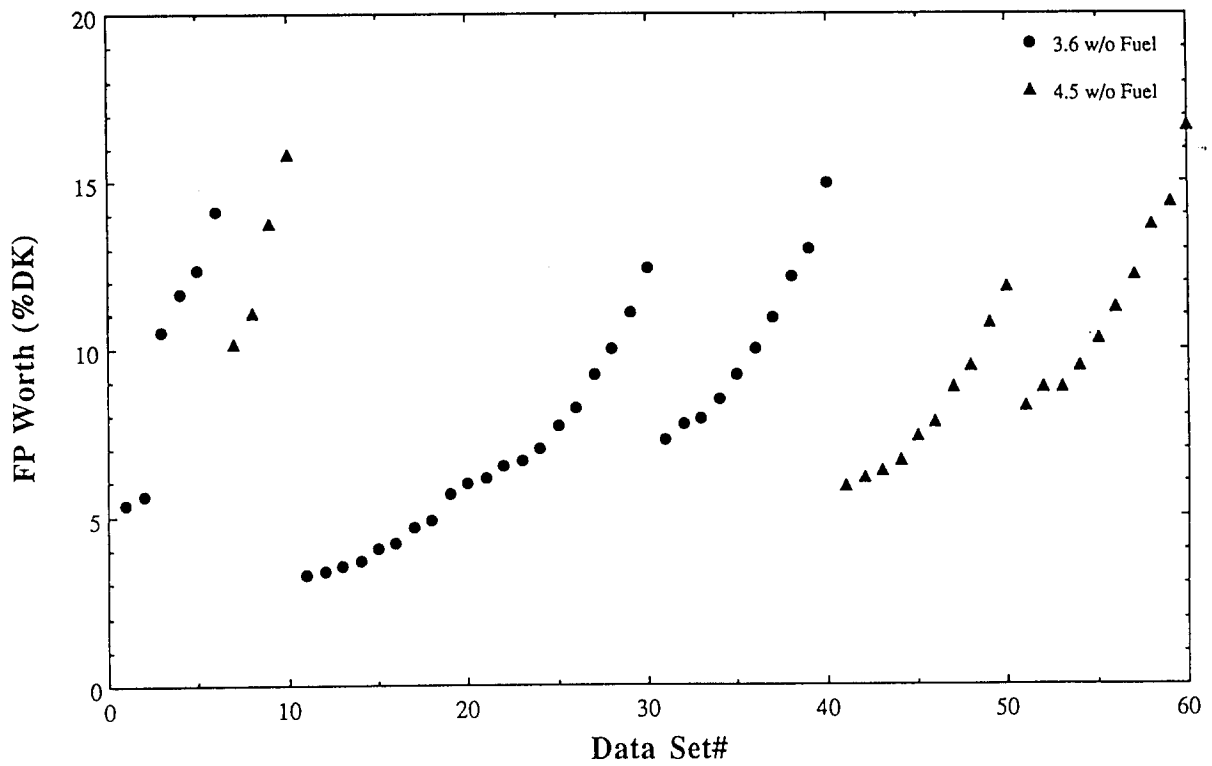


Fig. 8 Comparison of FP Worths by TGBLA Calculation

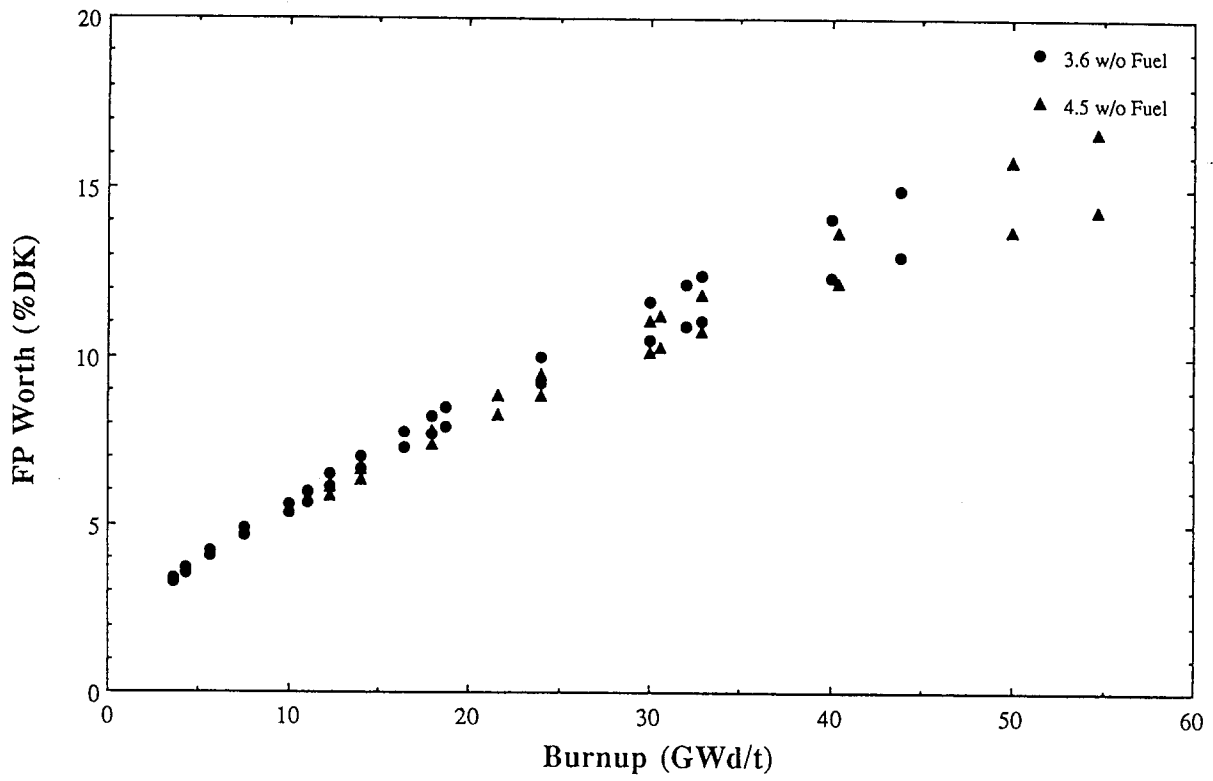


Fig. 9 Comparison of FP Worths by TGBLA Calculation

Appendix 3 Documents on Phase IIA Presented
at 1994 Meeting in Paris

Appendix 3.1 Preliminary Results (Figures and Tables)

Revised,

JAERI

Table 3.1 Summary of Participants, Data and Codes for Phase II A Analysis

No.	COUNTRY	INSTITUTE	PARTICIPANT	NUCLEAR		DATA	CALCULATION			REMARKS
				Origin	Library		No of Groups	CODE	MODEL	
1	Belgium	Belgonucleaire	Maidague			69	LWR-WIMS+ANISN	1-D		Collision Probability > 16-group S8 ANISN
2	France	CEA/DRN	Santamarina	JEF-1	CEA-86	99	APOLLO1+BISTRO	2-D		
3	France	CEA/PSN	Maubert	JEF-1+ENDF/B	CFA-86+H.R.	99	APOLLO1+MORET	3-D	-0.1	APOLLO1(Cell) > MORET(Monte Carlo)
4	Germany	BIS/KE	Schweer	JEF-1	(NJOY)	242	CGM+MORSE-K	3-D	-0.25	Only Zr-90 for Cladding
5	Germany	GRS	Gmal	ENDF-B/4,B/5	27BURNUPLIB	27	SCALE-4	3-D	-0.3	CSAS25
6	Italy	ENEA	Siciliano	JEF-1+ENDL-85	(NJOY)	(Continuous)	MCNP-3	3-D	-0.20	
7	Japan	JAERI(1)	Takano	JENDL-3	MGCL	137	JACS(KENO)	3-D	-0.1	MAIL3>KENOIV
8	Japan	JAERI(2)	Takano	JENDL-3	(NJOY)	(Continuous)	MCNP-4.2	3-D	-0.1	
9	Japan	JINS(1)	Miatake	ENDF-B/4,B/5	27BURNUPLIB	27	SCALE-4	3-D	-0.3	CSASI (NITAWL-II)>KENO-Va
10	Japan	JINS(2)	Miatake	ENDF-B/6	MGCL-JINS	137	MAIL-PI>KENO-V.a	3-D	-0.3	Excl. FP cases
11	Japan	PNC	Nojiri	ENDF-B/4,B/5	27BURNUPLIB	27	SCALE-4	3-D	-0.15	CSAS25
12	Japan	Tohoku Univ.	Suyama	JENDL-3	(NJOY)	(Continuous)	MCNP-4.2	3-D	-0.1	U-234 < ENDL-85, Pu-238 < BMCCS at 0k
13	Japan	Toshiba	Ando	JENDL-3,ENDF-B/4,B/5	B-4,5,J-3	95	TGBLA/ALEX	2-D	(1E-5)	Excl. Mo-95, Lumped Cr,Fe,Zr
14	Spain	CSN	Conde	ENDF-B/4,B/5,JEF-2	E4LTJB7	70	CASMO-3+SIMULATE-3	3-D	(1E-5)	Excl. Mo,Tc,Ru
15	Sweden	E.M. Systems	Mennerdahl	ENDF-B/4,B/5	27BURNUPLIB	27	SCALE-4.0	3-D	-0.15	
16	Switzerland	PSI	Grimm	JEF-1	BOXLIB	70	BOXER	1-D	(1E-5)	Gd from JENDL-2
17	U.K.	AEA Technology	Gulliford	JEF-2 DICE	MONKBTHRM	(Continuous)	MONK6B	3-D	-0.1	
18	U.K.	BNFL	Thorne	UKNDL+JEF2	MONK6B	(Continuous)	MONK6B	3-D	-0.25	
19	U.K.	DOT(1)	Stewart	UKNDL+JEF2	MONK6B	(Continuous)	MONK6B	3-D	-0.15	Am,Np,Ag,Eu < UKENDL
20	U.K.	DOT(2)	Stewart	UKNDL+JEF2	MONK6B	(Continuous)	MONK6B	3-D	-0.15	Am,Np,Ag,Eu < JEF
21	U.K.	DOT(3)	Stewart	UKNDL+JEF2	MONK6B	(Continuous)	MONK6B	3-D	-0.15	No Dataset Adjustment
22	U.S.A.	ORNL(1)	DeHart	ENDF-B/4,B/5	27BURNUPLIB	27	SCALE-4.2	3-D	-0.1	CSAS25
23	U.S.A.	ORNL(2)	DeHart	ENDF-B/5	44GROUPNDF5	44	SCALE-4.2	3-D	-0.1	CSAS25

13-Jun-94

Table 4.2 Multiplication Factors from Participants (4.5 w/o Initial Fuel Enrichment)

No.	COUNTRY	INSTITUTE	CODE	14	15	16	17	18	19	20	21	22	23	24	25	26
				Case												
				Burnup (GWd/t)	Fresh	30	30	30	50	50	50	50	50	50	50	50
				Cooling time (years)	N/A	1	1	1	1	1	1	1	5	5	5	5
				Fission Products	N/A	Yes	Yes	No	Yes	Yes	No	No	Yes	Yes	No	No
				Burnup Profile	N/A	Yes	No	Yes	Yes	No	Yes	No	Yes	No	Yes	No
1	Belgium	Belgonucleaire	LWR-WIMS>ANISN	1.4849	1.2145	1.2225	1.2986	1.3076	1.1024	1.0790	1.1986	1.1979	1.0725	1.0319	1.1795	1.1723
2	France	CEA/DRN	APOLLO-1>BISTRO	1.4831	1.1987	1.2001	1.2973	1.3059	1.0824	1.0535	1.2000	1.1977	1.0548	1.0075	1.1815	1.1733
3	France	CEA/PSN	APOLLO-1>MORET	1.4726	1.1993	1.1980	1.2973	1.3053	1.0809	1.0529	1.1996	1.1925	1.0524	1.0056	1.1779	1.1707
4	Germany	BIS/KE	CGM+MORSE-K	1.4820	1.1992	1.2035	1.2960	1.3041	1.0858	1.0558	1.2019	1.2014	1.0540	1.0116	1.1864	1.1714
5	Germany	GRS	SCALE-4	1.4578	1.1874	1.1937	1.2812	1.2951	1.0654	1.0494	1.1909	1.1856	1.0369	1.0033	1.1685	1.1679
6	Italy	ENEA	MCNP-3	1.4818	1.1951	1.2030	1.2936	1.3075	1.0852	1.0576	1.1840	1.1985	1.0468	1.0126	1.1613	1.1941
7	Japan	JAERI(1)	JACS(KENO)	1.4867	1.2110	1.2103	1.3029	1.3123	1.0947	1.0640	1.2080	1.2044	1.0542	1.0040	1.1802	1.1710
8	Japan	JAERI(2)	MCNP-4.2	1.4735	1.1944	1.1995	1.2944	1.3040	1.0812	1.0555	1.1969	1.1979	1.0530	1.0127	1.1770	1.1748
9	Japan	JINS(1)	SCALE-4	1.4626	1.1835	1.1896	1.2916	1.3004	1.0708	1.0519	1.1949	1.1885	1.0460	1.0091	1.1754	1.1688
10	Japan	JINS(2)	MAIL-PIJ>KENO5.a	1.4919			1.3148	1.3203			1.2162	1.2073			1.1873	1.1841
11	Japan	PNC	SCALE-4	1.4654	1.2013	1.1892	1.2950	1.2941	1.0699	1.0526	1.1909	1.1938	1.0460	1.0057	1.1746	1.1666
12	Japan	Tohoku Univ.	MCNP-4.2	1.4718	1.2011	1.1985	1.2968	1.3023	1.0841	1.0547	1.2019	1.1949	1.0553	1.0099	1.1812	1.1706
13	Japan	Toshiba	TGBLA	1.4792	1.2007	1.2038	1.2946	1.3051	1.0841	1.0590	1.1969	1.1963	1.0554	1.0138	1.1780	1.1716
14	Spain	CSN	CASMO-3>SIMULATE-3	1.4727	1.2096	1.2122	1.2961	1.3059	1.0995	1.0713	1.2019	1.1996	1.0715	1.0251	1.1831	1.1744
15	Sweden	E. M. Systems	SCALE-4	1.4671	1.1962	1.1966	1.2907	1.2993	1.0808	1.0555	1.1968	1.1959	1.0526	1.0081	1.1767	1.1693
16	Swiss.	PSI	BOXER	1.4767	1.1981	1.2011	1.2950	1.3053	1.0830	1.0579	1.1989	1.1989	1.0535	1.0119	1.1798	1.1742
17	U.K.	AEA	MONK6B	1.5018	1.2104	1.2124	1.3094	1.3186	1.0926	1.0659	1.2067	1.2103	1.0616	1.0200	1.1860	1.1842
18	U.K.	BNF	MONK6B	1.4974	1.2041	1.2101	1.3084	1.3183	1.0813	1.0611	1.2029	1.2034	1.0528	1.0185	1.1833	1.1786
19	U.K.	DOT(1)	MONK6B	1.4984	1.2049	1.2120	1.3060	1.3166	1.0895	1.0605	1.2092	1.2075	1.0627	1.0148	1.1918	1.1819
20	U.K.	DOT(2)	MONK6B	1.4984	1.2085	1.2114	1.3076	1.3157	1.0931	1.0612	1.2016	1.2043	1.0597	1.0169	1.1925	1.1818
21	U.K.	DOT(3)	MONK6B	1.4689	1.1929	1.1990	1.2948	1.3071	1.0825	1.0556	1.1985	1.1991	1.0534	1.0095	1.1835	1.1745
22	U.S.A.	ORNL(1)	SCALE-4.2(27G)	1.4676	1.1917	1.1968	1.2881	1.2998	1.0769	1.0543	1.1915	1.1945	1.0504	1.0102	1.1720	1.1687
23	U.S.A.	ORNL(2)	SCALE-4.2(44G)	1.4784	1.1980	1.2014	1.2959	1.3050	1.0827	1.0584	1.1942	1.1957	1.0552	1.0118	1.1760	1.1725
				Case 14	Case 15	Case 16	Case 17	Case 18	Case 19	Case 20	Case 21	Case 22	Case 23	Case 24	Case 25	Case 26
				Average	1.4792	1.2000	1.2029	1.2977	1.3068	1.0840	1.0585	1.1993	1.1985	1.0546	1.0125	1.1797
				2*sigma	0.0241	0.0152	0.0161	0.0148	0.0142	0.0176	0.0133	0.0135	0.0116	0.0154	0.0134	0.0138

Table 4.3 Relative Difference from Average k Value (3.6 w/o Initial Fuel Enrichment)

[Calculation/Average - 1.0]*100

No.	COUNTRY	INSTITUTE	CODE	Case															
				1	2	3	4	5	6	7	8	9	10	11	12	13			
				Fresh	10	10	10	10	10	30	30	30	30	30	30	30	30	30	30
				N/A	1	1	1	1	1	1	1	1	1	1	1	1	1	1	1
				N/A	Yes	Yes	No	No	No	Yes	Yes	Yes	No	No	No	Yes	Yes	No	No
				N/A	Yes	Yes	No	Yes	No	Yes	Yes	No	Yes	No	Yes	No	Yes	No	No
1	Belgium	Belgonucleaire	LWR-WIMS>ANISN	0.39	1.11	1.07	0.23	0.26	1.53	1.59	-0.01	0.07	1.39	1.65	-0.06	0.01			
2	France	CEA/DRN	APOLLO-1>BISTRO	0.20	0.03	0.07	0.12	0.12	0.01	-0.36	-0.10	-0.06	-0.11	-0.28	0.02	-0.07			
3	France	CEA/PSN	APOLLO-1>MORET	0.19	-0.09	0.06	-0.10	-0.43	-0.24	-0.50	-0.09	-0.27	0.18	-0.62	-0.04	-0.10			
4	Germany	BIS/IKE	CGM>MORSE-K	0.13	0.08	-0.14	0.11	0.17	-0.01	0.09	-0.16	0.21	-0.27	-0.09	-0.09	-0.36			
5	Germany	GRS	SCALE-4	-1.52	-0.55	-0.93	-1.31	-0.89	-1.07	-1.16	-0.50	-0.91	-0.82	-0.93	-0.72	-0.73			
6	Italy	ENEA	MCNP-3	-0.15	-0.04	0.06	0.24	0.15	-0.52	0.32	-0.29	0.14	-0.69	0.19	-0.38	0.16			
7	Japan	JAERI(1)	JACS(KENO)	0.54	0.54	0.55	0.42	0.64	1.07	0.40	0.52	0.22	0.98	0.57	0.61	0.36			
8	Japan	JAERI(2)	MCNP-4.2	-0.29	-0.41	-0.33	-0.24	-0.14	-0.32	-0.29	-0.31	-0.11	-0.32	-0.18	-0.10	-0.10			
9	Japan	JINS(1)	SCALE-4	-1.03	-1.18	-0.79	-0.80	-1.18	-1.14	-0.47	-0.75	-0.76	-0.45	-1.03	-0.81	-0.78			
10	Japan	JINS(2)	MAIL-PIJ>KENO5.a	0.89			0.99	0.79			1.17	0.49			1.10	0.87			
11	Japan	PNC	SCALE-4	-1.00	-0.86	-0.79	-1.06	-1.04	-0.83	-0.62	-0.67	-0.90	-1.30	-0.51	-0.59	-0.67			
12	Japan	Tohoku Univ.	MCNP-4.2	-0.36	-0.13	-0.36	-0.20	-0.43	0.17	-0.26	0.16	-0.21	-0.02	-0.33	0.16	-0.27			
13	Japan	Toshiba	TGBLA	-0.05	-0.02	0.07	-0.03	0.02	0.09	-0.03	-0.24	-0.16	0.03	0.10	-0.16	-0.18			
14	Spain	CSN	CASMO-3>SIMULATE-3	-0.38	0.17	0.22	-0.17	-0.14	1.06	0.87	0.06	0.10	1.03	0.98	0.12	0.04			
15	Sweden	E. M. Systems	SCALE-4	-0.73	-0.60	-0.67	-0.65	-0.58	-0.38	-0.53	-0.68	-0.40	-0.31	-0.44	-0.51	-0.34			
16	Swiss.	PSI	BOXER	-0.16	-0.24	-0.16	-0.15	-0.12	-0.04	-0.16	-0.13	-0.05	-0.14	-0.09	-0.08	-0.08			
17	U.K.	AEA	MONK6B	1.06	0.89	1.01	1.12	1.23	0.40	0.80	0.95	0.99	0.67	0.63	0.80	0.79			
18	U.K.	BNF	MONK6B	1.27	0.87	0.71	0.99	0.82	0.00	0.26	0.59	0.54	0.13	0.24	0.14	0.65			
19	U.K.	DOT(1)	MONK6B	1.37	0.90	1.04	0.85	0.95	0.83	0.51	0.81	0.81	0.50	0.14	0.78	0.75			
20	U.K.	DOT(2)	MONK6B	1.48	0.89	0.68	0.91	0.97	0.57	0.51	0.65	1.00	0.74	0.72	0.70	0.61			
21	U.K.	DOT(3)	MONK6B	-0.71	-0.38	-0.46	-0.34	-0.30	-0.24	-0.31	-0.12	-0.15	-0.09	-0.38	-0.01	-0.01			
22	U.S.A.	ORNL(1)	SCALE-4.2(27G)	-0.96	-0.90	-0.75	-0.83	-0.75	-0.60	-0.55	-0.61	-0.43	-0.75	-0.47	-0.52	-0.48			
23	U.S.A.	ORNL(2)	SCALE-4.2(44G)	-0.16	-0.08	-0.17	-0.10	-0.12	-0.34	-0.11	-0.23	-0.16	-0.40	0.14	-0.36	-0.06			

Table 4.4 Relative Difference from Average k Value (4.5 w/o Initial Fuel Enrichment)

[Calculation/Average - 1.0]*100

No.	COUNTRY	INSTITUTE	CODE	Case	14	15	16	17	18	19	20	21	22	23	24	25	26
				Burnup (GWdt)	Fresh												
				Cooling time (years)	N/A	1	1	1	1	1	1	1	1	5	5	5	5
				Fission Products	N/A	Yes	Yes	No	No	Yes	Yes	No	No	Yes	Yes	No	No
				Burnup Profile	N/A	Yes	No	Yes	No	Yes	No	Yes	No	Yes	No	Yes	No
1	Belgium	Belgonucleaire	LWR-WIMS>ANISN		0.39	1.21	1.63	0.07	0.06	1.70	1.93	-0.06	-0.06	1.70	1.92	-0.02	-0.20
2	France	CEA/DRN	APOLLO-1>BISTRO		0.27	-0.11	-0.24	-0.03	-0.07	-0.15	-0.48	0.06	-0.07	0.02	-0.49	0.15	-0.12
3	France	CEA/PSN	APOLLO-1>MORET		-0.44	-0.06	-0.41	-0.03	-0.11	-0.29	-0.53	0.03	-0.50	-0.21	-0.68	-0.15	-0.34
4	Germany	BIS/IKK	CGM+MORSE-K		0.19	-0.07	0.05	-0.13	-0.20	0.16	-0.26	0.22	0.24	-0.05	-0.09	0.57	-0.28
5	Germany	GRS	SCALE-4		-1.44	-1.06	-0.77	-1.27	-0.89	-1.72	-0.86	-0.69	-1.08	-1.68	-0.90	-0.95	-0.58
6	Italy	ENEA	MCNP-3		0.18	-0.41	0.00	-0.31	0.06	0.11	-0.09	-1.27	0.00	-0.74	0.01	-1.56	1.65
7	Japan	JAERI(1)	JACS(KENO)		0.51	0.91	0.61	0.40	0.42	0.99	0.52	0.73	0.49	-0.03	-0.84	0.04	-0.31
8	Japan	JAERI(2)	MCNP-4.2		-0.38	-0.47	-0.28	-0.25	-0.21	-0.26	-0.28	-0.19	-0.05	-0.15	0.02	-0.23	0.01
9	Japan	JINS(1)	SCALE-4		-1.12	-1.38	-1.11	-0.47	-0.49	-1.22	-0.62	-0.36	-0.83	-0.81	-0.33	-0.37	-0.50
10	Japan	JINS(2)	MAIL-PIJ>KENO5.a		0.86			1.32	1.04			1.41	0.73			0.64	0.80
11	Japan	PNC	SCALE-4		-0.93	0.11	-1.14	-0.20	-0.97	-1.30	-0.56	-0.70	-0.39	-0.81	-0.67	-0.43	-0.69
12	Japan	Tohoku Univ.	MCNP-4.2		-0.50	0.09	-0.37	-0.07	-0.34	0.01	-0.36	0.22	-0.30	0.07	-0.26	0.12	-0.35
13	Japan	Toshiba	TGBLA		0.00	0.06	0.07	-0.23	-0.12	0.00	0.05	-0.20	-0.18	0.08	0.13	-0.14	-0.26
14	Spain	CSN	CASMO-3>SIMULATE-3		-0.44	0.80	0.77	-0.12	-0.06	1.42	1.21	0.22	0.09	1.61	1.24	0.29	-0.02
15	Sweden	E. M. Systems	SCALE-4		-0.82	-0.32	-0.53	-0.54	-0.57	-0.30	-0.29	-0.20	-0.22	-0.19	-0.43	-0.26	-0.46
16	Swiss.	PSI	BOXER		-0.17	-0.16	-0.15	-0.20	-0.11	-0.10	-0.06	-0.03	0.03	-0.10	-0.06	0.01	-0.04
17	U.K.	AEA	MONK6B		1.53	0.86	0.79	0.91	0.91	0.79	0.70	0.62	0.98	0.67	0.74	0.53	0.81
18	U.K.	BNF	MONK6B		1.23	0.34	0.60	0.83	0.88	-0.25	0.24	0.30	0.41	-0.17	0.60	0.30	0.34
19	U.K.	DOT(1)	MONK6B		1.30	0.41	0.75	0.64	0.75	0.50	0.19	0.83	0.75	0.77	0.23	1.02	0.62
20	U.K.	DOT(2)	MONK6B		1.30	0.71	0.70	0.77	0.68	0.84	0.25	0.20	0.48	0.49	0.44	1.08	0.61
21	U.K.	DOT(3)	MONK6B		-0.69	-0.59	-0.33	-0.22	0.03	-0.14	-0.28	-0.06	0.05	-0.11	-0.29	0.32	-0.01
22	U.S.A.	ORNL(1)	SCALE-4.2(27G)		-0.78	-0.69	-0.51	-0.74	-0.53	-0.66	-0.40	-0.65	-0.34	-0.40	-0.22	-0.65	-0.51
23	U.S.A.	ORNL(2)	SCALE-4.2(44G)		-0.05	-0.17	-0.13	-0.13	-0.14	-0.12	-0.01	-0.42	-0.23	0.06	-0.07	-0.31	-0.18

Table 4.5 Effect of Burnup Profile in delta k (%)
 [$\Delta k = (k(\text{Profile=Yes}) - k(\text{Profile=No})) \cdot 100$]

No.	COUNTRY	INSTITUTE	CODE	4.50 w/o											
				3.60 w/o						30 GWd/t					
				10 GWd/t		30 GWd/t		30 GWd/t		30 GWd/t		30 GWd/t		30 GWd/t	
				1 year	5 years	1 year	5 years	1 year	5 years	1 year	5 years	1 year	5 years		
				A	B	C	D	E	F	G	H	I	J	K	L
				Yes	No	Yes	No	Yes	No	Yes	No	Yes	No	Yes	No
				Fission Products											
				Cooling time (years)											
				Burnup (GWd/t)											
				Fuel Enrichment (w/o)											
1	Belgium	Belgonucleaire	LWR-WIMS>ANISN	-0.68	-0.63	-0.07	-0.93	0.70	-0.86	-0.80	-0.90	2.34	0.07	4.05	0.71
2	France	CEA/DRN	APOLLO-1>BISTRO	-0.78	-0.59	0.42	-0.88	1.17	-0.67	-0.14	-0.86	2.89	0.23	4.73	0.82
3	France	CEA/PSN	APOLLO-1>MORET	-0.93	-0.13	0.30	-0.60	1.87	-0.72	0.13	-0.80	2.80	0.71	4.68	0.72
4	Germany	BIS/IKK	CGM+MORSE-K	-0.45	-0.66	-0.11	-1.29	0.78	-0.46	-0.43	-0.81	3.00	0.05	4.24	1.50
5	Germany	GRS	SCALE-4	-0.23	-1.14	0.10	-0.32	1.10	-0.77	-0.63	-1.39	1.60	0.54	3.35	0.06
6	Italy	ENEA	MCNP-3	-0.85	-0.46	-0.95	-1.36	0.00	-1.45	-0.79	-1.39	2.76	-1.45	3.42	-3.28
7	Japan	JAERI(1)	JACS(KENO)	-0.74	-0.89	0.76	-0.46	1.45	-0.49	0.07	-0.95	3.08	0.36	5.03	0.92
8	Japan	JAERI(2)	MCNP-4.2	-0.82	-0.72	-0.03	-1.08	0.82	-0.79	-0.51	-0.96	2.57	-0.10	4.03	0.22
9	Japan	JINS(1)	SCALE-4	-1.23	-0.06	-0.76	-0.82	1.63	-0.81	-0.61	-0.88	1.88	0.64	3.69	0.66
10	Japan	JINS(2)	MAIL-PIJ>KENOS.a		-0.31		0.00		-0.52		-0.55		0.89		0.32
11	Japan	PNC	SCALE-4	-0.82	-0.60	-0.23	-0.53	0.10	-0.68	1.21	0.09	1.73	-0.29	4.03	0.80
12	Japan	Tohoku Univ.	MCNP-4	-0.43	-0.27	0.49	-0.36	1.32	-0.27	0.26	-0.56	2.94	0.70	4.55	1.06
13	Japan	Toshiba	TGBLA	-0.86	-0.65	0.13	-0.93	0.91	-0.76	-0.30	-1.05	2.50	0.06	4.16	0.64
14	Spain	CSN	CASMO-3>SIMULATE-3	-0.79	-0.61	0.21	-0.87	1.06	-0.69	-0.26	-0.98	2.81	0.23	4.64	0.87
15	Sweden	E. M. Systems	SCALE-4	-0.64	-0.68	0.18	-1.17	1.13	-0.99	-0.04	-0.86	2.53	0.09	4.45	0.74
16	Swiss.	PSI	BOXER	-0.84	-0.63	0.14	-0.93	0.93	-0.79	-0.30	-1.03	2.51	0.00	4.16	0.56
17	U.K.	AEA	MONK6B	-0.89	-0.74	-0.45	-0.89	1.04	-0.78	-0.20	-0.92	2.67	-0.36	4.16	0.18
18	U.K.	BNF	MONK6B	-0.52	-0.35	-0.29	-0.77	0.87	-1.42	-0.60	-0.99	2.02	-0.05	3.43	0.47
19	U.K.	DOT(1)	MONK6B	-0.91	-0.73	0.36	-0.84	1.39	-0.76	-0.71	-1.06	2.90	0.17	4.79	0.99
20	U.K.	DOT(2)	MONK6B	-0.46	-0.67	0.08	-1.26	1.02	-0.68	-0.29	-0.81	3.19	-0.27	4.28	1.07
21	U.K.	DOT(3)	MONK6B	-0.62	-0.64	0.08	-0.79	1.30	-0.79	-0.61	-1.23	2.69	-0.06	4.39	0.90
22	U.S.A.	ORNL(1)	SCALE-4.2(27G)	-0.91	-0.68	-0.05	-1.05	0.66	-0.83	-0.51	-1.17	2.26	-0.30	4.02	0.33
23	U.S.A.	ORNL(2)	SCALE-4.2(44G)	-0.61	-0.55	-0.26	-0.91	0.39	-1.15	-0.34	-0.91	2.43	-0.15	4.34	0.35
			Average	-0.70	-0.58	0.00	-0.83	0.94	-0.79	-0.28	-0.91	2.44	0.07	4.03	0.51
			2*sigma	0.52	0.46	0.75	0.65	0.95	0.53	0.86	0.59	1.33	0.95	1.92	1.74

Table 4.6 Fission Density Data from Participants

No.	COUNTRY	INSTITUTE	CASE 2					CASE 6					CASE 19				
			3.6w/o, Burnup(10GWd/t), C.time(1y), F.P.(Yes)					3.6w/o, Burnup(30GWd/t), C.time(1y), F.P.(Yes)					4.5w/o, Burnup(50GWd/t), C.time(1y), F.P.(Yes)				
			Reg.-1	Reg.-2	Reg.-3	Reg.-4	Reg.-5	Reg.-1	Reg.-2	Reg.-3	Reg.-4	Reg.-5	Reg.-1	Reg.-2	Reg.-3	Reg.-4	Reg.-5
1	Belgium	Belgonucleaire	0.0200	0.0220	0.0600	0.1580	1.2520	0.1050	0.1130	0.2740	0.5550	1.1750	0.2430	0.2500	0.5670	0.9720	1.0870
2	France	CEADRN	0.0142	0.0161	0.0434	0.1117	0.8146	0.0549	0.0588	0.1412	0.2736	0.4715	0.0857	0.0883	0.1974	0.3247	0.3039
3	France	CEMIPSN	0.0163	0.0179	0.0506	0.1264	0.7886	0.0561	0.0603	0.1393	0.2739	0.4703	0.0794	0.0862	0.1946	0.3278	0.3119
4	Germany	BIS/IKK	0.0143	0.0165	0.0428	0.1105	0.8159	0.0515	0.0535	0.1284	0.2480	0.5186	0.0857	0.0850	0.1919	0.3216	0.3158
5	Germany	GRS	0.1296	0.1540	0.2168	0.2192	0.2804	0.1533	0.1685	0.2280	0.2630	0.1872	0.2378	0.2357	0.2633	0.2049	0.0583
6	Italy	ENEA	0.0701	0.1011	0.1860	0.2638	0.3789	0.1420	0.1658	0.2645	0.3188	0.1089	0.1949	0.2306	0.3029	0.2493	0.0223
7	Japan	JAERI(1)															
8	Japan	JAERI(2)	0.1247	0.1382	0.1856	0.2463	0.3052	0.2046	0.2134	0.2584	0.2560	0.0696	0.2415	0.2371	0.2665	0.2247	0.0302
9	Japan	JINS(1)	0.1372	0.1584	0.1945	0.2451	0.2647	0.1872	0.2044	0.2381	0.2406	0.1298	0.2253	0.2414	0.2590	0.2293	0.0449
10	Japan	JINS(2)															
11	Japan	PNC	0.1283	0.1383	0.1941	0.2414	0.2978	0.2033	0.2166	0.2574	0.2479	0.0749	0.2290	0.2380	0.2684	0.2225	0.0421
12	Japan	Tohoku Univ.															
13	Japan	Toshiba	0.1158	0.1354	0.1867	0.2504	0.3118	0.1974	0.2167	0.2634	0.2594	0.0633	0.2285	0.2409	0.2726	0.2280	0.0300
14	Spain	CSN	0.1236	0.1404	0.1856	0.2429	0.3076	0.2081	0.2216	0.2581	0.2486	0.0636	0.2420	0.2465	0.2663	0.2164	0.0289
15	Sweden	E. M. Systems	0.1321	0.1465	0.1907	0.2486	0.2821	0.2066	0.2162	0.2566	0.2530	0.0676	0.2376	0.2386	0.2679	0.2227	0.0332
16	Swiss.	PSI	0.1212	0.1384	0.1881	0.2486	0.3037	0.2019	0.2172	0.2614	0.2555	0.0640	0.2331	0.2413	0.2706	0.2248	0.0302
17	U.K.	AEA															
18	U.K.	BNF	0.1128	0.1238	0.1814	0.2734	0.3087	0.1931	0.1918	0.2143	0.2130	0.1878	0.2168	0.2289	0.2608	0.2396	0.0540
19	U.K.	DOT(1)	0.1259	0.1402	0.1904	0.2477	0.2958	0.2093	0.2196	0.2636	0.2529	0.0546	0.2456	0.2415	0.2670	0.2169	0.0289
20	U.K.	DOT(2)	0.1417	0.1604	0.2138	0.2729	0.2113	0.2121	0.2153	0.2605	0.2547	0.0574	0.2399	0.2451	0.2682	0.2206	0.0262
21	U.K.	DOT(3)	0.1208	0.1368	0.1908	0.2517	0.2999	0.2066	0.2135	0.2616	0.2501	0.0682	0.2375	0.2409	0.2683	0.2239	0.0294
22	U.S.A.	ORNL(1)	0.1267	0.1436	0.1929	0.2511	0.2857	0.2068	0.2127	0.2557	0.2542	0.0707	0.2280	0.2352	0.2669	0.2330	0.0368
23	U.S.A.	ORNL(2)	0.1178	0.1317	0.1786	0.2467	0.3252	0.1944	0.2028	0.2501	0.2529	0.0998	0.2337	0.2356	0.2647	0.2291	0.0369

Table 4.7 Adjusted Fission Densities (Data of Belgonucleaire, CEA/DRN, CEA/IPSN and BfS/IKE are Volume Averaged)

No	COUNTRY	INSTITUTE	CASE 2					CASE 6					CASE 19				
			3.6w/o, Burnup(10GWd/t), C.time(1y), F.P.(Yes)					3.6w/o, Burnup(30GWd/t), C.time(1y), F.P.(Yes)					4.5w/o, Burnup(50GWd/t), C.time(1y), F.P.(Yes)				
			Reg.-1	Reg.-2	Reg.-3	Reg.-4	Reg.-5	Reg.-1	Reg.-2	Reg.-3	Reg.-4	Reg.-5	Reg.-1	Reg.-2	Reg.-3	Reg.-4	Reg.-5
1	Belgium	Belgonucleaire	0.1288	0.1416	0.1931	0.2543	0.2821	0.1963	0.2113	0.2561	0.2594	0.0769	0.2298	0.2364	0.2681	0.2298	0.0360
2	France	CEA/DRN	0.1310	0.1485	0.2001	0.2575	0.2629	0.2039	0.2184	0.2623	0.2541	0.0613	0.2351	0.2422	0.2708	0.2227	0.0292
3	France	CEA/IPSN	0.1373	0.1508	0.2131	0.2662	0.2325	0.2070	0.2225	0.2570	0.2527	0.0607	0.2292	0.2423	0.2735	0.2303	0.0307
4	Germany	BfS/IKE	0.1319	0.1522	0.1974	0.2549	0.2635	0.2065	0.2146	0.2575	0.2486	0.0728	0.2393	0.2374	0.2679	0.2245	0.0309
5	Germany	GRS	0.1296	0.1540	0.2168	0.2192	0.2804	0.1533	0.1685	0.2280	0.2630	0.1872	0.2378	0.2357	0.2633	0.2049	0.0583
6	Italy	ENEA	0.0701	0.1011	0.1860	0.2638	0.3789	0.1420	0.1658	0.2645	0.3188	0.1089	0.1949	0.2306	0.3029	0.2493	0.0223
7	Japan	JAERI(1)															
8	Japan	JAERI(2)	0.1247	0.1382	0.1856	0.2463	0.3052	0.2046	0.2134	0.2564	0.2560	0.0696	0.2415	0.2371	0.2665	0.2247	0.0302
9	Japan	JINS(1)	0.1372	0.1584	0.1945	0.2451	0.2647	0.1872	0.2044	0.2381	0.2406	0.1298	0.2253	0.2414	0.2590	0.2293	0.0449
10	Japan	JINS(2)															
11	Japan	PNC	0.1283	0.1383	0.1941	0.2414	0.2978	0.2033	0.2166	0.2574	0.2479	0.0749	0.2290	0.2380	0.2684	0.2225	0.0421
12	Japan	Tohoku Univ.															
13	Japan	Toshiba	0.1158	0.1354	0.1867	0.2504	0.3118	0.1974	0.2167	0.2634	0.2594	0.0633	0.2285	0.2409	0.2726	0.2280	0.0300
14	Spain	CSN	0.1236	0.1404	0.1856	0.2429	0.3076	0.2081	0.2216	0.2581	0.2486	0.0636	0.2420	0.2465	0.2663	0.2164	0.0289
15	Sweden	E. M. Systems	0.1321	0.1465	0.1907	0.2486	0.2821	0.2066	0.2162	0.2566	0.2530	0.0676	0.2376	0.2386	0.2679	0.2227	0.0332
16	Swiss.	PSI	0.1212	0.1384	0.1881	0.2486	0.3037	0.2019	0.2172	0.2614	0.2555	0.0640	0.2331	0.2413	0.2706	0.2248	0.0302
17	U.K.	AEA															
18	U.K.	BNF	0.1128	0.1238	0.1814	0.2734	0.3087	0.1931	0.1918	0.2143	0.2130	0.1878	0.2168	0.2289	0.2608	0.2396	0.0540
19	U.K.	DOT(1)	0.1259	0.1402	0.1904	0.2477	0.2958	0.2093	0.2196	0.2636	0.2529	0.0546	0.2456	0.2415	0.2670	0.2169	0.0289
20	U.K.	DOT(2)	0.1417	0.1604	0.2138	0.2729	0.2113	0.2121	0.2153	0.2605	0.2547	0.0574	0.2399	0.2451	0.2682	0.2206	0.0262
21	U.K.	DOT(3)	0.1208	0.1368	0.1908	0.2517	0.2999	0.2066	0.2135	0.2616	0.2501	0.0682	0.2375	0.2409	0.2683	0.2239	0.0294
22	U.S.A.	ORNL(1)	0.1267	0.1436	0.1929	0.2511	0.2857	0.2068	0.2127	0.2557	0.2542	0.0707	0.2280	0.2352	0.2669	0.2330	0.0368
23	U.S.A.	ORNL(2)	0.1178	0.1317	0.1786	0.2467	0.3252	0.1944	0.2028	0.2501	0.2529	0.0998	0.2337	0.2356	0.2647	0.2291	0.0369
		Average	0.1241	0.1411	0.1937	0.2517	0.2895	0.1969	0.2086	0.2538	0.2545	0.0863	0.2315	0.2387	0.2691	0.2259	0.0347
		2' sigma	0.0293	0.0260	0.0208	0.0239	0.0691	0.0361	0.0317	0.0256	0.0365	0.0786	0.0223	0.0087	0.0174	0.0179	0.0180

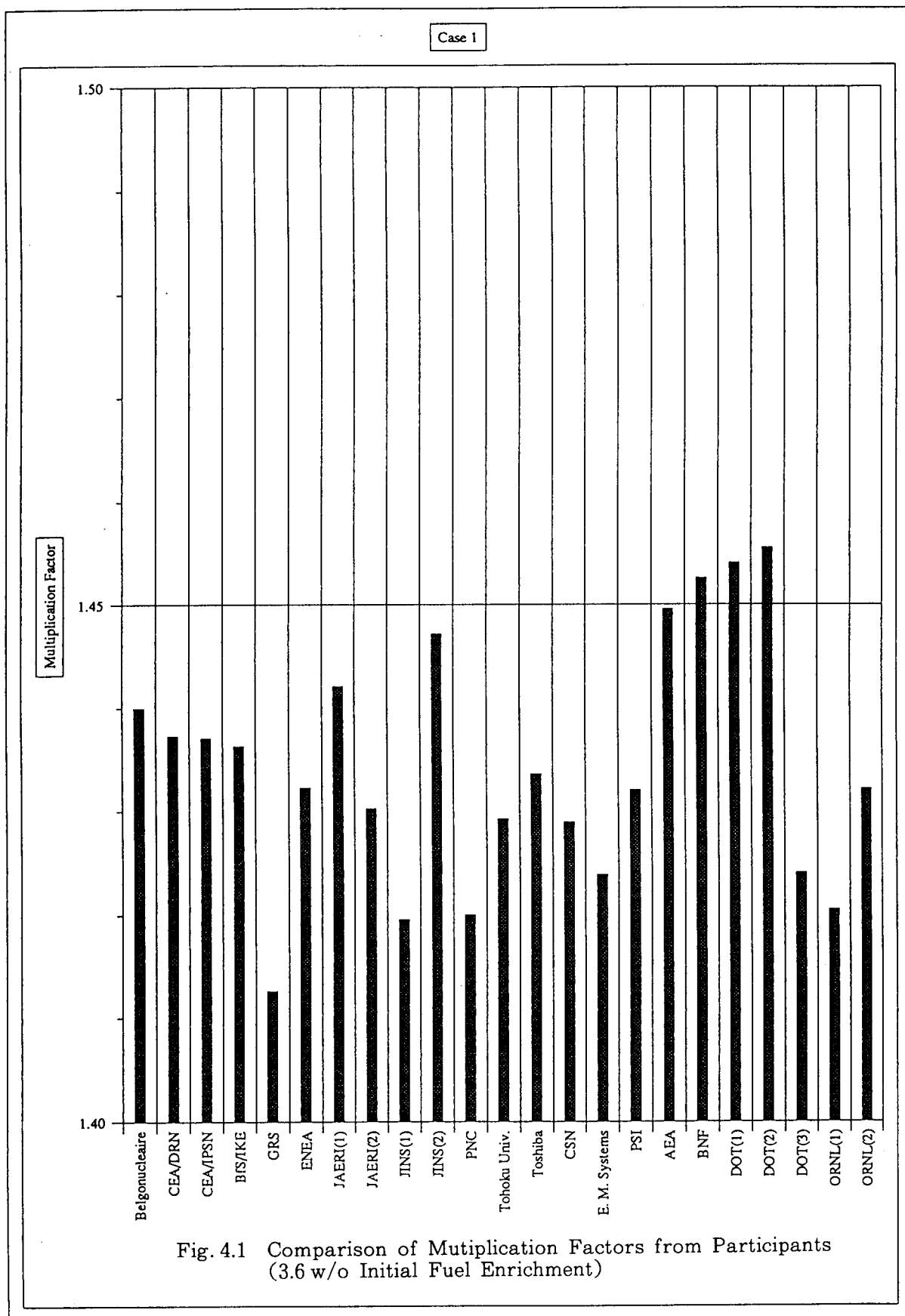


Fig. 4.1 Comparison of Multiplication Factors from Participants (3.6 w/o Initial Fuel Enrichment)

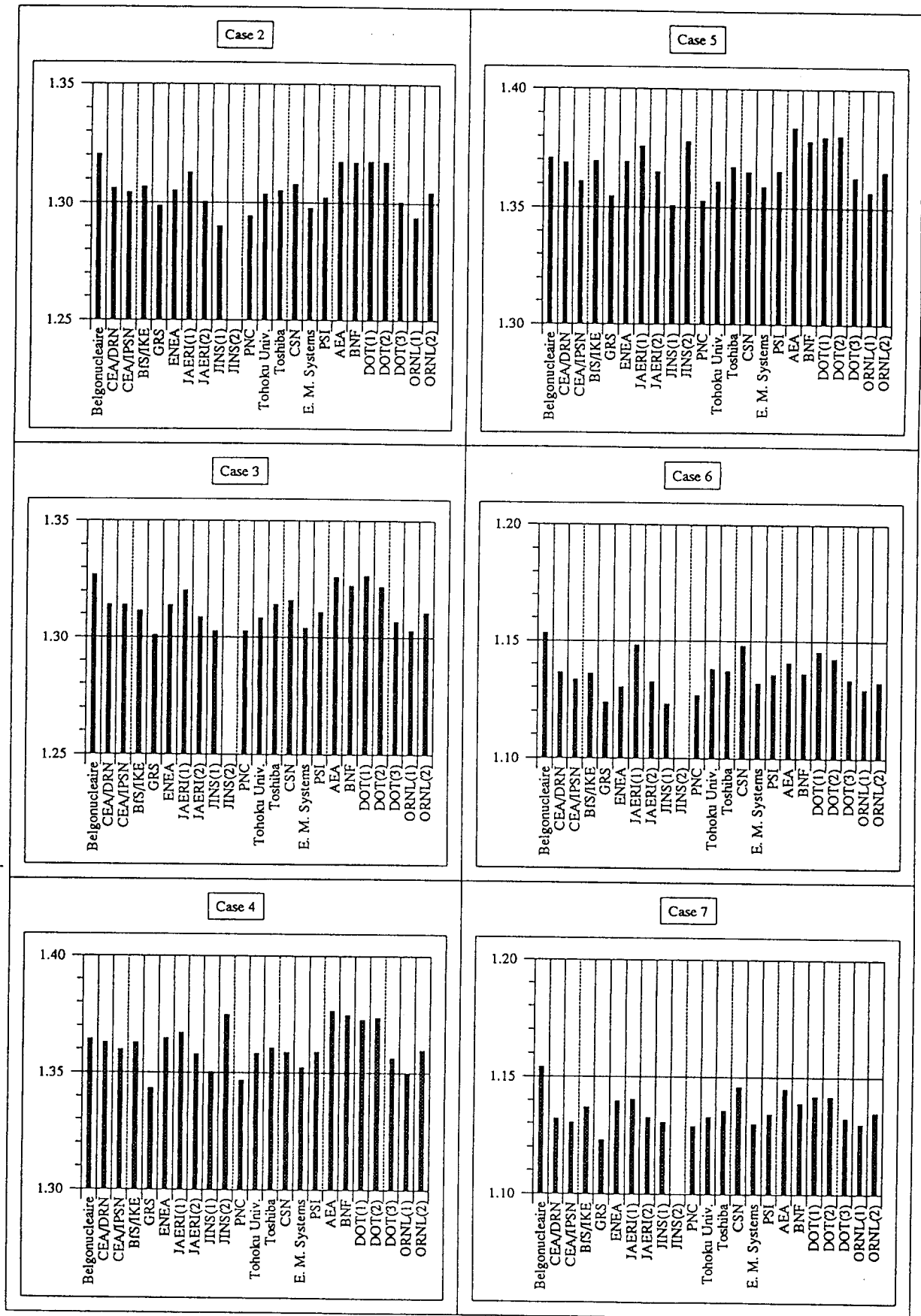


Fig. 4.1 (Continued)

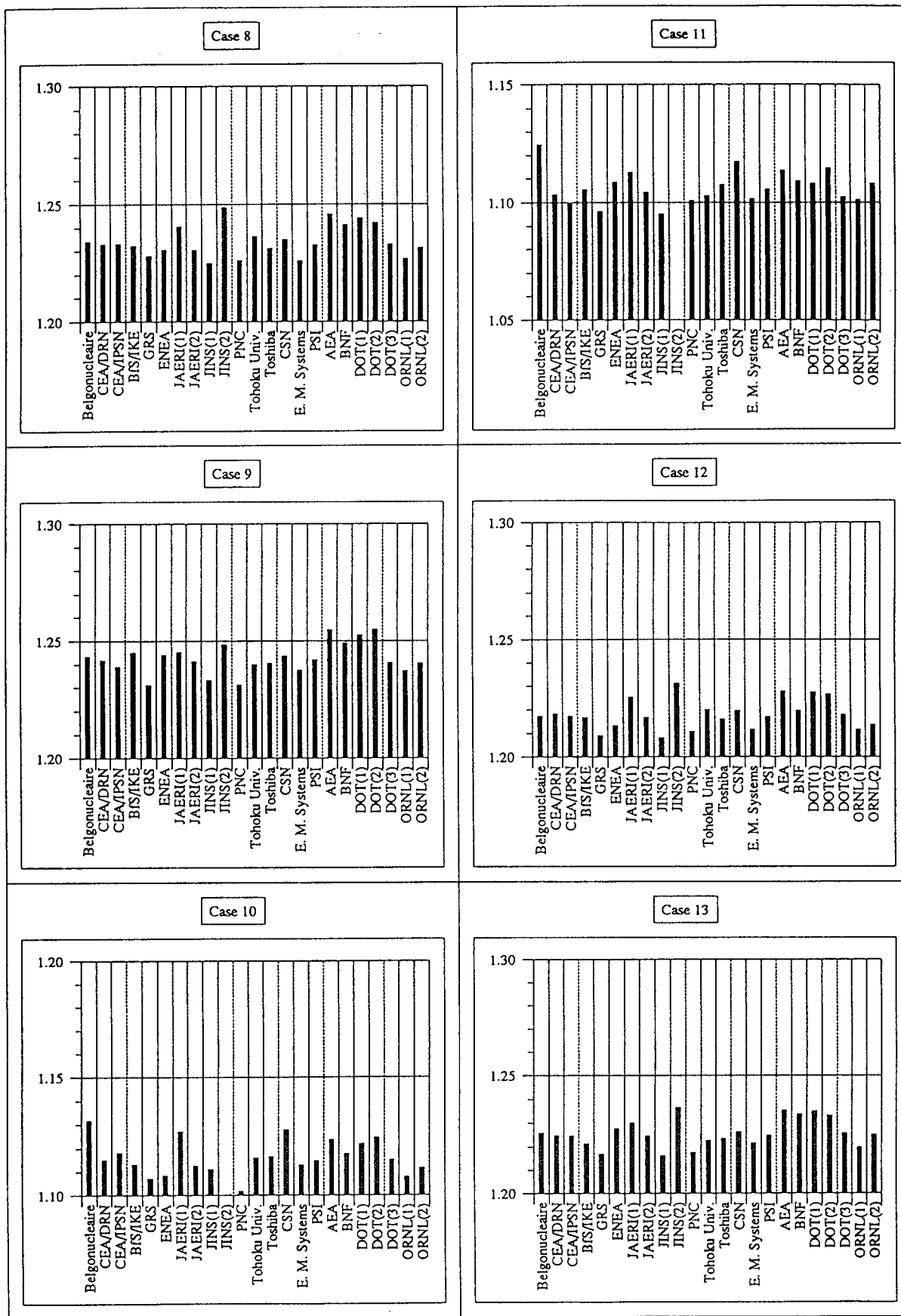


Fig. 4.1 (Continued)

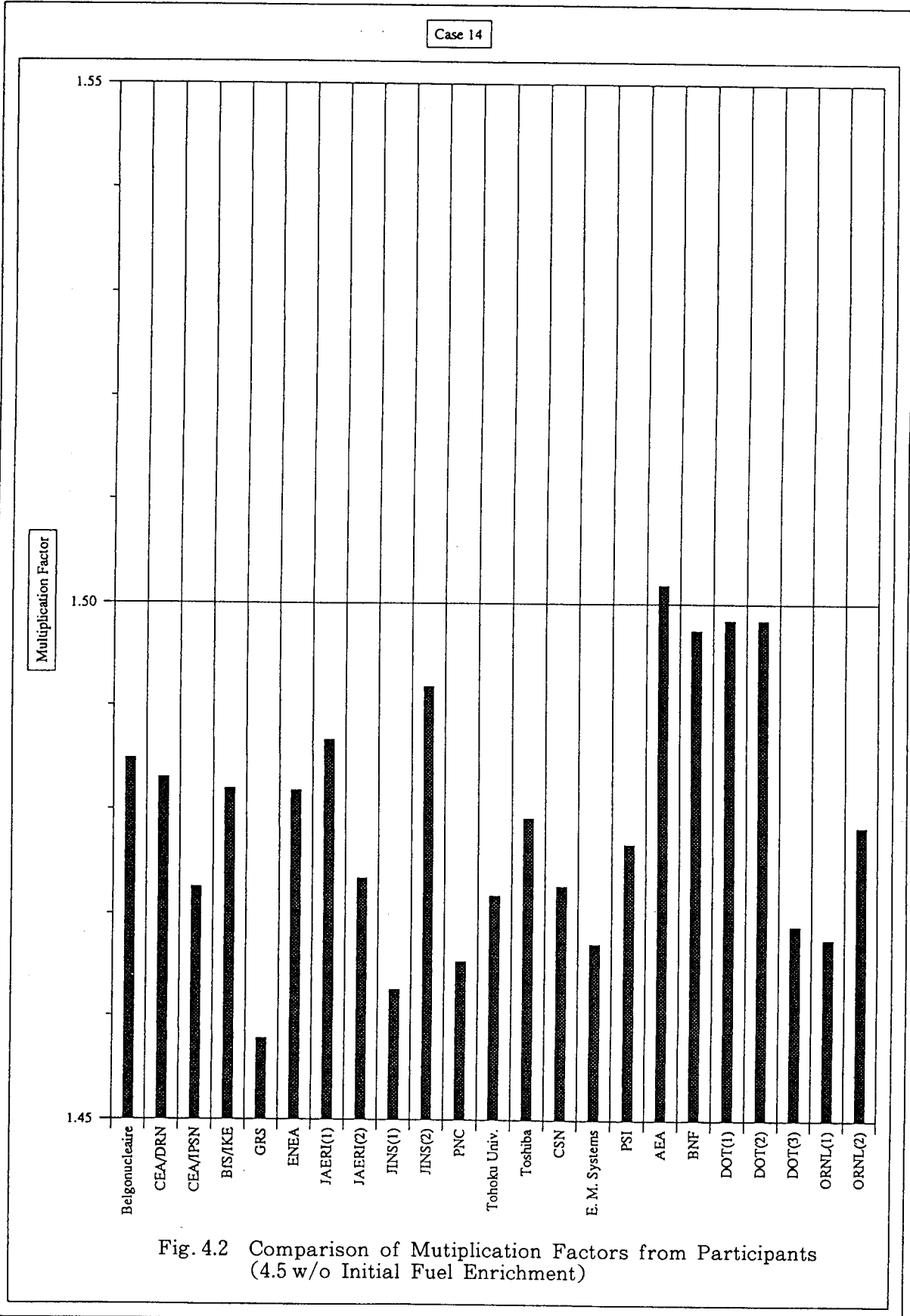


Fig. 4.2 Comparison of Mutiplication Factors from Participants (4.5 w/o Initial Fuel Enrichment)

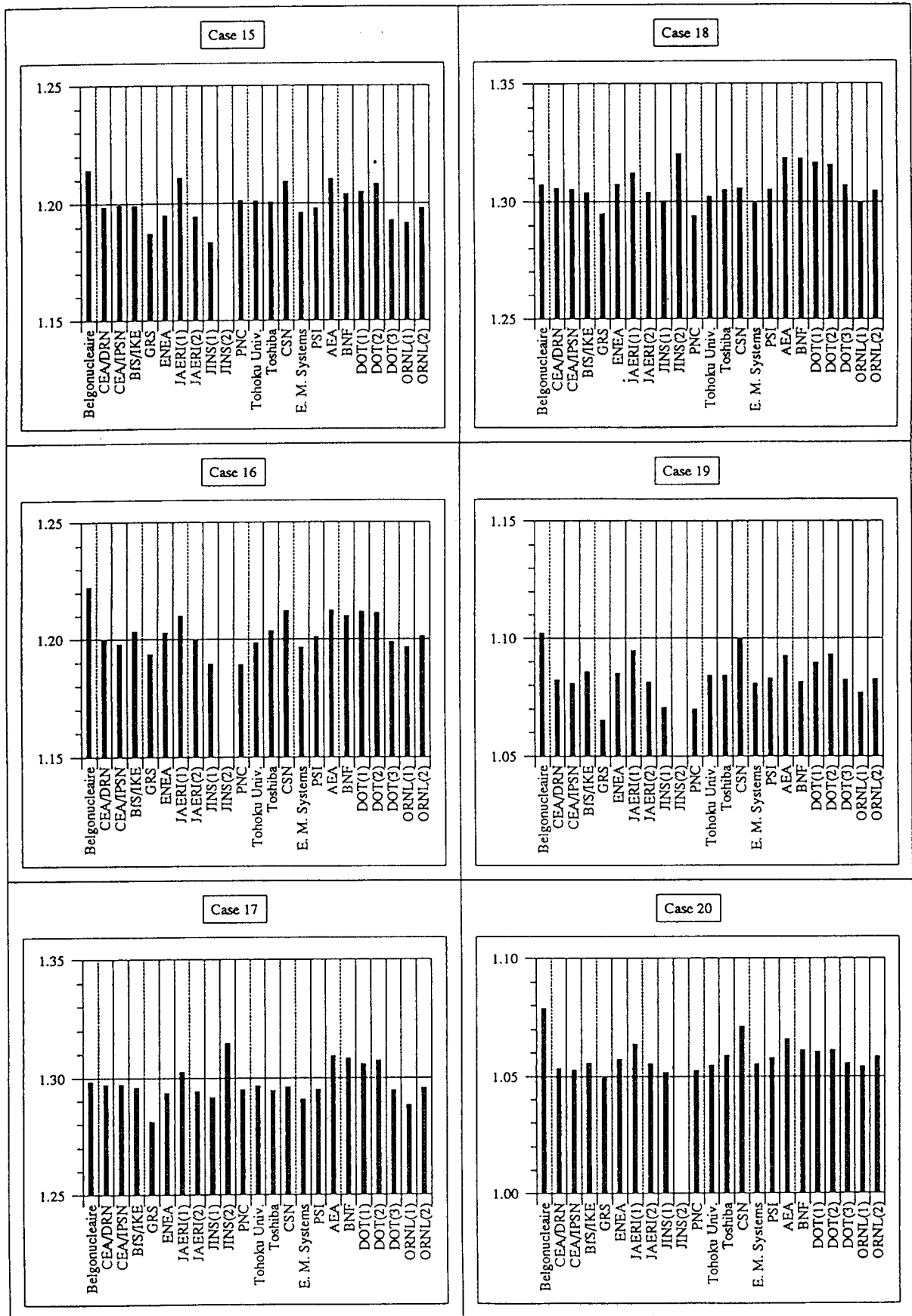


Fig. 4.2 (Continued)

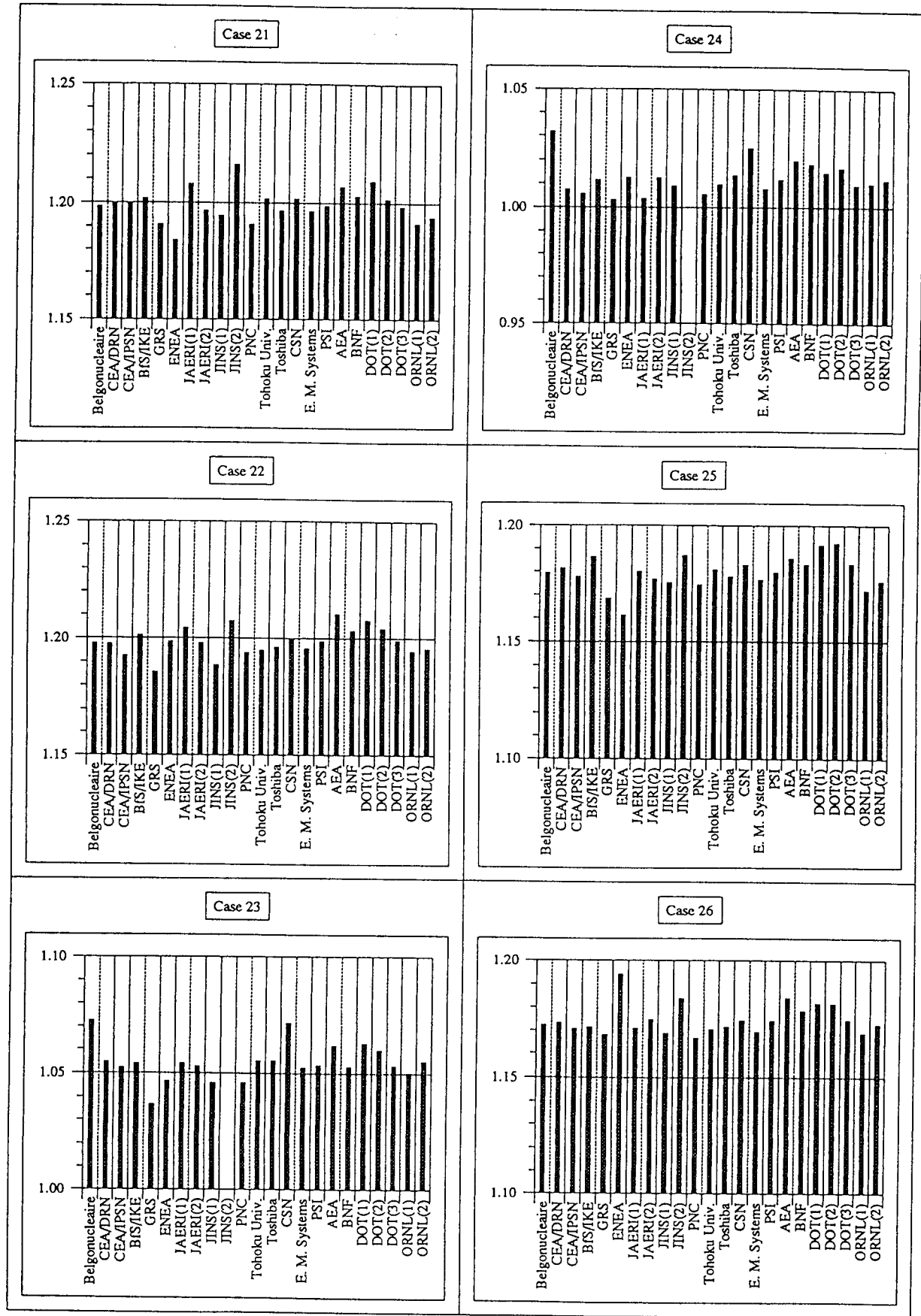


Fig. 4.2 (Continued)

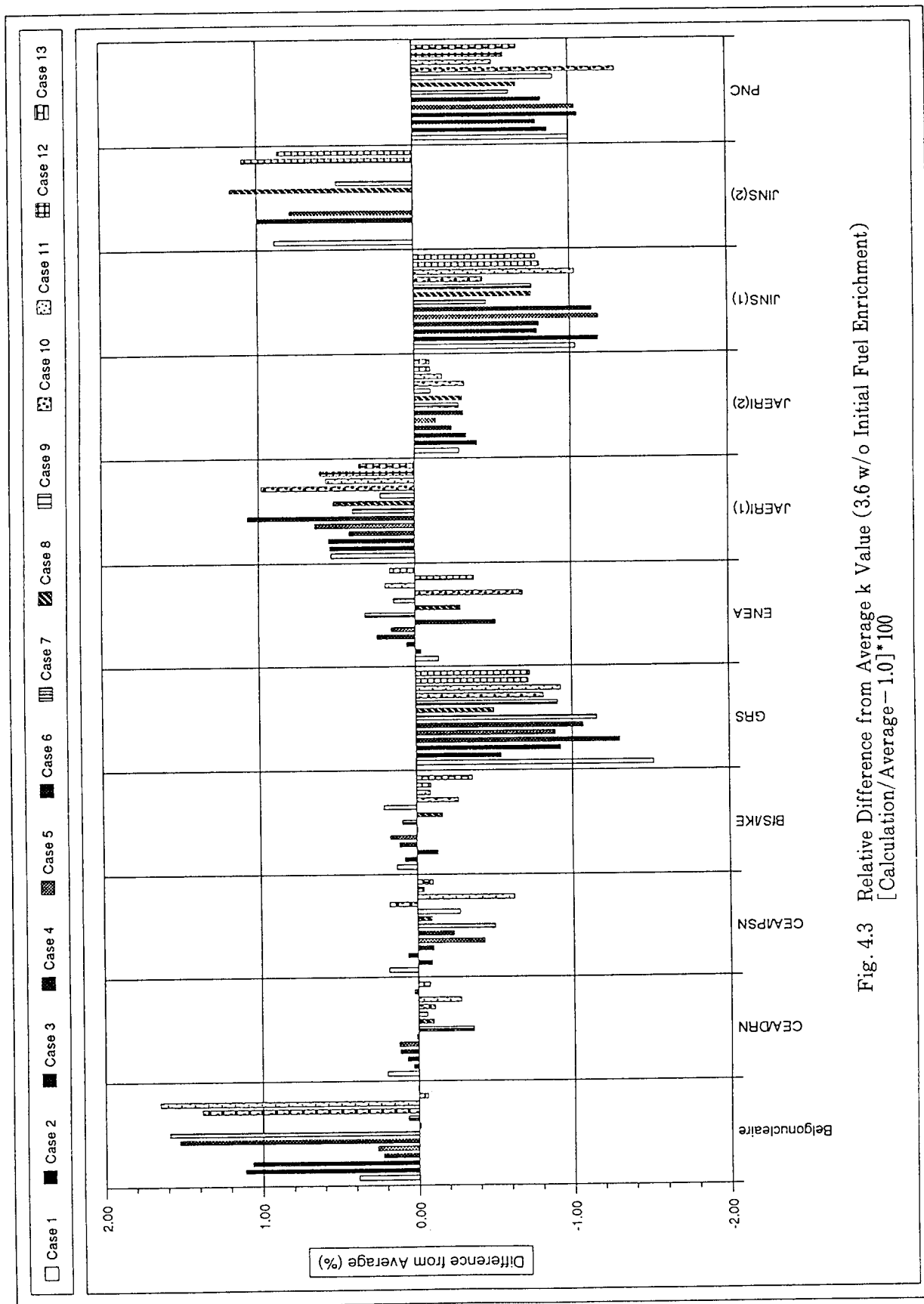


Fig. 4.3 Relative Difference from Average k Value (3.6 w/o Initial Fuel Enrichment)
 [Calculation/Average - 1.0] * 100

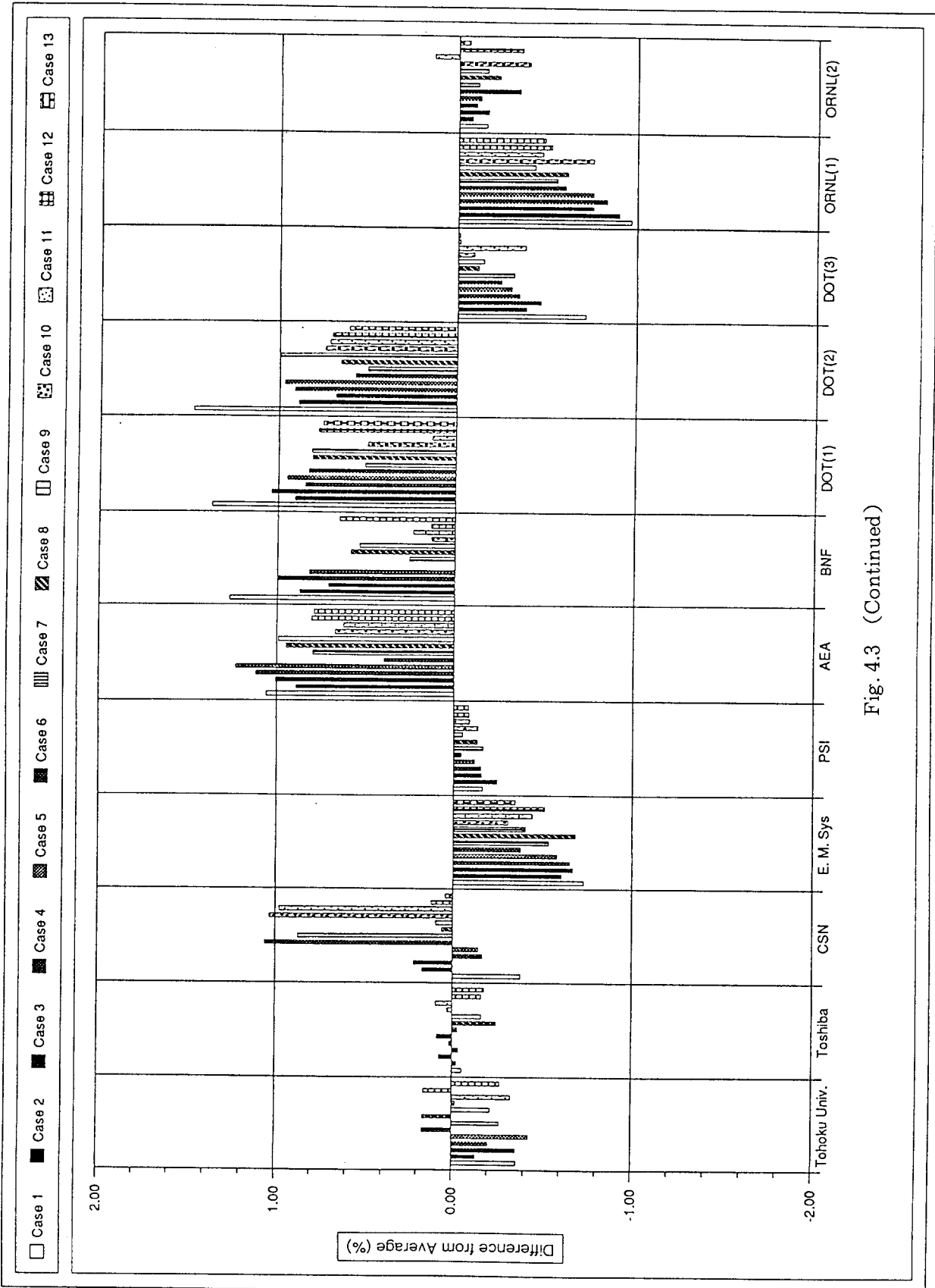


Fig. 4.3 (Continued)

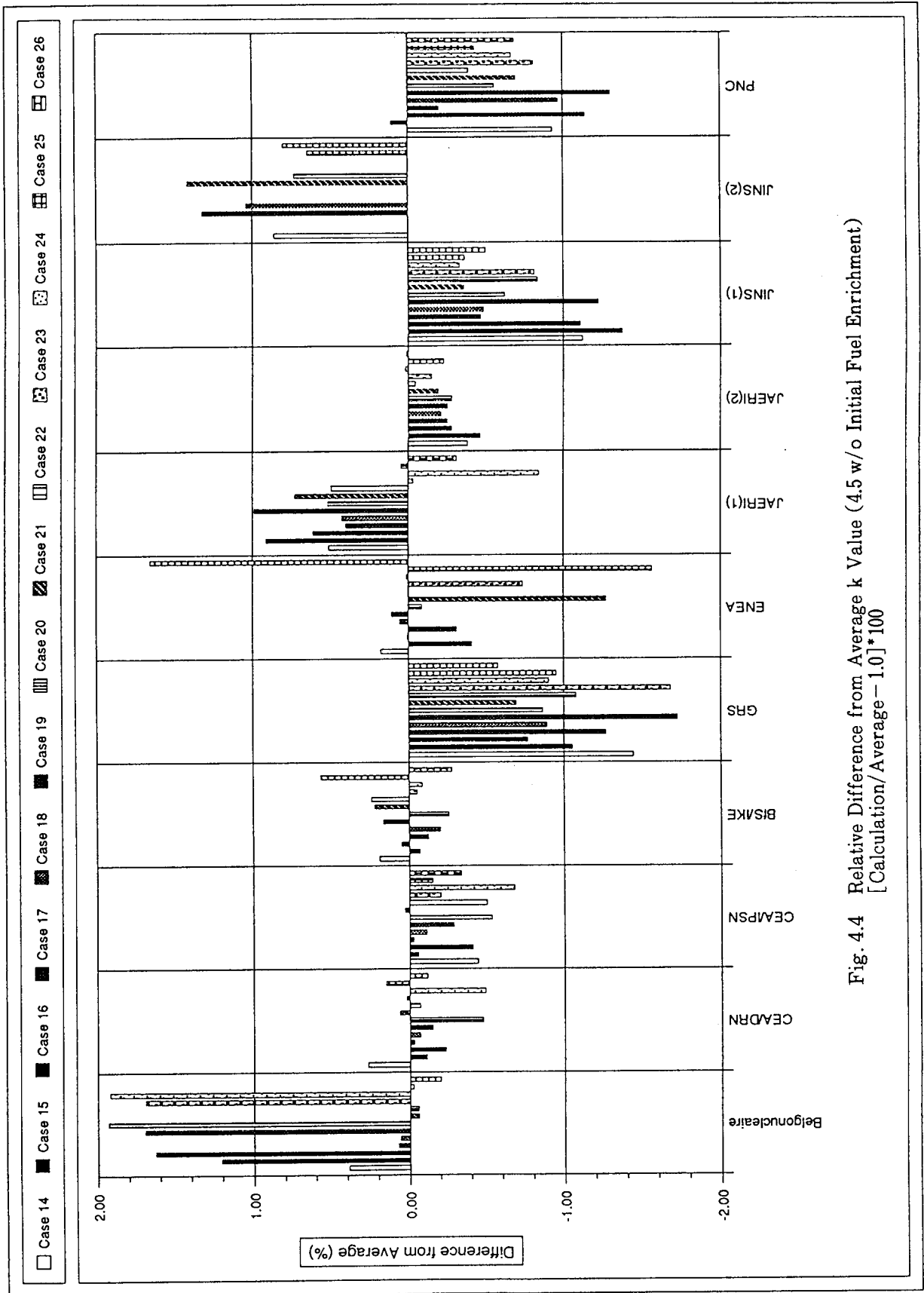


Fig. 4.4 Relative Difference from Average k Value (4.5 w/o Initial Fuel Enrichment)
 [Calculation/Average - 1.0] * 100

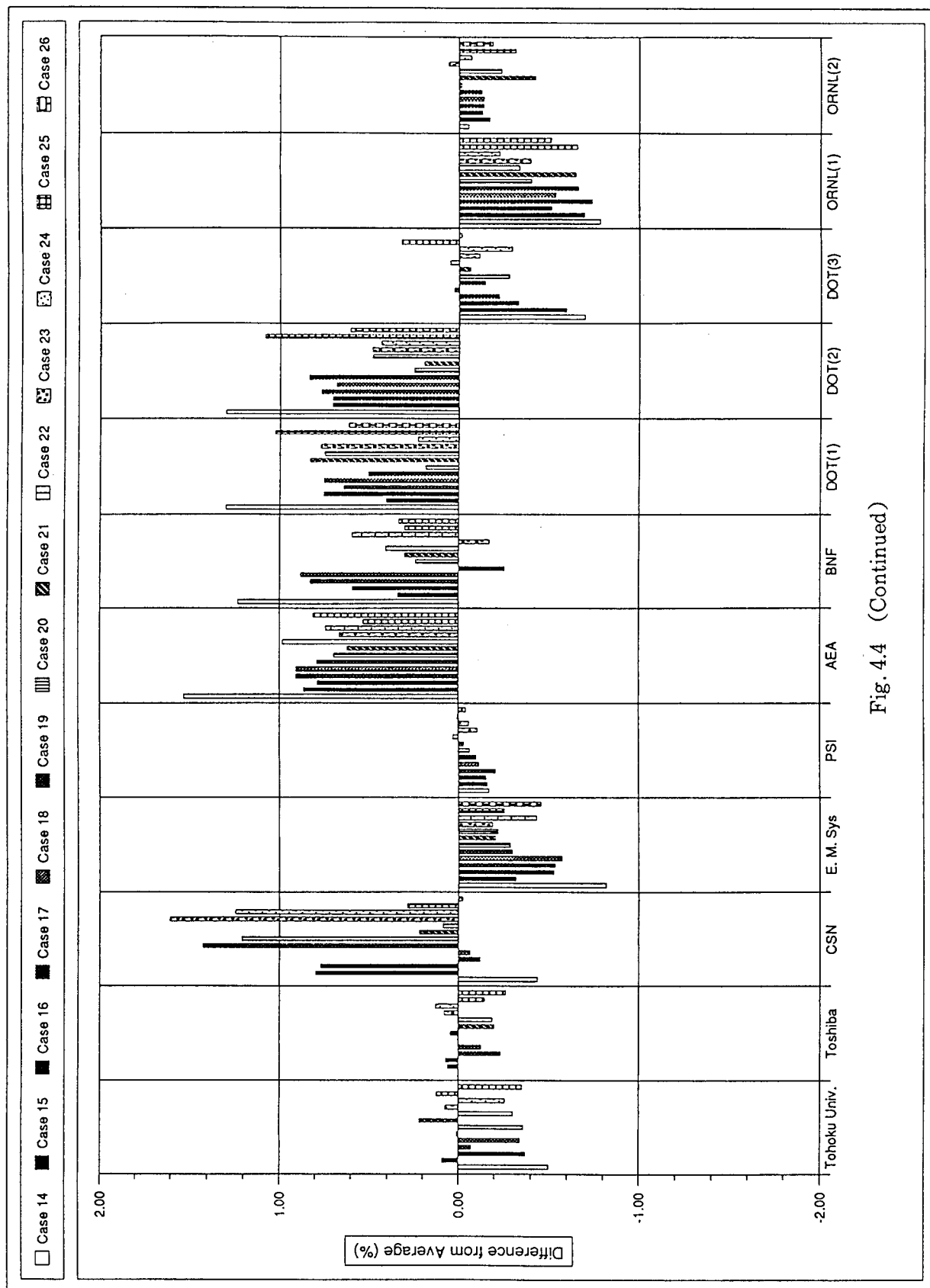


Fig. 4.4 (Continued)

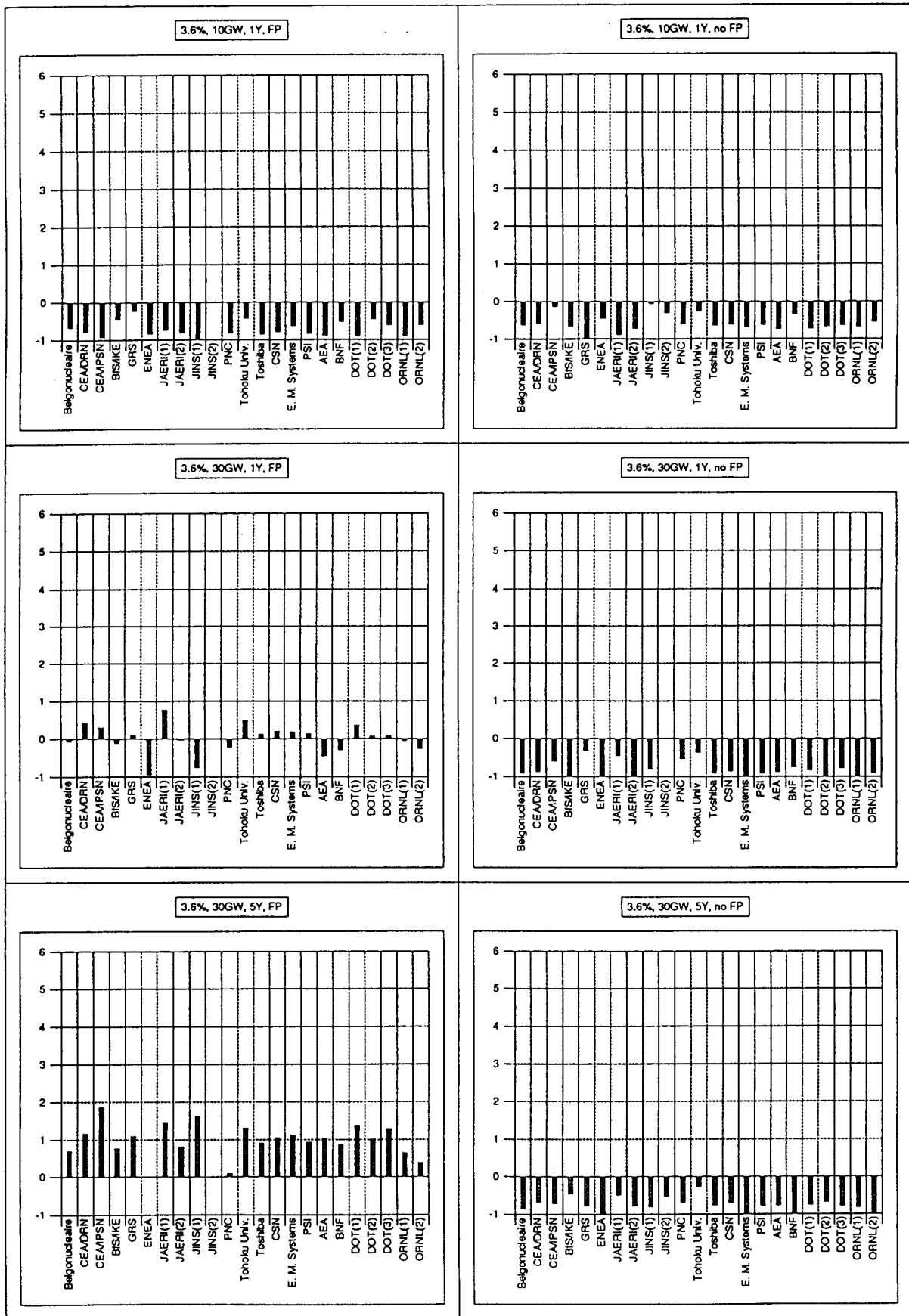


Fig. 4.5 Effect of Burnup Profile in delta k (%)

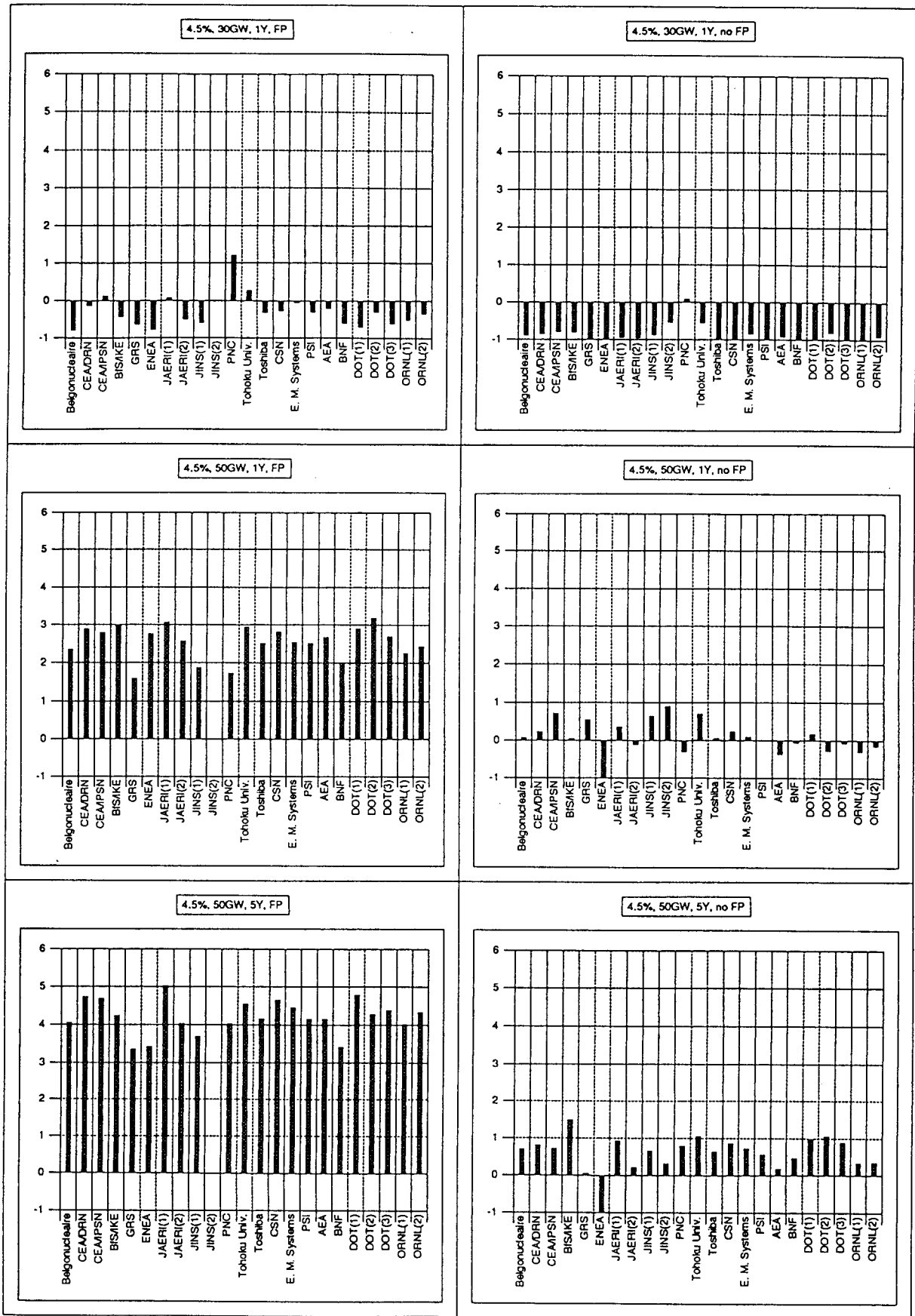


Fig. 4.5 (Continued)

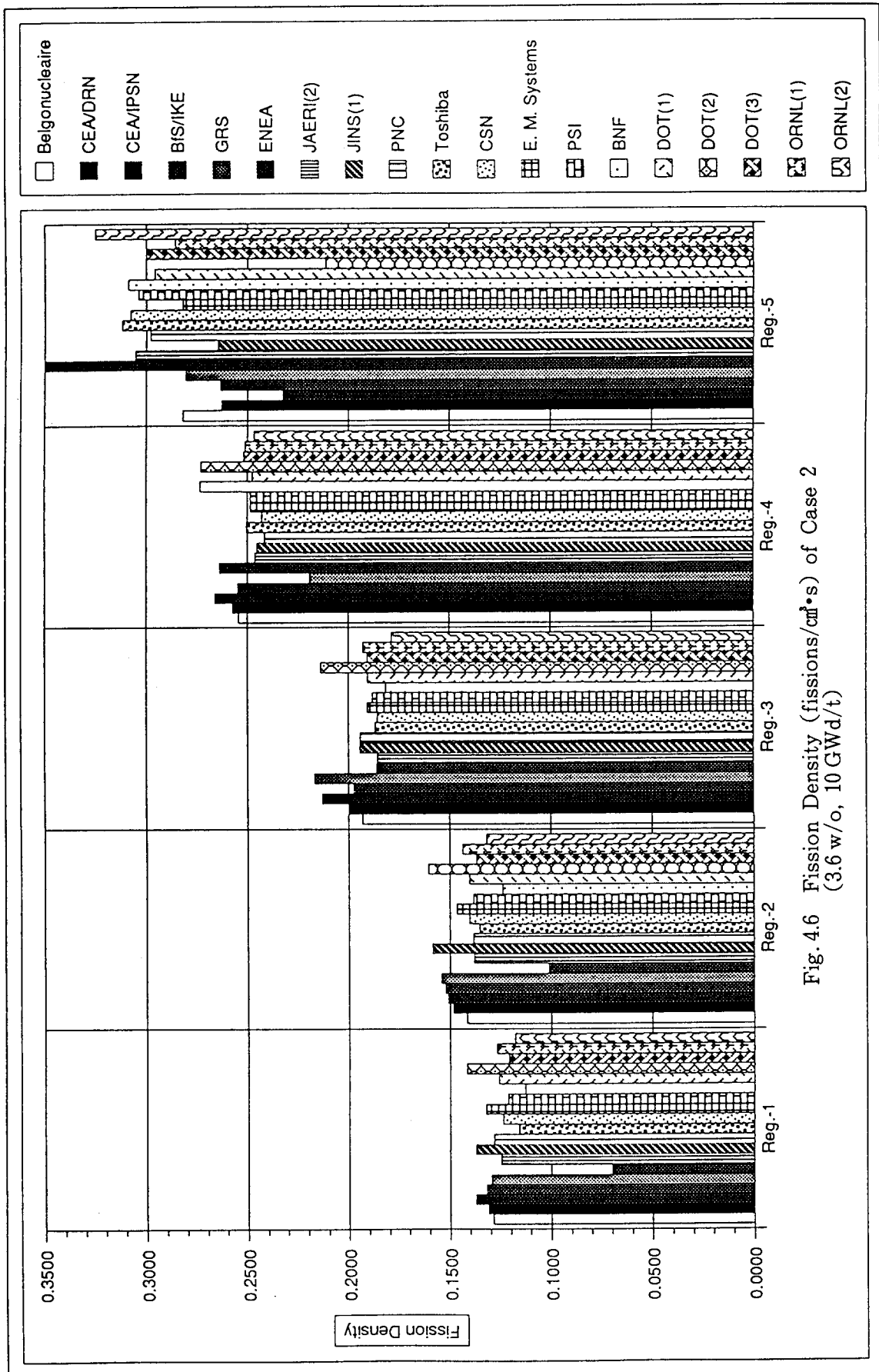


Fig. 4.6 Fission Density (fissions/cm²·s) of Case 2 (3.6 w/o, 10 GWd/t)

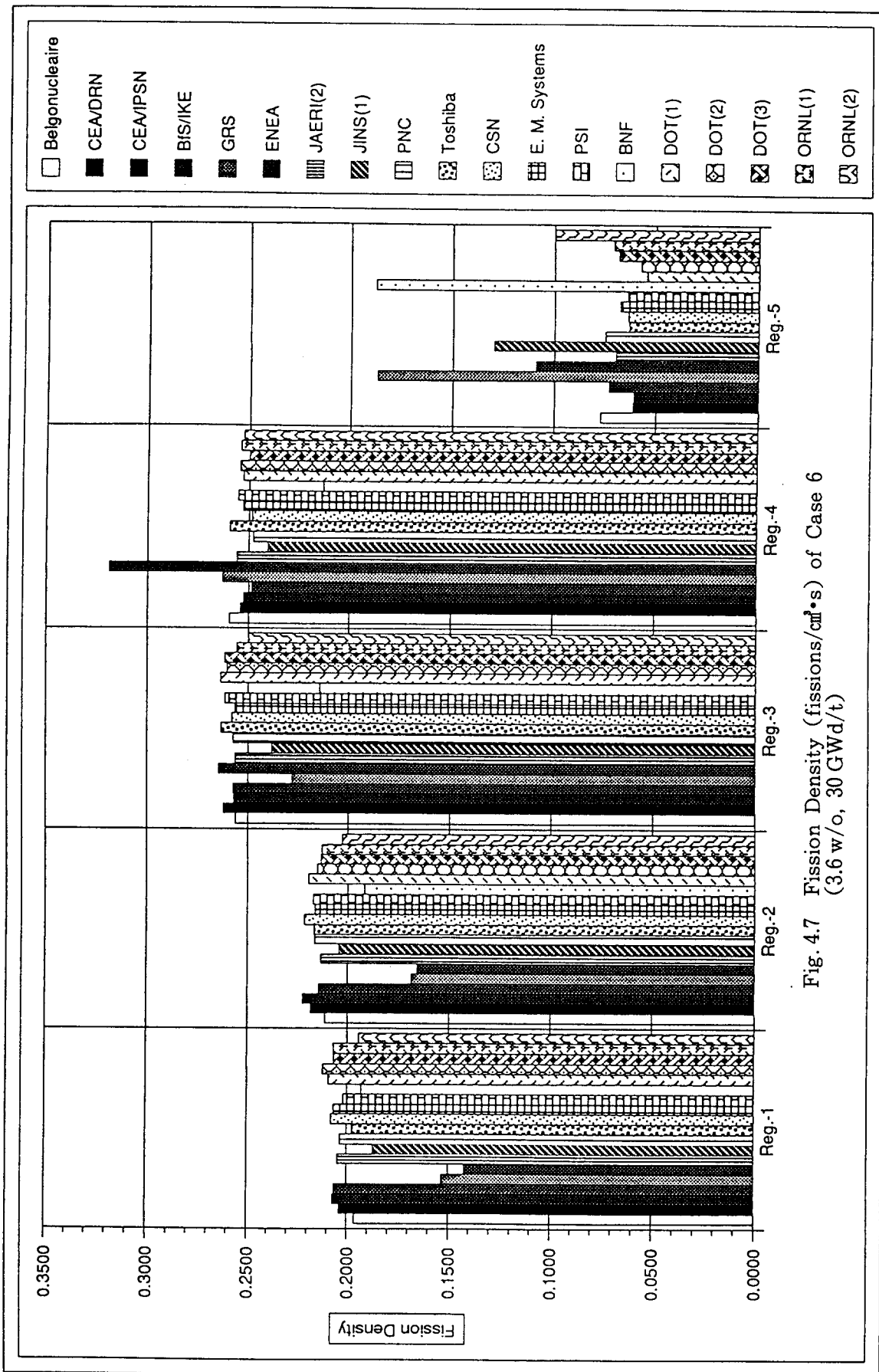


Fig. 4.7 Fission Density (fissions/cm²·s) of Case 6 (3.6 w/o, 30 GWd/t)

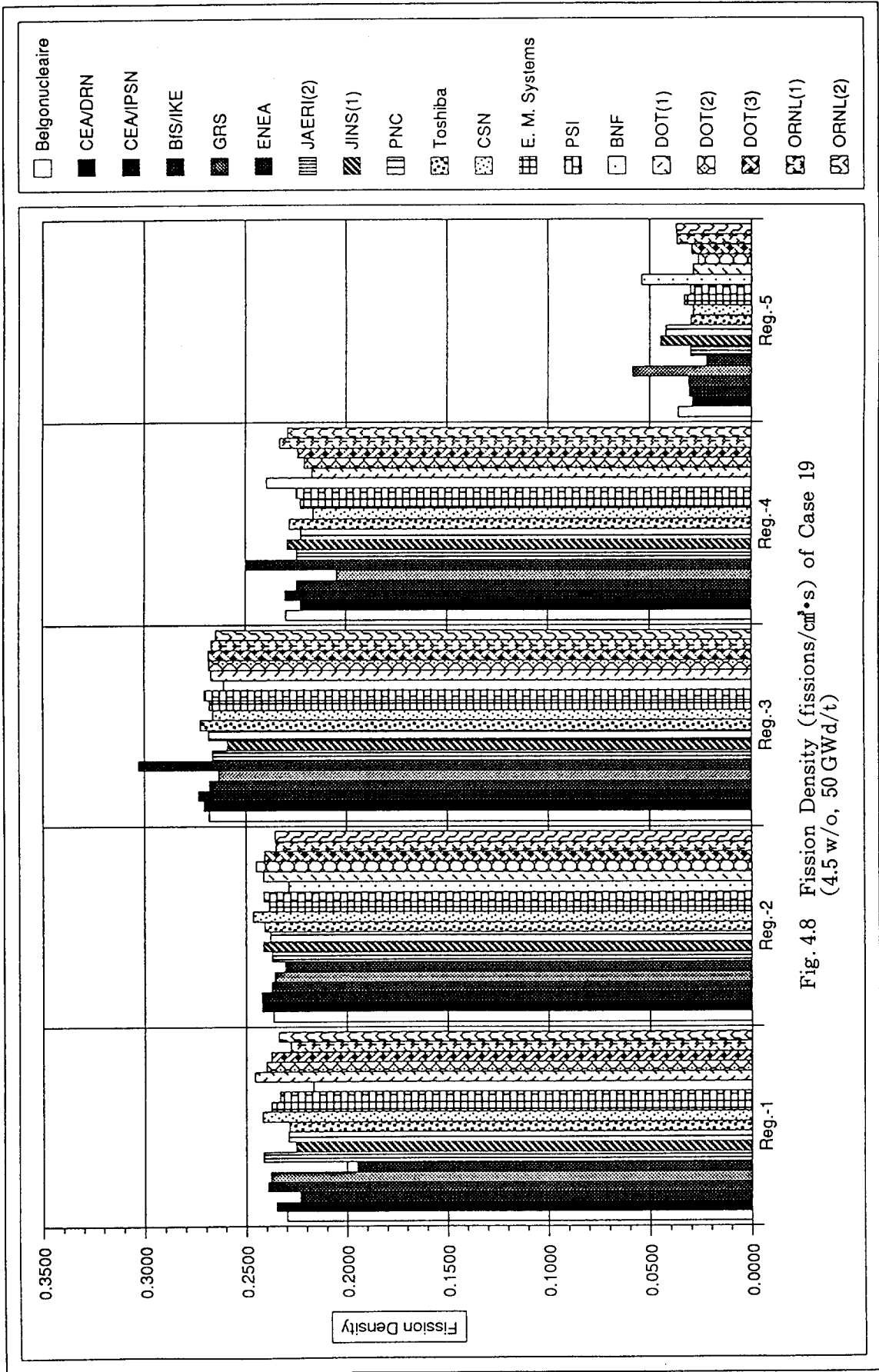


Fig. 4.8 Fission Density (fissions/cm²·s) of Case 19 (4.5 w/o, 50 GWd/t)

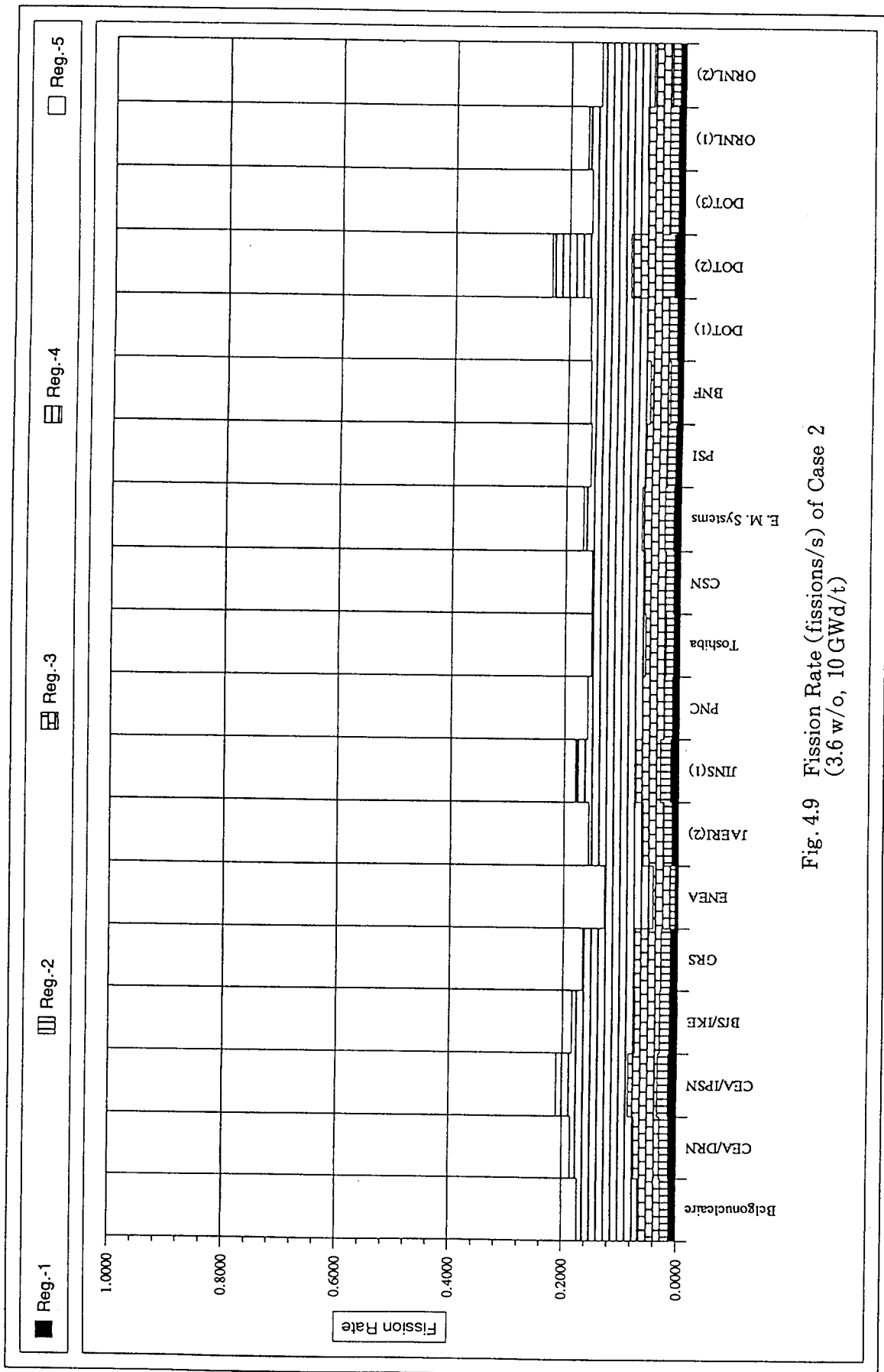
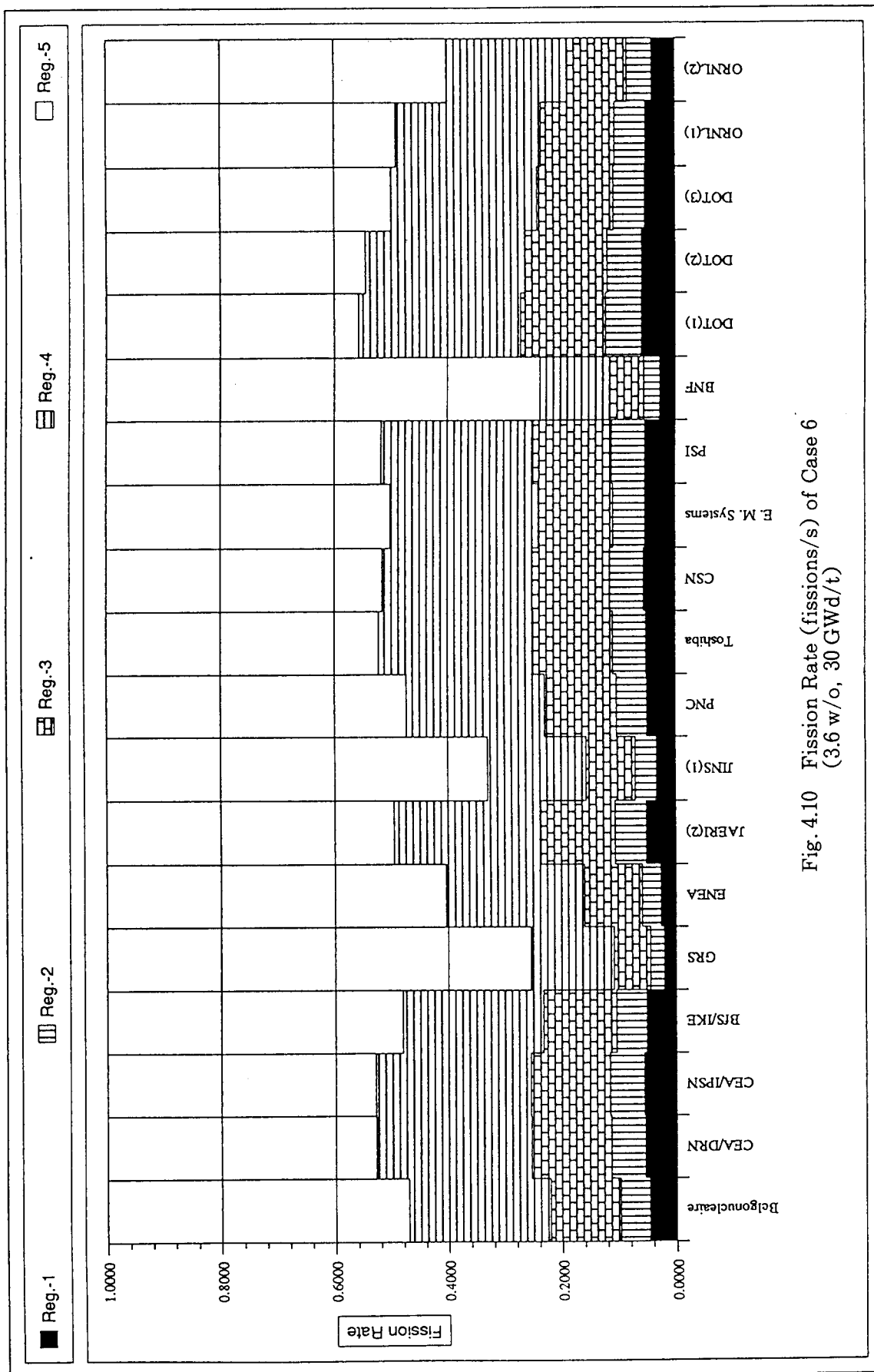


Fig. 4.9 Fission Rate (fissions/s) of Case 2
(3.6 w/o, 10 GWd/t)



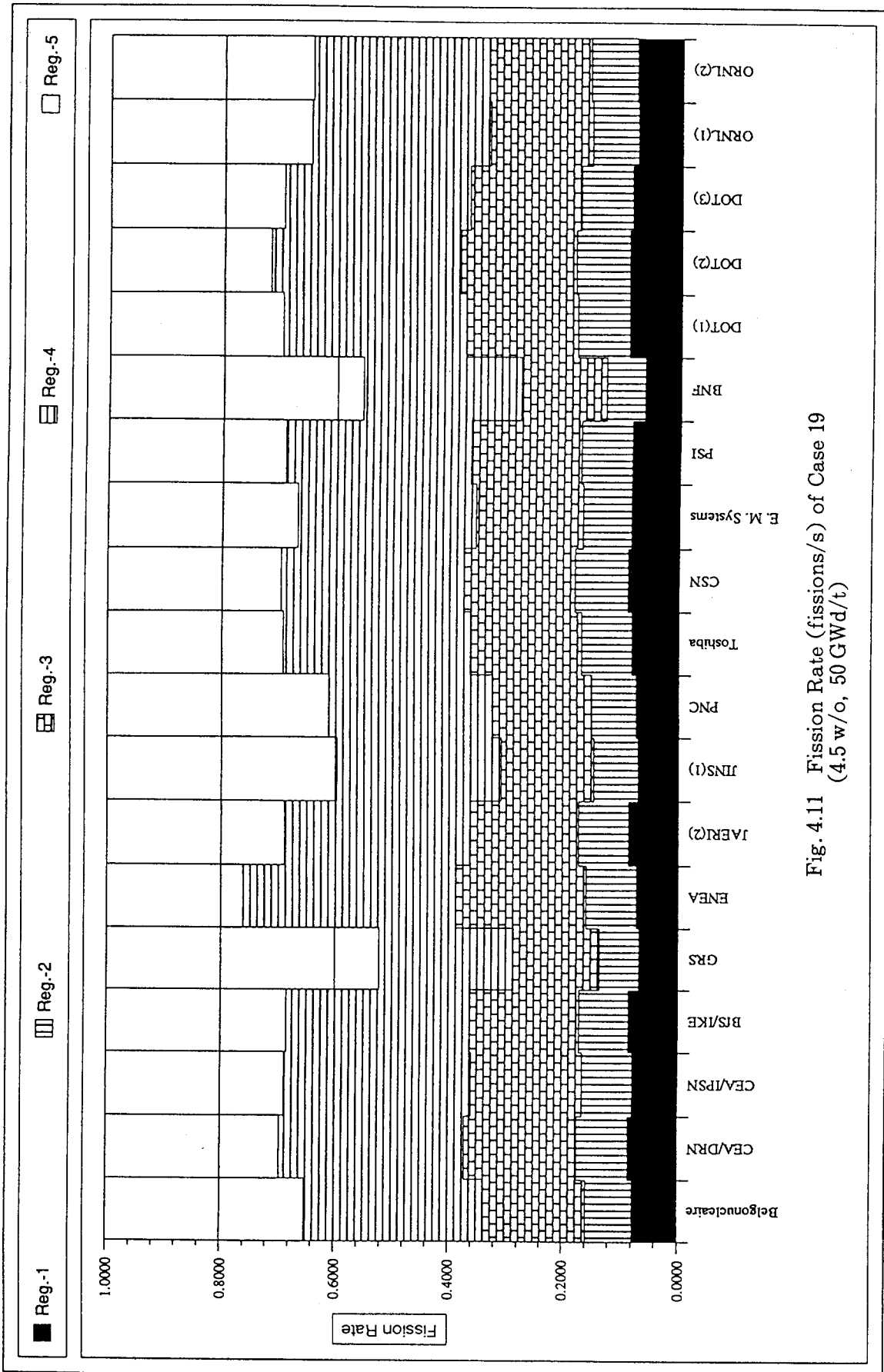
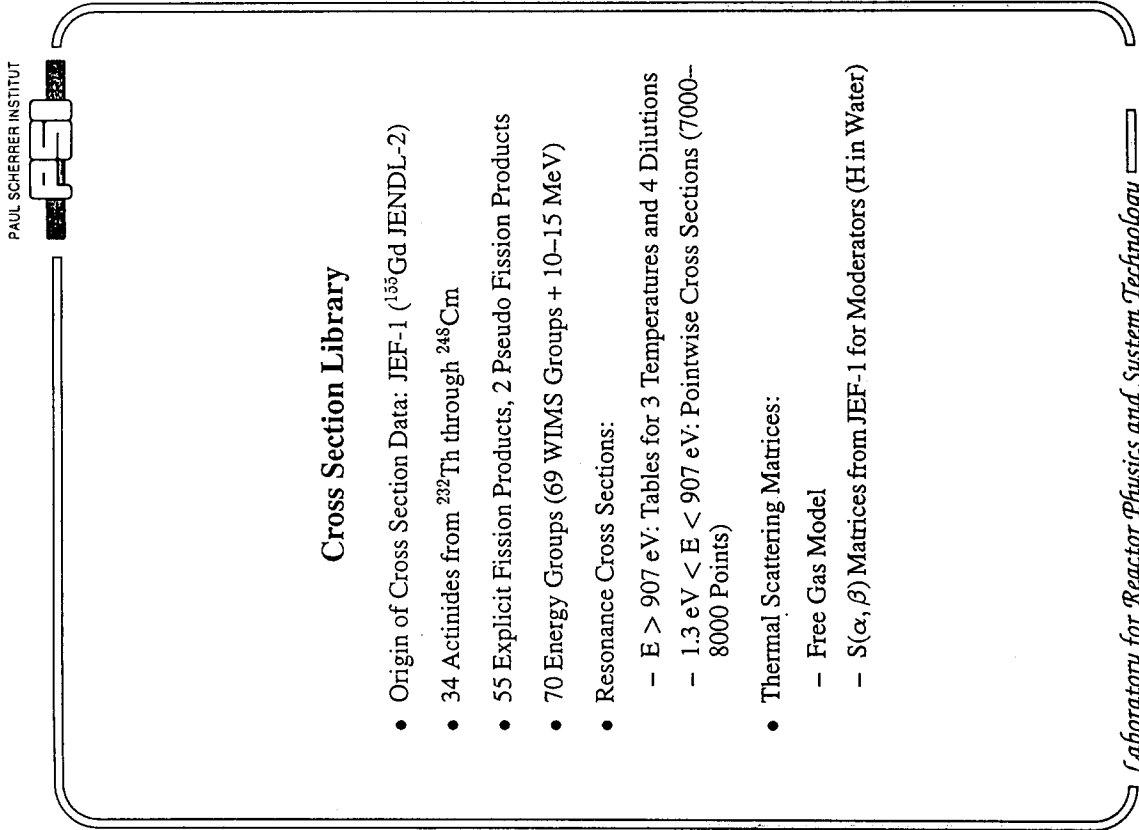


Fig. 4.11 Fission Rate (fissions/s) of Case 19 (4.5 w/o, 50 GWd/t)

Appendix 3.2 PSI Calculation for NEA Burnup Credit
Criticality Benchmark, Phase IIA

PSI

Organization of BOXER



Cross Section Library

- Origin of Cross Section Data: JEF-1 (¹⁵⁵Gd JENDL-2)
- 34 Actinides from ²³²Th through ²⁴⁸Cm
- 55 Explicit Fission Products, 2 Pseudo Fission Products
- 70 Energy Groups (69 WIMS Groups + 10-15 MeV)
- Resonance Cross Sections:
 - E > 907 eV: Tables for 3 Temperatures and 4 Dilutions
 - 1.3 eV < E < 907 eV: Pointwise Cross Sections (7000-8000 Points)
- Thermal Scattering Matrices:
 - Free Gas Model
 - S(α,β) Matrices from JEF-1 for Moderators (H in Water)

Laboratory for Reactor Physics and System Technology

Calculational Methods

BOXER code for the calculation of two-dimensional light water reactor configurations

Cell calculations:

- Resonance Self Shielding:
 - Table Interpolation ($E > 907$ eV)
 - Collision Probability Calculation in 2 Regions (1.3 eV $< E < 907$ eV)
- Fluxes per Zone in 70 Groups: Integral Transport Method (Cylindrical Geometry)
- Fission Source Flat, Scattering Source Flat in Each Zone or Polynomial of Radius
- Cells Calculated with White Boundary Conditions or with Outgoing Partial Current from First Cell as Fixed Surface Source
- Fundamental Mode by B_1 Calculation for Homogenized Cell

Laboratory for Reactor Physics and System Technology

Two-dimensional calculations:

- Transport: Transmission probability method QP1
 - Adjacent meshes coupled by continuity of mesh surface current moments
 - Outgoing current moments from solution of the integral transport equation
 - Mesh surface current approximated by a linear function in space and a first order spherical harmonics expansion in each quadrant of the hemisphere of the flight directions:

$$J(x, \theta, \phi) = \bar{J} + J_1 x + J_2 \cos\theta \cos\phi + J_3 \cos\theta \sin\phi$$
 - Linear space dependence of scattering and fission source within mesh
 - Scattering anisotropy: P_1
- Diffusion: Mesh-centered finite differences

Laboratory for Reactor Physics and System Technology



Sensitivity Studies

Effect of Doubling Energy Group Number (8 to 16):

	Δk_{eff}	Max. Change in Fission Density per Region
Case 2	+71 pcm	0.4%
Case 19	+35 pcm	0.3%

Effect of Doubling Mesh Number (77 to 154):

	Δk_{eff}	Max. Change in Fission Density per Region
Case 2	0 pcm	0.1%
Case 19	-3 pcm	<0.1%

Laboratory for Reactor Physics and System Technology

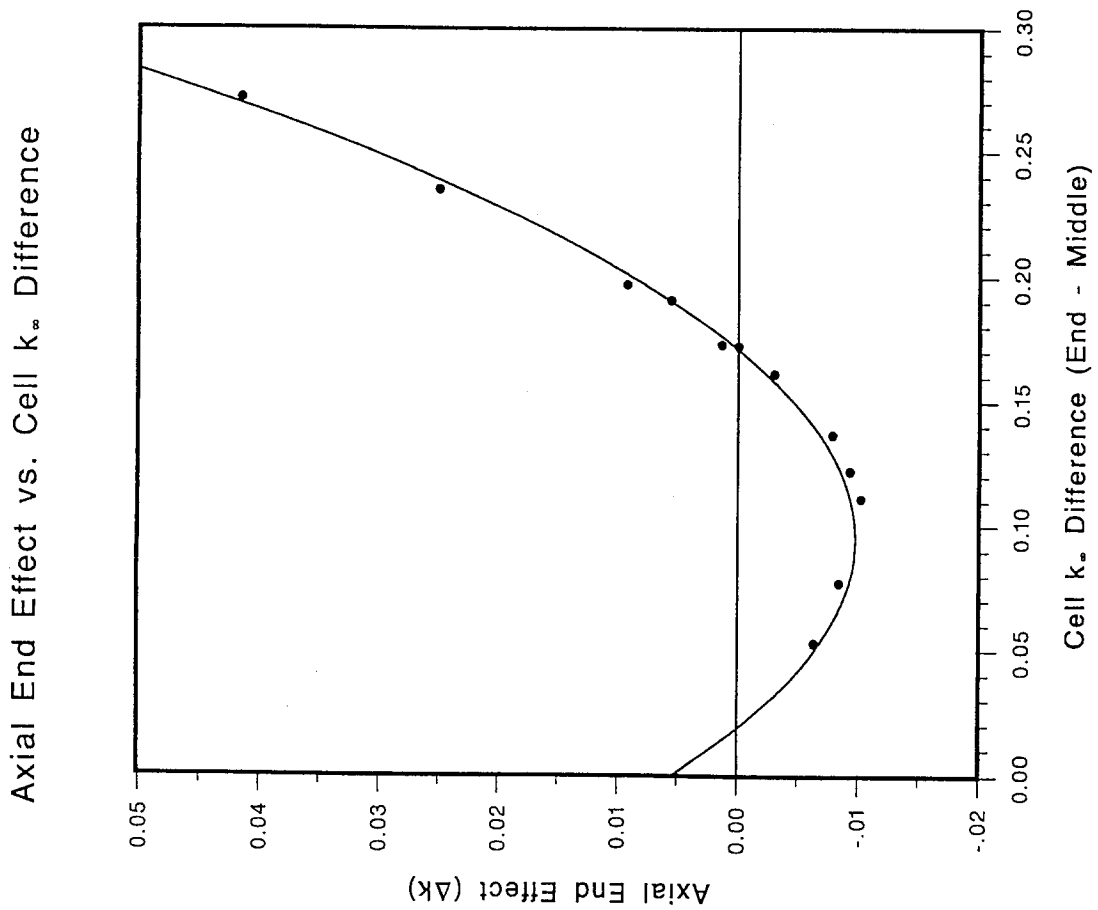
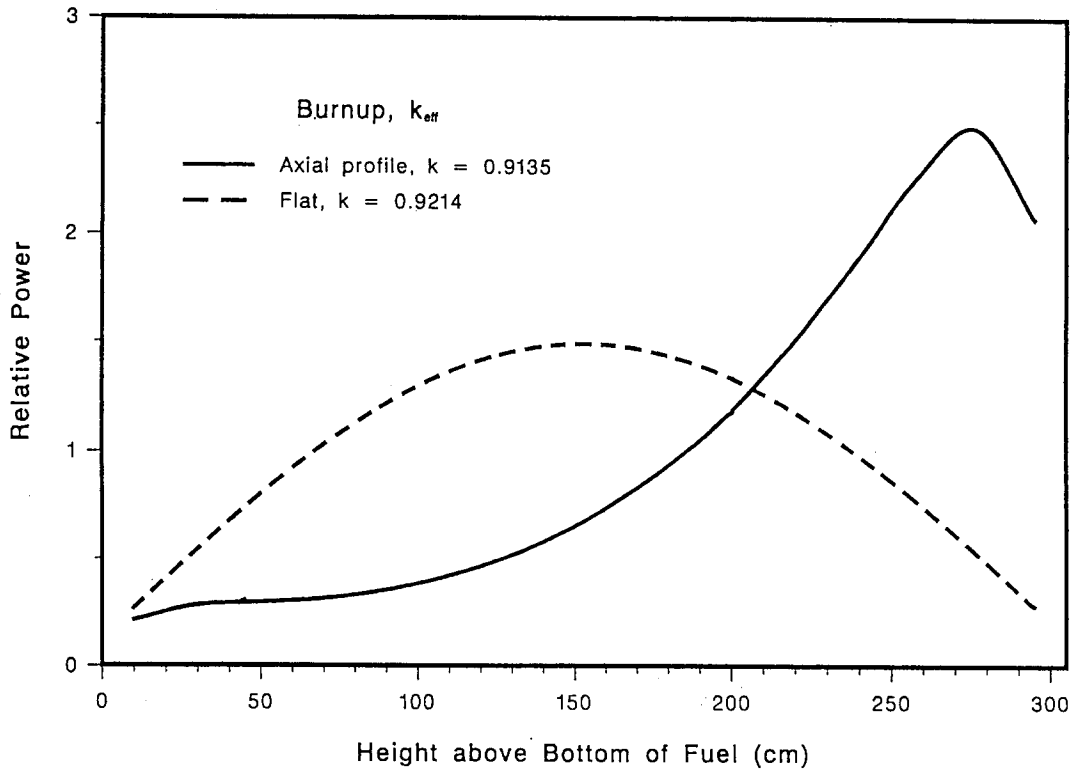


Calculations

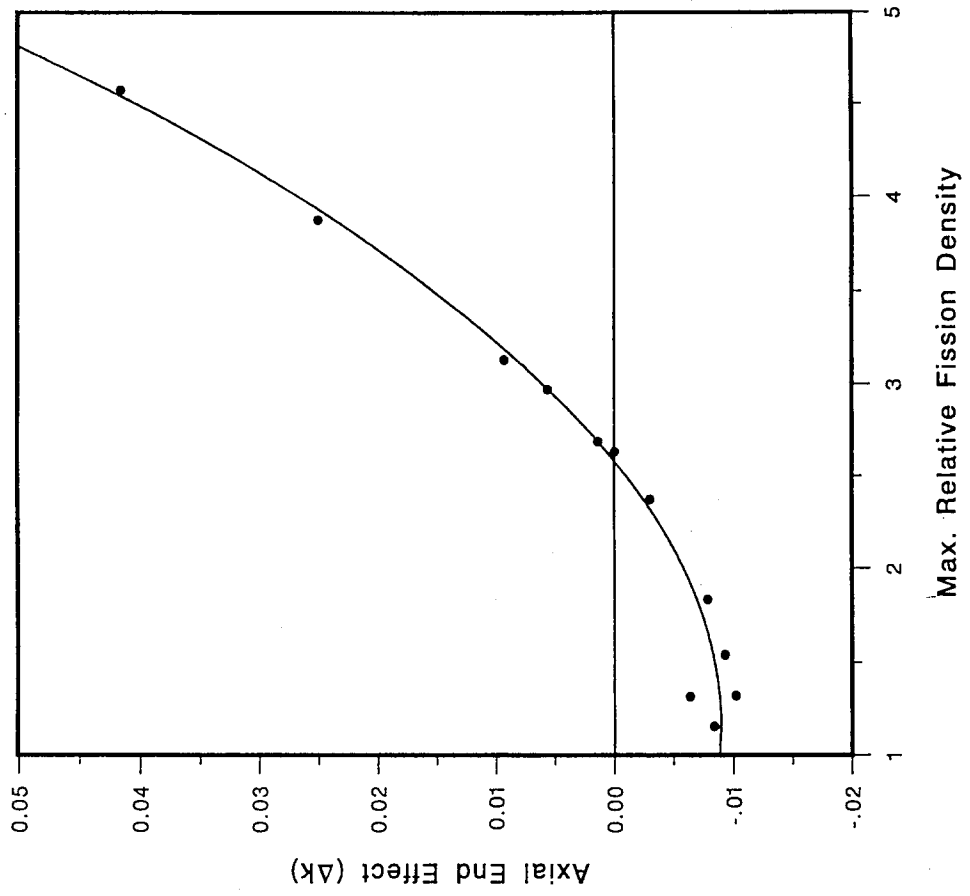
- Cell Calculation with White Boundary Conditions for Each Axial Fuel Region
- End Plugs Homogenized with Surrounding Water by Cell Calculation
- 1-D Transport Calculations for Half of Axial Configuration
- Mesh Widths from 1 cm Near Material Interfaces to 5 cm in the Middle of Zone 5, Total 77 Meshes
- 8 Energy Groups
- Flux Convergence 10^{-5}

Laboratory for Reactor Physics and System Technology

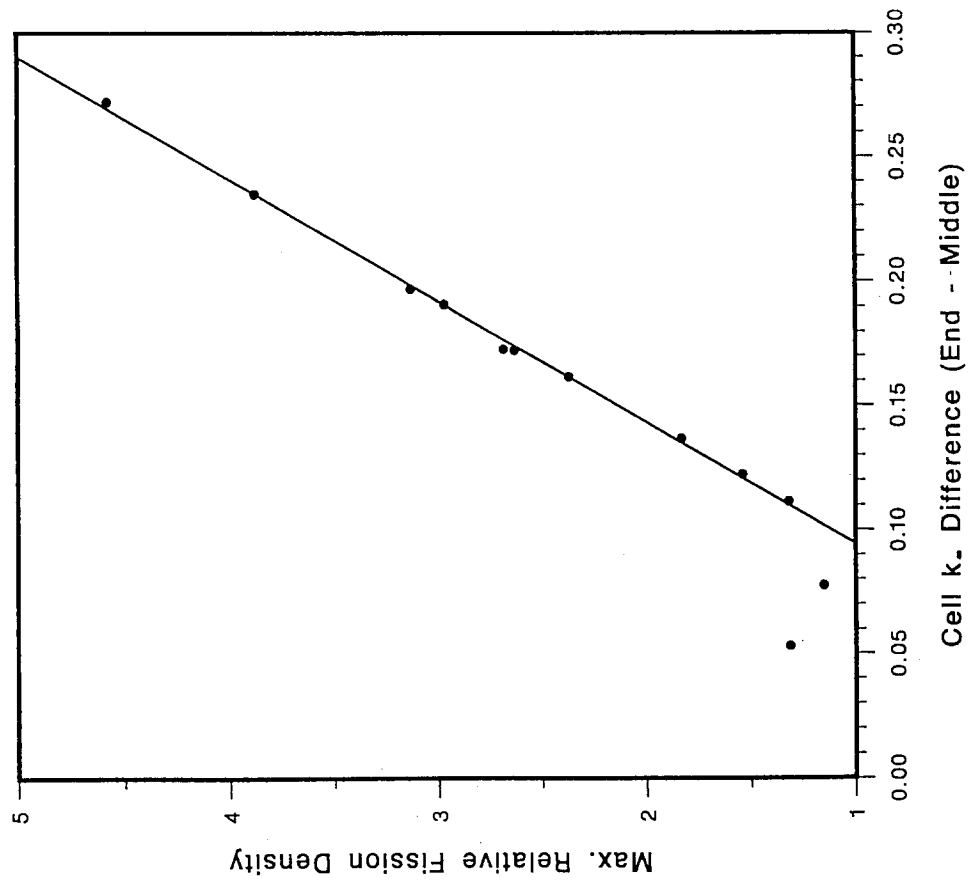
Axial Power Distribution in a Discharged PWR Assembly at HZP
 36.84 GWd/t Burnup, Relative to Average Power



Axial End Effect vs. Max. Fission Density



Max. Fission Density vs. Cell k_{∞} Difference



**Appendix 3.3 The Effect of Axial Burnup Profile,
CEA/DRN**

OECD/NEA Criticality Group Meeting
Paris 11-13 July 1994

**The Effect of the Axial Burnup Profile
OECD Burnup Credit Criticality Benchmark - Phase IIA**

B. ROQUE, A. SANTAMARINA, J.C. ESTIOT

C.E.A./DRN - Cadarache, 13108 Saint-Paul-Lez-Durance, France

ABSTRACT

The effect of the actual axial burnup profile in PWR assemblies on fuel cycle criticality is studied in the Phase II of the Burnup Credit (BUC) Criticality Benchmark. Results of the Phase IIA, corresponding to an infinite array of PWR spent fuel rods, are presented in this paper. Axial flux distributions, with the flat BU model and with the actual burnup profile, are analyzed and provide elements for understanding the Keff values.

I. INTRODUCTION

Today the neutron capture of F.P. are not accounted for in safety-criticality calculations of transport casks, storage and dissolvers.

The concept of allowing reactivity credit for spent fuel offers both economic and risk incentives. As an example burnup credit may potentially increase cask capacity by as much as 2 [1] ; increased cask capacity means fewer spent fuel shipments, which lowers costs and increases safety. In reprocessing plants, accounting for burnup credit enables the operator to avoid the use of Gd soluble poison in the dissolver and reduces mass limitations in dissolver loading [2].

For the criticality calculation of a spent fuel system, burnup profile of the spent fuel needs to be considered.

The effect of the axial burnup profile (end effect) on criticality calculations of spent fuel storage and casks is studied in Phase II of the OECD Benchmark on Burnup Credit Criticality.

The Phase II is divided in two programs :

- Phase II.A [3], devoted to the criticality calculation of an infinite array of PWR burnt fuel rods, is performed to grasp the effect of axial burnup profile on criticality.
- Phase II.B will assessed the criticality of actual spent fuel casks [4].

This paper presents the CEA results based on the deterministic calculation route.

II. CALCULATION ROUTE

The calculations were performed using the French APOLLO-BISTRO deterministic calculation scheme used in criticality studies [5].

The fuel pin cell (figure 1) was computed using the APOLLO1 transport code, which solves the Boltzmann Integral equation by the Collision Probability Method in a multigroup model [6]. The "CEA-86" 99-group library [7], based on the JEF1 file and CEA evaluations, was used.

All BUC nuclides are accounted for in the spent fuel calculations : U, Pu, Np and Am isotopes are described, as well as the 15 selected F.Ps Mo-95, Tc-99, Ru-101, Rh-103, Ag-109, Cs-133, Sm-147, Sm-149, Sm-150, Sm-151, Sm-152, Nd-143, Nd-145, Eu-153, Gd-155.

The 2D-transport calculations (figure 2) were carried out using the efficient BISTRO S_N code [8] : 15 energy-group collapsed cross-sections from APOLLO1 were automatically handled by BISTRO for the RZ calculations in a S_{16} quadrature. Anisotropic scattering is accounted by means of a P1 Legendre polynomial expansion. A refined axial mesh $\Delta z = 1$ cm was implemented in order to detail the flux gradient at the fuel/reflector interface.

III. CALCULATION RESULTS

The end effect is a function of the initial fuel enrichment, the burnup and the cooling time.

The selected parameters of benchmark Phase IIA are [3] :

- 3.6% and 4.5% w/o initial enrichment,
- 10 and 30 GWd/t burnups (3.6% enriched fuel),
- 30 and 50 GWd/t burnups (4.5% enriched fuel),
- 1 and 5 years of cooling times.

Moreover, calculations are run with and without Fission Product in order to investigate the F.P. role on the end effect.

The K_{eff} calculated values of the various PWR cases (radial infinite array) are summarized in Table 1.

The effect of the axial burnup profile on BUC reactivity is assessed through the result comparison between multiplication factor calculations with a flat burnup distribution and K_{eff} calculations with the actual burnup distribution.

IV. RESULT ANALYSIS AND AXIAL BURNUP PROFILE EFFECT

The Reactivity loss, corresponding to Burnup Credit, is :

$$BUC = |\Delta\rho| = \rho(BU) - \rho(\text{fresh})$$

The reactivity variation is defined as $\Delta\rho = \text{Ln} \frac{K_{\text{final}}}{K_{\text{initial}}}$ and expressed in pcm (10⁻⁵).

Table 2 summarizes the BUC reactivity versus burnup for cooling time $T = 1$ year. This table shows the high level of burnup credit, which amounts to (at $BU = 30$ GWd/t) :

$$\begin{aligned} |\Delta\rho| &= 23510 \text{ pcm} && (\text{Actinide depletion} + 15 \text{ F.P}) \\ |\Delta\rho| &= 15330 \text{ pcm} && (\text{without F.P}) \end{aligned}$$

Table 2 points out that the simplified \overline{BUC} calculations, with the flat average burnup distribution, give conservative values up to $\overline{BU} = 30$ GWd / t. For higher burnups the flat burnup model overestimates the BUC reactivity worth (+9% at $\overline{BU} = 50$ GWd / t), and the actual axial burnup profile should be accounted for in BUC calculations of PWR assembly casks and storage.

The mismatch in the assembly K_{eff} values, between the flat burnup calculation and the exact axial burnup calculation, arises from the corresponding axial flux shape :

- in the flat average burnup model, due to the homogeneous composition of the assembly, the axial flux is a cosine (see figure 3),

- in the exact calculation, the axial flux is already flattered at $\overline{\text{BU}} = 10 \text{ GWd/t}$ as shown in figure 4. With higher burnups, two peaks of the neutron flux are appearing close to the bottom and the top of the fuel rods, i.e. $Z = \pm 160 \text{ cm}$ from the middle plane (see figure 5 corresponding to a 3.6% enriched PWR assembly irradiated at $\overline{\text{BU}} = 30 \text{ GWd/t}$, and figures 6, 7 corresponding to a 4.5% enriched assembly irradiated up to 30 GWd/t and 50 GWd/t respectively).

In agreement with the specifications of the benchmark [3], the axial fission rates integrated over the 5 fissile volumes (see fig. 2) are given in Table 3. The results stress the neutronic weight increase of the fuel pin extremity with the assembly exposure.

V. CONCLUSION

The effect of the assembly axial burnup profile in burnup credit calculations was investigated. Due to a strong shift of the flux towards the fuel pin extremities with increasing burnup, the simplified flat burnup model is not suited to burnup credit calculations of PWR casks and storage for highly irradiated assemblies, i.e. $\overline{\text{BU}} > 30 \text{ GWd/t}$.

REFERENCES

- [1] M.C. BRADY, T.L. SANDERS
 "A validated methodology for evaluating burnup credit in spent fuel casks" -
 Proceedings of the ICNC'91 Conference, Vol 1, II-68, Oxford Sept 9-13, 1991.
- [2] B. ROQUE, A. SANTAMARINA
 "La prise en compte du credit burnup dans la Sûreté-Criticité - Quantification des gains
 dans le cadre du dissolvant-roue"
 CEA - Report SPRC-LEPh N°93/223
- [3] M. TAKANO, M. BRADY, A. SANTAMARINA
 "Burnup Credit Criticality Benchmark - Phase II-A : Effect of axial burnup profile"
 NEA/NSC/DOC (93) 15 October 1993.
- [4] E. SARTORI
 "Summary record of the NSC Meeting on the burnup credit criticality benchmark"
 (ORNL, USA, 15-17 Sept. 1993) NEA/NSC/DOC (93) 23.
- [5] A. SANTAMARINA
 "Development and Validation of a criticality calculation scheme based on French
 deterministic transport codes".
 Proceedings of the ICNC'91 Conference, Vol. 1, pp. II.24-II.33,
 Oxford (UK), 9-13 September 1991.
- [6] A. KAVENOKY, R. SANCHEZ
 "The APOLLO assembly spectrum code"
 Proc. Int. Conf. on React. Physics.
 Paris (France) 23-30 April 1987.
- [7] A. SANTAMARINA, H. TELLIER
 "The French CEA-86 multigroup cross-section library and its integral qualification".
 Proc. Int. Conf. on Nucl. Data MITO (Japan) 30 May 1988.
- [8] G. PALMIOTTI, J.M. RIEUNIER, G. GHO, M. SALVATORES
 "Optimised Two-Dimensional SN Transport (BISTRO)"
 Nucl. Sci. Eng. 104, 26-33 1990

Table 1 PWR assembly Keff values from 2D-calculations

	CASE N°	B.U. Profile	Cooling Time	B.U.	Keffectif
FUEL 3.6%	1		0 year	0 GWj/t	1.4373
	2	Yes	1 year	10 GWj/t	1.3062
	3	No	1 year	10 GWj/t	1.3140
	4 (No F.P.)	Yes	1 year	10 GWj/t	1.3629
	5 (No F.P.)	No	1 year	10 GWj/t	1.3688
	6	Yes	1 year	30 GWj/t	1.1362
	7	No	1 year	30 GWj/t	1.1320
	8 (No F.P.)	Yes	1 year	30 GWj/t	1.2330
	9 (No F.P.)	No	1 year	30 GWj/t	1.2418
	10	Yes	5 years	30 GWj/t	1.1152
	11	No	5 years	30 GWj/t	1.1035
	12 (No F.P.)	Yes	5 years	30 GWj/t	1.2183
	13 (No F.P.)	No	5 years	30 GWj/t	1.2250
FUEL 4.5%	14		0 year	0 GWj/t	1.4831
	15	Yes	1 year	30 GWj/t	1.1987
	16	No	1 year	30 GWj/t	1.2001
	17 (No F.P.)	Yes	1 year	30 GWj/t	1.2973
	18 (No F.P.)	No	1 year	30 GWj/t	1.3059
	19	Yes	1 year	50 GWj/t	1.0824
	20	No	1 year	50 GWj/t	1.0535
	21 (No F.P.)	Yes	1 year	50 GWj/t	1.2000
	22 (No F.P.)	No	1 year	50 GWj/t	1.1977
	23	Yes	5 years	50 GWj/t	1.0548
	24	No	5 years	50 GWj/t	1.0075
	25 (No F.P.)	Yes	5 years	50 GWj/t	1.1815
	26 (No F.P.)	No	5 years	50 GWj/t	1.1733

Table 2 Burnup credit reactivity versus assembly exposure

INITIAL, ENRICHISSEMENT	BURN - UP	F. P	BURNUP CREDIT ($10^{-5} \Delta K/K$)	
			With BU profile	Flat BU
e = 3.6 %	10 GWd/t	Yes	9560	8970
		No	5310	4880
	30 GWd/t	Yes	23510	23880
		No	15330	14620
e = 4.5 %	30GWd/t	Yes	21290	21170
		No	13380	12720
	50 GWd/t	Yes	31490	34200
		No	21180	21370

Table 3 Integrated axial fission rates versus assembly exposure

CAS	ZONE	INTEGRATED FISSION RATE $F_i = \int \int \Sigma_f \Phi dE dV$ with $\sum_i F_i = 1$	NORMALISED FISSION DENSITY $\bar{F}_i = \frac{(F_i/V_i)}{(F_{tot}/V_{tot})}$
	1	0.0142	0.5186
	2	0.0161	0.5877
2	3	0.0434	0.7937
B.U.=10 GWd/t	4	0.1117	1.0217
	5	0.8146	1.0426
	1	0.0549	2.0060
	2	0.0588	2.1508
6	3	0.1412	2.5828
B.U.=30 GWd/t	4	0.2736	2.5010
	5	0.4715	0.6036
	1	0.0857	3.1361
	2	0.0883	3.2290
19	3	0.1974	3.6102
B.U.=50 GWd/t	4	0.3247	2.9682
	5	0.3039	0.3889

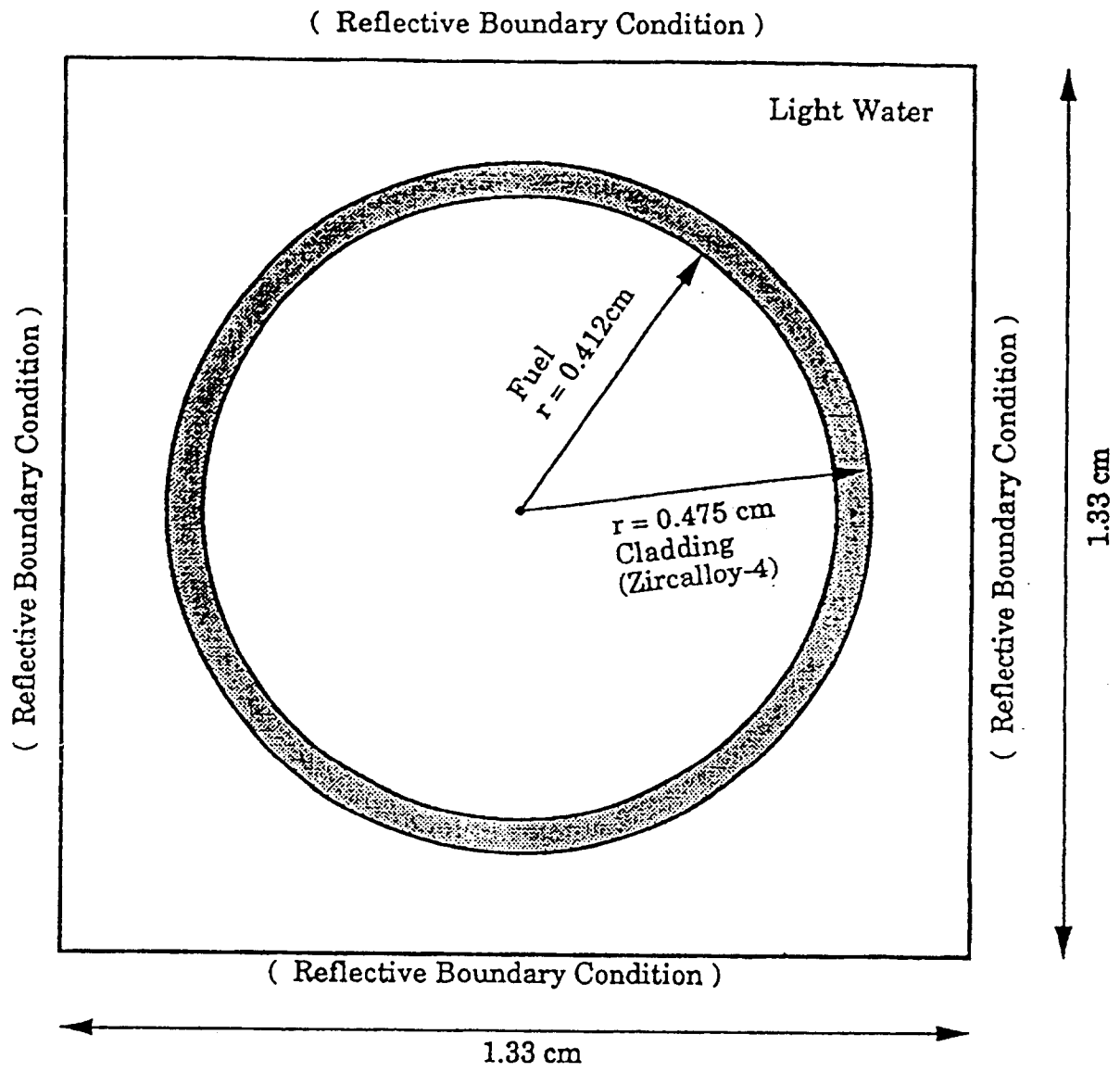


Fig. 1 Radial Dimensions

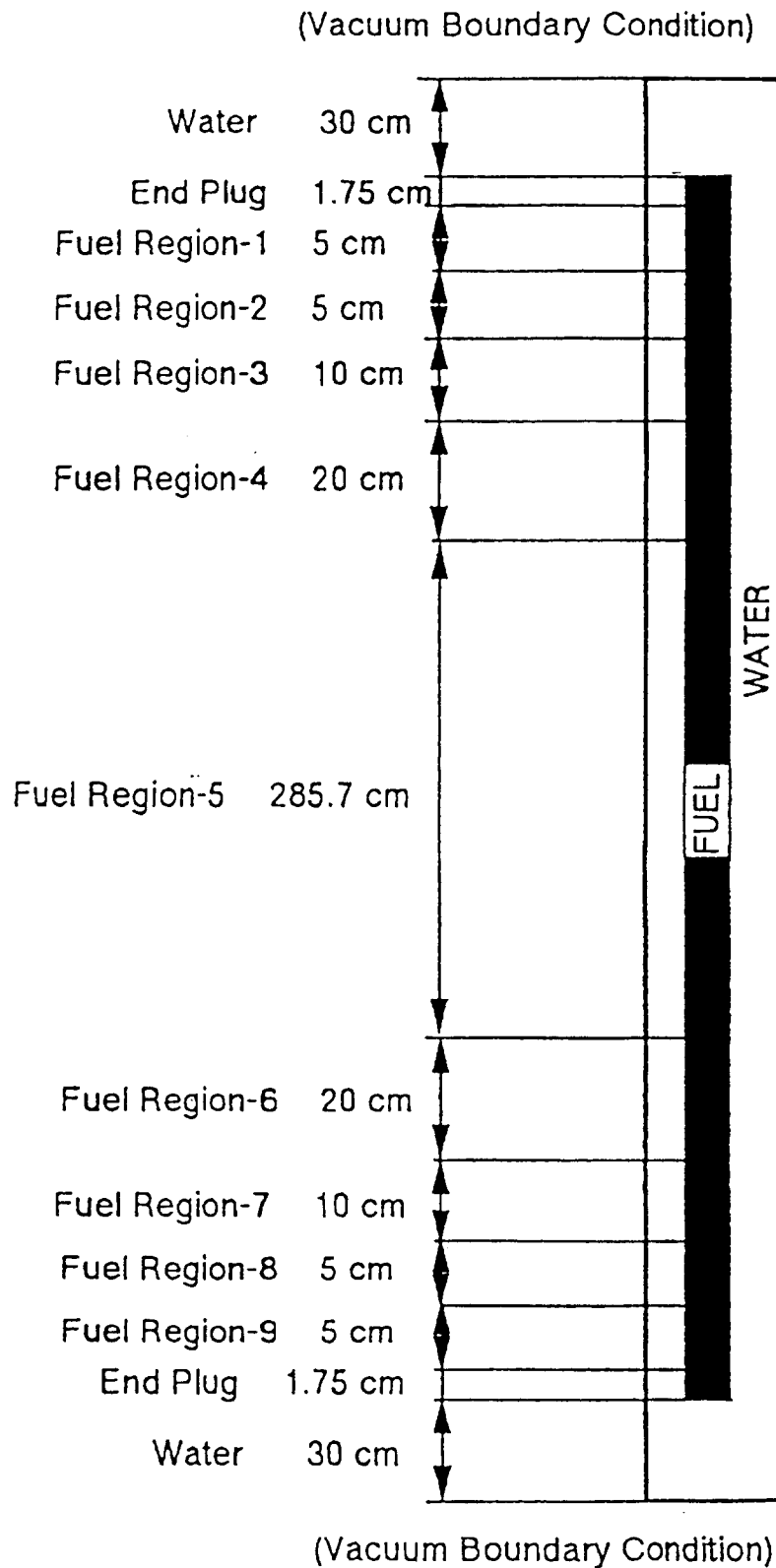


Fig. 2 Axial Dimensions

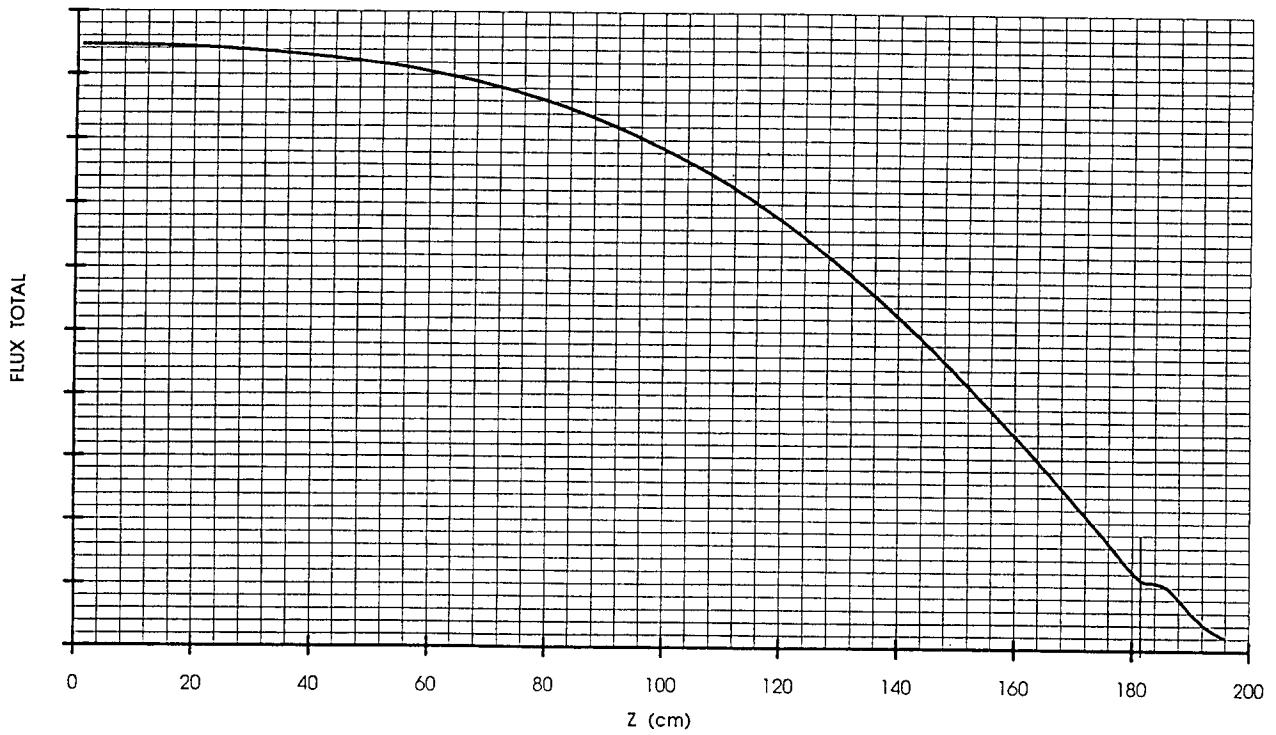


Fig. 3 BISTRO axial flux distribution in the flat BU calculations

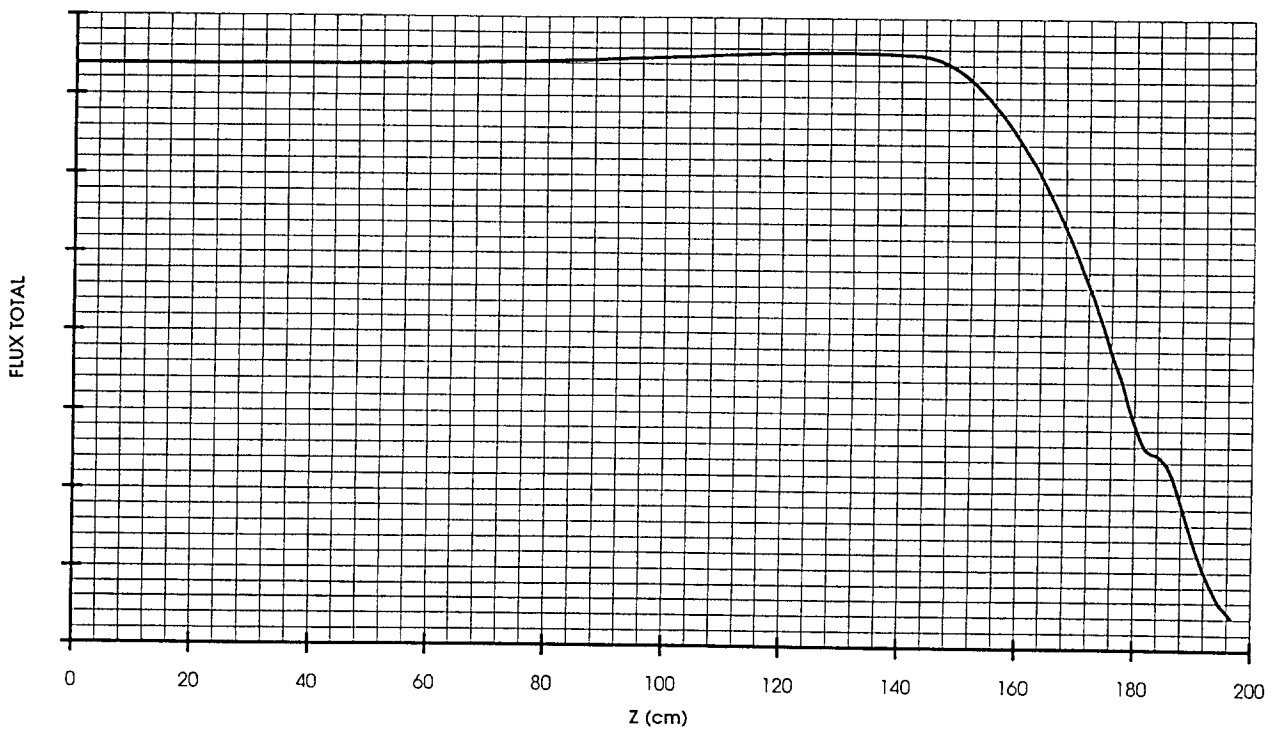


Fig. 4 Axial flux distribution in the 10 GWd/t PWR assembly
(with BU profile: case n°2)

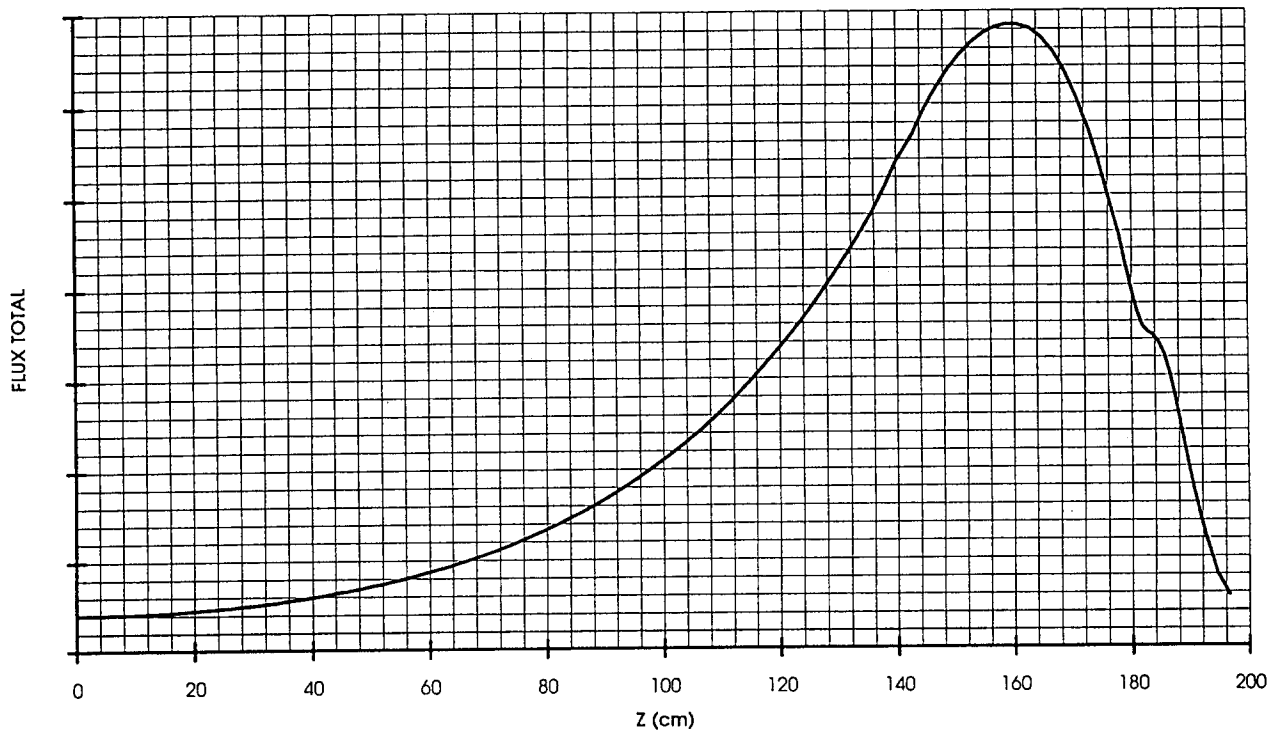


Fig. 5 Axial flux distribution in the 30 GWd/t PWR assembly
(with BU profile: case n°6, $e = 3.6\%$)

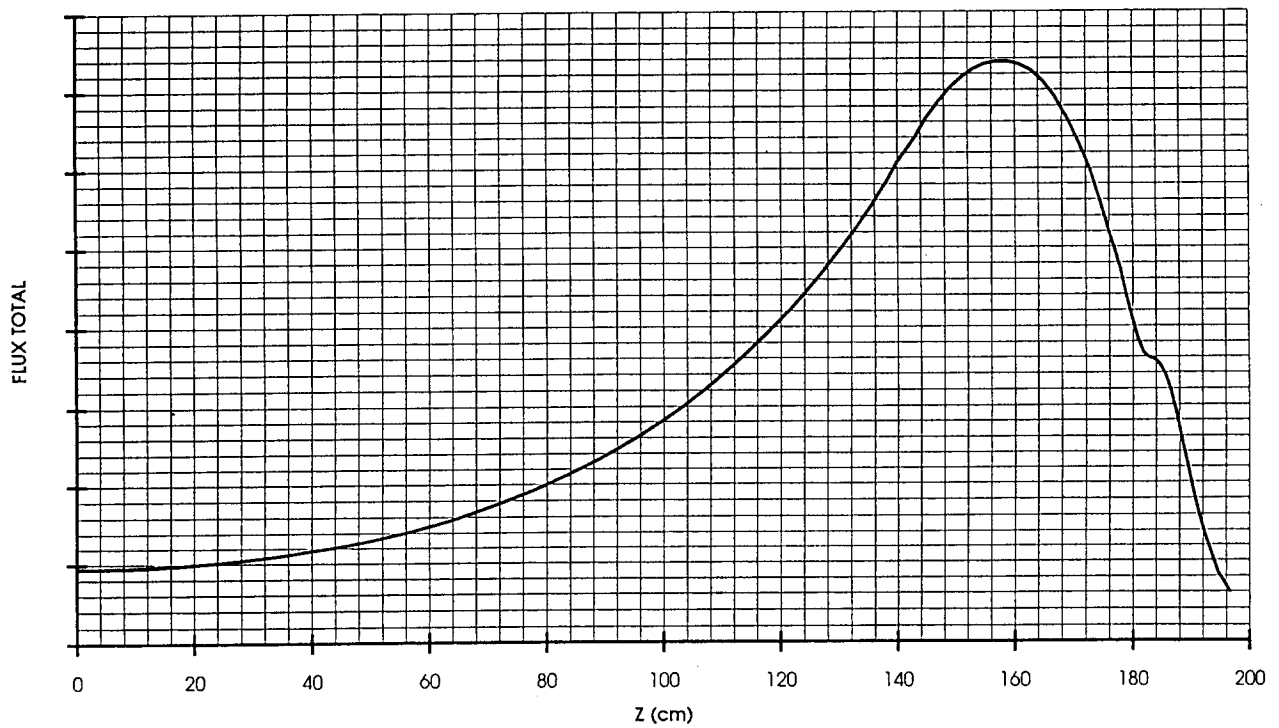


Fig. 6 Axial flux distribution in the 30 GWd/t PWR assembly
(with BU profile: case n°15, $e = 4.5\%$)

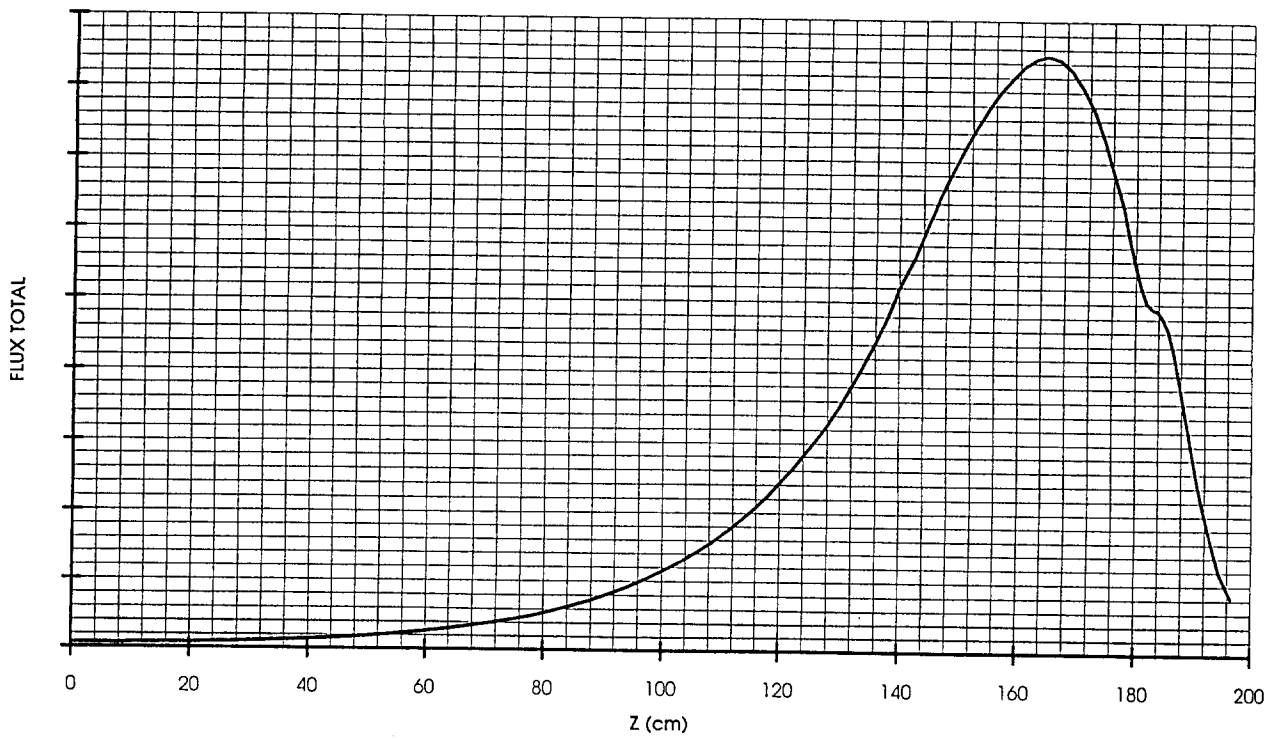


Fig. 7 Axial flux distribution in the 50 GWd/t PWR assembly
(with BU profile: case n°19, e = 4.5 %)

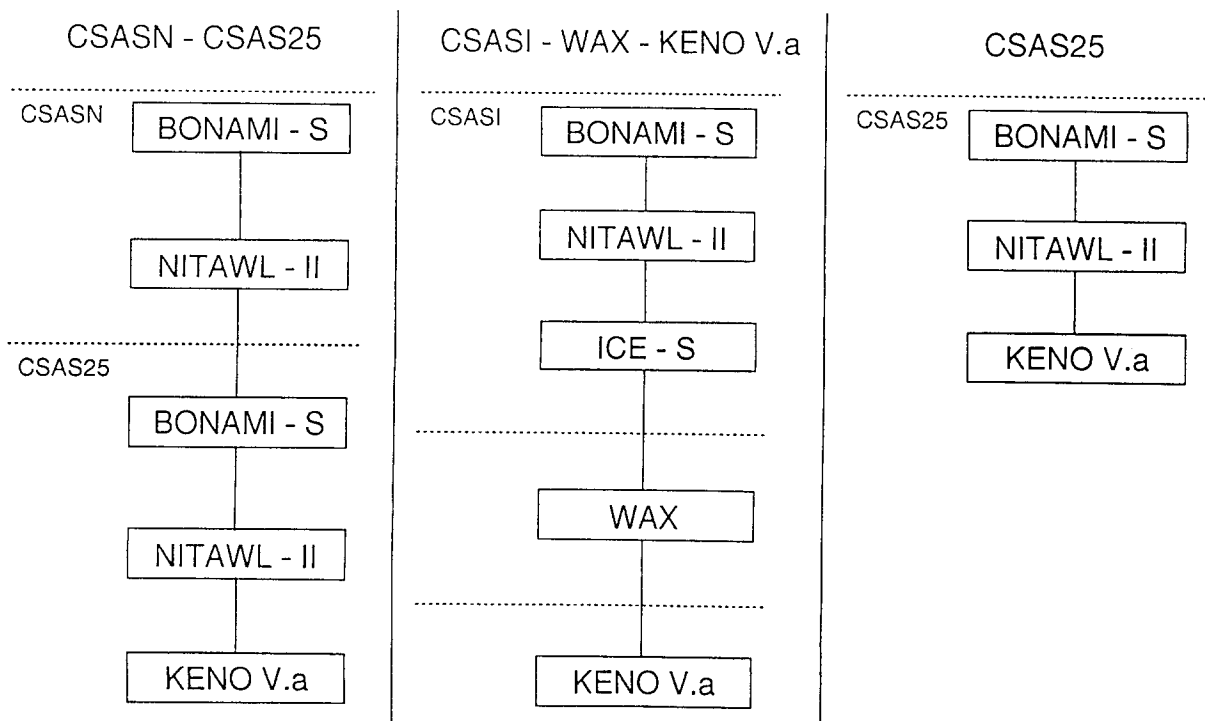
Appendix 3.4 Comparison of SCALE-4 CSAS Modules for
Criticality Calculations,
PNC

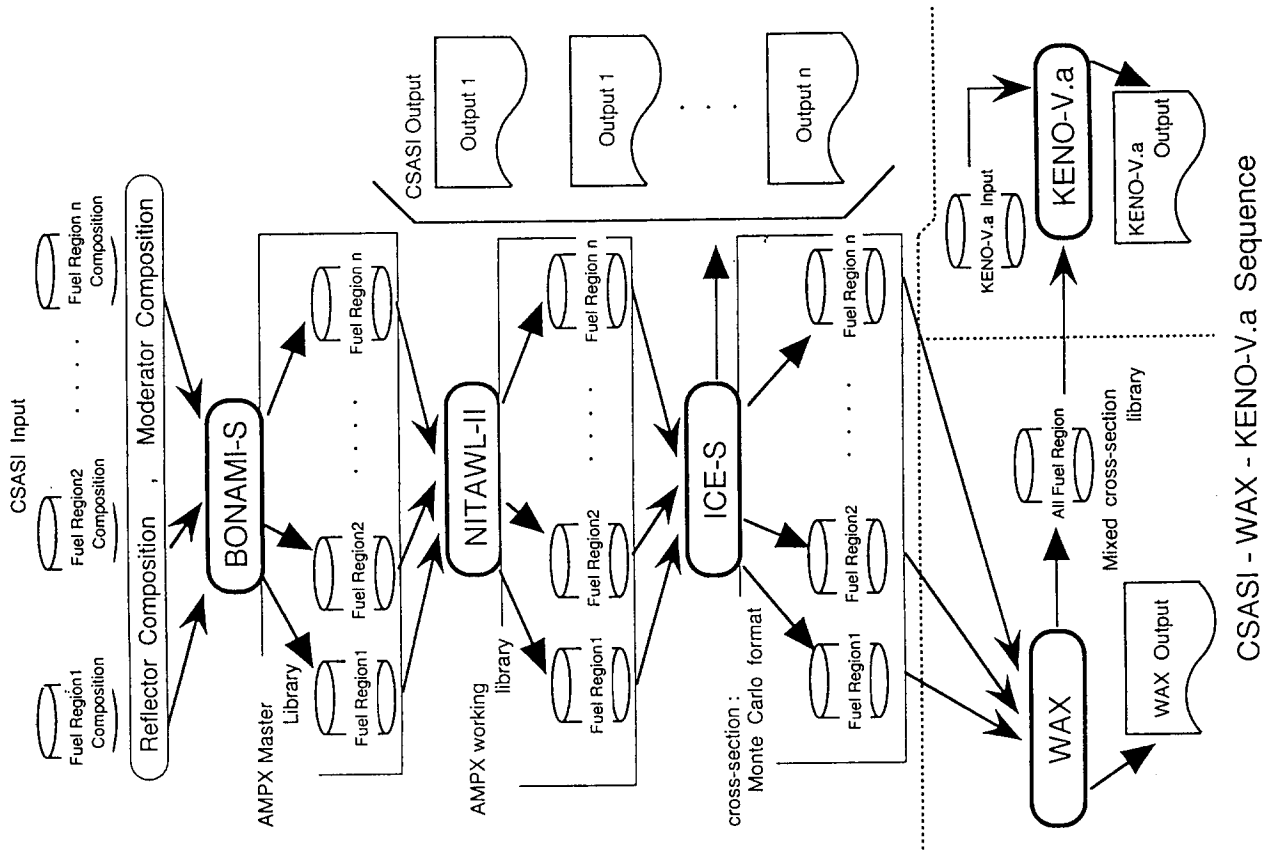
Comparison of SCALE-4 CSAS Modules
for Criticality Calculations
of an Infinite Array of PWR Spent Fuel Rods

Ichiro NOJIRI, Yasuhiro FUKASAKU, Osamu NARITA

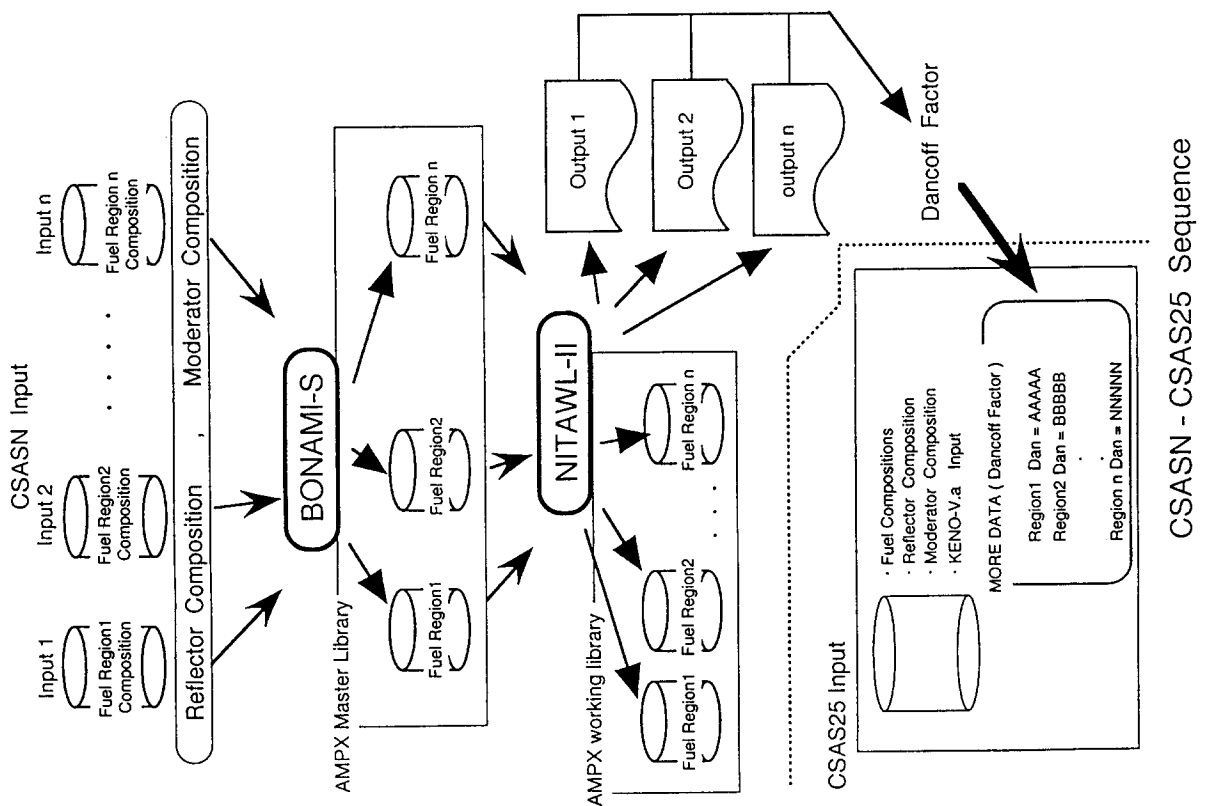
PNC Tokai Works, Japan

Selected CSAS modules for Calculations

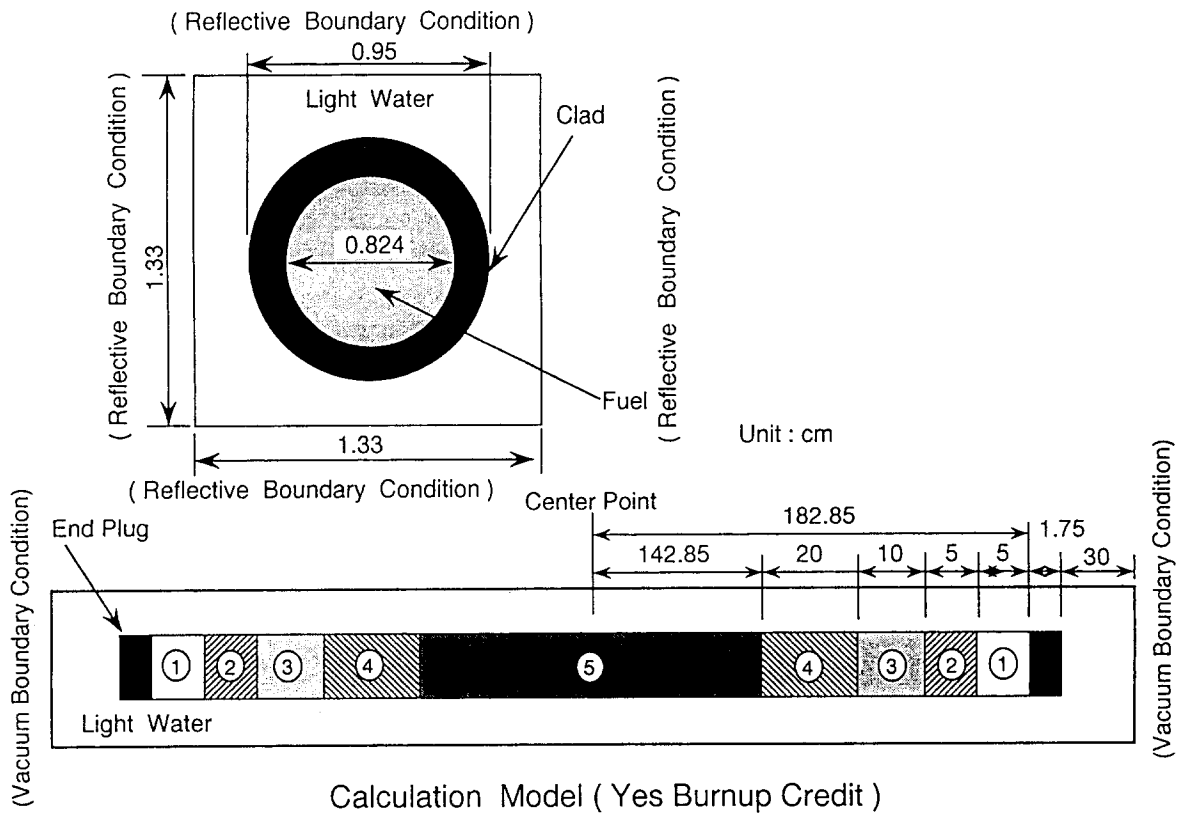




CSASI - WAX - KENO-V.a Sequence

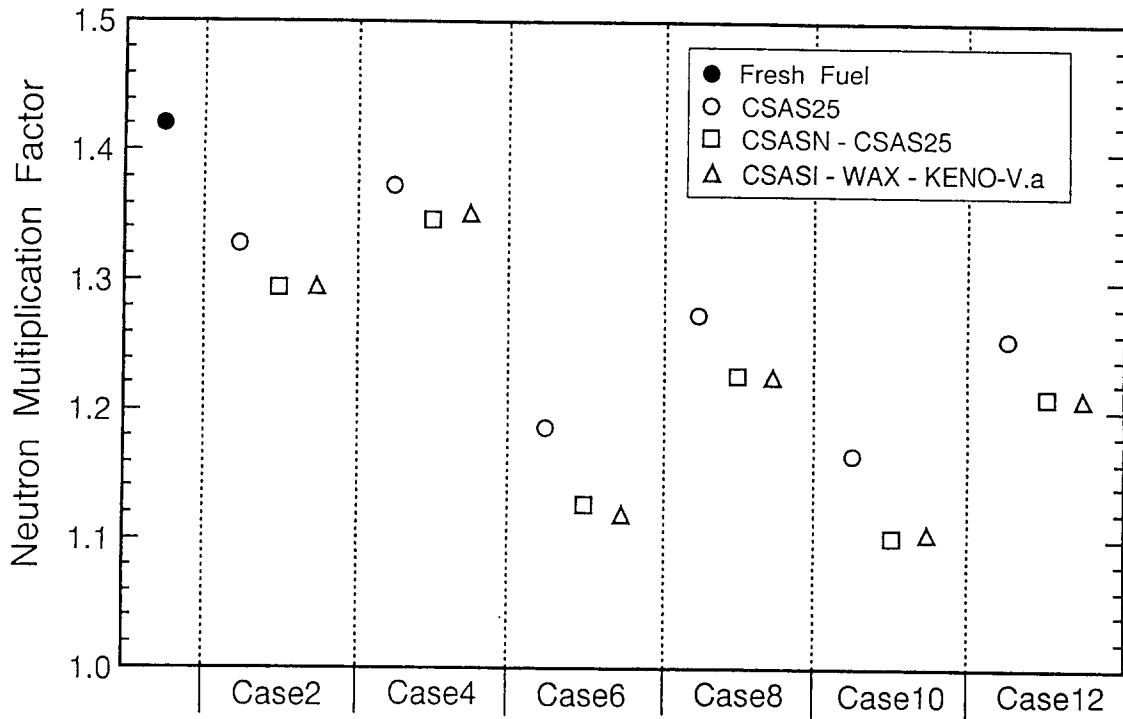


CSASN - CSAS25 Sequence

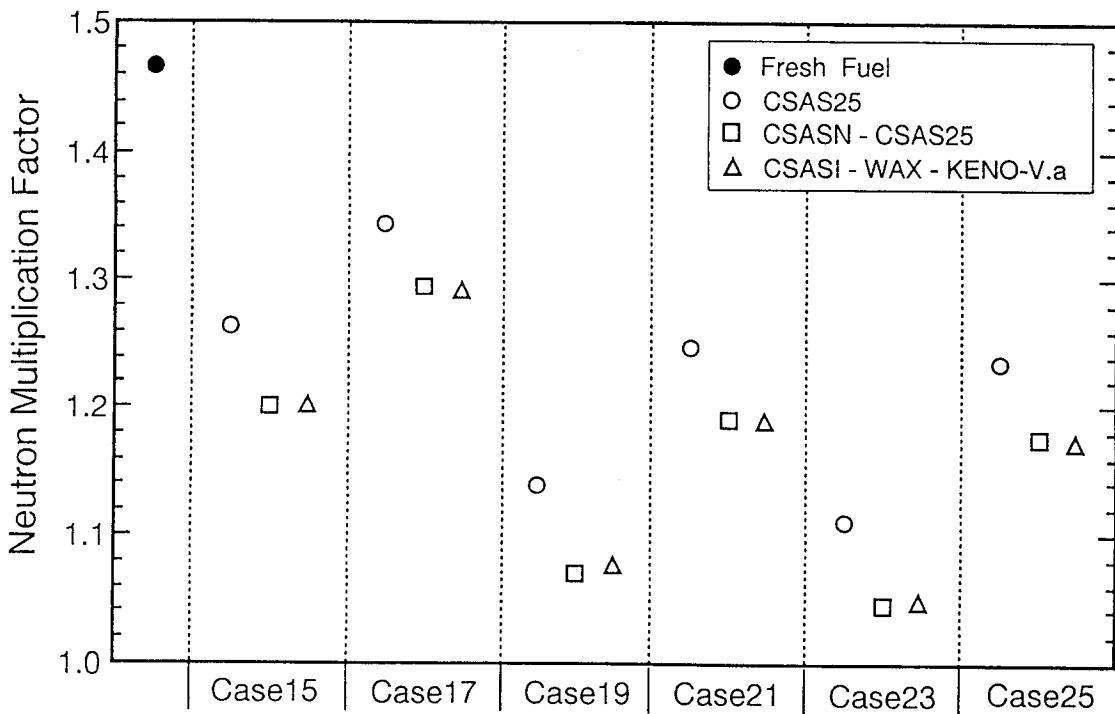


Calculation Results of Neutron Multiplication Factor for Each Case

Initial Fuel Enrichment	Case	CSAS25	CSASN-CSAS25	CSASI-WAX-KENO-V.a
		$K_{eff} \pm \sigma$	$K_{eff} \pm \sigma$	$K_{eff} \pm \sigma$
3.6wt%	2	1.328 ± 0.0016	1.294 ± 0.0015	1.294 ± 0.0016
	4	1.374 ± 0.0017	1.347 ± 0.0015	1.352 ± 0.0017
	6	1.186 ± 0.0019	1.127 ± 0.0015	1.119 ± 0.0015
	8	1.274 ± 0.0017	1.226 ± 0.0015	1.224 ± 0.0015
	10	1.166 ± 0.0017	1.102 ± 0.0016	1.104 ± 0.0016
	12	1.255 ± 0.0018	1.211 ± 0.0017	1.208 ± 0.0016
4.5wt%	15	1.264 ± 0.0019	1.201 ± 0.0017	1.201 ± 0.0017
	17	1.343 ± 0.0018	1.295 ± 0.0016	1.289 ± 0.0016
	19	1.138 ± 0.0020	1.070 ± 0.0017	1.076 ± 0.0019
	21	1.247 ± 0.0019	1.191 ± 0.0017	1.187 ± 0.0017
	23	1.111 ± 0.0020	1.046 ± 0.0017	1.047 ± 0.0018
	25	1.234 ± 0.0019	1.175 ± 0.0017	1.171 ± 0.0017



Comparison of Neutron Multiplication Factor for Each Case (1)
Initial Fuel Enrichment : 3.6wt%



Comparison of Neutron Multiplication Factor for Each Case (2)
Initial Fuel Enrichment : 4.5wt%

Appendix 4 List of Participants

Burnup Credit Criticality Benchmark: Phase IIA

BELGIUM

MALDAGUE, Thierry	Tel.	+32 (2) 774 0630
VANDERBORCK, Y.	Tel.	+32 (2) 774 0511
Belgonucléaire S.A. Avenue Ariane 4 B-1200 BRUXELLES	Fax	+32 (2) 774 0614

FRANCE

MAUBERT, Louis	Tel.	+33 (1) 46 54 74 30
NOURI, Ali	Tel.	+33 (1) 46 54 89 15
POULLOT, Gilles	Tel.	+33 (1) 46 54 85 66
ROUSSIGNOL, Jacques		
CEA/IPSN/DRS/SEC CEN Fontenay-aux-Roses B.P. No. 6 F-92265 FONTENAY-AUX-ROSES	Fax	+33 (1) 46 57 29 98
ROQUE, Bénédicte	Tel.	+33 42 25 36 48
SANTAMARINA, Alain	Tel.	+33 42 25 70 46
C.E. - Cadarache Bât. 230 CEA/DRN/DER F-13108 ST. PAUL LEZ DURANCE CEDEX	Fax	+33 42 25 48 49

GERMANY

BERNNAT, Wolfgang	Tel.	+49 (711) 685 2118
Universität Stuttgart Institut für Kernenergetik und Energiesysteme Postfach 801140 D-70550 STUTTGART 80	Fax	+49 (711) 685 2010
GMAL, Bernhard	Tel.	+49 (89) 32004 494
HEINICKE, Walter		
MOSER, Eberhard	Tel.	+49 (89) 32004 187
WEBER, Wolf-Jürgen	Tel.	+49 (89) 32004 185
Gesellschaft für Anlagen- und Reaktorsicherheit Postfach 1328 D-85739 GARCHING	Fax	+49 (89) 32004 491

SCHWEER, Hans Heinrich Tel. +49 (531) 592 7685
 Bundesamt für Strahlenschutz Fax +49 (531) 592 7616
 Albert Schweitzerst. 18
 D-38226 SALZGITTER

ITALY

SICILIANO, Francesco Tel. +39 (835) 974 213
 ENEA - Centro Comb Trisaia Fax +39 (835) 974 292
 S.S. 106 Jonica, Km 419+500
 I-75025 POLICORO (Matera)

JAPAN

ANDO, Yoshihira Tel. +81 (44) 288 8132
 YAMAMOTO, Munenari Tel. +81 (44) 288 8130

Toshiba Corporation Fax +81 (44) 299 2853
 Nuclear Engineering Lab.
 4-1 Ukishima-cho,
 Kawasaki-ku
 KAWASAKI 210

HIRAKAWA, Naohiro
 IWASAKI, Tomohiko
 SUYAMA, Kenya Tel. +81 (22) 217 7910

University of Tohoku Fax +81 (22) 217 7900
 Dept. of Nuclear Engineering
 Aoba, Aramaki-ku
 SENDAI-SHI 980

MITAKE, Susumu Tel. +81 (3) 5470 5470

NUPEC Fax +81 (3) 5470 5454
 Institute of Nuclear Safety
 17-1, Toranomom 3-chome
 Minato-ku, TOKYO 105

NAITO, Yoshitaka Tel. +81 (29) 282 5757
 TAKANO, Makoto Tel. +81 (29) 282 5943
 OKUNO, Hiroshi Tel. +81 (29) 282 5103

JAERI
Shirakata-Shirane
TOKAI-MURA 319-11

Fax +81 (29) 282 6199

NOJIRI, Ichiro

Tel. +81 (29) 282 1111

PNC
Muramatsu
TOKAI-MURA 319-11

Fax +81 (29) 287 1841

SATO, Osamu

Tel. +81 (3) 3277 0595

Mitsubishi Research
Institute, Inc.
Time & Life Bldg.
2-3-6 Otemachi
Chiyoda-ku, TOKYO 100

Fax +81 (3) 3270 9004

SPAIN

CONDE LOPEZ, Jose M.

Tel. +34 (1) 346 02 53

RECIO SANTAMARIA, Manuel

Tel. +34 (1) 346 02 10

Nuclear Engineering D.
CSN
Justo Dorado, 11
28003 MADRID

Fax +34 (1) 346 05 88

SWEDEN

MENNERDAHL, Dennis

Tel. +46 (8) 756 5812

D. Mennerdahl Systems
Starvägen 12
S-183 51 TÄBY

Fax +46 (8) 756 5872

SWITZERLAND

GRIMM, Peter

Tel. +41 (56) 310 20 71

PARATTE, Jean-Marie

Tel. +41 (56) 310 20 70

Paul Scherrer Institute
CH-5232 VILLIGEN PSI

Fax +41 (56) 310 21 99

WHITESIDES, G. Elliott (Chair) Tel. +1 (423) 574 5304
Oak Ridge National Labs. Fax +1 (423) 574 9646
P.O. Box 2008
Oak Ridge, Tennessee 37830

OECD/NEA (Secretariat)

SARTORI, Enrico Tel. +33 (1) 4524 1072
OECD/NEA Data Bank Fax +33 (1) 4524 1110
Le Seine-Saint Germain
12 boulevard des Iles
F-92130 ISSY-LES-MOULINEAUX

国際単位系 (SI) と換算表

表1 SI基本単位および補助単位

量	名称	記号
長さ	メートル	m
質量	キログラム	kg
時間	秒	s
電流	アンペア	A
熱力学温度	ケルビン	K
物質質量	モル	mol
光度	カンデラ	cd
平面角	ラジアン	rad
立体角	ステラジアン	sr

表3 固有の名称をもつSI組立単位

量	名称	記号	他のSI単位による表現
周波数	ヘルツ	Hz	s ⁻¹
力	ニュートン	N	m·kg/s ²
圧力, 応力	パスカル	Pa	N/m ²
エネルギー, 仕事, 熱量	ジュール	J	N·m
工率, 放射束	ワット	W	J/s
電気量, 電荷	クーロン	C	A·s
電位, 電圧, 起電力	ボルト	V	W/A
静電容量	ファラド	F	C/V
電気抵抗	オーム	Ω	V/A
コンダクタンス	ジーメンズ	S	A/V
磁束	ウェーバ	Wb	V·s
磁束密度	テスラ	T	Wb/m ²
インダクタンス	ヘンリー	H	Wb/A
セルシウス温度	セルシウス度	°C	
光照射度	ルーメン	lm	cd·sr
放射線量当量	ルクス	lx	lm/m ²
放射線量当量	ベクレル	Bq	s ⁻¹
放射線量当量	グレイ	Gy	J/kg
放射線量当量	シーベルト	Sv	J/kg

表2 SIと併用される単位

名称	記号
分, 時, 日	min, h, d
度, 分, 秒	°, ', "
リットル	l, L
トン	t
電子ボルト	eV
原子質量単位	u

1 eV = 1.60218 × 10⁻¹⁹ J
1 u = 1.66054 × 10⁻²⁷ kg

表4 SIと共に暫定的に維持される単位

名称	記号
オングストローム	Å
バイン	b
バル	bar
ガリ	Gal
キュリー	Ci
レントゲン	R
ラド	rad
レム	rem

1 Å = 0.1 nm = 10⁻¹⁰ m
1 b = 100 fm = 10⁻²⁸ m²
1 bar = 0.1 MPa = 10⁵ Pa
1 Gal = 1 cm/s² = 10⁻² m/s²
1 Ci = 3.7 × 10¹⁰ Bq
1 R = 2.58 × 10⁻⁴ C/kg
1 rad = 1 cGy = 10⁻² Gy
1 rem = 1 cSv = 10⁻² Sv

表5 SI接頭語

倍数	接頭語	記号
10 ¹⁸	エクサ	E
10 ¹⁵	ペタ	P
10 ¹²	テラ	T
10 ⁹	ギガ	G
10 ⁶	メガ	M
10 ³	キロ	k
10 ²	ヘクト	h
10 ¹	デカ	da
10 ⁻¹	デシ	d
10 ⁻²	センチ	c
10 ⁻³	ミリ	m
10 ⁻⁶	マイクロ	μ
10 ⁻⁹	ナノ	n
10 ⁻¹²	ピコ	p
10 ⁻¹⁵	フェムト	f
10 ⁻¹⁸	アト	a

(注)

- 表1-5は「国際単位系」第5版, 国際度量衡局 1985年刊行による。ただし, 1 eV および 1 uの値は CODATA の1986年推奨値によった。
- 表4には海里, ノット, アール, ヘクタールも含まれているが日常の単位なのでここでは省略した。
- bar は, JISでは流体の圧力を表わす場合に限り表2のカテゴリに分類されている。
- EC閣僚理事会指令では bar, barn および「血圧の単位」mmHgを表2のカテゴリに入れている。

換算表

力	N (=10 ⁵ dyn)	kgf	lbf
	1	0.101972	0.224809
	9.80665	1	2.20462
	4.44822	0.453592	1

粘度 1 Pa·s (= N·s/m²) = 10 P (ポアズ) (g/(cm·s))

動粘度 1 m²/s = 10⁴ St (ストークス) (cm²/s)

圧	MPa (=10 bar)	kgf/cm ²	atm	mmHg (Torr)	lbf/in ² (psi)
	1	10.1972	9.86923	7.50062 × 10 ³	145.038
力	0.0980665	1	0.967841	735.559	14.2233
	0.101325	1.03323	1	760	14.6959
	1.33322 × 10 ⁻⁴	1.35951 × 10 ⁻³	1.31579 × 10 ⁻³	1	1.93368 × 10 ⁻²
	6.89476 × 10 ⁻³	7.03070 × 10 ⁻²	6.80460 × 10 ⁻²	51.7149	1

エネルギー・仕事・熱量	J (=10 ⁷ erg)	kgf·m	kW·h	cal (計量法)	Btu	ft·lbf	eV
	1	0.101972	2.77778 × 10 ⁻⁷	0.238889	9.47813 × 10 ⁻⁴	0.737562	6.24150 × 10 ¹⁸
	9.80665	1	2.72407 × 10 ⁻⁶	2.34270	9.29487 × 10 ⁻³	7.23301	6.12082 × 10 ¹⁹
	3.6 × 10 ⁶	3.67098 × 10 ⁵	1	8.59999 × 10 ⁵	3412.13	2.65522 × 10 ⁶	2.24694 × 10 ²⁵
	4.18605	0.426858	1.16279 × 10 ⁻⁶	1	3.96759 × 10 ⁻³	3.08747	2.61272 × 10 ¹⁹
	1055.06	107.586	2.93072 × 10 ⁻⁴	252.042	1	778.172	6.58515 × 10 ²¹
	1.35582	0.138255	3.76616 × 10 ⁻⁷	0.323890	1.28506 × 10 ⁻³	1	8.46233 × 10 ¹⁸
	1.60218 × 10 ⁻¹⁹	1.63377 × 10 ⁻²⁰	4.45050 × 10 ⁻²⁵	3.82743 × 10 ⁻²⁰	1.51857 × 10 ⁻²²	1.18171 × 10 ⁻¹⁹	1

1 cal = 4.18605 J (計量法)
= 4.184 J (熱化学)
= 4.1855 J (15 °C)
= 4.1868 J (国際蒸気表)

仕事率 1 PS (仏馬力)
= 75 kgf·m/s
= 735.499 W

放射能	Bq	Ci
	1	2.70270 × 10 ⁻¹¹
	3.7 × 10 ¹⁰	1

吸収線量	Gy	rad
	1	100
	0.01	1

照射線量	C/kg	R
	1	3876
	2.58 × 10 ⁻⁴	1

線量当量	Sv	rem
	1	100
	0.01	1

